

Doctoral theses at NTNU, 2020:305

Vladimír Hamouz

Retention and detention-based roofs for stormwater management in urban environments in cold climates

ISBN 978-82-326-4958-7 (printed ver.)
ISBN 978-82-326-4959-4 (electronic ver.)
ISSN 1503-8181

Doctoral theses at NTNU, 2020:305

NTNU
Norwegian University of
Science and Technology
Thesis for the degree of
Philosophiae Doctor
Faculty of Engineering
Department of Civil and Environmental
Engineering

 **NTNU**
Norwegian University of
Science and Technology

 **NTNU**

 **NTNU**
Norwegian University of
Science and Technology

Vladimír Hamouz

Retention and detention-based roofs for stormwater management in urban environments in cold climates

Thesis for the degree of Philosophiae Doctor

Trondheim, October 2020

Norwegian University of Science and Technology
Faculty of Engineering
Department of Civil and Environmental Engineering



Norwegian University of
Science and Technology

NTNU

Norwegian University of Science and Technology

Thesis for the degree of Philosophiae Doctor

Faculty of Engineering

Department of Civil and Environmental Engineering

© Vladimír Hamouz

ISBN 978-82-326-4958-7 (printed ver.)

ISBN 978-82-326-4959-4 (electronic ver.)

ISSN 1503-8181

Doctoral theses at NTNU, 2020:305



Printed by Skipnes Kommunikasjon AS

Abstract

The combined effect of urbanization and climate change, which results in an increased level of imperviousness, is currently causing stress to urban drainage systems in urban areas unable to preserve the hydrological cycle of natural catchments. A considerable portion of urban environments' impervious fractions is comprised of rooftops, which have increasingly been retrofitted with green roofs. Vegetated rooftops may contribute to reducing the impact of climate change and urbanization by retaining and detaining runoff, thereby reducing overall runoff volume and peak runoff rates. However, they do not always fulfil the requirements for stormwater detention. Moreover, in climates with limited evapotranspiration, a non-vegetated configuration may be a more favourable option for stormwater management.

A field station for testing different rooftops was established in 2017 on the coast of Trondheim, Norway. Two different solutions comprised of vegetated (green) and non-vegetated (grey) configurations were evaluated with respect to their hydrological performance between years 2017 and 2019. The first solution (*Solution 1*) consisted of an extensive green roof with a 30- mm thick layer of Sedum mats, a non-vegetated grey roof with a 200-mm thick layer of expanded clay, and a reference black roof. The second solution (*Solution 2*) offered a detention-based green roof with a 100-mm thick layer of expanded clay, a non-vegetated grey roof with a 100-mm thick layer of expanded clay covered by paving stones and the reference black roof.

The extensive and detention-based green roofs provided stormwater retention between 24- 37 % of the total long-term continuous runoff in the warm period, experiencing a normalized daily retention of 0.86 mm/day for *Solution 1* and 1.05 mm/day for *Solution 2*. Regarding detention performance, the grey roof outperformed the extensive green roof for the ten largest recorded events for *Solution 1*. However, underlaying the extensive green roof with expanded clay for *Solution 2* resulted in the improvement of the detention performance in

addition to providing reasonable stormwater retention. With respect to *Solution 2*, while the detention-based green roof performed similarly to the grey roof in terms of peak delay, it outperformed the grey roof in volume reduction (retention) by more than four times. Nevertheless, the event-based retention and detention performances of the individual roof may vary since they are a result of the local climate as well as events interpretation.

The detention performance of the detention-based green roof, consisting of Sedum mats underlaid with expanded clay, was tested for current and future climate conditions under extreme precipitation. Events having a return period of 20 years, including a climate factor of 1.4 corresponding to different locations in Trondheim, Oslo and Bergen, were created using an artificial rainfall generator. It was found that the peak delay and attenuation may not provide an ideal evaluation of the roof primarily due to the temporal resolution and specificity of individual rainfall patterns. While peak delay exponentially decreased from 31 minutes to 2 minutes, the centroid delay exponentially decreased from almost 500 to 10 minutes with increasing initial water content. The time of concentration for the black roof was within 5 minutes independent of rainfall intensity, whereas in the case of the detention-based green roof, it was extrapolated between 30 and 90 minutes, being strongly dependent on the rainfall intensity ranging between 0.8 to 2.5 mm/min. The roof performance decreased due to increased initial water content and was most sensitive to longer rainfalls with lower intensity than short, intense rainfalls.

The Environmental Protection Agency (EPA) Storm Water Management Model (SWMM) 5.1.012 with Low Impact Development (LID) Controls was used to evaluate the model performance of the roofs from *Solution 1* on the building scale before the calibrated roof models were applied on a catchment scale. High-resolution data from previously monitored roofs and physical parameters within the individual LID layers (soil and drainage mat) were selected for model calibration. The calibrated parameters of the green and grey roofs were compared to several other roofs from another study, including roofs located in Oslo, Bergen and Sandnes, with different types of construction, geometry, and climates. The SWMM model provided a significantly positive match between observed and simulated runoff using a Nash-Sutcliffe model efficiency (NSME) between 0.56 and 0.96 and a volume error between -4 to 29 % for all configurations, including different locations in Bergen, Oslo, Sandnes and Trondheim. The calibrated roof models used during the winter period showed poor performance levels for long-term simulation runs. These were expressed with an NSME of 0.56 (green roof) and 0.37 (grey roof) and a volume error of 30% (green roof) and 11% (grey roof). Even though optimal

parameter sets were proposed for each configuration, the model parameters obtained at one site were only partly transferable due to the issue of model equifinality. This could be linked to the choice of a one-year training period and the fact that model transferability is greater when moving from wetter to drier periods.

The PCSWMM model version 7.2.2780, which is a user interface for EPA SWMM 5, was used for simulating runoff from an urban catchment at Risvollan in the city of Trondheim. The calibrated green or grey roof models for *Solution 1* were used in the catchment instead of conventional rooftops, and their resulting detention impact on the catchment outlet was evaluated according to nine scenarios. There was a focus on peak runoff reduction in terms of the runoff exceedance of three thresholds (100, 50 and 25 L/s) at the catchment outlet. It was found that as little as 11 % of the roof area can substantially reduce maximum flows, reduce the number of events, including the volume per event as well as the duration of the events themselves. Concerning the peak flows, the reduction performance increases in line with an increase of the area for potential retrofitting by green or grey roofs and with a decrease of the catchment slope. The implementation of grey roofs outperformed the extensive green roofs in all areas: event duration, number of events and volume of exceedance per event.

The green roofs showed a greater variation in their measured moisture content than the grey roofs did due to the transpiration process. However, the relatively high moisture levels in the expanded clay did not affect the detention performance under normal daily conditions. A reduction of detention performance occurred when running consecutive extreme events over the course of one day. In this case, the moisture levels increased with respect to events with a 20-year return period for future climate (2071-2100) and 200-year return period for the current climate. While the extensive green roof was mostly efficient for retention, the detention-based green roof underlaid with expanded clay provided an additional detention effect. Thus, the roof implementation's impact on an urban catchment's vulnerable points will mainly occur when using a configuration containing expanded clay.

Considering its initial saturation point and chosen type, rooftop retrofitting as a form of source control will, in most cases, contribute to a change in the runoff characteristics of conventional roofs. This thesis provides information for decision-makers and urban stormwater planners on how to target and focus on implementing rooftop solutions as stormwater measures. The hydrological performance of the detention-based green roof under extreme precipitation

confirms and strengthens the applicability of the retrofitted rooftop solutions in an urban environment under both current and future climate conditions.

Preface

This doctoral thesis is submitted for the partial fulfilment of the requirements for the degree of *Philosophiae Doctor* (Ph.D.). The study has been completed at the Department of Civil and Environmental Engineering, Faculty of Engineering, Norwegian University of Science and Technology in Trondheim, with Professor Tone Merete Muthanna as main supervisor and Professor Tore Kvande as co-supervisor.

This work is the result of a four-year Ph.D. programme in which 75 % was dedicated to research and 25 % to compulsory work for the department. This work included assisting in the Master-level course TVM4130 Urban Water Systems, supervising exchange students as well as students writing their thesis and helping out during field work. Funding was provided by the Research Council of Norway and several other partners through the Centre for Research-based Innovation project *Klima 2050* (project number 237859/030).

This thesis presents work completed on stormwater management in urban areas using retention and detention-based roofs that has resulted in five scientific papers. The candidate has been the main author on four of the five papers, while Paper 4 was written in collaboration with another main author. Further information about these authors' contributions may be found in the papers and co-author statements in *Co-Author Statements*.

Chapter 1 introduces the topic addressed in this thesis and presents the main factors that need to be considered when designing and modelling roofs for stormwater management. Chapter 2 offers the materials used and methods performed to accomplish this work. Chapter 3 summarizes and discusses the main results from the papers included in this thesis in order to answer all relevant research questions. Chapter 4 outlines a conclusion from this thesis and provides a number of recommendations for future work. *Appendix A* provides supplementary materials for the main results. The selected papers of this thesis are listed in *Appendix B*.

Appendix also presents the abstracts and bibliographies of the secondary papers and conference presentations and the co-author statements pertaining to the publication of this thesis.

In accordance with the requirements of the Faculty of Engineering at NTNU, the present thesis comprises an introduction to research work, which is composed of five scientific papers.

Acknowledgments

I would like to thank the Research Council of Norway and the Centre for Research-based Innovation for funding my research through the project *Klima 2050*.

Special thanks go to my main supervisor, Professor Tone Merete Muthanna, for believing that I was the right person for this Ph.D. position, inspiring fruitful discussions and always offering constructive criticism. I have appreciated your friendliness, kindness, patience and constant support.

Thank you so much, Tone; it is all because of you that I have reached this stage!

My appreciation also goes to my co-supervisor, Professor Tore Kvande, for his support and management skills during the project and help during the construction – and reconstruction – of the field station at Høvringen.

Next, I would like to express my gratitude to my co-authors: Jardar Lohne, Jaran Raymond Wood, Birgitte Gisvold Johannessen, Ashenafi Seifu Gragnes, Per Møller-Pedersen, Vincent Jean-Michel Thierry Pons, Edvard Sivertsen, Gema Sakti Raspati and Jean-Luc Bertrand-Krajewski. My thanks also go to the students who helped me (or whom I helped) during the final four years of my research project: Jon Christian Wilmann, Solène Chalvet, Lotte Askeland Schärer, Li Li.

I would like to stress the importance of having a great officemate, fun sports mate and excellent mentor during my first years of study: Thank you, Carlos! And I cannot forget my wonderful colleagues Chunbo, Ushanth, Manuel, Michal, Marcell, Mauro, Erle, Ana, Ana, Adina, colleagues from the project *Klima2050*, and many others as well as the university futsal team NTNUI and the department football team FK Steindølene for all the good times during my time here in Trondheim.

Acknowledgments

Huge thanks go to my family, especially my mom: you have always supported me and always believed in me. You never argued about all the decisions I made, but just gave me your full support.

Last but not least, thank you, Jani, for joining me on this crazy trip! Thanks for following me up here to Norway and especially for giving up weekends and free time while I have been going through the super busy – and hard – last year of my studies.

Table of Contents

Abstract	i
Preface	v
Acknowledgments	vii
Table of Contents	ix
List of Figures	xi
List of Tables	xiii
List of Publications	xvii
Chapter 1 Introduction	1
1.1 Background	4
1.2 Research questions	7
Chapter 2 Materials and Methods	9
2.1 Roof configuration	9
2.2 Hydrometeorological data - Høvringen	11
2.3 Hydrometeorological data - Risvollan Urban Hydrological Station (RUHS)	13
2.4 Methods in Paper 1	14
2.5 Methods in Paper 2	15
2.6 Methods in Paper 3	18
2.7 Methods in Paper 4	20
2.8 Methods in Paper 5	21

Chapter 3 Results and Discussion	25
3.1 Results and discussion of Paper 1 (extended version).....	25
3.2 Results and discussion of Paper 2.....	30
3.3 Results and discussion of Paper 3.....	35
3.4 Results and discussion of Paper 4.....	39
3.5 Results and discussion of Paper 5.....	43
3.6 Uncertainty in observation input and hydrological modelling	46
Chapter 4 Conclusions and recommendations	49
4.1 Conclusions	49
4.2 Recommendations for future work	51
References	53
Appendix A: Supplementary materials	59
Appendix B: Selected papers	65

List of Figures

Figure 1 Location map of the city of Trondheim (yellow cross), the Høvringen field site (blue star), and Risvollan catchment (red star).	9
Figure 2 Two sets of rooftop solutions (marked as Solution 1 and Solution 2) monitored between 2017 and 2019.	10
Figure 3 Three different rooftops at Høvringen on 11.6.2019. NB.: each of the rooftops with size 8×11 meters receives additional stormwater from surrounding separation walls and parapets with an area of 12m ²	11
Figure 4 Rainfall simulator over the detention-based green roof on 11.6.2019.	16
Figure 5 Risvollan catchment with the stormwater drainage network and flat roofs (yellow shaded) chosen for the green and grey roofs' implementation. (Paper 5 - Hamouz et al. – in review)	22
Figure 6 Comparison between peak runoff, centroid delay and T50 for different rainfall patterns. (Paper 2 - Hamouz et al. - Accepted for publication)	32
Figure 7 Comparison between peak runoff, peak attenuation and centroid delay for different locations, including a climate factor of 1.4. (Paper 2 - Hamouz et al. - Accepted for publication)	34
Figure 8 Comparison of observed and simulated runoff from the green (left) and grey (right). Event C3 from the calibration period was chosen (Table 10). More plots from the calibration period may be found in Paper 3 (Hamouz and Muthanna, 2019).	37
Figure 9 Comparison of observed and simulated runoff from the green (left) and grey (right) for the largest event V2 from the validation period in 2017. More plots from the validation period may be found in Paper 3 (Hamouz and Muthanna, 2019).	37
Figure 10 Comparison of the event record with the Depth-Duration-Frequency (DDF) curves for Solution 1	60

Figure 11 Comparison of the event record with the Depth-Duration-Frequency (DDF) curves for **Solution 2**.....60

Figure 12 Observed maximum black roof runoffs and runoffs corresponding to the extensive green and grey roofs for **Solution 1**.....61

Figure 13 Observed maximum black roof runoffs and runoffs corresponding to the detention-based green and grey roofs for **Solution 2**.....61

Figure 14 Probability exceedance of the black, extensive green and grey roof runoffs for **Solution 1**.62

Figure 15 Probability exceedance of the black, detention-based green and grey roof runoffs for **Solution 2**.62

List of Tables

Table 1 Summary of the tested rainfall events extracted from DDF curves for the three locations of Trondheim, Oslo, and Bergen with and without climate factor. The green column shows the events with a primary focus of 20 RP; the rest was transposed to other locations. (Paper 2 - Hamouz et al. - Accepted for publication).....	17
Table 2 LID Green roof control editor and its parameters with initial values and lower and upper bounds. (Hamouz and Muthanna, 2019).....	19
Table 3 Tested rooftops scenarios (more about the scenarios may be found in Paper 5).....	24
Table 4 Long-term precipitation/runoff records for Solution 1 and Solution 2. Values in the brackets are percental volume errors with respect to raw precipitation.....	26
Table 5 Long-term runoff measurements for Solution 1 and Solution 2, including runoff reduction, retention and normalized daily retention for the green and grey roofs with respect to the black roof.	27
Table 6 Ten events according to max 5-min precipitation intensity for Solution 1 , including peak delay for the extensive green and grey roofs with respect to the black roof.	28
Table 7 Ten events according to max 5-min precipitation intensity for Solution 1 , including peak reduction and volume reduction for the extensive green and grey roofs with respect to the black roof.	28
Table 8 Ten events according to max 5-min precipitation intensity for Solution 2 , including peak delay for the detention-based green and grey roofs with respect to the black roof.....	29
Table 9 Ten events according to max 5-min precipitation intensity for Solution 2 , including peak reduction and volume reduction for the detention-based green and grey roofs with respect to the black roof.	29
Table 10 Individual events used for evaluating the model performance within the calibration (C) and validation (V) period and comparison to the black roof runoff. The table shows overall	

model performance for long-term continuous calibration, validation and cold periods. (Hamouz and Muthanna, 2019)	38
Table 11 Model evaluation from individual model calibration (Johannessen et al., 2019).....	40
Table 12 Final model parameters for Papers 3 and 4 and comparison to the SWMM manual and other studies.	43
Table 13 Impact of the green and grey roofs’ implementation for different exceedance thresholds 100, 50 and 25 L/s with respect to the evaluation criteria. Scenarios A, B, and C from Table 3. (Paper 5 - Hamouz et al. in review)	44
Table 14 Impact of the green and grey roofs’ implementation with doubled roof size for different exceedance thresholds 100, 50 and 25 L/s with respect to the evaluation criteria. Scenario A, D, and E from Table 3. (Paper 5 - Hamouz et al. in review)	45
Table 15 Material characteristics of green roof substrate and expanded clay	59
Table 16 Ten largest events within the cold period according to the maximum black roof runoff for Solution 1 , including peak delay for the extensive green and grey roofs with respect to the black roof.	63
Table 17 Ten largest events within the cold period according to the maximum black roof runoff for Solution 1 , including peak and volume reduction for the extensive green and grey roofs with respect to the black roof.....	63
Table 18 Ten largest events within the warm period according to the maximum black roof runoff for Solution 1 , including peak delay for the extensive green and grey roofs with respect to the black roof.	63
Table 19 Ten largest events within the warm period according to the maximum black roof runoff for Solution 1 , including peak and volume reduction for the extensive green and grey roofs with respect to the black roof.....	63
Table 20 Ten largest events within the cold period according to the maximum black roof runoff for Solution 2 , including peak delay for the detention-based green and grey roofs with respect to the black roof.	64
Table 21 Ten largest events within the cold period according to the maximum black roof runoff for Solution 2 , including peak and volume reduction for the detention-based green and grey roofs with respect to the black roof.....	64
Table 22 Ten largest events within the warm period according to the maximum black roof runoff for Solution 2 , including peak delay for the detention-based green and grey roofs with respect to the black roof.....	64

Table 23 Ten largest events within the **warm** period according to the maximum black roof runoff for **Solution 2**, including peak and volume reduction for the detention-based green and grey roofs with respect to the black roof. 64

List of Publications

Selected papers

1. Hamouz, V., Lohne, J., Wood, J., & Muthanna, T. (2018). Hydrological performance of LECA-based roofs in cold climates. *Water*, 10(3), 263. <https://doi.org/10.3390/w10030263>
2. Hamouz, V., Pons, V., Sivertsen, E., Raspati, G. S., Bertrand-Krajewski, J-L., & Muthanna, T. M. (2020) Detention-based green roofs for stormwater management under extreme precipitation due to climate change. *Blue-Green Systems*, 2(1), 250-266. <https://doi.org/10.2166/bgs.2020.101>
3. Hamouz, V., & Muthanna, T. M. (2019). Hydrological modelling of green and grey roofs in cold climate with the SWMM model. *Journal of Environmental Management*, 249, 109350. <https://doi.org/10.1016/j.jenvman.2019.109350>
4. Johannessen, B. G., Hamouz, V., Gragne, A. S., & Muthanna, T. M. (2019). The transferability of SWMM model parameters between green roofs with similar build-up. *Journal of Hydrology*, 569, 816-828. <https://doi.org/10.1016/j.jhydrol.2019.01.004>
5. Hamouz, V., Møller-Pedersen P., & Muthanna, T. M., Modelling runoff reduction through implementation of green and grey roofs in urban catchments using PCSWMM. (In review: *Urban Water Journal*)

Secondary papers

1. Hamouz, V., & Muthanna, T. M. (2017). Hydrological performance of a blue-grey roof in a cold climate. I: Proceedings of the 14th IWA/IAHR International Conference on Urban Drainage. 10-15 September 2017, Prague, Czech Republic.

2. Hamouz, V., & Muthanna, T. M. (2018). Modelling of Green and Grey Roofs in Cold Climates Using EPA's Storm Water Management Model. In International Conference on Urban Drainage Modelling (pp. 385-391). Springer, Cham.

Chapter 1 Introduction

This chapter presents the background, including the problem statement, aims, and scope of the doctoral thesis. The research questions, which have been formulated to accomplish the thesis' goal, are introduced, and the thesis' structure is presented.

According to the United Nations (UN, 2019), in 2018, 55% of the world's population was living in urban areas, whereas in Norway, an entire 82 % of the country's population lives in urban environments. Projections for 2050 show that there is an increasing shift in the human population from rural to urban areas as well as an overall growth in the world's population; these percentages are expected to rise to 68 % for the world and 90 % for Norway. Traditional urbanization leads to increased catchment imperviousness due to replacing natural areas with roads, parking lots, paved sidewalks and rooftops. All of these changes alter the hydrological cycle in urban areas; consequently, only a small amount of rainfall generates runoff that is rapidly transported to underground conduits and open channels, causing reduced evapotranspiration, infiltration, storage and groundwater recharge, etc. (Beven, 2011; Dunne and Black, 1970; Gill et al., 2007; Leopold, 1968; Semadeni-Davies et al., 2008). This results in an increased number of runoff events and higher volume in the runoff itself, which is transported through the drainage system. This in turn reduces catchments' concentration time, causing local peak runoffs following high-intensity rainfalls. In addition, urban drainage systems, which are already stressed by being connected to newly built impervious surfaces, are exposed to even more severe outcomes of climate change due to anticipated greater rainfall amounts and higher rainfall intensities (Dyrrdal and Førland, 2019; Hanssen-Bauer et al., 2017; Hoegh-Guldberg et al., 2018; Ipcc, 2014; 2018; Mailhot and Duchesne, 2009; Stocker, 2014;

Willems et al., 2012). The existing infrastructure is typically not suitable for handling the combined effect of ever-increasing urbanization and climate change (Mentens et al., 2006). Moreover, during dry periods, impervious surfaces accumulate pollutants that are washed off during the first flush of rainfall events (Borris et al., 2014; Deletic, 1998; Kim et al., 2006). Consequently, vulnerable places in urban catchments are exposed to floods, and overloaded drainage systems discharge contaminated stormwater using sewer overflow structures (a phenomenon called combined sewer overflows - CSO) into receiving bodies of water (Jia et al., 2015).

CSOs are typically caused by rainfall or melted water and initiated by peak runoff; therefore, it is crucial to decrease stormwater entering the drainage network as much as possible – or at least detain stormwater at the location where it falls (Semadeni-Davies et al., 2008). Outfitting new constructions and retrofitting existing buildings with sustainable urban drainage systems (SUDS) are thus key to creating successful and sustainable urban redevelopment, and they should be applied as efficient measures to counteract imperviousness in urban environments (Fletcher et al., 2015; Mentens et al., 2006; Torgersen et al., 2014; VanWoert et al., 2005). As an example of flood or CSO prevention, underground detention tanks were a typical solution in the late 20th century (Burkhard et al., 2000; Duan et al., 2016; O'Loughlin et al., 1995). Currently, there has been a shift towards blue-green infrastructure, e.g. reopening streams and using bioretention cells (LeFevre et al., 2015; Trowsdale and Simcock, 2011). These solutions certainly provide a desirable level of stormwater management. While bioretention cells provide improvement to both water quality and the evapotranspiration process (Davis et al., 2009), underground tanks disable the evapotranspiration process. However, densely urbanized areas have in most cases limited space for retrofitting either on the surface or below it (Barbosa et al., 2012; Lamond et al., 2015). This encourages municipalities and urban planners to rethink stormwater management by placing a new focus on building rooftops. Rooftops in developed cities cover almost half of the impervious surfaces (Lamond et al., 2015; Stovin et al., 2012). Even though rooftop retrofitting might have certain disadvantages in terms of placing additional weight loads on buildings or being difficult to apply to private properties, it has multiple benefits in terms of hydrology, building physics, investment, biodiversity, air pollutant removal and usage as recreational areas (Ahiablame and Shakya, 2016; Berndtsson, 2010; Besir and Cuce, 2018; Bianchini and Hewage, 2012; Castleton et al., 2010; Oberndorfer et al., 2007; Saadatian et al., 2013; Vijayaraghavan, 2016; Yang et al., 2008).

In 2008 the Norwegian Water Association adopted national guidelines for surface stormwater management that apply a three-step approach (Lindholm et al., 2008): Step 1 aims to infiltrate all minor events onsite, Step 2 aims to detain all medium events, while Step 3 ensures safe floodways for all extreme events (according to the authors, rainfall intensity classification is location-specific). Rooftop solutions such as vegetated green (Berndtsson, 2010; Carter and Jackson, 2007; Stovin et al., 2012) or non-vegetated roofs (Berghage et al., 2009; Hamouz et al., 2018) belong to the first and second of the so-called “three-step stormwater treatment train” as forms of source control (Fletcher et al., 2015; Woods-Ballard et al., 2007). The main drivers behind using retrofitted rooftops as source control are runoff detention and retention (Cipolla et al., 2016; DeNardo et al., 2003; Johannessen et al., 2018). Retention may be considered as long-term or short-term (event-based) performance and occurs through the combined process of evaporation for non-vegetated and evapotranspiration for vegetated solutions. Detention examines the event-based impact of the retrofitted roof on runoff with respect to temporal delays or percental attenuation, and stormwater designers have increasingly called for detention when planning new projects (Stovin et al., 2017; Villarreal, 2007).

Regardless of the above factors, a retrofitted rooftop’s overall performance largely depends on the local climate. For instance, performance in cold and wet climates is limited due to these climates’ higher levels of initial moisture, freezing and thawing cycle, snow cover, varying temperatures and precipitation (Bengtsson et al., 2005; Johannessen et al., 2018; Johannessen et al., 2017; Locatelli et al., 2014; Stovin et al., 2013; Stovin et al., 2017; Vanuytrecht et al., 2014; Villarreal, 2007). One of the measures taken to avoid surface ponding in the wet seasons and standing water freezing in the cold seasons is to increase the infiltration capacity of SUDS, including rooftops (Paus, 2016). This means that in order to achieve the desired detention effect in highly permeable systems, it is crucial to consider a total transport time through the system.

As rooftop retrofitting becomes an increasingly more popular solution for handling stormwater, the knowledge of the different solutions’ hydrological performance in variable climates and geographical locations must be developed further, especially on a larger (catchment) scale rather than a small pilot test (or building) scale. However, it may be challenging to apply observations from the field directly for design purposes, as there is a large variation in reported performances due to climatic conditions or material properties (Alfredo et al., 2009; Carson et al., 2013; Hakimdavar et al., 2014; Voyde et al., 2010). Applying modelling software in combination with observed data provides a tool for utilizing observed data in combination with simulations under variable climatic conditions in order to increase the depth of knowledge

about these roofs' performance (Devia et al., 2015; Li and Babcock, 2014; Niazi et al., 2017; Palla and Gnecco, 2015; Peng and Stovin, 2017). Moreover, only a few studies have investigated the use of retrofitted rooftops under conditions of extreme precipitation because capturing extreme rainfall is difficult due to its infrequent and random occurrences (Bengtsson, 2005; Villarreal and Bengtsson, 2005).

1.1 Background

Urban drainage systems

Flooding events in urban areas resulting from extreme precipitation have been increasingly reported (Changnon and Demissie, 1996; Copenhagen, 2012; Madsen et al., 2014; Nie et al., 2009; Teegavarapu, 2012; Zhou, 2014). This situation has resulted in urban drainage systems undergoing changes, moving from closed pipe systems to sustainable stormwater solutions over the past several decades (Chocat et al., 2007; Delleur, 2003; Fletcher et al., 2015). Indeed, urban drainage has become a complex system that involves diverse approaches where both the design and decision-making process are driven by multiple objectives (Barbosa et al., 2012; Marsalek and Chocat, 2002; Zhou, 2014). A number of principles and practices have been employed which use different terminology based on the location in which they are utilized or scope they cover. These include: Low Impact Development (LID), Best Management Practice (BMP), Sustainable Urban Drainage System (SUDS), Green Infrastructure (GI), Water Sensitive Urban Drainage (WSUD), or Nature-Based Solution (NBS). Fletcher et al. (2015) found significant overlap between various terms in urban drainage terminology, which is defined as: “(i) mitigation of changes to hydrology and evolution towards a flow regime as much as feasible towards natural levels for local environmental objectives and (ii) improvement of water quality and reduction of pollutants.”

Hydrological performance of retention and detention-based roofs

Retention occurs during dry periods when stormwater is evaporated from the surface and transpired by plants into the atmosphere. Retention may be studied as a long-term or short-term (event-based) performance of the tested configuration. Green roofs are the most commonly studied objects; consequently, their annual runoff reduction has been extensively investigated (Berndtsson, 2010; Berretta et al., 2014; Carson et al., 2013; Garofalo et al., 2016; Gregoire and Clausen, 2011; Stovin et al., 2015). The results from previous studies show a large variation in performance due to factors related to precipitation volume, precipitation dynamics (precipitation patterns), antecedent conditions, growth medium, plant species, roof

slope, location and temperature or daylight variations throughout the year (Berndtsson, 2010; Li and Babcock, 2014). However, while increasing media depth has been reported to increase retention through larger storage capacity (Alfredo et al., 2009; Soulis et al., 2017; VanWoert et al., 2005), full-scale roofs have provided increased detention through prolonged horizontal runoff (Carson et al., 2013; Fassman-Beck et al., 2013).

In terms of retention performance, VanWoert et al. (2005) has studied the total rainfall retention for different media. The retention ranged from 27.2% for gravel ballast to 50.4% for a bare growing media, and 60.6% for a green treatment. Similarly, Mentens et al. (2006) have compared the annual runoffs from green and gravel-covered roofs. They presented a 25% reduction for the gravel roof and a 50% reduction for the green roof. Berghage et al. (2009) have reported the annual rainfall retention from three different setups. The retention ranged from 14.1% for an asphalt roof to 29.7% for a media roof, and 52.6% for a vegetated roof. When comparing expanded clay-based (non-vegetated) and vegetated setups, higher levels of retention were observed using vegetated beds (Stovin et al., 2015), with an annual volumetric retention of 54.5% for an expanded clay-based setup and 75.1% for a green roof. Johannessen and Muthanna (2016) have presented an annual runoff reduction of 17–30% for three coastal cities in Norway. In a study focused on a long dry period, major differences were found in retention through evapotranspiration by vegetated and non-vegetated configurations (Poë et al., 2015). Berretta et al. (2014) have studied moisture loss from a growing medium during a dry period in both cold and warm months. They presented a mean moisture loss ranging from 0.34 mm/day to 1.65 mm/day from March to July. Particular attention should be given to the regeneration of roof storage capacity, which depends on physical configuration, precipitation patterns, and evaporation during dry periods (Stovin et al., 2013). Johannessen et al. (2017) have investigated potential evapotranspiration in cold and wet regions across 14 locations in northern Europe and concluded that retention on green roofs varied between 0% and 1% for Nordic countries during the winter period. Overall, the average retention performance is useful in a context where stormwater discharge to the sewer system is chargeable.

The detention effect occurs when temporarily detained stormwater is subsequently released after rainfall (Locatelli et al., 2014; Stovin et al., 2017; Villarreal, 2007). Even though the evapotranspiration effect, which restores storage capacity during dry periods, may be negligible during a rainfall event (especially when extreme rainfall occurs), it may affect runoff characteristics through initial water content and thus impact detention performance. The main point of interest is the way in which the intense flow is transformed into a natural flat flow.

Comparing detention performance, Liu and Minor (2005) and Villarreal (2007) have presented an intensive green roof's peak flow reductions and peak delays on an event basis. The peak reductions varied between 25% and 65%, and the peak delays varied between 20 min and 40 min. Stovin et al. (2015) have concluded that peak reduction for rainfall greater than 10 mm varied from 29% for an expanded clay-based bed to 68% for a sedum roof. They also noted that vegetated beds comprised of brick-based substrates consistently offer a higher level of attenuation compared with the expanded clay-based substrate. Stovin et al. (2012) have investigated the performance of an extensive green roof subjected to events and having a return period of over one year. They presented a per-event peak reduction of 59% (for both mean and median), and a per-event peak-to-peak delay of 54.16 min (mean) and 18 min (median). Li and Babcock (2014) have reviewed the typical hydrological performance of green roofs. It was shown that these roofs attenuate a peak flow of 22% to 93%, and delay a peak flow of 0 to 30 min. A considerable amount of research has been published about green roofs in terms of their long-term performance (retention) (Berndtsson, 2010; Carter and Rasmussen, 2006; Li and Babcock, 2014; Poë et al., 2015). However, only a few researchers have strictly focused on detention performance or developing solutions that ensure a combined version of retention and detention performance. At the same time, a rooftop solution, which focuses only on detention capability in climates where retention is somewhat limited, has not yet been established and studied. Moreover, a large amount of research has been focused on the hydrological performance of small-scale roofs, whereas evidence of full-scale roofs is limited (Johannessen et al., 2018; Nawaz et al., 2015; Stovin et al., 2012).

Green roof modelling

A large part of the research has been conducted in the form of monitoring studies in order to understand the hydrological performance of green roofs. However, it remains challenging to predict these roof's general hydrological performance, as each performance reflects a specific type of green roof and its location. There have been several attempts to simulate green roof runoffs on an individual roof scale (Carson et al., 2013; Hilten et al., 2008; Johannessen et al., 2019; Kasmin et al., 2010; Krebs et al., 2016; Locatelli et al., 2014; Metselaar, 2012; Stovin et al., 2012; Villarreal, 2007) or a catchment scale (Ashbolt et al., 2013; Carter and Jackson, 2007; Krebs et al., 2013, 2014; Palla and Gnecco, 2015; Rosa et al., 2015; Warsta et al., 2017). These models may either be categorized as data-based methods, where runoff is calculated as an empirical function of rainfall, or process-based methods, where the runoff is calculated from the green roof water balance (Carson et al., 2017; Li and Babcock, 2014; Stovin et al., 2013).

Urban hydrology is a complex system in which a model must account for an array of possible physical processes: surface runoff, infiltration, groundwater, snowmelt, flow routing, surface ponding, and water quality routing. Green roof systems, which calculate the runoff by solving a water balance equation, account for precipitation, irrigation, storage, and evapotranspiration processes (Rossman, 2015). So even though green roofs might operate on a simple system consisting of several layers, all the processes within each layer must be controlled dynamically. Based on these considerations, the physically-based SWMM model has been considered the best choice to use for further work, as it includes all previously mentioned processes as well as snowmelt simulation (Elliott and Trowsdale, 2007; Moghadas et al., 2016).

1.2 Research questions

The overall main objective has been to study and quantify the role of vegetated (green) and non-vegetated (grey) roofs play as part of stormwater management in cold climates using full-scale pilots. This is done through evaluating different roof configurations, the implications of hydrometeorological patterns, and further, investigating catchment scale tools for performance estimates and design.

In order to address the main objective, the following four specific objectives were formulated:

1. Investigate the retention and detention performance for different configurations of green and grey roofs for stormwater management. Which configuration provides the best retention and detention performances in a cold climate?
2. What is the influence of rainfall intensity and pattern, including extreme events, on the performance of the detention-based green roofs?
3. Investigate the use of catchment scale modelling tools for design and performance estimates with respect to vegetated and non-vegetated roofs.
4. To what extent does retention and detention-based roof implementation contribute to runoff reduction on a catchment level in urban areas?

Chapter 2 Materials and Methods

Two field sites, the Høvringen field site and Risvollan Urban Hydrological Station (RUHS), served as data sources for the research (Figure 1). The Høvringen field site provided input data for Papers 1, 2, 3 and 4, and Risvollan Urban Hydrological Station provided input data for Paper 5.

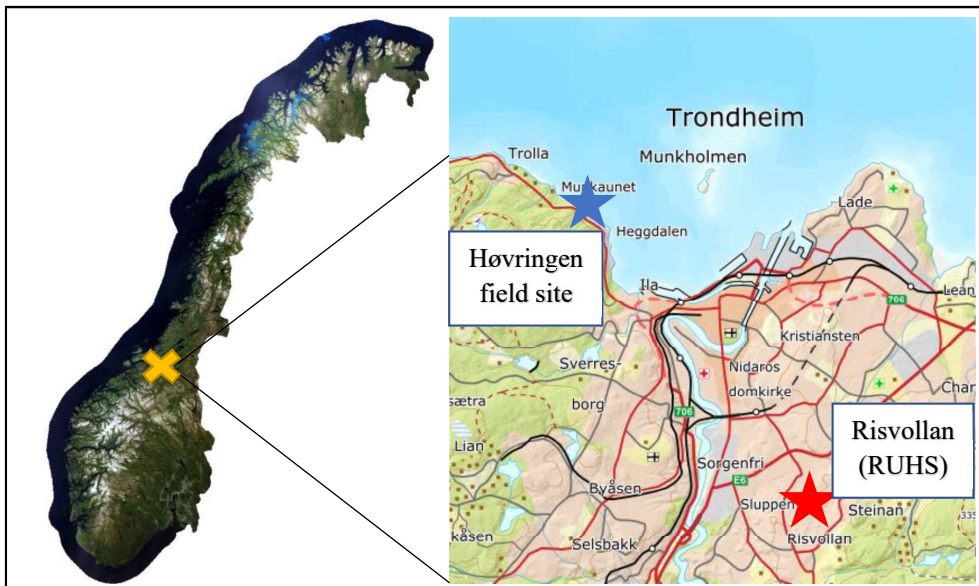


Figure 1 Location map of the city of Trondheim (yellow cross), the Høvringen field site (blue star), and Risvollan catchment (red star).

2.1 Roof configuration

Between 2017 and 2019 the Høvringen field site was used for monitoring hydrometeorological data while testing different full-scale rooftop solutions for stormwater management (Figure 2, Figure 3). This consisted of three configurations (reference black, vegetated, and non-vegetated roof) at a given time for comparing their hydrological performance; a total of two complete

solutions were constructed during this period. Each of the rooftops with size 8×11 meters receives additional stormwater from surrounding separation walls and parapets with an area of 12m² (roof disposition can be seen in Figure 3). Runoff is measured using a weight-based system with two tanks located downstream of the drainage outlet (a 110 mm pipe) (additional description can be found in each paper).

In April 2017, the first complete solution (*Solution 1*) was finished, providing hydrometeorological data for Papers 1, 3, 4, and (partially) 5. It involved a black roof, an extensive green roof (vegetated configuration), and a grey roof (a non-vegetated configuration, and in Paper 1 called a LECA-based roof). At the end of June and beginning of July 2018, the rooftops were changed to a second solution (*Solution 2*), which consisted of a black roof, a detention-based green roof and a different type of grey roof (material characteristics are shown in *Appendix A: Supplementary materials*, Table 15). Based on the second solution, the detention-based green and black roof were used for Paper 2. Additionally, the monitored data from all the roof types and solutions were used to compare individual roof performance in terms of retention and detention (unpublished extension of Paper 1).

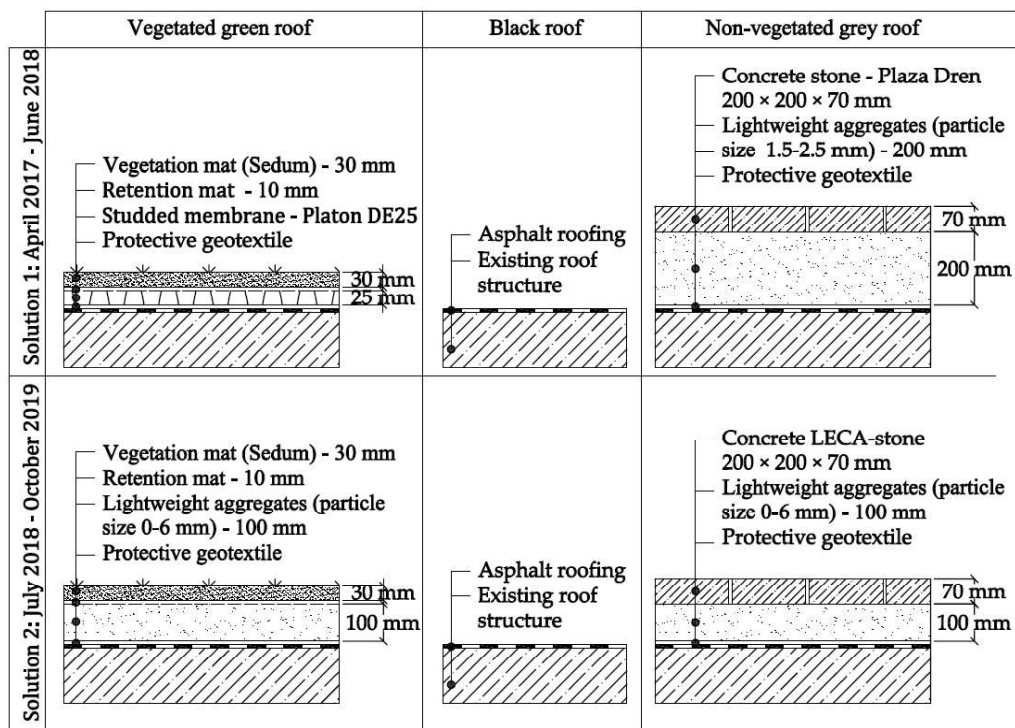


Figure 2 Two sets of rooftop solutions (marked as *Solution 1* and *Solution 2*) monitored between 2017 and 2019.



Figure 3 Three different rooftops at Høvringen on 11.6.2019. NB.: each of the rooftops with size 8×11 meters receives additional stormwater from surrounding separation walls and parapets with an area of 12m^2 .

2.2 Hydrometeorological data - Høvringen

Precipitation was measured by a heated tipping bucket rain gauge Lambrecht meteo GmbH 1518 H3 with a resolution of 0.1 mm at 1-min intervals and with uncertainty $\pm 2\%$. Runoff was measured using a weight-based system (uncertainty class C3 according to OIML R60) with two tanks downstream of the drainage outlets. These collection tanks were automatically emptied either every 30 min or whenever the collected water reached tank capacity. All the data were recorded at 1-min intervals using a data logger CR 1000 Campbell Scientific, Inc. The air temperature and relative humidity were registered using a temperature and humidity sensor Vaisala HMP155A with uncertainty $\pm 0.03\text{ }^\circ\text{C}$ for temperature and $\pm 0.6\%$ for relative humidity in a range between 0-40 % and $\pm 1\%$ for relative humidity in a range between 40-97 %. The soil temperature was registered using a temperature sensor Campbell Scientific 109 with uncertainty $\pm 0.03\text{ }^\circ\text{C}$. Finally, the wind speed was measured using an ultrasonic anemometer Lufft VENTUS 240W with an uncertainty $\pm 2\%$.

Precipitation measurement

A heated tipping bucket rain gauge was used to collect and register the amount of precipitation in either a liquid or solid form. It is a widely used, low-maintenance, reliable instrument that

ensures year-round measurements, especially in snowy regions, due to having two separate controlled heating circuits. These circuits maintain an optimal temperature, which prevents the sensor becoming frozen with snow. They also ensure that evaporation from the heated surface is minimized. Precipitation is captured by collecting a surface of 200 cm². It is then transferred through a funnel to the tipping bucket, which can hold 2 cm³ (2g equivalent to a precipitation rate of 0.1 mm per square meter) of water. Since this bucket has been installed unprotected from the wind, some under catches may be experienced, especially when precipitation falls in a solid or mixed form. The raw precipitation data were corrected for aerodynamic effects using a dynamic correction model in accordance with a manual detailing the operational correction of Nordic precipitation data (Førland et al., 1996). However, the adjusted precipitation was lower during certain periods than the measurement taken from the black roof. It was for this reason that the black reference roof was used, as it provided a simple correction coefficient based on registered flow. In addition, the precipitation gauge was cleaned and calibrated on an annual basis.

During 2016 – before the green and grey roofs were installed – rainfall measurements were performed over a period of four months using manual rain gauges (simple plastic non-digital cones which must be handled manually and require eight gauges per roof) in order to record the rainfall distribution over the roofs and see if the roofs were receiving equal amounts of precipitation during non-snowy periods. No significant difference was found between the individual plots' registered volumes.

Flow measurement

The runoff collection from each of the roofs was measured using a weight-based system with two tanks downstream of the drainage outlets. The collection tanks had two conditions for emptying: they were automatically emptied every 30 min and when the weight of the water approached the tank's capacity (30 kg).

In addition, the weight-based tanks were cleaned and calibrated annually by the provider (VisionTech AS). The weight-based system allowed measuring flows ranging from very low to very high values; therefore, this system is suitable for measuring flow generated from natural precipitation. However, during the data collection period for Paper 2, it was noticed that the tanks had a limited maximum capacity. In the case of the black roof, the collection tanks overflowed while the highest level of inflow intensity was being run.

Moisture measurement

The soil moisture (water content) was measured using a 5TM soil moisture and temperature sensor. This sensor determines volumetric water content (VWC) by measuring the dielectric constant of the soil (or other media) using capacitance/frequency domain technology. The sensor uses a 70 MHz frequency, which minimizes salinity and textural effects, thereby ensuring its measurement uncertainty in most soils and soil-free media. The sensors were tested under laboratory conditions, and calibration equations were provided. Due to a larger measured span in the field measurement than in the laboratory, the soil moisture was expressed by its degree of saturation. Additional laboratory experiments for estimating maximum water holding capacity (MWHC) were conducted according to the procedure provided in the German Green Roofing Guideline, published by the Landscape Development and Landscaping Research Society (FLL, 2008).

2.3 Hydrometeorological data - Risvollan Urban Hydrological Station (RUHS)

Hydrometeorological data from RUHS from the years 2017 and 2018 were only used in Paper 5 (additional information can be found in section 2.8 Methods in Paper 5). The reason for using data gathered during this particular year was that the calibration and validation data for Papers 3 and 4 were gathered during this same year. The Norwegian University of Science and Technology (NTNU), in collaboration with the city of Trondheim and the Norwegian Water Resources and Energy Directorate (NVE), controls a gauging station located at the catchment outlet. The station is equipped with a data logger CR 1000 Campbell Scientific, Inc. which registers e.g. precipitation, air temperature, wind speed and stormwater flow. During 2017 alone, 1,146 mm of precipitation was registered by a heated tipping bucket rain gauge Lambrecht meteo GmbH having a resolution of 0.1 mm at 1-min intervals and with uncertainty $\pm 2\%$ and 502 mm of runoff using a V-notch weir equipped by a pressure sensor IMCTL Submersible level & temperature transmitter at 1-min intervals with uncertainty $\pm 0.1\%$. The air temperature was measured using a temperature probe Vaisala HMP45 ranging from $-15.8\text{ }^{\circ}\text{C}$ to $28.5\text{ }^{\circ}\text{C}$ with an average value of $5.9\text{ }^{\circ}\text{C}$ and uncertainty $\pm 0.2\text{ }^{\circ}\text{C}$ at $20\text{ }^{\circ}\text{C}$. The wind speed was measured using an ultrasonic anemometer Young 85004 ranging from 0.56 km/h to 8.51 km/h with an average value of 2.59 km/h and uncertainty $\pm 2\%$ for wind speed within 0 to 108 km/h. According to the local climate, the year was divided into a cold period from October to April and a warm period from May to September. This was based on the fact that negative

temperatures, snowfall, and snowmelt considerably impact runoff characteristics, whereas, during the warm period, the rainfall is directly transferred to the runoff.

The municipality of Trondheim provided data, as it has a drainage stormwater network that contains 222 manholes and 222 stormwater conduits with a total length of 4,633 m and a diameter ranging from 110 mm to 800 mm that conveys the runoff to the catchment outlet. It should be noted that most of the information linked to the pipe depth or inverted elevation was missing.

2.4 *Methods in Paper 1*

The monitored data from the field station were analysed for long-term continuous periods and individual precipitation events within *Solution 1* and *Solution 2*. Single precipitation events were defined according to a minimum period of 6 h of antecedent dry weather period (ADWP), as commonly used by several previous studies (Stovin et al., 2012; VanWoert et al., 2005). A threshold precipitation depth of 0.5 mm was used to exclude insignificant precipitation events. Similarly, a threshold discharge of 0.1 L/min was set to specify the start and end of runoff events. The moisture content in expanded clay was recorded using Decagon 5TM soil moisture and temperature sensors (delivered at the end of June). The moisture sensors were pre-calibrated in the laboratory for minimum and maximum degrees of saturation (0% and 100% saturation). Events were identified and sorted into five groups based on the type of precipitation: *rain*, *rain on snow*, *snow*, *snowmelt*, and *mixed*. The events which were designated as “mixed” typically had a long duration (several days) and experienced several changes in precipitation type during this period.

Retention performance

Retention was considered to be long-term permanent water removal for the lifetime of individual solutions. Retention capacity was determined to be percentual runoff reduction, retained volume or normalized daily retention for total periods as well as partial (cold¹ and warm²) periods:

$$Ret = P - R, \quad (1)$$

where P is precipitation, R is runoff and Ret is retention.

¹ Period with snow and temperatures that can influence runoff (≤ 0 °C).

² Period without snow and negative temperatures.

The retention at any given time was the sum of the evaporation (evapotranspiration) and the water currently stored in the green or grey roof medium.

Detention performance

The detention capacity of the green and grey roofs was assessed as the ability to attenuate and delay peak flows as well as reduce the total volume in comparison with to the response of the black roof for the ten largest events within each configuration and test period. This analysis was carried out on an event basis. In some cases, several peaks were observed in a single event due to its lengthy duration (several days). The individual approach was applied to these cases. The peak flow reduction was determined as follows:

$$\text{Peak Reduction} = 1 - \frac{Q_{GR,max}}{Q_{BR,max}} \quad (2)$$

where $Q_{GR,max}$ is the maximum flow recorded per event from the green/grey roof, and $Q_{BR,max}$ is the maximum flow recorded per event from the black roof. The peak delay was determined as follows:

$$\text{Peak Delay} = T_{GR,max} - T_{BR,max} \quad (3)$$

where $T_{GR,max}$ is the time of maximum flow recorded per event from the green/grey roof and $T_{BR,max}$ is the time of maximum flow recorded per event from the black roof. Additionally, any delays were analysed as delays of individual events' centroid. Volume reduction was determined as follows:

$$\text{Volume Reduction} = 1 - \frac{V_{GR,tot}}{V_{BR,tot}} \quad (4)$$

where $V_{GR,tot}$ is the total volume recorded per event from the green/grey roof, and $V_{BR,tot}$ is the total volume recorded per event from the black roof.

2.5 Methods in Paper 2

The vegetated roof configuration (in Paper 2 called the detention-based green roof) and the abovementioned black roof from Solution 2 were used for running extreme precipitation (Figure 2). The field site at Høvringen was equipped with a setup using a grid of non-regulated nozzles (4 nozzles in 4 lines) connected to the water supply, which was used to generate the precipitation (Figure 4). The nozzles were placed 1.5 m above the roof structure to ensure the water's maximal spreading effect. A simple method to measure flow rates from each nozzle and assess water distribution over the roof with respect to different inflows was performed by volume measurement over time. The water distribution error was recorded line by line, and the

enlarged uncertainty (BIPM et al., 2009) with respect to the water spatial distribution was $\pm 3\%$. Additionally, eight plexiglass tubes were buried vertically along the longitudinal edge of the roof for visual observation and estimation of spatial water distribution within the roof at the beginning and the end of each individual event during the tests. The inflow rates were measured by an electromagnetic flowmeter Siemens Sitrans FM MAG 5000 with uncertainty $\pm 0.4\%$ of the flow rate and regulated using two valves, which allowed for changes in inflow duration and intensity. A gate valve was used to fine-tune the flow, and a ball valve was used to open or close the system. The decision was made to run rainfalls with different durations, intensities, and inter-event periods (ranging from 5 minutes to more than 74 minutes) to enable different initial water contents in the roof and differently shaped hyetographs. The range of intensities (from 0.8 to 2.5 mm/min) was limited by the minimal flow due to nozzle spread and maximum flow by the capacity of the flow measuring tanks.



Figure 4 Rainfall simulator over the detention-based green roof on 11.6.2019.

Precipitation was the only aspect of climate change considered in this study. Firstly, the concentration time of the detention-based green roof was tested for different inflow intensities (0.8, 1.0, 1.2, 1.4, 1.7, 2.0, and 2.5 mm/min) and compared to the concentration time of the black roof (this can be seen in Paper 2). The duration of each event was to ensure that inflow and outflow intensities were equal or within the measurement uncertainty for inflow (2 %) and outflow (2 %). Moreover, precipitation depths for the 20-year return period (RP) from Depth-Duration-Frequency (DDF) curves for three different cities (Bergen (BER), Oslo (OSL), and Trondheim (TRO)) were extracted (Table 1). It should be kept in mind that the designations Bergen (BER), Oslo (OSL), and Trondheim (TRO) in Paper 2 were related to events differentiation and were thus different from those used in Paper 4, where they represented rooftop configurations. These precipitation depths were multiplied by a climate factor of 1.4 to

estimate expected rainfall in the period between 2071-2100, including a worst-case scenario with Representative Concentration Pathway (RCP) 8.5 for short-term events (<https://www.klimaservicesenter.no/>).

Secondly, different hyetographs (TRO 2, 2a, 2b, 2c, and 2d), keeping the same rainfall depth (16 mm) and duration (16 minutes) were tested in order to identify the rainfall pattern to which the roof runoff is most sensitive (Table 1 and Figure 6):

- I) mean intensity of 1.0 mm/min over 16 minutes (TRO 2),
- II) 2-minute peak of 2.6 mm/min in the beginning and 14-minute intensity of 0.8 mm/min (TRO 2a),
- III) 7-minute intensity of 0.8 mm/min, 2-minute peak of 2.6 mm/min in the middle and 7-minute intensity of 0.8 mm/min (TRO 2b),
- IV) 14-minute intensity of 0.8 mm/min and 2-minute peak of 2.6 mm/min in the end (TRO 2c),
- V) three 2-minute peaks of 2.6 mm/min (TRO 2d).

Thirdly, the list of events was expanded for two other cities, Bergen and Oslo (as mentioned before), with precipitation depths for the 20-year RP multiplied by the climate factor of 1.4. According to 20-year RP from DDF curves, four rainfall depths were selected for Trondheim (TRO 1, TRO 2, TRO 3, and TRO 4), two events for Bergen (BER 1, and BER 2) and two events for Oslo (OSL 1 and OSL 2), as shown in Table 1 and Figure 7.

Table 1 Summary of the tested rainfall events extracted from DDF curves for the three locations of Trondheim, Oslo, and Bergen with and without climate factor. The green column shows the events with a primary focus of 20 RP; the rest was transposed to other locations. (Paper 2 - Hamouz et al. - Accepted for publication)

ID	Intensity	Depth	Duration	Number of hyetographs	Return Period			Return period CF=1.4		
					TRO	OSL	BER	TRO	OSL	BER
-	[mm/min]	[mm]	[mm:ss]	[Nr. per day]	[YYYY]	[YYYY]	[YYYY]	[YYYY]	[YYYY]	[YYYY]
TRO 1	1.7	12	07:00	9	200	20 - 25	100	20	5	5 - 10
TRO 2	1.0	16	16:00	8	200	5 - 10	100	20	2	5
TRO 2a	1.0	16	16:00	7	200	5 - 10	100	20	2	5
TRO 2b	1.0	16	16:00	8	200	5 - 10	100	20	2	5
TRO 2c	1.0	16	16:00	6	200	5 - 10	100	20	2	5
TRO 2d	1.0	16	16:00	6	200	5 - 10	100	20	2	5
TRO 3	2.6	9	03:30	9	200	100 - 200	100	20	10	5 - 10
TRO 4	0.8	20	26:00	6	200	5 - 10	100	20	2	5
OSL 1	1.7	23	16:00	5	>>200	200 - >200	>>200	>200	20	200 - >200
OSL 2	1.0	45	44:00	3	>>200	200 - >200	>>200	>200	20	200
BER 1	1.7	16	09:00	6	>200	50 - 100	>200	50	5 - 10	20
BER 2	1.0	28	23:00	5	>200	20	>200	50	5	20

For all simulated rainfall events, a set of condition indicators:

- *Initial Relative Water Content [mm]* – initial water content based on water balance;
- *Peak Relative Water Content [mm]* – the highest value of water content observed before peak runoff;
- *Peak Rainfall [mm/min]* - maximum rainfall at 1 min time intervals;

and performance indicators was estimated:

- *Peak Runoff [mm/min]* - maximum runoff at 1 min time intervals;
- *Peak Attenuation [-]* = $\frac{\text{Peak Rainfall} - \text{Peak Runoff}}{\text{Peak Rainfall}}$ - percentual runoff reduction;
- *Peak Delay [min]* - the time between the peak rainfall (the maximum and the last peak when observing multiple peaks) and peak runoff;
- *Centroid Delay [min]* – a delay between the mass centre of the rainfall and mass centre of the associated runoff;
- *T50 [min]* - a delay between 50 % of the volume of the rain supplied on the roof and 50 % of the volume released out of the roof.

2.6 Methods in Paper 3

The Storm Water Management Model (SWMM) 5.1.012, including the Low Impact Development (LID) Controls module specifically designed for modelling SUDS (Sustainable Urban Drainage Systems), was used for the long-term and short-term simulations of runoff quantity using the rainfall/runoff process with 1-minute time increase. The LID module consists of three layers (surface, soil and drainage mat); however, only parameters included in the soil and drainage layers were selected for calibration (Table 2). There were four parameters in the soil layer (the porosity, field capacity, conductivity and conductivity slope) and two parameters in the drainage mat (void fraction and roughness) that were calibrated. The initial green and grey roof parameters, as well as the lower and upper boundaries used during the calibration, were estimated from field measurements and the literature (Carson et al., 2017; Krebs et al., 2016; Peng and Stovin, 2017; Rosa et al., 2015), or defaults (Rossman and Huber, 2016a; Rossman and Huber, 2016b).

Table 2 LID Green roof control editor and its parameters with initial values and lower and upper bounds. (Hamouz and Muthanna, 2019)

Control name	Green roof		Grey roof		Data source
Parameter	Initial value	Range	Initial value	Range	
SURFACE					
Berm Height (mm)	500	-	500	-	A
Vegetation Volume Fraction	0.1	-	0	-	B
Surface Roughness (Manning's n)	0.05	-	0.015	-	C
Surface Slope (%)	2	-	2	-	A
SOIL					
Thickness (mm)	30	-	200	-	A
Porosity (volume fraction) *	0.5	0.45-0.60	0.6	0.45-0.65	b, c, d, e, f
Field Capacity (volume fraction) *	0.3	0.20-0.45	0.1	0.02-0.2	b, c, d, e, f
Wilting Point (volume fraction)	0.05	-	0.01	-	b, c, d, e, f, g
Conductivity (mm/h) *	25	10-1000	1432	500-3000	b, c, d, e, f
Conductivity Slope *	15	5-60	10	5-60	b, c, d, e, h
Suction Head (mm)	110	-	10	-	b, c, d, g
DRAINAGE MAT					
Thickness (mm)	10	-	10	-	A
Void Fraction*	0.5	0.01-1	0.5	0.01-1	B
Roughness (Manning's n) *	0.1	0.01-0.4	0.1	0.01-0.4	B
* parameters for calibration					
Site specific	a		Laboratory analysis	e	Data source
(Rossman, 2015)	b		(FLL, 2008)	f	
(Rossman and Huber, 2016a)	c		(Rosa et al., 2015)	g	
(Rossman and Huber, 2016b)	d		(Palla and Gnecco, 2015)	h	

A long-term continuous calibration was chosen in order to prevent eventual validation issues while comparing events having different characteristics. Data (for *Solution 1*) gathered between the 11th of May 2017 and 31st of July 2017 served for the model calibration. The calibration period included five larger events, while six events were used for model validation (Table 10). Two objective functions were applied to evaluate the model performance by the Nash-Sutcliffe Model Efficiency (NSME) and volume error (VE) in both the calibration and validation periods using a long-term continuous dataset as well as an event-based dataset. In general, the closer the NSME (eq. 5) is to 1, the more accurately the model can predict the observed performance, while an NSME greater than 0.5 indicates an acceptable model performance (Rosa et al., 2015). Regarding water balance evaluation, the volume error (VE) (eq. 6) was used to calculate discrepancies between observed and simulated runoffs.

$$NSME = 1 - \frac{\sum_1^n (Q_{obs,i} - Q_{sim,i})^2}{\sum_1^n (Q_{obs,i} - \overline{Q_{obs}})^2}, \quad (5)$$

$$VE = \frac{V_{obs} - V_{sim}}{V_{obs}} * 100, \quad (6)$$

where $Q_{obs,i}$ is the observed discharge and $Q_{sim,i}$ is the simulated discharge, $\overline{Q_{obs,i}}$ is the mean of observed discharge, and V_{obs} and V_{sim} are the observed and simulated runoff volumes, respectively. The final parameters were achieved by applying the Shuffled Complex Evolution

(SCE) algorithm (Duan et al., 1992). The SCE method is based on four concepts that aim for achieving efficient global optimization. The calibration process was based on random sampling from a predefined variable range where each parameter had its lower and upper boundaries delineated. The SCE algorithm uses an initial guess to generate a sequence of improving approximate solutions to reach the highest NSME, where the n-th approximation was derived from the previous ones. The termination criteria of the calibration process were based on the principle of convergence (Duan et al., 1992).

2.7 Methods in Paper 4

Similarly, as in Paper 3, the runoff from various rooftop configurations was simulated using SWMM version 5.1.012, including the green roof LID module. The intention in Paper 4 was to discover whether or not the model could provide comparable parameters representing the individual layers within the green roof LID module. Whereas in Paper 3 the number of parameters for calibration was only six, in Paper 4 the number of parameters for calibration was extended to 12. Initial parameter values, as well as lower and upper boundaries for the calibration, were estimated from examining field observations and laboratory experiments from other studies (Cipolla et al., 2016; Krebs et al., 2016; Palla and Gnecco, 2015; Peng and Stovin, 2017; Rosa et al., 2015) or from SWMM manuals (Rossman, 2015; Rossman and Huber, 2016b). Various field sites containing not only extensive green roofs but also black bitumen reference roofs and a non-vegetated media (grey roof) of various scales were modelled. Continuous-time series from the field rooftops and short-term (event-based) data records from the laboratory were used as inputs to the hydrological model. Test plots (8–15m²) as well as full-scale (100m²) field sites were set up in different cities representing Norway's typical coastal climate and various rainfall patterns. These cities were Bergen (BER), Oslo (OSL), Sandnes (SAN) and Trondheim. In Trondheim, data from two different test sites, Risvollan (RIS) and Høvringen, were included (HOV). Moreover, laboratory tests were conducted to supplement field studies. Each monitored roof was identified by its location and a number (e.g. BER1 and BER3). At two sites (OSL1 and HOV2), a black bitumen roof was used as a reference roof, while a grey roof was tested at one site (HOV1). Three groups of extensive green roofs from three different suppliers (A, B and C), which henceforth should be referred to as Type A, Type B and Type C, were tested; more information about the individual types may be found in (Johannessen et al., 2019).

The optimal model parameters were identified through model calibration using the Shuffled Complex Evolution (SCE) algorithm (Duan et al., 1992). The Nash–Sutcliffe Efficiency (NSME) (eq. 5) (Nash and Sutcliffe, 1970) and the volume error (VE) (eq. 6) were used for model evaluation. Parameter spans providing acceptable model performance were defined as the 5–95% percentile of all parameters fulfilling the requirement of $NSME > 0.5$ or $|VE| < 25\%$. A two-step calibration procedure separating the volume calibration (retention performance) from the peak runoff calibration (detention performance) was carried out. Retention-related parameters (soil field capacity, wilting point and soil recovery constant) were calibrated with continuous time-series first and evaluated based on volume errors. These parameters were then kept constant while the remaining detention-related parameters were calibrated on selected events having high-intensity precipitation and evaluated with NSME.

2.8 Methods in Paper 5

The study contains data from two field research stations located in Trondheim, Norway. The first field station is used for testing different rooftop solutions (Figure 1, Figure 2 and Figure 3, [63°26'47.5"N 10°20'11"E](#)) and is equipped with a meteorological station, including a high-resolution precipitation gauge. Data from this field station was used as input to the roof configurations, this data originate from previous published studies (more information may be found in Papers 1 and 3 (Hamouz et al., 2018; Hamouz and Muthanna, 2019)). The second site is a research urban hydrological catchment (Figure 5, catchment outlet [63°23'55.1"N 10°25'22"E](#)) established by the Norwegian University of Science and Technology (NTNU) together the city of Trondheim and Norwegian Water Resources and Energy Directorate (NVE), used for long-term monitoring and data collection of hydraulic and hydrological processes in the urban area (Hailegeorgis and Alfredsen, 2018; Matheussen, 2004).

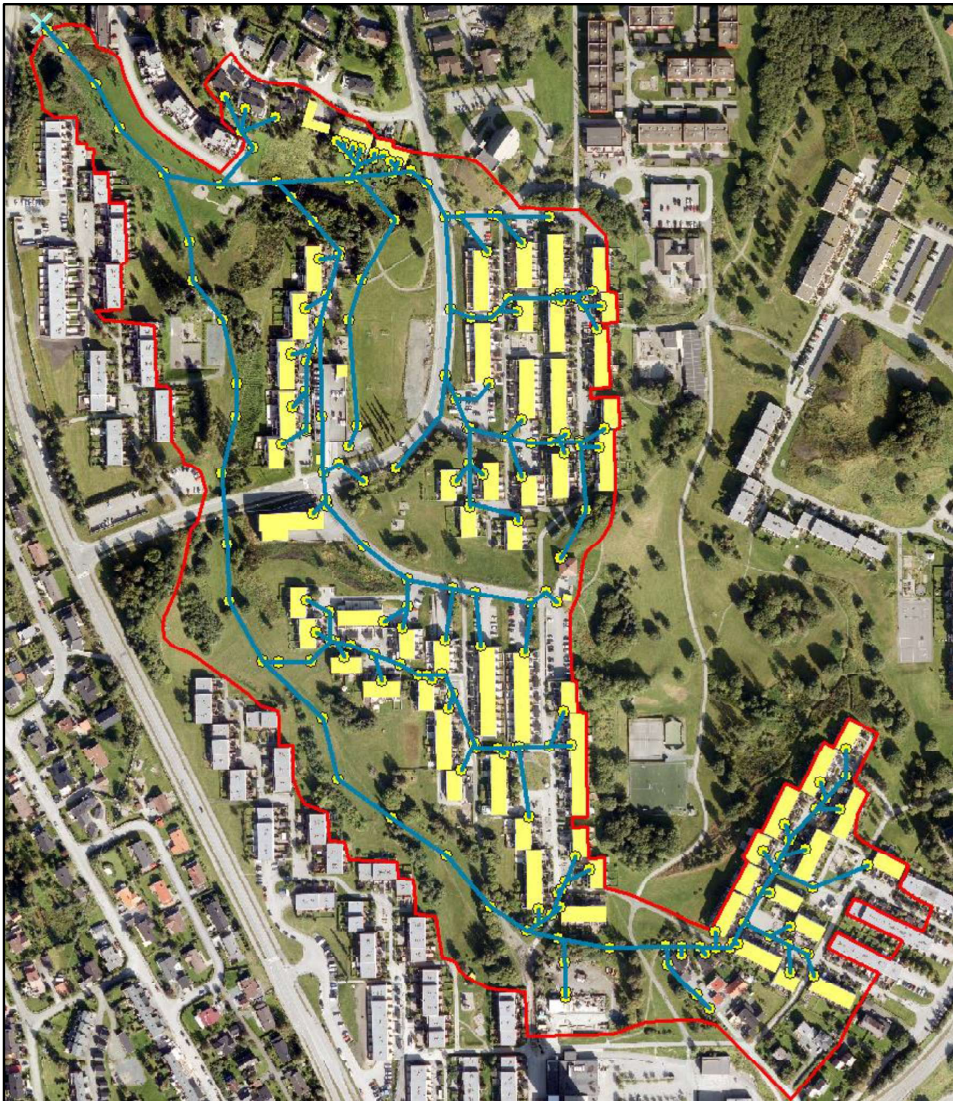


Figure 5 Risvollan catchment with the stormwater drainage network and flat roofs (yellow shaded) chosen for the green and grey roofs' implementation. (Paper 5 - Hamouz et al. – in review)

The Risvollan experimental urban catchment has separate sewers for wastewater and stormwater and is located at a ground elevation ranging from 85 to 134 m above sea level at Risvollan in Trondheim, Norway. It occupies 20.6 ha which is characterized as 57 % pervious and 43 % impervious landuse. The catchment delineation and discretization were carried out in ArcGIS Desktop 10.7 (Environmental Systems Research Institute, California, USA) using high-resolution aerial photographs (<https://kartkatalog.geonorge.no>), and a digital elevation model (DEM) was made out of light detection and ranging (LiDAR) data with a resolution of 25 cm (<https://hoydedata.no/LaserInnsyn/>). All green areas were considered to be pervious,

and thus equal to 57 %, whereas the impervious areas were represented by 8.9 % roads, 6.3 % parking lots, 2.9 % paths, 11.9 % courtyards, 1.2 % playgrounds, 1% pitched rooftops and 10.7 % flat roofs.

This study used the PCSWMM Professional model version 7.2.2785 (64-bit) (Computation Hydraulics International, Ontario, Canada) with the SWMM 5.1.013 hydrology and hydraulics engine, which was primarily developed for modelling of water quantity and quality in urban areas for both short- and long-term simulation runs (James et al., 2010). The PCSWMM model is a modelling software for stormwater, wastewater, watershed, and water distribution systems (<https://www.pcswmm.com/>), including import functions for entity and attribute data from GIS (Geographic Information System) formats as well as coordinate system of the desired location. The PCSWMM model is also the spatial decision support system for stormwater management modelling, which was essential for this study. Sub-catchments in the PCSWMM model are characterized by the area, width (or flow length), slope, impervious cover, depression storage on the pervious and impervious areas, and Manning's roughness for the pervious and impervious areas. The parametrization of the sub-catchment area, width (length), slope, and the fraction of impervious cover was performed using GIS. In particular, the parameters identified from spatial analysis – sub-catchment width, slope, and the impervious cover – were found to contain errors and were therefore inspected during the sensitivity analysis (Liong et al., 1991), e.g. information about where stormwater from courtyards flows in order to determine stormwater redistribution between subareas. The sensitivity-based radio tuning calibration (SRTC) tool within the PCSWMM model served to identify sensitive parameters within the model and the minimum number of key parameters for model calibration using long-term simulation runs (James et al., 2010). Sensitivity was tested on 17 parameters: eight parameters in the sub-catchment layer, three parameters in the Green-Ampt infiltration model, four parameters in the Snow Pack layer, one parameter in the conduits, and one parameter in the network junction. Each parameter was increased and decreased by ± 10 , and ± 50 %, and its quality of fit was evaluated for the continuous period as well as the period without snowfall and negative temperatures.

The model's performance during the sensitivity analysis, the parameters' optimization and individual events were evaluated using a coefficient of determination (R^2) (eq. 7), Nash-Sutcliffe model efficiency (eq. 5), volume error (eq. 6) and mean flow error (MFE) (eq. 8).

$$R^2 = 1 - \frac{RSS}{TSS}, \quad (7)$$

$$MFE = \frac{MF_{obs} - MF_{sim}}{MF_{obs}} * 100, \quad (8)$$

where RSS is the sum of squares of residuals, TSS is the total sum of squares, MF_{obs} is the observed mean flow, and MF_{sim} is the simulated mean flow.

Rooftop retrofitting scenarios

According to the spatial analysis, the study catchment accounts for 10.7 % of flat roofs (yellow-shaded in Figure 5). In total, nine scenarios were created in this study. Flat roofs were changed from a conventional black roof, which was used as a reference called “Scenario A”, to either a vegetated green “Scenario B, D, F, and H” or a non-vegetated grey roof “Scenario C, E, G, and I” (scenarios A B C D and E can be found in Table 3, supplementary scenarios F, G, H and I can be found in Paper 5). While the scenarios A, B and C retained actual roof area located in the catchment, the scenarios D and E fictionally tested double roof area. The vegetated green and non-vegetated grey roofs were calibrated using the EPA SWMM Green roof LID module. More information may be found in Paper 3 (Hamouz and Muthanna, 2019). It was tested how the green and grey roof implementation impacts runoff in the catchment in terms of peak flows, volume reduction, and exceedance of three thresholds (100, 50 and 25 L/s). The thresholds were defined by flow analysis subdividing the high-resolution 1-min flow dataset into three groups according to flow magnitude. The roof area was fictionally doubled (Table 3) to investigate how this change in proportion between impervious cover and green and grey roofs would affect the runoff. Additionally, placement of the green and grey roofs was investigated to be located upstream and downstream to check whether the location of the retrofitted roofs would be important for runoff alteration in the catchment outlet or not. In this case, the actual roof area (10.7 % for the whole catchment) was fictionally used in either downstream sub-catchments or upstream sub-catchments, however only in subcatchments where the flat roofs appear originally.

Table 3 Tested rooftops scenarios (more about the scenarios may be found in Paper 5)

Designation	Roof area	Scenario type	Note
A	Actual ³	Do nothing	Table 13, Table 14
B	Actual ³	Green roofs	Table 13
C	Actual ³	Grey roofs	Table 13
D	Double ⁴	Green roofs	Table 14
E	Double ⁴	Grey roofs	Table 14

³ According to the spatial analysis.

⁴ Two times of the actual roof area.

Chapter 3 Results and Discussion

This chapter presents the main results achieved from the five scientific papers, focusing on their relevant findings and connections to one another. Results from the papers will not be discussed in detail, as the full version of selected papers is provided in Appendix B: Selected papers.

3.1 Results and discussion of Paper 1 (extended version)

The first research question aimed to explore which tested rooftop configuration provided the best hydrological performance for stormwater management. The knowledge gained from the monitoring of hydrometeorological data related to Paper 1 was applied to other papers: *“Investigate the retention and detention performances of different configurations of green and grey roofs for stormwater management. Which configuration provides the best retention and detention performances in a cold climate?”*

Retention and detention performances of the LECA-based roof (grey roof) from Paper 1 were extended to the individually tested solutions (*Solution 1* and *Solution 2*, description of individual configurations may be found in *Chapter 2 Materials and Methods*) to find the best configuration for stormwater management. In this case, Paper 1 served as a concept for developing methodology and discussing results before a larger quantity of data was recorded.

Retention performance

The retention was investigated and compared in *Solution 1* and *Solution 2*. However, the duration of each solution for assessment varied. For *Solution 1*, the hydrometeorological data was monitored for 417 days starting in April 2017 (NB.: in April 2017, the first green roof was

installed at the field station at Høvringen, which completed *Solution 1* with green, grey and black roof) whereas, data recorded for *Solution 2* lasted 316 days. It was found that sums of raw precipitation were lower than precipitation adjusted for aerodynamic effects (Table 4), -26 mm and -33 mm respectively for *Solution 1* and for *Solution 2*.

Moreover, even larger differences were found when comparing raw precipitation from precipitation gauge with runoff records from the black roof, -52 mm (-5 %) for *Solution 1* and -148 (-14 %) mm for *Solution 2*. The long-term observation was distributed into the warm and cold periods in order to investigate the source of the largest errors. It was detected that the largest under-catch occurred during the cold periods for both solutions, -51 mm (-11 %) for *Solution 1* and -119 (-22 %) mm for *Solution 2*. Due to this, the black roof was used as a reference.

Table 4 Long-term precipitation/runoff records for *Solution 1* and *Solution 2*. Values in the brackets are percental volume errors with respect to raw precipitation.

	Period	Days	Precipitation		Total runoff		
			Raw [mm]	Adjusted [mm]	Grey [mm]	Black [mm]	Green [mm]
Solution 1	April/17 - June/18	417	997	1023	983 (1%)	1049 (-5%)	824 (17%)
Solution 2	July/18 - May/19	316	1071	1104	1151 (-7%)	1220 (-14%)	1070 (0.1%)
Solution 1	Cold period	188	468	486	505 (-8%)	518 (-11%)	490(-5%)
	Warm period	229	529	537	478 (10%)	530 (-0.2%)	334 (37%)
Solution 2	Cold period	180	505	535	616 (-22%)	624 (-24%)	617 (-22%)
	Warm period	136	567	569	535 (6%)	596 (-5%)	453 (20%)

Note to solution 1: cold period - November/17 - April/18; warm period -April/17 - October/17 + May/18 - June/18
 Note to solution 2: cold period - November/18 - April/19; warm period -July/18 - October/18 + May/19

The total retention of the green and grey roofs with respect to the black roof for the examined periods may be found as either percental runoff reduction, retained volume or normalized daily retention. The green roof was able to retain 225 mm of runoff (21 % of the total black roof runoff) for *Solution 1* and 149 mm of runoff (12 % of the entire black roof runoff) for *Solution 2* (Table 5). The retention of the grey roof was lower retaining 65 mm and 68 mm respectively for *Solution 1* and for *Solution 2*.

Retention performance in a cold climate like Trondheim has a strong seasonality in the performance. Though the temperature and wind measurements varied little during the two warm periods, the seasonal duration can vary greatly. For *Solution 1*, the warm period lasted 93 days longer than *Solution 2*. This makes it important to consider the normalized daily retention during which the green roof retained 0.86 mm per day for *Solution 1* compared to 1.05 mm per day for *Solution 2*.

Overall, the green roof configuration had more than double the retention of the grey roof in all the cases (Table 5). This clearly demonstrates that the green roof should be favoured in terms of retention before the grey roof.

Table 5 Long-term runoff measurements for Solution 1 and Solution 2, including runoff reduction, retention and normalized daily retention for the green and grey roofs with respect to the black roof.

Period	Days	Total runoff			Runoff reduction		Total retention		Norm. daily retention		
		Grey [mm]	Black [mm]	Green [mm]	Grey [%]	Green [%]	Grey [mm]	Green [mm]	Grey [mm/day]	Green [mm/day]	
Sol. 1	417	983	1049	824	6 %	21 %	65	225	0.16	0.54	
Sol. 2	316	1151	1220	1070	6 %	12 %	68	149	0.22	0.47	
Sol. 1	Cold	188	505	518	490	3 %	5 %	13	28	0.07	0.15
	Warm	229	478	530	334	10 %	37 %	52	197	0.23	0.86
Sol. 2	Cold	180	616	624	617	1 %	1 %	8	7	0.04	0.04
	Warm	136	535	596	453	10 %	24 %	61	143	0.45	1.05

Detention performance

A total of 151 events were registered in *Solution 1* in the period between April 2017 and June 2018 and 103 events in *Solution 2* in the period between July 2018 and May 2019. The majority of these events were precipitation in the form of rain, including 91 events for *Solution 1* and 64 for *Solution 2*. The detention performance of the green and grey roof was evaluated using peak flow delay, peak flow reduction and volume reduction for the ten largest registered 5-min intensities for all tested periods involved in *Solution 1* and *Solution 2* (Table 6, Table 7, Table 8, Table 9). In addition, largest events within the cold and warm period according to the maximum black roof runoff for *Solution 1* and *Solution 2* were included for comparison in *Appendix A: Supplementary materials* (Table 16-Table 23). Observed maximum black roof runoffs and runoffs corresponding to the green and grey roofs can be found in *Appendix A: Supplementary materials* in Figure 12 and Figure 13 and probability exceedance of the black, green and grey roof maximum daily runoffs in Figure 14 and Figure 15.

The record of events for each *Solution* lacked extreme precipitations, containing only one event with a 2-year return period for each *Solution* (*Appendix A: Supplementary materials* in Figure 10 and Figure 11). The events ranged greatly in duration (from 8 minutes to more than four days), precipitation depth (from 3.4 to 61.7 mm) and mean intensity (from 0.5 to 25.6 mm/h); consequently, there was also a considerable variation in peak delays. While some long-duration events depending on precipitation pattern and intensity can produce very long delays, the most observed delays for “normal” shorter events are in a range of minutes. The grey roof outperformed the extensive green roof in terms of detention being more sensitive to precipitation which generated larger volume and less sensitive to intense precipitation.

Table 6 Ten events according to max 5-min precipitation intensity for **Solution 1**, including peak delay for the extensive green and grey roofs with respect to the black roof.

	Event		Duration [hours]	Precipitation depth [mm]	Mean int. [mm/h]	Max 5-min int. [mm/h]	Peak delay		
	nr	Type					Start	[black vs. grey]	[black vs. green]
Solution 1	50	Rain	19.08.2017	28:47	58.1	2.0	40.8	12:17	0:02
	41	Rain	26.07.2017	0:08	3.4	25.6	21.6	0:00	0:01
	53	Rain	29.08.2017	7:15	11.4	1.6	21.6	7:35	5:23
	6	Mixed	20.04.2017	69:34	39.5	0.6	17.6	2:30	0:14
	34	Rain	12.07.2017	19:35	9.0	0.5	16.3	0:01	10:49
	91	ROS	08.12.2017	25:38	24.0	0.9	13.2	0:34	0:03
	56	Rain	13.09.2017	5:25	8.2	1.5	12.0	0:00	0:01
	81	Rain	09.11.2017	17:03	14.0	0.8	12.0	7:22	0:44
	89	Rain	01.12.2017	101:04	61.7	0.6	12.0	25:36	no delay
	23	Rain	17.06.2017	74:38	60.4	0.8	11.6	36:42	35:31
ROS states rain on snow.						Median		4:56	0:14
						Mean		9:15	5:52

The grey roof performed better than the extensive green roof with respect to peak reduction, producing a median of 93 % and mean of 86 % peak reduction. The peak reduction provided a clearer and more clustered results with the exception of event 91, which was registered as rain on snow. The green roof provided a median event-based retention of 9 % in comparison to the grey roof, which had a median of 6 % for *Solution 1*. Regarding the largest events, there was found to be a positive correlation between precipitation depth and retained water in the roof. The events that had a negative volume reduction were influenced by antecedent events. Thus, part of the water was conveyed between the events. Due to this factor, the initial runoff may also be used as a performance corrector, or predictor, in addition to the degree of saturation. Higher initial runoffs correlated to higher degrees of saturation in the media from previous events.

Table 7 Ten events according to max 5-min precipitation intensity for **Solution 1**, including peak reduction and volume reduction for the extensive green and grey roofs with respect to the black roof.

	Event nr	Peak reduction	Peak reduction	Volume reduction	Volume reduction	Grey degree	Green degree
		[black vs. grey]	[black vs. green]	[black vs. grey]	[black vs. green]	of saturation	of saturation
Solution 1	50	93 %	75 %	4 %	9 %	33 %	37 %
	41	97 %	95 %	92 %	95 %	32 %	21 %
	53	97 %	95 %	48 %	64 %	32 %	36 %
	6	85 %	30 %	-5 %	7 %	-	-
	34	97 %	88 %	-5 %	8 %	36 %	59 %
	91	43 %	0 %	0 %	-1 %	47 %	57 %
	56	95 %	92 %	34 %	92 %	32 %	16 %
	81	93 %	87 %	7 %	9 %	33 %	63 %
	89	82 %	50 %	43 %	7 %	11 %	18 %
	23	80 %	38 %	5 %	11 %	-	-
Median		93 %	81 %	6 %	9 %		
Mean		86 %	65 %	22 %	30 %		

Table 8 Ten events according to max 5-min precipitation intensity for **Solution 2**, including peak delay for the detention-based green and grey roofs with respect to the black roof.

Event nr	Type	Start	Duration [hours]	Precipitation depth [mm]	Mean int. [mm/h]	Max 5-min int. [mm/h]	Peak delay	Peak delay	
							[black vs. grey]	[black vs. green]	
Solution 2	9	Rain	10.08.2018	29:49	57.2	1.9	30.0	no delay (-1)	0:00
	2	Rain	18.07.2018	9:40	6.8	0.7	19.2	0:01	no runoff
	8	Rain	09.08.2018	0:09	2.2	15.0	19.2	0:02	0:04
	29	Rain	25.09.2018	30:58	20.2	0.7	16.8	1:20	1:20
	44	Rain	22.10.2018	14:46	22.9	1.5	13.2	7:14	7:11
	6	Rain	05.08.2018	31:36	26.1	0.8	12.0	0:01	0:01
	12	Rain	18.08.2018	41:10	13.2	0.3	12.0	0:01	0:07
	88	ROS	24.03.2019	16:32	40.8	2.5	12.0	no delay	no delay
	7	Rain	09.08.2018	3:45	3.8	1.0	10.8	0:10	0:15
	21	Rain	12.09.2018	11:06	16.3	1.5	10.8	2:34	0:45
	ROS states rain on snow.						Median	0:06	0:11
						Mean	1:25	1:12	

In *Solution 2*, the peak delay and peak reduction were comparable for both the green and grey roofs. Still, the green roof outperformed the grey roof in all the indicators (Table 8 and Table 9). The reason for this was due to the green roof build-up (more information may be found in *Chapter 2 Materials and Methods*), which was upgraded with a detention layer consisting of expanded clay. This combination ensured that evapotranspiration could take part in the regeneration process and create a thicker storage zone where the retardation of the lateral flow provided extra detention. The evapotranspiration can be in the median volume reduction of 42 % and only 24 % for the grey roof (Table 9).

Table 9 Ten events according to max 5-min precipitation intensity for **Solution 2**, including peak reduction and volume reduction for the detention-based green and grey roofs with respect to the black roof.

Event nr	Peak reduction	Peak reduction	Volume reduction	Volume reduction	Grey degree of saturation	Green degree of saturation	
	[black vs. grey]	[black vs. green]	[black vs. grey]	[black vs. green]			
Solution 2	9	88 %	90 %	1 %	7 %	27 %	37 %
	2	97 %	100 %	79 %	100 %	19 %	13 %
	8	98 %	100 %	57 %	95 %	28 %	36 %
	29	93 %	94 %	5 %	10 %	28 %	45 %
	44	82 %	83 %	2 %	5 %	33 %	52 %
	6	91 %	95 %	12 %	85 %	20 %	14 %
	12	97 %	98 %	-3 %	18 %	23 %	40 %
	88	30 %	28 %	-6 %	-21 %	35 %	59 %
	7	98 %	99 %	69 %	98 %	27 %	34 %
	21	92 %	95 %	23 %	66 %	21 %	31 %
	Median	93 %	95 %	9 %	42 %		
Mean	87 %	88 %	24 %	46 %			

A number of events were recorded as long-duration events lasting more than one day using the six hours of ADWP. A total of 19 and 25 events were logged exceeding 24 hours duration, and 5 and 9 events exceeded 48 hours duration for *Solution 1* and *Solution 2* respectively. Several of the larger events, which were used to assess the detention performance, were included in these categories. These events were more complicated for evaluation, as peak runoff could appear under different precipitation patterns. While the extensive green roof and the reference black roof were more sensitive to relatively short, intense periods of rainfall, the detention-based green and grey roofs were able to transform these events. On the other hand, events having a long duration could generate worse performance, producing larger volumes of runoff

from these roofs. This can be explained by the volume build up over the long duration of the event, causing a larger peak when the storage capacity is full. Considering long-duration events and their maximum runoffs as the representative value may overestimate the overall performance in terms of the peak delay, even though it is more natural to compare events according to maximum registered values. The irregularity of natural rainfall patterns, combined with the variability in the detention effect in specific events, complicates the identification of peak-to-peak delays.

In summary, the retention and detention performance of these configurations show following:

- *Solution 1*: The extensive green roof provided stormwater retention during the warm period by evapotranspiring 37 % (with a normalized daily retention rate of 0.86 mm/day) of total black roof runoff. In terms of the detention performance, the grey roof outperformed the extensive green roof in peak reduction with a median of 93 % for the largest recorded events.
- *Solution 2*: underlaying the detention-based green roof with expanded clay resulted in an improvement of the detention performance in addition to improving stormwater retention with a long-term runoff reduction of 24 % during the warm period translated to a normalized daily retention rate of 1.05 mm/day. The detention-based green performed similarly to the grey roof in terms of peak delay (producing a median of 11 minutes vs. 6 minutes) and peak reduction (with a median of 95 % vs. 93 %) but outperformed the grey roof in volume reduction more than four times over (producing a median of 42 % vs. 9 %).

3.2 Results and discussion of Paper 2

The second research question investigated the use of the retention and detention-based roofs for managing extreme precipitation under different initial moisture conditions in the current and future changing climate: “*What is the influence of rainfall intensity and pattern, including extreme events, on the performance of the detention-based green roofs?*”

The detention impact of a detention-based green roof, consisting of Sedum mats underlaid with expanded clay, was tested for current and future climate conditions during extreme precipitation using an artificial rainfall generator. Figure 6 shows several indicators selected to assess the effect of the hyetograph’s shape. A clear relationship was found between initial water content and peak runoff, similar to others (Li and Babcock, 2014; Locatelli et al., 2014; Villarreal and Bengtsson, 2005). Peak runoffs increased exponentially with respect to the initial

available space in the roof and relative water content. On the other hand, the centroid delay and T50 exponentially decreased with respect to the initial water content in the roof. It was found that having the peak at the end (TRO 2b) or the middle (TRO 2c) of the rainfall event caused the poorest performance (highest peak runoff).

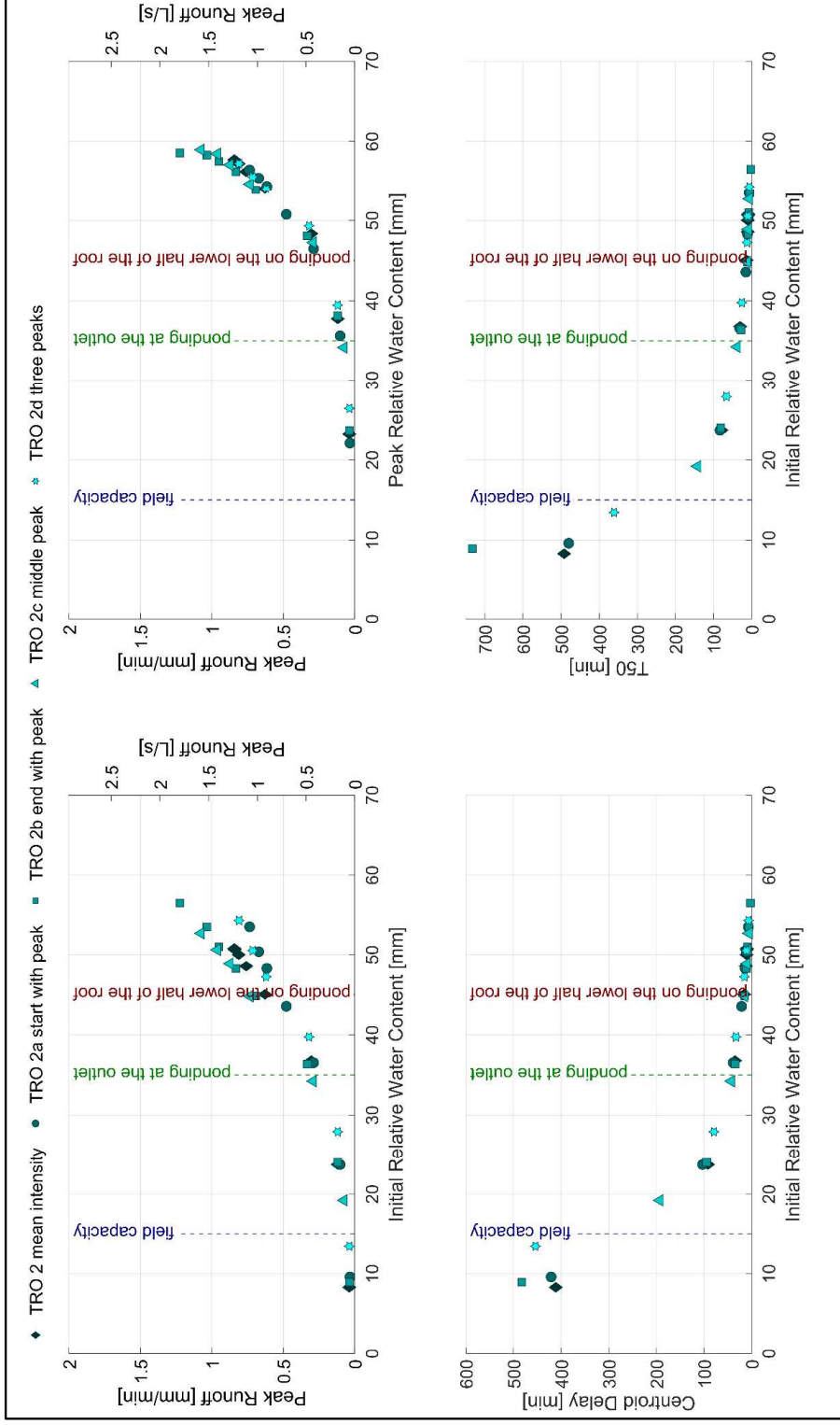


Figure 6 Comparison between peak runoff, centroid delay and T50 for different rainfall patterns. (Paper 2 - Hamouz et al. - Accepted for publication)

When analysing peak runoff versus initial moisture content (Figure 7), it is noticeable that the events corresponding to Oslo generally generated higher runoffs than events in Bergen and Trondheim. Depending on the location and antecedent amounts of rainfall, initial conditions can change considerably. However, according to DDF curves and climate (Johannessen et al., 2018; Peel et al., 2007), Oslo is likely to have lower initial water content than Trondheim or Bergen. Considering its low initial water content, the roof was more sensitive to longer periods of rainfall with lower intensity (e.g., OSL 1 performed worse than OSL 2 when initial water content was lower than field capacity). When starting with a high moisture level, the peak runoff was close to the peak rainfall, and the roof was more vulnerable to shorter patterns with higher intensity (e.g., OSL 1 performed better than OSL 2 when the initial water content was higher than 30 mm). The same analysis may be done with OSL 2 and BER 1, or BER 1 and BER 2, but the shift appeared with higher water content (50 mm). Consequently, it was not possible to make an easy conclusion about performance depending on the location (Bergen, Oslo and Trondheim). This is because in addition to the DDF curves, the design should be based on different patterns depending on a range of initial water content levels, and those initial conditions should also depend on location. The annual precipitation and number of precipitation days were found for each location: Bergen (205 ±18 days, 2715 ±450 mm), Oslo (122 ±15 days, 861 ±146 mm) and Trondheim (174 ±14 days, 1191 ±184 mm) according to the Norwegian Meteorological Institute (<https://www.met.no/>). This shows that initial conditions are likely to change according to their location, meaning that the initial moisture condition is an important design consideration.

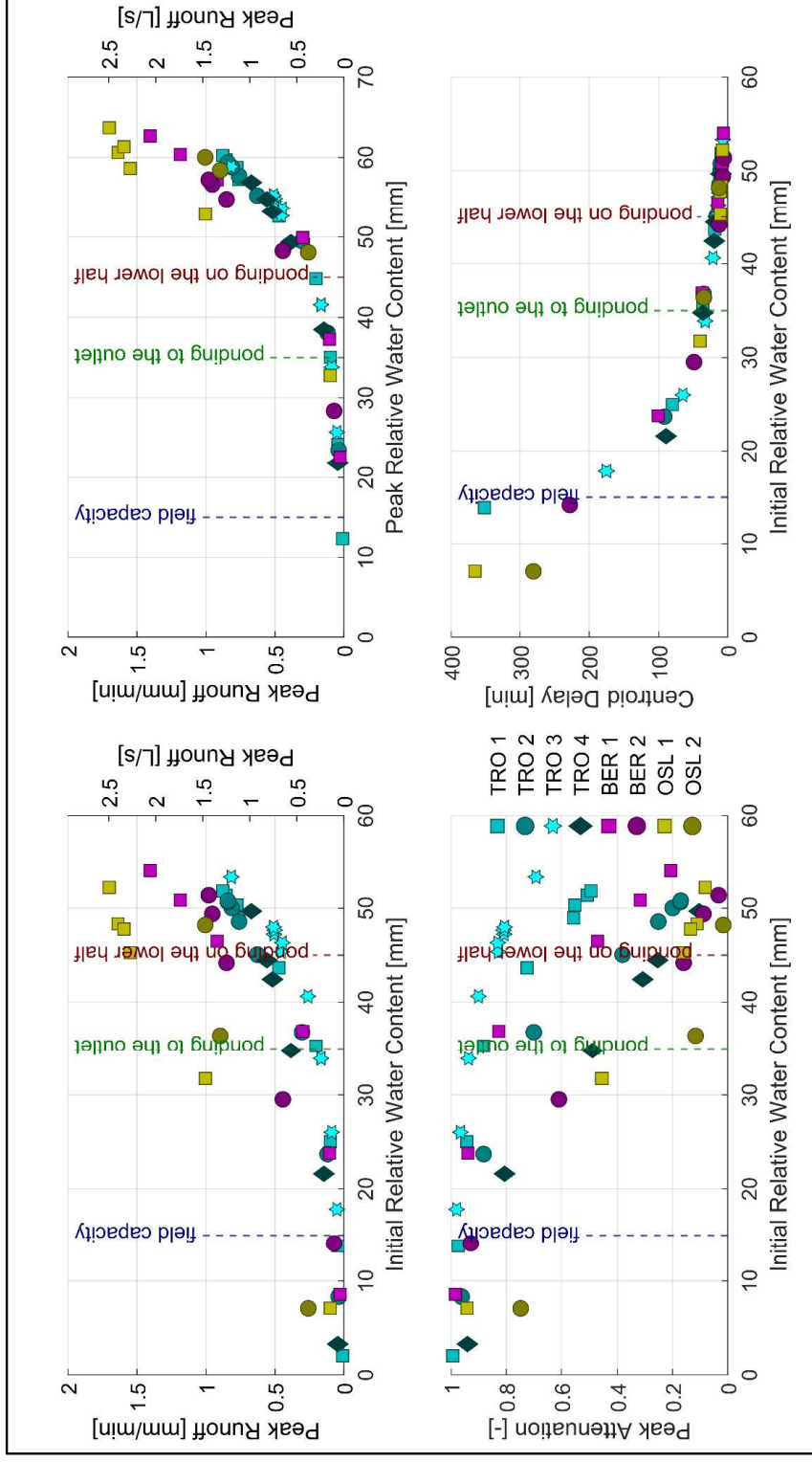


Figure 7 Comparison between peak runoff, peak attenuation and centroid delay for different locations, including a climate factor of 1.4. (Paper 2 - Hamouz et al. - Accepted for publication)

One natural event was found with a return period between two and five years, which generated the maximum value of 0.602 mm/min for the black roof and 0.063 mm/min for the detention-based green roof. According to the extreme precipitation tests, the level of outflow reaching 0.06 mm/min would equal a relative water content of approximately 30 mm. Given this initial water content, the detention-based green roof would generate the following performance:

- centroid delay and T50 of 50 minutes for all the tested rains (Figure 6, Figure 7),
- peak attenuation larger than 50 % for the event in all tested locations (Figure 7),
- peak runoff lower than 0.25 mm/min (< 0.37 L/s) for the events from Trondheim,
- peak runoff lower than 0.5 mm/min (< 0.73 L/s) for the events from Bergen,
- peak runoff lower than 1 mm/min (< 1.47 L/s) for the events from Oslo.

Since peak flows generated by the roof followed an exponential curve, it was possible to generalize an outflow curve as well as water content decreasing over time (both curves can be found in Paper 2 in Figure 5 - Median-observed drainage curve for the green roof with 5th and 95th percentile). It was observed that water content in the roof decreased from ponding in the lower half of the roof (45 mm) to the outlet (35 mm) within 80 minutes and to the field capacity (15 mm) within approximately 12 hours. Thus, the roof can regenerate its storage capacity for large flows within a relatively short period and at the same time provide water detention, which is represented by centroid delay or T50.

3.3 Results and discussion of Paper 3

The third research question was shared in Papers 3 and 4, aiming to simulate long-term continuous runoff from retention and detention-based roofs and provide an optimal parameter set which could be applied for design purposes using the EPA's Stormwater Management Model: *“Investigate the use of catchment scale modelling tools for design and performance estimates for vegetated and non-vegetated roofs.”*

The long-term (retention) and event-based (detention) observations for *Solution 1* examined in Paper 1 were used as input in Paper 3. The long-term continuous data applied for runoff simulations using initial uncalibrated parameter sets indicated a correlation between the observed and simulated runoffs from the green roof with the NSME set at 0.5. However, the same did not apply for the simulated runoff from the grey roof with the NSME set at -2.87, where calibration was required. Due to this occurrence, six parameters in two LID layers (namely the soil and drainage mat) were calibrated. Their values prior to and after calibration

are presented in Table 2. Some of the parameters (berm height, surface slope, thickness) were kept fixed to preserve the physical description of the field setup as well as avoid overparameterization. Substantial improvements to the model's performance was achieved after the calibration of both the green and grey roof parameters. The NSME calculated from the observed and simulated runoff from the green roof improved from 0.50 to 0.94; it improved from insufficient -2.87 to 0.78 from the grey roof. It should be noted that the NSME values include inter-event periods (periods without rain) since the increased detention effect (that led to higher baseflow) made it challenging to determine when the runoff stopped.

In general, a more suitable fit for long-term continuous model simulation was found during the calibration period of the green roof rather than of the grey roof. Visually speaking, the models simulated the runoffs well (Figure 8, Figure 9). The simulated runoff from both the green and grey roofs tended to underestimate the observed peak flow responses to rainfalls with the highest intensity. This indicated that the rain gauge measurement of the most intense rainfall was uncertain. At the same time, the model had difficulties in simulating the tails of grey roof runoff more than it did in the green roof. The simulated cumulative runoffs (total volumes) were close to the observed data.

Five events classified as C1-C5 were chosen to evaluate the model's performance in terms of event-based simulation during the calibration period (event C3 is presented in Figure 8). One can see the difficulties associated with the simulation and the underestimation of the runoff tails in the grey roof (Figure 8), leading to the model's ability to simulate runoff detention being partly limited. Thus, the equations describing the detention processes as well as the detention parameters, namely 1) porosity, 2) soil conductivity, 3) soil conductivity slope and 4) soil suction head within soil layers and 5) the parameters in the drainage mat estimating the baseflow, should be further investigated in order to improve runoff prolongation.

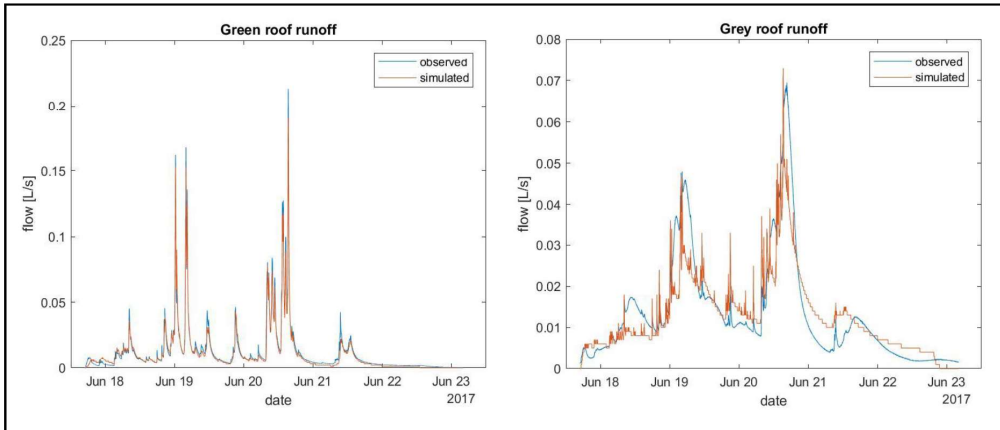


Figure 8 Comparison of observed and simulated runoff from the green (left) and grey (right). Event C3 from the calibration period was chosen (Table 10). More plots from the calibration period may be found in Paper 3 (Hamouz and Muthanna, 2019).

Six events classified as V1-V6 were chosen to evaluate the model's performance in terms of event-based simulation during the validation period (event V2 is presented in Figure 9). During this study, only one event having a 2-year return period was registered by the rain gauge at Høvringen, Trondheim, in August 2017 (Figure 9).

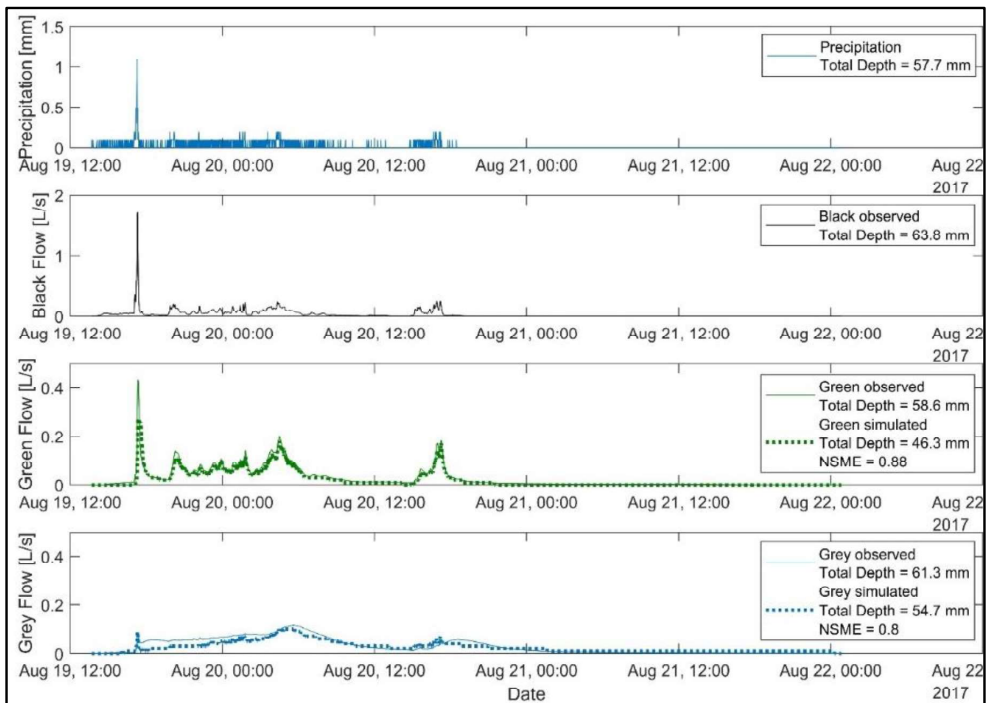


Figure 9 Comparison of observed and simulated runoff from the green (left) and grey (right) for the largest event V2 from the validation period in 2017. More plots from the validation period may be found in Paper 3 (Hamouz and Muthanna, 2019).

Events V2 and V6 provided interesting results, reaching the NSME of 0.8 and higher for both roofs; in addition, the volume error fell within reasonable limits. Both events lasted several days, and relatively large volumes were registered. It may therefore be concluded that these events are of interest since the SWMM model showed its ability to reproduce registered runoffs, and the roofs were able to reduce the maximal flow (Table 10). The green roof runoff was simulated reasonably well except for one event in September during the validation period (V4), which followed a dry period lasting nearly one week, intensely drying the roof's storage capacity. Regarding the long-term datasets, the green roof model's performance worsened with respect to the NSME, sinking from 0.94 to 0.88 (and VE rising from 3 % to 29 %) during the validation period, while the grey roof model experienced an improvement in terms of the NSME, rising from 0.78 to 0.81 (Table 10).

Table 10 Individual events used for evaluating the model performance within the calibration (C) and validation (V) period and comparison to the black roof runoff. The table shows overall model performance for long-term continuous calibration, validation and cold periods. (Hamouz and Muthanna, 2019)

CALIBRATION /VALIDATION	RUNOFF SIMULATION									
	BLACK OBSERVED	GREEN OBSERVED	GREEN SIMULATED	VE	NSME	GREY OBSERVED	GREY SIMULATED	VE	NSME	
	[mm]	[mm]	[mm]	[%]	[-]	[mm]	[mm]	[%]	[-]	
C1	18.3	5.6	6.5	-15.9	0.44	15.4	8.4	45.3	0.33	
C2	15.9	6.9	8.0	-16.3	0.61	14.8	12.4	16.1	0.44	
C3	62.4	57.5	52.7	8.3	0.98	62.6	60.6	3.1	0.78	
C4	25.5	19.6	19.3	1.5	0.89	22.7	22.9	-0.7	0.61	
C5	3.0	0.2	0.0	96.6	-0.13	0.2	0.2	30.8	0.59	
V1	13.9	6.3	2.6	59.4	0.38	12.5	10.8	13.5	0.24	
V2	63.8	58.6	46.3	21.0	0.88	61.3	54.7	10.7	0.80	
V3	12.2	5.6	2.3	59.4	0.26	9.2	10.5	-14.0	0.06	
V4	7.7	0.7	0.8	-10.0	-0.90	5.0	6.9	-38.6	-1.74	
V5	26.3	24.4	16.7	31.5	0.86	25.7	27.5	-6.7	0.53	
V6	97.3	94.6	77.6	17.9	0.84	96.6	92.1	4.7	0.80	
Calibration period	241.5	147.4	143.3	2.8	0.94	214.4	193.5	9.7	0.78	
Validation period	331.2	259.7	185.1	28.7	0.88	315.6	279.7	11.4	0.81	
Cold period	390.0	371.0	259.0	30.2	0.56	384.0	340.0	11.5	0.37	

In comparison, the volume errors between the simulated and observed runoffs from the grey roof counted 10 % and from the green roof 3 % during the calibration period, 11 % and 29 % during the validation period and 12 % and 30 % during the cold period, respectively. The limitations of these simulations include the actual dataset duration, which spans over less than one year, and the fact that there was only one event with a return period greater than 2 years. This may also raise the question of whether or not it is appropriate to validate the model using different seasonal periods within the same year.

A few points that explain the runoff mismatch were noted. Firstly, the volume errors were caused by inaccurately estimated seasonal evapotranspiration rates, which occur during dry periods and cause a regeneration of the roof's storage capacity. Secondly, the volume errors were caused by inaccurate model simulations of runoffs. It was noted that while the actual ET

rates decay over time during the dry period, the SWMM model assumes fixed ET rates (Peng and Stovin, 2017). Thirdly, the model runoff outputs had a coarser resolution than the observed runoff, which made the volume comparison more challenging. Fourthly, the measurement of intense rainfall is uncertain and, in most cases, underestimated, leading to lower simulated volumes. The model was less accurate for short, intense rainfalls following a long antecedent dry period. This shows that the model storage capacity of the green roof was regenerated without considering the local climate (e.g., condensation of atmospheric vapor). Median and mean values of the observed flow used during calibration were 0.0012 L/s (median) vs. 0.003 L/s (mean), and during validation 0.006 L/s (median) vs. 0.0036 L/s (mean). Thus, there was a baseflow that was twice as high during calibration and only a slightly peaky runoff during validation. This might signify that the wetter period of the year “performed” better than the dryer period (Wilby, 2005), raising the question of using these different periods of the year for validation. The visual comparison of the data spread concerning observed and simulated runoffs from the green and grey roofs from all periods as well as their mathematical expression (value of norm of residuals, mean squared error MSE, coefficient of determination R^2 and correlation coefficient) may be found in Paper 3 (Hamouz and Muthanna, 2019).

3.4 Results and discussion of Paper 4

The third research question was shared in Papers 3 and 4; its aim was to simulate long-term continuous runoff from retention and detention-based roofs using the EPA's Stormwater Management Model and provide an optimal parameter set which could be used for design purposes: *“Investigate the use of catchment scale modelling tools for design and performance estimates for vegetated and non-vegetated roofs.”*

Individual model evaluation

The calibrated model parameters found in Paper 3 were compared to the calibrated parameters from different locations in Paper 4. The individual model calibration resulted in volume errors ranging from -4 to 28% during the calibration period and from -5 to 17% during the validation period (Table 11). While some of the models showed acceptable volume errors (models with errors less than < 6%), others exhibited large volume errors (models with errors larger than 20%). This is most likely because the model does not fully represent the evapotranspiration processes taking place, as suggested by earlier studies (Peng and Stovin, 2017); however, errors could also be caused by measurement inaccuracies and uncertainties. The model represents evapotranspiration by the Hargreaves method combined with a soil recovery coefficient and

does not include the influence of soil moisture, which has been shown to have an important impact on evapotranspiration in green roofs (Berretta et al., 2014; Stovin et al., 2013). The calibration was based on one soil recovery coefficient for the entire modelling period; however, it is possible that individual coefficients for each month might improve the performance. Larger volume errors were found for all tested configurations at Høvringen (HOV). One explanation for this might be the uncertainties involved with precipitation measurements relating to the field station being located at Høvringen, which lies along a coastline exposed to an open fjord area; consequently, this area undergoes high levels of wind stress. The ability of the individual model to reproduce the observed runoff was evaluated by NSME coefficients (Table 11). All model runs provided NSME greater than 0.56 with an average of 0.80 for both the calibration and validation periods, which may be considered an adequate performance for a rainfall-runoff model based on field observations (Rosa et al., 2015).

Table 11 Model evaluation from individual model calibration (Johannessen et al., 2019)

Id	NSME		VE	
	Calibration events	Validation events	Calibration period	Validation period
RIS1	0.65	0.85	4 %	9 %
BER1	0.77	0.75	-4 %	3 %
SAN1	0.66	0.75	4 %	1 %
BER4	0.77	0.82	-1 %	3 %
SAN3	0.92	0.87	21 %	17 %
RIS3	0.60	0.56	5 %	4 %
BER3	0.85	0.85	0 %	6 %
SAN2	0.87	0.80	12 %	10 %
HOV3	0.90	0.88	28 %	14 %
OSL1	0.80	0.66	2 %	-5 %
HOV2	0.96	0.95	18 %	9 %
HOV1	0.90	0.83	25 %	17 %
LAB1	0.89			
LAB2	0.84			
LAB3	0.84			
LAB4	0.82			
LAB6	0.60			

Model parameters - Reference roofs

Optimal model parameters for all calibrated models are listed in Table 12, including parameters from Paper 3, the SWMM manual and other studies. Three models of reference roofs (OSL1, HOV2, LAB1) were calibrated, resulting in model parameters that could be useful for design purposes when comparing different roof configurations to conventional roofs (Table 12). Optimal model parameters from individual calibration were comparable, indicating that the SWMM model reproduces the runoff satisfactorily and may be used for modelling reference roofs of variable sizes and locations. Recommended model parameters for reference roofs based on this study are a Manning's roughness coefficient of 0.01, also found by (Cipolla et al., 2016), and a depression storage of 0.03.

Green roof model retention performance

The available water storage capacity in green roofs in the SWMM green roof module is defined by the pore space between the field capacity and the wilting point combined with the soil thickness. No storage capacity is included in the drainage layer of the model, even if the properties of the drainage layer might allow for water to be stored there, i.e., in cups in the conjugated plastic drainage layers or soaked up in the textile retention drainage mats. The individual model calibrations showed a large variation in optimal parameters for both field capacities (17–44%) and wilting points (1–15%) for the same material at different sites, and the resulting parameters seem to be influenced by local climate conditions (Table 12). Regarding some of the configurations, the monthly variations may be explained by variations in precipitation patterns occurring during drier conditions in certain months and producing lower soil moisture content, which in turn reduces the actual evapotranspiration. Both the significant volume errors and variations in the calibrated parameters for soil recovery coefficients, field capacities and wilting points confirm previous findings. These findings indicate that the modelling of evapotranspiration in the SWMM LID module, when based on the Hargreaves method combined with a soil recovery coefficient, does not adequately represent the actual evapotranspiration; further, it does not adequately represent the retention processes (Feng and Burian, 2016; Peng and Stovin, 2017).

Green roof drainage layers parameters

The drainage layer parameters are expected to play an essential role in runoff generation, especially for full-scale roofs, as they will define the detention process associated with the horizontal water movement. The detention processes occur when the water content in the roof exceeds the field capacity, resulting in runoff, which is mainly driven by gravitational forces; however, it is also affected by the friction and capillary forces. The only flat green roof included in the study resulted in a drainage layer void fraction of 0.64 and a Manning's n of 0.07. Model studies using similar conjugated plastic drainage layers resulted in comparable calibrated void fractions of 0.4–0.6 but lower Manning's roughness coefficients of 0.01–0.03 (Krebs et al., 2016; Palla and Gnecco, 2015; Peng and Stovin, 2017). These studies were based on table scale green roof units with drainage lengths of 2–3 m, which could explain the differences in the findings. While the SWMM manual suggests a void fraction of 0.2–0.4 and Manning's n values of 0.01–0.03, it does so without specifying the drainage layer build-up (Rossman and Huber, 2016b). The sloped green roofs included in the study were all equipped with textile retention mats as their bottommost layer, while the total thickness of the drainage layer varied between

the different types. The drainage layer parameters were the parameters that showed the largest variation between individual models for the same type and between the different types, despite the similarities of the bottommost layer. This indicated that the SWMM green roof module has a limited ability to represent the water movement through the drainage layer, a process considered by the authors to be quite important for modelling detention properly on large-scale roofs. This limitation of the model was also mentioned by Krebs et al. (2016), who also applied a textile retention mat as the bottommost layer, and by Peng and Stovin (2017), who applied a slightly different configuration having a plastic drainage layer as the bottommost layer. Soil conductivity varied both between and within the different types of green roofs (42–1276 mm/h), while there was slightly less variation in the obtained parameters for conductivity slope (14–60) and suction head (6–71). The SWMM manual suggests Soil Conductivity values in the range of 1000–2500 mm/h (Rossman and Huber, 2016b), while the German Green Roofing Guidelines state a requirement for water permeability in the range of 36–4200 mm/h (FLL, 2008). Krebs et al. (2016) applied a pre-grown vegetation mat (Type A) over a thicker substrate and found a Soil Conductivity of 38 mm/h, while (Palla and Gnecco, 2015) and (Peng and Stovin, 2017) found it to be 1000 mm/h.

Grey roof model parameters

Two models of grey roofs, one from the laboratory (LAB6) and one from the field site (HOV1), were calibrated in the same way as the green roofs. Both grey roofs were based on an expanded clay but had varying particle size, roof size, and type of experiment (continuous versus events). The drainage parameters of HOV1 showed greater values than all the other configurations (Manning's $n=0.48$). This corresponds well to the observed runoff, with prolonged runoff compared to the green roofs; however, the calibrated parameters might be too high, as high flows tended to be slightly underestimated. Since the soil conductivity (vertical movement) was very high, the horizontal movement through the expanded clay layer was expected to provide substantial detention. Porosity was found to be lower for the grey roof than for the green roofs and conductivity higher, while conductivity slope and suction heads were found to be comparable. Laboratory-measured porosity was 54 % for the HOV1 material, which was significantly higher than the calibrated model porosity of 35 %. Field capacity and the wilting point, which determined the soil retention, were found to both be 15 % according to the calibrated model parameters for HOV1. Laboratory measurements of the same material gave a field capacity of 16 %, which was consistent to the model parameter, while the wilting point was measured at 13 %, indicating there was a slight potential retention capacity in the material

that was not found in the model parameters. Identical values for field capacity and wilting point in the model correspond to no available storage capacity and explain the model's large volume error (Table 11). This is an indication that the model does not correctly represent the retention processes. The LAB6 model produced a porosity level close to the laboratory-measured 54 %, while the field capacity (10 %) and wilting point (7%) deviated largely from the model-derived parameters of 27% and 10%, respectively.

It was found that individual parameters fell into the range of recommended values from the SWMM manual or others (Table 12). However, the complete parameter sets should be used for specific tested locations in order to preserve model performance.

Table 12 Final model parameters for Papers 3 and 4 and comparison to the SWMM manual and other studies.

Roof parameters	Paper 3 - GreyRoof	Paper 4 – GreyRoof	Paper 3 GreenRoof	Paper 4 - GreenRoof	SWMM*	Others**
Soil Parameters						
Field Capacity (%)	10	21 (15-27)	27	31 (17-44)	30-50	29-49
Wilting Point (%)	-	13 (10-15)	-	9 (1-15)	5-20	2-7
Porosity (%)	45	46 (35-57)	56	60 (43-70)	45-60	41-66
Conductivity (mm/h)	2975	1723 (80-3366)	11	460 (43-1183)	1000-3500	25-1000
Conductivity Slope	28	34 (19-48)	32	30 (14-60)	30-55	15-60
Suction Head	-	64 (49-79)	-	46 (6-77)	2-4	61-110
Drain Parameters						
Void Fraction	0.663	0.560 (0.40-0.72)	0.016	0.151 (0.01-0.64)	0.20-0.40	0.40-0.60
Manning's n	0.205	0.415 (0.35-0.48)	0.010	0.154 (0.07-0.24)	0.01-0.03	0.01-0.03

*(Rossman and Huber, 2016b)

** (Carson et al., 2017; Krebs et al., 2016; Palla and Gnecco, 2015; Peng and Stovin, 2017; Rosa et al., 2015)

3.5 Results and discussion of Paper 5

In the fourth research question, the calibrated model of the retention detention-based roofs was applied to the PCSWMM model in order to test the impact of the retention and detention-based roofs on catchment outlet: *“To what extent can the retention and detention-based roof implementation contribute to runoff reduction on a catchment level in urban areas?”*

Papers 1-4 provided valuable information about a site (building) scale modelling of the retention and detention-based roofs. The performance and ability to replicate runoff from the roofs using the hydrological model was interpreted to catchment scale (Paper 5). In addition to the model performance assessment (more about this may be found in Paper 5), the calibrated model of the catchment was used for simulation of the catchment runoff while artificially retrofitting all the flat roofs in the catchment (10.7 %) with either the green or grey roofs (Table 13). It was found that the green and grey roofs can equally reduce the maximum flow by 17 %. Moreover, three exceedance thresholds were chosen to test how often, how long, and how much volume of stormwater runoff from the catchment exceeded flow equal to 100, 50 and 25 L/s. The implementation of either solution with the green roofs or the solution with the grey roofs

showed essential improvements, specifically in terms of peak flows. This may be observed for the largest exceedance threshold where the reductions were the most considerable. The impact of the roof's implementation decreased together with the reduction of the exceedance threshold (from 100 L/s down to 25L/s). The grey roof implementation outperformed the green roofs in all the aspects: duration, number, and volume of exceedance and even in the long-term continuous simulation which was found to be overestimated.

Table 13 Impact of the green and grey roofs' implementation for different exceedance thresholds 100, 50 and 25 L/s with respect to the evaluation criteria. Scenarios A, B, and C from Table 3. (Paper 5 - Hamouz et al. in review)

Evaluation criteria	Do nothing - Scenario A	GreenRoof's performance - Scenario B	GreyRoof's performance - Scenario C	Impact of GreenRoofs	Impact of GreyRoofs
Maximum Flow [L/s]	174	145	145	17 %	17 %
Exceedance threshold [L/s]	Duration of Exceedances [h]			Impact of GreenRoofs	Impact of GreyRoofs
100	1.4	1.1	0.6	23 %	54 %
50	20.0	17.1	11.3	14 %	44 %
25	118.0	109.3	85.9	7 %	27 %
Exceedance threshold [L/s]	Number of Exceedances			Impact of GreenRoofs	Impact of GreyRoofs
100	8	8	5	0 %	38 %
50	67	60	47	10 %	30 %
25	214	198	184	7 %	14 %
Exceedance threshold [L/s]	Volume of Exceedances [m ³]			Impact of GreenRoofs	Impact of GreyRoofs
100	132	61	47	53 %	64 %
50	1323	992	630	25 %	52 %
25	6046	5104	3829	16 %	37 %

Further, an extra scenario in the green and grey roof implementation was emphasized with respect to changes in the roof area versus impervious cover (Table 14). The roof area was artificially enlarged to twice the area in each of the sub-catchments, simulating a scenario with urban densification, where the flat roof is present, to a total of 21.4 % of flat roofs for retrofitting in the entire catchment. This was done due to the fact that rooftops in urban environments, specifically in city centres, may account for up to 50 % of the impervious surface area (Dunnnett and Kingsbury, 2008). In this case, it was found that the green roofs were able to reduce the maximum flow by 30 % and grey roofs as much as 35 % (Table 14). Both roof scenarios were very effective in reducing volume (78 % for green and 98 % for grey roofs), which exceeded the threshold equal to 100 L/s. In comparison to the green roof, the grey roof kept high levels of reduction for all exceedance thresholds.

Table 14 Impact of the green and grey roofs' implementation with doubled roof size for different exceedance thresholds 100, 50 and 25 L/s with respect to the evaluation criteria. Scenario A, D, and E from Table 3. (Paper 5 - Hamouz et al. in review)

Evaluation criteria	Do nothing - Scenario A	2xGreenRoof's performance - Scenario D	2xGreyRoof's performance - Scenario E	Impact of 2x GreenRoofs	Impact of 2x GreyRoofs
Maximum Flow [L/s]	174	123	113	30 %	35 %
Exceedance threshold [L/s]	Duration of Exceedances [h]			Impact of GreenRoofs	Impact of GreyRoofs
100	1.4	1.0	0.1	31 %	90 %
50	20.0	19.8	4.5	1 %	78 %
25	118.0	122.6	62.4	-4 %	47 %
Exceedance threshold [L/s]	Number of Exceedances			Impact of GreenRoofs	Impact of GreyRoofs
100	8	7	3	13 %	63 %
50	67	46	21	31 %	69 %
25	214	179	136	16 %	36 %
Exceedance threshold [L/s]	Volume of Exceedances [m ³]			Impact of GreenRoofs	Impact of GreyRoofs
100	132	29	3	78 %	98 %
50	1323	1092	209	17 %	84 %
25	6046	5878	2107	3 %	65 %

The paper presents a method to examine an urbanized area using modelling tools and identify potential areas for retrofitting; moreover, it is a follow-up to Paper 1 (Hamouz et al., 2018), Paper 3 (Hamouz and Muthanna, 2019) and Paper 4 (Johannessen et al., 2019). It provides an important contribution towards utilizing retrofitted rooftops for the detention of stormwater at the place where it is generated. The potential for reducing the runoff may thereby be determined. This can be a valuable tool for urban planners when deciding whether to keep rooftops impervious or focus on green and/or grey roof retrofitting strategies. Still, it should be kept in mind that the rooftop retrofitting alone helps to reduce urban runoff and therefore rooftops runoff should be additionally treated by disconnecting and redirecting in other decentralized drainage systems like bioretention cells or raingardens (Davis et al., 2009; Gleick, 2014; Jarden et al., 2016). The overall performance is however also dependent on other situations, e.g., summer/winter conditions (Johannessen et al., 2017; Li and Babcock, 2014), initial saturation (Alfredo et al., 2009; Berretta et al., 2014), roof size, media and slope (Getter et al., 2007; Hakimdavar et al., 2014; VanWoert et al., 2005). Last but not least, deep percolation within a catchment with native soils formed from fjord or marine deposits is limited. Therefore, the use of rooftops retrofitting can be a favourable stormwater solution rather than infiltration-based measures.

Rooftop retrofitting showed the greatest effectiveness for the largest flows (100 L/s) than smaller flows (50 L/s and 25 L/s). Concerning combined sewer overflows, rooftop retrofitting with the grey roof would decrease an overflow's duration by 54 %, the number of overflows by 38 % and the volume of overflow by 64 %. While the total area of the flat roof was less than

11 %, it is possible to find urban areas having a total roof area greater than 50 %, which would have a great impact on urban hydrology. Moreover, a greater impact on the urban runoff (reducing CSOs or underground detention tanks) would be expected if rooftop configuration is used in stormwater treatment train combined with other stormwater measures like permeable pavement, rain garden, detention basin.

3.6 Uncertainty in observation input and hydrological modelling

In order to improve the applicability and reliability of hydrological models of retention and detention-based roofs and the high quality of hydrometeorological data measurement (precipitation, flow, wind speed, temperature, water content, etc.), it is essential to start with an optimization method and model conceptualization.

The difficulty of defining events using the 6-hour ADWP (resulting in some long events) indicated that it might not be the best-suited time definition for the climate zone. These long-duration events also cause decreasing mean intensity of individual events. Considering a maximum runoff as the representative value for an event may overestimate the overall performance in terms of the peak delay, even though it is more natural to compare events according to maximum registered values. The irregularity of natural rainfall patterns, combined with the variability in the detention effect in specific events, complicates the identification of peak-to-peak delays.

Although the calibrated SWMM models reproduced the observed runoffs sufficiently, the calibration revealed that there might be several parameter sets that perform equally well (Paper 3 and 4). This makes the parameters uncertain and valid only for the tested roof setups (in this case the green and grey roofs from *Solution 1*, more information may be found in Chapter 2 Materials and Methods) and climatic conditions of the study site. The reason for the parameter's sets being skewed could be due to the optimization algorithm, which, instead of finding the global minimum, may have found only local minima. A sensitivity analysis of the tested parameters showed that porosity is the most sensitive parameter for the green roof. In terms of the grey roof, the porosity and conductivity slopes were found to be the most sensitive parameters.

During the calibration of the hydrological model, the parameter identifiability was problematic due to an equifinality in the model (Papers 3 and 4). The equifinality states the non-uniqueness of the optimized parameter sets, indicating a greater risk of uncertainty. The issue here is that similarly performing optimized parameter sets may not all be equivalent in terms of

transferability and sensitivity. This will also affect the distribution of parameters into identifiable regional patterns, which is a common limitation in the conceptual water balance model (Beven, 2011). Two similar models may have different optimized parameter sets, and it is also likely that the optimized parameter sets should be transferred in their entirety and not as individual parameters (Beven and Binley, 1992; Beven and Freer, 2001). Information contained in the optimized parameter set is specific to the modelled roof, and thus may not be transferable to another roof model (a singularity problem). This might be due to data error compensation (precipitation or/and runoff), as the precipitation measurements are affected both by the wind and under catches of intense rain. Another likely issue is the bias contained the model by the optimization period and its specific climatic conditions in addition to the model conceptualization error (Poissant et al., 2017).

There is a possible explanation for the mismatch between observed and simulated runoffs during the winter period (Paper 3). The SWMM model simulates runoff from rainfall, or snow accumulation from snowfall, according to the observed air temperature. This temperature, however, does not correspond to the temperature inside the medium (substrate) or around the roof outlet where runoff is measured. Having negative air temperatures and positive medium temperatures may therefore lead to continuously observed runoff, while the model accounts for snow accumulation.

The water balance was inspected during the catchment modelling (Paper 5) in the model with and without implemented roofs. It was found that the model accounted for an evaporation loss of 2.7% for set-up without roof implementation. Whereas the evaporation loss from the green roof implementation was 5.4 %, and the grey roof implementation was even higher at 5.8 %. This shows that the LID Green roof module does not adequately simulate the evaporation loss from the roof with and without vegetation (the evaporation loss for the grey roof was overestimated).

After several rainfalls, the observed base flow in the stormwater pipe lasted for several extended periods (Paper 5). This was, however, not the case for the simulated runoff, which disappeared sooner after the rain stopped. Water redistribution between sub-catchments and subareas may differ from season to season and from event to event. This may also apply to pipe infiltration from ground water, which presumably changes from season to season.

It was noticed that the input data (primarily precipitation and flow data) contained unexpected events, e.g., due to calibration of the rain gauge or maintenance of the drainage network due to

the use of a flushing device (regular pipe cleaning by the municipality). It concedes an uncertainty regarding the simulated results. The model could not accurately model all the periods of the year and all the events due to parameter uncertainty, uncertainty in the model's structure, uncertainty in flow redistribution between individual sub-catchments and subareas, and uneven precipitation distribution over the catchment (especially during extreme events).

The implementation of retrofitted rooftops upstream and downstream revealed the importance of concentration time for particular sections within the entire catchment. This means that the roof implementation may change the travel time to the catchment outlet less favourably with respect to peak runoffs. For catchments with multiple subareas, the concentration time must be considered individually.

Chapter 4 Conclusions and recommendations

This chapter concludes the thesis and summarizes the finding organized around the research questions presented in Section 1.2 Research questions. It also provides suggestions for future work based on the experiences and results obtained in the present study.

4.1 Conclusions

Long-term and short-term hydrological performance of retention and detention-based (vegetated and non-vegetated) roofs were analysed to identify best practice for the design of these roofs with respect to stormwater management. The hydrological performance of two complete solutions consisting of green and grey roofs were compared to a reference black roof.

Two different solutions comprised of vegetated (green) and non-vegetated (grey) configurations were compared in terms of hydrological performance between 2017 and 2019. While the first solution (*Solution 1*) consisted of:

- an extensive green roof with a 30-mm thick layer of Sedum,
- a non-vegetated grey roof with a 200-mm thick layer of expanded clay,
- and a reference black roof,

the second solution (*Solution 2*) contained:

- a detention-based green roof with a 100-mm thick layer of expanded clay,
- a non-vegetated grey roof with a 100-mm thick layer of expanded clay,
- and the reference black roof.

It was found that the green roofs provided a higher level of retention than the grey roofs, especially during warm periods between 24-37 % of the long-term continuous runoff between May and October due to combined evapotranspiration. In comparison, the grey roofs had a limited retention rate of 10 % for both *Solutions 1* and *Solutions 2*. However, the grey roofs, which consisted of expanded clay as the primary storage medium, provided better runoff detention than the extensive green roof. Therefore, in the second solution, the 30-mm thick layer extensive green roof was underlaid with a 100-mm thick layer of expanded clay. This configuration provided the best combination of retention and detention performance for stormwater management. One special benefit observed was the dampening effect of the expanded clay layer, making it much more robust when handling short-duration intense rainfalls, which are a common disadvantage of the thinnest extensive roofs.

The detention performance of a detention-based green roof, consisting of sedum mats underlaid with expanded clay, was tested for current and future climate conditions under extreme precipitation using an artificial rainfall generator. Rainfall events were derived from DDF curves for three different cities, Bergen, Oslo and Trondheim and tested at the field station in Trondheim. The events corresponded to events with 20-year RP, including a climate factor of 1.4, for the future climate between 2071 and 2100 (the worst scenario with RCP 8.5) or to a variable return period between 2-year and more than 200-year RP for the current climate. It was confirmed that the use of a variable shape of short-duration hyetograph would lead to different performance. The rainfall pattern that peaked at the end caused the worst performance, and initial water content had a more considerable influence on the performance than the shape of the hyetograph. The roof can regenerate its storage capacity for large flows within a relatively short time and provide desired stormwater detention, which is represented by centroid delay or T50.

Although the EPA SWMM model was able to replicate green and grey roof runoffs in both the calibration and validation periods, it was challenging to identify individual parameters. Using observed precipitation and runoff data from multiple sites and configurations in the model showed a positive correlation between observed and simulated runoffs for both objective functions, the Nash-Sutcliffe model efficiency and volume error. The calibration revealed several parameters sets that provided comparable model performance. Therefore, the complete parameter sets should be used when transferring the models. The parameter identifiability was recognised during the calibration of the hydrological model due to an equifinality in the model.

It is a common limitation in the conceptual water balance model and indicates a greater parameter-related uncertainty.

In the watershed scale modelling study using PCSWMM, it was found that retrofitting of all flat roofs with the green or grey roofs would have a positive effect on urban hydrology. The roof implementation showed essential improvements, specifically in terms of peak flows. While both green and grey roofs had the same effect on reducing the largest flow by decreasing it by 17 %, the grey roof provided better results with respect to other performance indicators. For example, when considering 100 L/s as an activation threshold for combined sewer overflows at the catchment outlet, rooftop retrofitting with the grey roof would decrease the duration of these overflows by 54 %, the number of overflows by 38 % and the volume of overflows by 64 %. A scenario of doubling the total grey roof area would cause a reduction of the maximum flow by 35 %. The performance, in terms of reduction of maximum flows, increases in line with an increase of the area for potential retrofitting by green and/or grey roofs and with a decrease of the catchment slope. Concerning the exceedance thresholds, the grey roofs' implementation outperformed the green roofs in all aspects: duration, number, and volume of exceedance.

4.2 Recommendations for future work

Based on the experiences and results obtained in the present study, a few suggestions for future work may be offered. There is a certain limitation in having only about one year of observed data per each solution. It could therefore be good to test the solutions for more extended periods (several years) to obtain a broader and more detailed performance span in addition to an improved basis for statistics on larger events as well as frequent daily events.

- Investigations on the lateral flow part of the roof in order to understand and describe this part better, as the resistance to lateral flow clearly influences detention.
- Obtain more performance indicators for the tested extreme events and run events with longer durations for Bergen, Oslo and Trondheim as well as different locations.
- Use the test data on extreme precipitation for calibrating the EPA SWMM model and compare the obtained parameters with the parameters from Papers 3 and 4.
- Use data from other monitored SUDS (e.g., green roof, grey roof, rain garden) and model runoff as a stormwater treatment train.

References

- Ahiablame, L. and Shakya, R. 2016. Modeling flood reduction effects of low impact development at a watershed scale. *Journal of environmental management* 171, 81-91.
- Alfredo, K., Montalto, F. and Goldstein, A. 2009. Observed and modeled performances of prototype green roof test plots subjected to simulated low-and high-intensity precipitations in a laboratory experiment. *Journal of Hydrologic Engineering* 15(6), 444-457.
- Barbosa, A.E., Fernandes, J.N. and David, L.M. 2012. Key issues for sustainable urban stormwater management. *Water research* 46(20), 6787-6798.
- Bengtsson, L. 2005. Peak flows from thin sedum-moss roof. *Hydrology Research* 36(3), 269-280.
- Bengtsson, L., Grahn, L. and Olsson, J. 2005. Hydrological function of a thin extensive green roof in southern Sweden. *Hydrology Research* 36(3), 259-268.
- Berghage, R.D., Beattie, D., Jarrett, A.R., Thuring, C., Razaeei, F. and O'Connor, T.P. 2009. Green roofs for stormwater runoff control, Citeseer.
- Berndtsson, J.C. 2010. Green roof performance towards management of runoff water quantity and quality: A review. *Ecological Engineering* 36(4), 351-360.
- Berretta, C., Poë, S. and Stovin, V. 2014. Moisture content behaviour in extensive green roofs during dry periods: The influence of vegetation and substrate characteristics. *Journal of Hydrology* 511, 374-386.
- Besir, A.B. and Cuce, E. 2018. Green roofs and facades: A comprehensive review. *Renewable and Sustainable Energy Reviews* 82, 915-939.
- Beven, K. and Binley, A. 1992. The future of distributed models: model calibration and uncertainty prediction. *Hydrological processes* 6(3), 279-298.
- Beven, K. and Freer, J. 2001. Equifinality, data assimilation, and uncertainty estimation in mechanistic modelling of complex environmental systems using the GLUE methodology. *Journal of hydrology* 249(1-4), 11-29.
- Beven, K.J. (2011) *Rainfall-runoff modelling: the primer*, John Wiley & Sons.
- Bianchini, F. and Hewage, K. 2012. Probabilistic social cost-benefit analysis for green roofs: a lifecycle approach. *Building and Environment* 58, 152-162.
- BIPM, I., IFCC, I., ISO, I. and IUPAP, O. 2009. Evaluation of measurement data—An introduction to the “Guide to the expression of uncertainty in measurement” and related documents. *JCGM* 104, 1-104.
- Borris, M., Viklander, M., Gustafsson, A.M. and Marsalek, J. 2014. Modelling the effects of changes in rainfall event characteristics on TSS loads in urban runoff. *Hydrological Processes* 28(4), 1787-1796.
- Burkhard, R., Deletic, A. and Craig, A. 2000. Techniques for water and wastewater management: a review of techniques and their integration in planning. *Urban water* 2(3), 197-221.
- Carson, T., Keeley, M., Marasco, D.E., McGillis, W. and Culligan, P. 2017. Assessing methods for predicting green roof rainfall capture: A comparison between full-scale observations and four hydrologic models. *Urban Water Journal* 14(6), 589-603.

- Carson, T., Marasco, D., Culligan, P. and McGillis, W. 2013. Hydrological performance of extensive green roofs in New York City: observations and multi-year modeling of three full-scale systems. *Environmental Research Letters* 8(2), 024036.
- Carter, T. and Jackson, C.R. 2007. Vegetated roofs for stormwater management at multiple spatial scales. *Landscape and urban planning* 80(1), 84-94.
- Carter, T.L. and Rasmussen, T.C. 2006. Hydrologic behavior of vegetated roofs. *JAWRA Journal of the American Water Resources Association* 42(5), 1261-1274.
- Castleton, H.F., Stovin, V., Beck, S.B. and Davison, J.B. 2010. Green roofs; building energy savings and the potential for retrofit. *Energy and buildings* 42(10), 1582-1591.
- Changnon, S.A. and Demissie, M. 1996. Detection of changes in streamflow and floods resulting from climate fluctuations and land use-drainage changes. *Climatic change* 32(4), 411-421.
- Chocat, B., Ashley, R., Marsalek, J., Matos, M., Rauch, W., Schilling, W. and Urbonas, B. 2007. Toward the sustainable management of urban storm-water. *Indoor and built environment* 16(3), 273-285.
- Cipolla, S.S., Maglionico, M. and Stojkov, I. 2016. A long-term hydrological modelling of an extensive green roof by means of SWMM. *Ecological Engineering* 95, 876-887.
- Copenhagen, T.c.o. 2012. Cloudburst Management Plan 2012. Copenhagen, T.a.E.A. (ed).
- Davis, A.P., Hunt, W.F., Traver, R.G. and Clar, M. 2009. Bioretention technology: Overview of current practice and future needs. *Journal of Environmental Engineering* 135(3), 109-117.
- Deletic, A. 1998. The first flush load of urban surface runoff. *Water research* 32(8), 2462-2470.
- Delleur, J.W. 2003. The evolution of urban hydrology: past, present, and future. *Journal of hydraulic engineering* 129(8), 563-573.
- DeNardo, J., Jarrett, A., Manbeck, H., Beattie, D. and Berghage, R. 2003. Stormwater detention and retention abilities of green roofs, pp. 1-7.
- Devia, G.K., Ganasri, B. and Dwarakish, G. 2015. A review on hydrological models. *Aquatic Procedia* 4, 1001-1007.
- Duan, H.-F., Li, F. and Yan, H. 2016. Multi-objective optimal design of detention tanks in the urban stormwater drainage system: LID implementation and analysis. *Water Resources Management* 30(13), 4635-4648.
- Duan, Q., Sorooshian, S. and Gupta, V. 1992. Effective and efficient global optimization for conceptual rainfall-runoff models. *Water resources research* 28(4), 1015-1031.
- Dunne, T. and Black, R.D. 1970. Partial area contributions to storm runoff in a small New England watershed. *Water resources research* 6(5), 1296-1311.
- Dunnett, N. and Kingsbury, N. (2008) *Planting green roofs and living walls*, Timber press Portland, OR.
- Dyrddal, A.V. and Førland, E.J. 2019. Klimapåslag for korttidsnedbør - Anbefalte verdier for Norge, Norwegian Climate Service Center.
- Fassman-Beck, E., Voyde, E., Simcock, R. and Hong, Y.S. 2013. 4 Living roofs in 3 locations: Does configuration affect runoff mitigation? *Journal of hydrology* 490, 11-20.
- Feng, Y. and Burian, S. 2016. Improving Evapotranspiration Mechanisms in the US Environmental Protection Agency's Storm Water Management Model. *Journal of Hydrologic Engineering* 21(10), 06016007.
- Fletcher, T.D., Shuster, W., Hunt, W.F., Ashley, R., Butler, D., Arthur, S., Trowsdale, S., Barraud, S., Semadeni-Davies, A. and Bertrand-Krajewski, J.-L. 2015. SUDS, LID, BMPs, WSUD and more—The evolution and application of terminology surrounding urban drainage. *Urban Water Journal* 12(7), 525-542.
- FLL (2008) *Guidelines for the planning, construction and maintenance of green roofing: Green roofing guideline*, Forschungsgesellschaft Landschaftsentwicklung Landschaftsbau, Landscape, Research, Development & Construction Society, Bonn, Germany.
- Førland, E., Allerup, P., Dahlström, B., Elomaa, E., Jönsson, T., Madsen, H., Perälä, J., Rissanen, P., Vedin, H. and Vejen, F. 1996. Manual for operational correction of Nordic precipitation data. *Klima Report* 24, 96.
- Garofalo, G., Palermo, S., Principato, F., Theodosiou, T. and Piro, P. 2016. The Influence of Hydrologic Parameters on the Hydraulic Efficiency of an Extensive Green Roof in Mediterranean Area. *Water* 8(2), 44.

- Getter, K.L., Rowe, D.B. and Andresen, J.A. 2007. Quantifying the effect of slope on extensive green roof stormwater retention. *Ecological engineering* 31(4), 225-231.
- Gill, S.E., Handley, J.F., Ennos, A.R. and Pauleit, S. 2007. Adapting cities for climate change: the role of the green infrastructure. *Built environment* 33(1), 115-133.
- Gleick, P.H. 2014. *The world's water.: the biennial report on freshwater resources* Volume 8.
- Gregoire, B.G. and Clausen, J.C. 2011. Effect of a modular extensive green roof on stormwater runoff and water quality. *Ecological Engineering* 37(6), 963-969.
- Hailegeorgis, T.T. and Alfredsen, K. 2018. High spatial–temporal resolution and integrated surface and subsurface precipitation-runoff modelling for a small stormwater catchment. *J. Hydrol.* 557, 613-630.
- Hakimdavar, R., Culligan, P.J., Finazzi, M., Barontini, S. and Ranzi, R. 2014. Scale dynamics of extensive green roofs: Quantifying the effect of drainage area and rainfall characteristics on observed and modeled green roof hydrologic performance. *Ecological engineering* 73, 494-508.
- Hamouz, V., Lohne, J., Wood, J.R. and Muthanna, T.M. 2018. Hydrological Performance of LECA-Based Roofs in Cold Climates. *Water* 10(3), 263.
- Hamouz, V. and Muthanna, T.M. 2019. Hydrological modelling of green and grey roofs in cold climate with the SWMM model. *Journal of environmental management* 249, 109350.
- Hanssen-Bauer, I., Drange, H., Førland, E., Roald, L., Børsheim, K., Hisdal, H., Lawrence, D., Nesje, A., Sandven, S. and Sorteberg, A. 2017. Climate in Norway 2100. Background information to NOU Climate adaptation (In Norwegian: Klima i Norge 2100. Bakgrunnsmateriale til NOU Klimatilpassing), Oslo: Norsk klimasenter.
- Hoegh-Guldberg, O., Jacob, D., Taylor, M., Bindi, M., Brown, S., Camilloni, I., Diedhiou, A., Djalante, R., Ebi, K. and Engelbrecht, F. 2018. Impacts of 1.5 °C global warming on natural and human systems.
- Ipcc 2014 Summary for policymakers. In: *Impacts, Adaptation, and Vulnerability. Part A: Global and Sectoral Aspects. Contribution of Working Group II to the Fifth Assessment Report of the Intergovernmental Panel on Climate Change.* Cambridge University Press, C.U.K. and New York, N.Y.U.S.A.p. (eds).
- Ipcc 2018 Summary for Policymakers. In: *Global Warming of 1.5°C. An IPCC Special Report on the impacts of global warming of 1.5°C above pre-industrial levels and related global greenhouse gas emission pathways, in the context of strengthening the global response to the threat of climate change, sustainable development, and efforts to eradicate poverty.* World Meteorological Organization, G.S.p. (ed).
- James, W., Rossman, L.A. and James, W.R.C. 2010 *User's guide to SWMM 5: Based on original USEPA SWMM documentation, CHI.*
- Jarden, K.M., Jefferson, A.J. and Grieser, J.M. 2016. Assessing the effects of catchment-scale urban green infrastructure retrofits on hydrograph characteristics. *Hydrological Processes* 30(10), 1536-1550.
- Jia, H., Yao, H., Tang, Y., Shaw, L.Y., Field, R. and Tafuri, A.N. 2015. LID-BMPs planning for urban runoff control and the case study in China. *Journal of environmental management* 149, 65-76.
- Johannessen, B., Muthanna, T. and Braskerud, B. 2018. Detention and retention behavior of four extensive green roofs in three nordic climate zones. *Water* 10(6), 671.
- Johannessen, B.G., Hamouz, V., Gragne, A.S. and Muthanna, T.M. 2019. The transferability of SWMM model parameters between green roofs with similar build-up. *Journal of Hydrology* 569, 816-828.
- Johannessen, B.G., Hanslin, H.M. and Muthanna, T.M. 2017. Green roof performance potential in cold and wet regions. *Ecological Engineering* 106, 436-447.
- Johannessen, B.G. and Muthanna, T. 2016. Hydraulic performance of extensive green roofs in cold climate. *Contrôle à la source/Source control.*
- Kim, L.-H., Zoh, K.-D., Jeong, S.-m., Kayhanian, M. and Stenstrom, M.K. 2006. Estimating pollutant mass accumulation on highways during dry periods. *Journal of Environmental Engineering* 132(9), 985-993.
- Krebs, G., Kuoppamäki, K., Kokkonen, T. and Koivusalo, H. 2016. Simulation of green roof test bed runoff. *Hydrological processes* 30(2), 250-262.

- Lamond, J.E., Rose, C.B. and Booth, C.A. 2015. Evidence for improved urban flood resilience by sustainable drainage retrofit. *Proceedings of the Institution of Civil Engineers-Urban Design and Planning* 168(2), 101-111.
- LeFevre, G.H., Paus, K.H., Natarajan, P., Gulliver, J.S., Novak, P.J. and Hozalski, R.M. 2015. Review of dissolved pollutants in urban storm water and their removal and fate in bioretention cells. *Journal of Environmental Engineering* 141(1), 04014050.
- Leopold, L.B. 1968. *Hydrology for urban land planning: A guidebook on the hydrologic effects of urban land use.*
- Li, Y. and Babcock, R.W. 2014. Green roof hydrologic performance and modeling: a review. *Water Science and Technology* 69(4), 727-738.
- Lindholm, O.G., Endresen, S., Thorolfsson, S.T., Sægrov, S., Jakobsen, G. and Aaby, L. 2008. *Veiledning i klimatilpasset overvannshåndtering. Rapport 162, 2008.*
- Liong, S., Chan, W. and Lum, L. 1991. Knowledge-based system for SWMM runoff component calibration. *Journal of Water Resources Planning and Management* 117(5), 507-524.
- Liu, K. and Minor, J. 2005. Performance evaluation of an extensive green roof. Presentation at Green Rooftops for Sustainable Communities, Washington DC 1, 1-11.
- Locatelli, L., Mark, O., Mikkelsen, P.S., Arnbjerg-Nielsen, K., Jensen, M.B. and Binning, P.J. 2014. Modelling of green roof hydrological performance for urban drainage applications. *Journal of hydrology* 519, 3237-3248.
- Madsen, H., Lawrence, D., Lang, M., Martinkova, M. and Kjeldsen, T. 2014. Review of trend analysis and climate change projections of extreme precipitation and floods in Europe. *J. Hydrol.* 519, 3634-3650.
- Mailhot, A. and Duchesne, S. 2009. Design criteria of urban drainage infrastructures under climate change. *Journal of Water Resources Planning and Management* 136(2), 201-208.
- Marsalek, J. and Chocat, B. 2002. International report: stormwater management. *Water science and technology* 46(6-7), 1-17.
- Matheussen, B.V. 2004. Effects of anthropogenic activities on snow distribution, and melt in an urban environment.
- Mentens, J., Raes, D. and Hermy, M. 2006. Green roofs as a tool for solving the rainwater runoff problem in the urbanized 21st century? *Landscape and urban planning* 77(3), 217-226.
- Nawaz, R., McDonald, A. and Postoyko, S. 2015. Hydrological performance of a full-scale extensive green roof located in a temperate climate. *Ecological Engineering* 82, 66-80.
- Niazi, M., Nietch, C., Maghrebi, M., Jackson, N., Bennett, B.R., Tryby, M. and Massoudieh, A. 2017. Storm water management model: performance review and gap analysis. *Journal of Sustainable Water in the Built Environment* 3(2), 04017002.
- Nie, L., Lindholm, O., Lindholm, G. and Syversen, E. 2009. Impacts of climate change on urban drainage systems—a case study in Fredrikstad, Norway. *Urban Water Journal* 6(4), 323-332.
- O'Loughlin, G., Beecham, S., Lees, S., Rose, L. and Nicholas, D. 1995. On-site stormwater detention systems in Sydney. *Water Science and Technology* 32(1), 169-175.
- Oberndorfer, E., Lundholm, J., Bass, B., Coffman, R.R., Doshi, H., Dunnett, N., Gaffin, S., Köhler, M., Liu, K.K. and Rowe, B. 2007. Green roofs as urban ecosystems: ecological structures, functions, and services. *BioScience* 57(10), 823-833.
- Palla, A. and Gnecco, I. 2015. Hydrologic modeling of Low Impact Development systems at the urban catchment scale. *Journal of Hydrology* 528, 361-368.
- Paus, K.A.H. 2016. Toxic metal removal and hydraulic capacity in bioretention cells in cold climate regions.
- Peel, M.C., Finlayson, B.L. and McMahon, T.A. 2007. Updated world map of the Köppen-Geiger climate classification. *Hydrology and earth system sciences discussions* 4(2), 439-473.
- Peng, Z. and Stovin, V. 2017. Independent validation of the SWMM green roof module. *Journal of Hydrologic Engineering* 22(9), 04017037.
- Poë, S., Stovin, V. and Berretta, C. 2015. Parameters influencing the regeneration of a green roof's retention capacity via evapotranspiration. *Journal of Hydrology* 523, 356-367.
- Poissant, D., Arsenaault, R. and Brissette, F. 2017. Impact of parameter set dimensionality and calibration procedures on streamflow prediction at ungauged catchments. *Journal of Hydrology: Regional Studies* 12, 220-237.

- Rosa, D.J., Clausen, J.C. and Dietz, M.E. 2015. Calibration and verification of SWMM for low impact development. *JAWRA Journal of the American Water Resources Association* 51(3), 746-757.
- Rossman, L. 2015. *SWMM 5.1 Storm Water Management Model User's Manual*, US Environmental Protection Agency, Cincinnati, OH.
- Rossman, L. and Huber, W. 2016a. *Storm Water Management Model Reference Manual Volume I—Hydrology (Revised)*. US Environmental Protection Agency: Cincinnati, OH, USA.
- Rossman, L. and Huber, W. 2016b. *Storm Water Management Model Reference Manual: Volume III—Water Quality*. US Environmental Protection Agency, Office of Research and Development, National Risk Management Laboratory: Cincinnati, OH, USA.
- Saadatian, O., Sopian, K., Salleh, E., Lim, C., Riffat, S., Saadatian, E., Toudeshki, A. and Sulaiman, M. 2013. A review of energy aspects of green roofs. *Renewable and Sustainable Energy Reviews* 23, 155-168.
- Semadeni-Davies, A., Hernebring, C., Svensson, G. and Gustafsson, L.-G. 2008. The impacts of climate change and urbanisation on drainage in Helsingborg, Sweden: Combined sewer system. *Journal of Hydrology* 350(1), 100-113.
- Soulis, K.X., Valiantzas, J.D., Ntoulas, N., Kargas, G. and Nektarios, P.A. 2017. Simulation of green roof runoff under different substrate depths and vegetation covers by coupling a simple conceptual and a physically based hydrological model. *Journal of environmental management* 200, 434-445.
- Stocker, T. (2014) *Climate change 2013: the physical science basis: Working Group I contribution to the Fifth assessment report of the Intergovernmental Panel on Climate Change*, Cambridge University Press.
- Stovin, V., Poë, S. and Berretta, C. 2013. A modelling study of long term green roof retention performance. *Journal of environmental management* 131, 206-215.
- Stovin, V., Poë, S., De-Ville, S. and Berretta, C. 2015. The influence of substrate and vegetation configuration on green roof hydrological performance. *Ecological Engineering* 85, 159-172.
- Stovin, V., Vesuviano, G. and De-Ville, S. 2017. Defining green roof detention performance. *Urban Water Journal* 14(6), 574-588.
- Stovin, V., Vesuviano, G. and Kasmin, H. 2012. The hydrological performance of a green roof test bed under UK climatic conditions. *Journal of Hydrology* 414, 148-161.
- Teegavarapu, R.S. (2012) *Floods in a changing climate: extreme precipitation*, Cambridge University Press.
- Torgersen, G., Bjerkholt, J.T. and Lindholm, O.G. 2014. Addressing Flooding and SuDS when Improving Drainage and Sewerage Systems—A Comparative Study of Selected Scandinavian Cities. *Water* 6(4), 839-857.
- Trowsdale, S.A. and Simcock, R. 2011. Urban stormwater treatment using bioretention. *J. Hydrol.* 397(3-4), 167-174.
- Vanuytrecht, E., Van Mechelen, C., Van Meerbeek, K., Willems, P., Hermy, M. and Raes, D. 2014. Runoff and vegetation stress of green roofs under different climate change scenarios. *Landscape and Urban Planning* 122, 68-77.
- VanWoert, N.D., Rowe, D.B., Andresen, J.A., Rugh, C.L., Fernandez, R.T. and Xiao, L. 2005. Green roof stormwater retention. *Journal of environmental quality* 34(3), 1036-1044.
- Vijayaraghavan, K. 2016. Green roofs: A critical review on the role of components, benefits, limitations and trends. *Renewable and sustainable energy reviews* 57, 740-752.
- Villarreal, E.L. 2007. Runoff detention effect of a sedum green-roof. *Hydrology Research* 38(1), 99-105.
- Villarreal, E.L. and Bengtsson, L. 2005. Response of a Sedum green-roof to individual rain events. *Ecological Engineering* 25(1), 1-7.
- Voyde, E., Fassman, E. and Simcock, R. 2010. Hydrology of an extensive living roof under sub-tropical climate conditions in Auckland, New Zealand. *Journal of hydrology* 394(3), 384-395.
- Wilby, R.L. 2005. Uncertainty in water resource model parameters used for climate change impact assessment. *Hydrological Processes: An International Journal* 19(16), 3201-3219.
- Willems, P., Arnbjerg-Nielsen, K., Olsson, J. and Nguyen, V. 2012. Climate change impact assessment on urban rainfall extremes and urban drainage: methods and shortcomings. *Atmospheric research* 103, 106-118.

- Woods-Ballard, B., Kellagher, R., Martin, P., Jefferies, C., Bray, R. and Shaffer, P. (2007) *The SUDS Manual*, Ciria London.
- Yang, J., Yu, Q. and Gong, P. 2008. Quantifying air pollution removal by green roofs in Chicago. *Atmospheric environment* 42(31), 7266-7273.
- Zhou, Q. 2014. A review of sustainable urban drainage systems considering the climate change and urbanization impacts. *Water* 6(4), 976-992.

Appendix A: Supplementary materials

Table 15 Material characteristics of green roof substrate and expanded clay

Parameter	Units	Expanded clay 1.5-2.5 mm	Expanded clay 0-6 mm	Green roof substrate	Method
Particle density	g/cm ³	1.05±0.05	0.92±0.03	-	*Porous plate
Particle density	g/cm ³	0.91	0.89	1.64	Calculated
Bulk density	g/cm ³	0.48±0.01	0.43±0.00	-	*Porous plate
Bulk density	g/cm ³	0.41±0.03	0.39±0.06	1.02±0.09	**FLL
Porosity	% v/v	54.2±1.8	53.7±1.5	-	*Porous plate
Porosity	% v/v	54.7±1.8	56.2±0.3	38.2±0.2	**FLL
Wilting point	% v/v	12.6±0.1	6.5±1.5	-	*Porous plate
Field capacity	% v/v	15.2±0.5	9.1±0.5	-	*Porous plate
Maximum water holding capacity	% v/v	18.3±1.3	30.1±1.8	29.5±1.9	**FLL
Hydraulic conductivity	cm/h	143.2±38.2	105.2±28.3	-	***Darcy's law

* Porous plate apparatus method, laboratory of the Norwegian University of Life Sciences in Ås
** FLL (2008)
*** Flow of a fluid through a porous medium

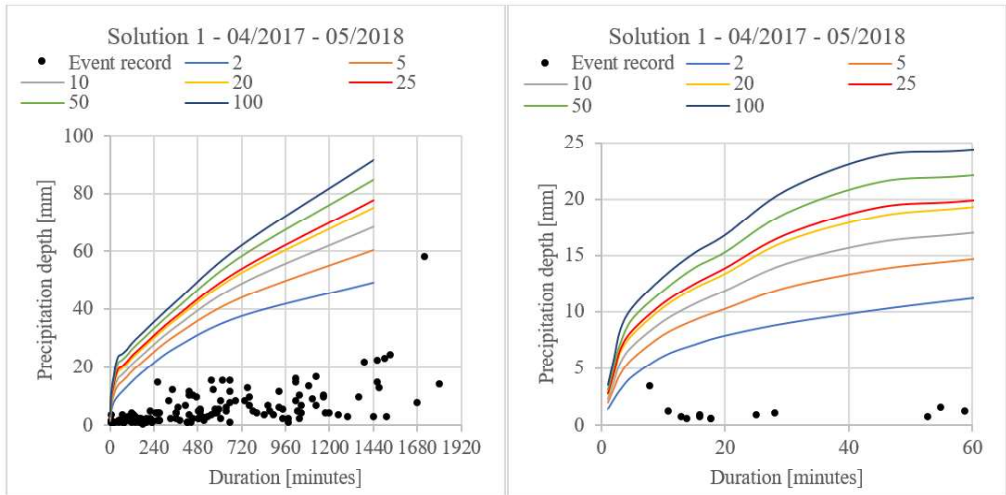


Figure 10 Comparison of the event record with the Depth-Duration-Frequency (DDF) curves for **Solution 1**.

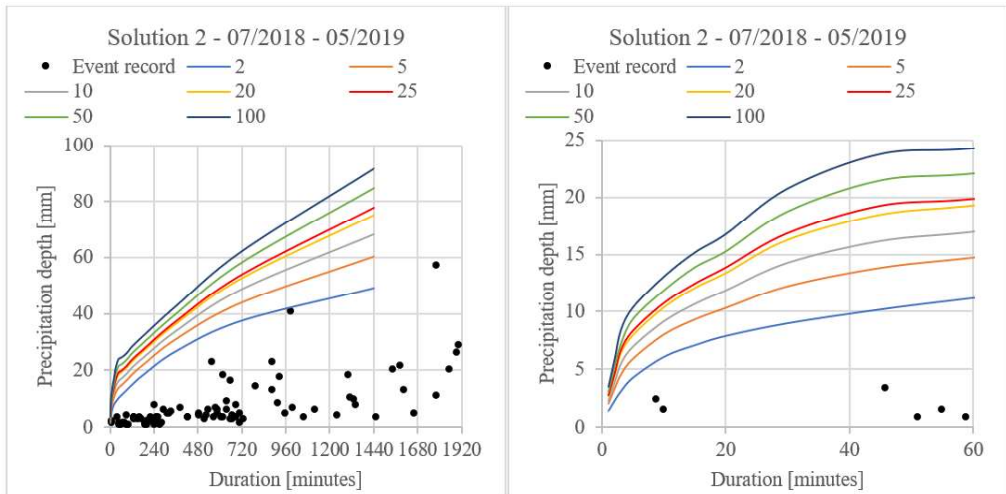


Figure 11 Comparison of the event record with the Depth-Duration-Frequency (DDF) curves for **Solution 2**.

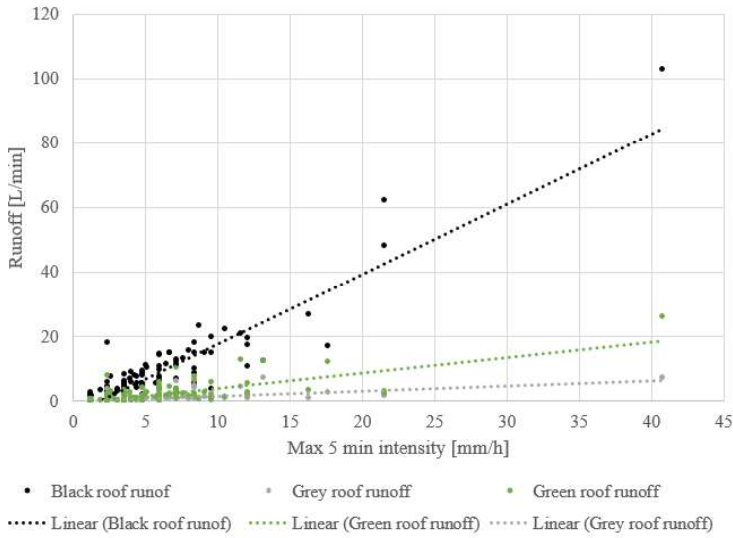


Figure 12 Observed maximum black roof runoffs and runoffs corresponding to the extensive green and grey roofs for **Solution 1**.

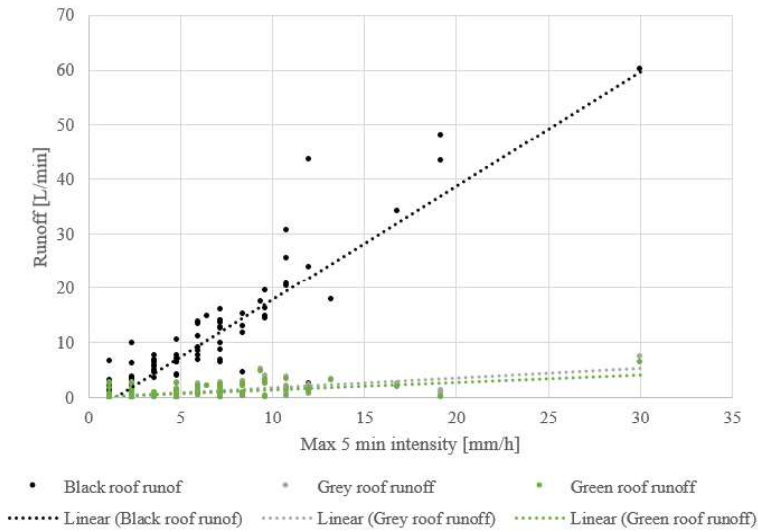


Figure 13 Observed maximum black roof runoffs and runoffs corresponding to the detention-based green and grey roofs for **Solution 2**.

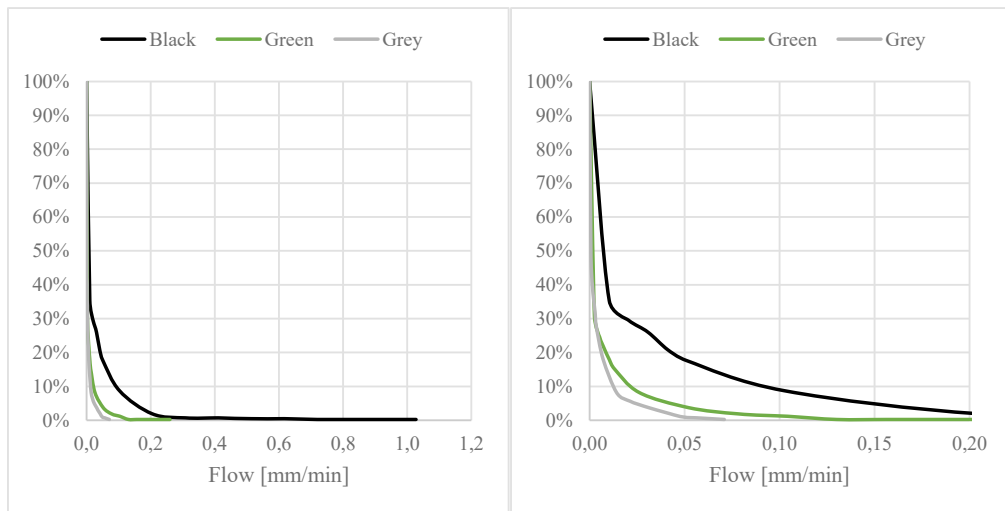


Figure 14 Probability exceedance of the black, extensive green and grey roof runoffs for **Solution 1**.

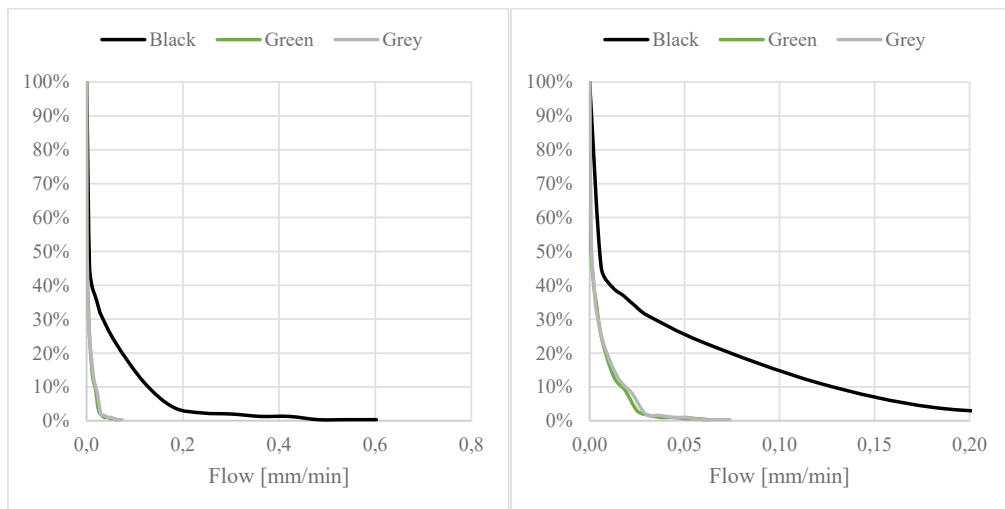


Figure 15 Probability exceedance of the black, detention-based green and grey roof runoffs for **Solution 2**.

Table 16 Ten largest events within the **cold** period according to the maximum black roof runoff for **Solution 1**, including peak delay for the extensive green and grey roofs with respect to the black roof.

Event nr	Type	Start	Duration [hours]	Precipitation depth [mm]	Mean int. [mm/h]	Max 5-min int. [mm/h]	Peak delay	
							[black vs. grey]	[black vs. green]
81	Rain	09.11.2017	17:03	14.0	0.8	12.0	7:22	0:44
79	Rain	05.11.2017	23:19	21.3	0.9	2.4	4:13	1:07
6	Mixed	20.04.2017	69:34	39.5	0.6	17.6	2:30	0:14
84	ROS	14.11.2017	25:13	22.5	0.9	9.6	23:48	no delay
91	ROS	08.12.2017	25:38	24.0	0.9	13.2	0:34	0:03
4	Mixed	09.04.2017	39:28	16.8	0.4	5.0	4:27	0:29
82	Rain	11.11.2017	18:51	16.2	0.9	7.2	4:06	0:07
89	Rain	01.12.2017	101:04	61.7	0.6	12.0	25:36	no delay
97	Rain	21.12.2017	75:49	34.7	0.5	8.4	16:37	0:10
141	Rain	20.04.2018	30:04	13.7	0.5	6.0	2:39	0:42
Median							4:20	0:21
Mean							9:11	0:27

Table 17 Ten largest events within the **cold** period according to the maximum black roof runoff for **Solution 1**, including peak and volume reduction for the extensive green and grey roofs with respect to the black roof.

Event nr	Peak reduction	Peak reduction	Volume reduction	Volume reduction	Grey degree of saturation	Green degree of saturation
	[black vs. grey]	[black vs. green]	[black vs. grey]	[black vs. green]		
81	93 %	87 %	7 %	9 %	33 %	63 %
79	81 %	56 %	16 %	13 %	32 %	59 %
6	85 %	30 %	-5 %	7 %		
84	95 %	91 %	9 %	7 %	33 %	70 %
91	43 %	0 %	0 %	-1 %	47 %	57 %
4	93 %	76 %	8 %	18 %		
82	87 %	68 %	26 %	22 %	33 %	68 %
89	82 %	50 %	43 %	7 %	11 %	18 %
97	55 %	26 %	8 %	7 %	18 %	37 %
141	80 %	52 %	-22 %	34 %	44 %	51 %
Median	84 %	54 %	8 %	8 %		
Mean	79 %	53 %	9 %	12 %		

Table 18 Ten largest events within the **warm** period according to the maximum black roof runoff for **Solution 1**, including peak delay for the extensive green and grey roofs with respect to the black roof.

Event nr	Type	Start	Duration [hours]	Precipitation depth [mm]	Mean int. [mm/h]	Max 5-min int. [mm/h]	Peak delay	
							[black vs. grey]	[black vs. green]
50	rain	19.08.2017	28:47	58.1	2.0	40.8	12:17	0:02
41	rain	26.07.2017	0:08	3.4	25.6	21.6	0:00	0:01
53	rain	29.08.2017	7:15	11.4	1.6	21.6	7:35	5:23
34	rain	12.07.2017	19:35	9.0	0.5	16.3	0:01	10:49
42	rain	31.07.2017	1:38	2.8	1.7	8.8	0:00	0:04
31	rain	09.07.2017	6:05	3.9	0.6	10.6	0:29	0:30
23	rain	17.06.2017	74:38	60.4	0.8	11.6	36:42	35:31
66	rain	07.10.2017	9:17	15.2	1.6	9.6	6:30	0:01
64	rain	05.10.2017	2:03	3.8	1.9	8.4	0:00	0:01
56	rain	13.09.2017	5:25	8.2	1.5	12.0	0:00	0:01
Median							0:15	0:03
Mean							6:21	5:14

Table 19 Ten largest events within the **warm** period according to the maximum black roof runoff for **Solution 1**, including peak and volume reduction for the extensive green and grey roofs with respect to the black roof.

Event nr	Peak reduction	Peak reduction	Volume reduction	Volume reduction	Grey degree of saturation	Green degree of saturation
	[black vs. grey]	[black vs. green]	[black vs. grey]	[black vs. green]		
50	93 %	75 %	4 %	9 %	33 %	37 %
41	97 %	95 %	92 %	95 %	32 %	21 %
53	97 %	95 %	48 %	64 %	32 %	36 %
34	97 %	88 %	-5 %	8 %	36 %	59 %
42	100 %	100 %	33 %	71 %	33 %	14 %
31	97 %	95 %	-9 %	69 %	34 %	55 %
23	80 %	38 %	5 %	11 %		
66	88 %	71 %	-10 %	-4 %	36 %	64 %
64	96 %	89 %	69 %	58 %	34 %	49 %
56	95 %	92 %	34 %	92 %	32 %	16 %
Median	96 %	91 %	19 %	61 %		
Mean	94 %	84 %	26 %	47 %		

Table 20 Ten largest events within the **cold** period according to the maximum black roof runoff for **Solution 2**, including peak delay for the detention-based green and grey roofs with respect to the black roof.

Event nr	Type	Start	Duration [hours]	Precipitation depth [mm]	Mean int. [mm/h]	Max 5-min int. [mm/h]	Peak delay	Peak delay	
							[black vs. grey]	[black vs. green]	
Solution 2	93	Rain	29.03.2019	61:31	55.9	0.9	10.8	no delay	no delay
	98	Rain	29.04.2019	0:46	3.3	4.2	7.2	0:31	no runoff
	50	Rain	16.11.2018	5:34	5.4	1.0	6.0	2:19	0:06
	55	ROS	24.12.2018	64:25	52.2	0.8	7.2	4:19	0:10
	86	ROS	19.03.2019	21:40	17.9	0.8	8.4	1:55	0:06
	57	Rain	28.12.2018	34:24	26.3	0.8	7.2	15:19	14:07
	58	Rain	31.12.2018	35:43	28.2	0.8	7.2	no delay	0:11
	59	ROS	02.01.2019	102:07	72.7	0.7	8.4	36:29	36:26
	61	ROS	10.01.2019	58:20	28.1	0.5	6.0	3:01	1:04
	78	ROS	24.02.2019	5:18	4.5	0.9	7.2	7:23	0:05
Median							3:40	0:10	
Mean							8:54	6:31	

Table 21 Ten largest events within the **cold** period according to the maximum black roof runoff for **Solution 2**, including peak and volume reduction for the detention-based green and grey roofs with respect to the black roof.

Event nr	Peak reduction	Peak reduction	Volume reduction	Volume reduction	Grey degree	Green degree	
	[black vs. grey]	[black vs. green]	[black vs. grey]	[black vs. green]	of saturation	of saturation	
Solution 2	93	42 %	49 %	0 %	-4 %	32 %	52 %
	98	98 %	100 %	91 %	100 %	20 %	20 %
	50	97 %	96 %	25 %	38 %	24 %	45 %
	55	84 %	86 %	26 %	29 %	7 %	15 %
	86	81 %	84 %	18 %	21 %	16 %	35 %
	57	81 %	82 %	-11 %	-14 %	34 %	53 %
	58	86 %	85 %	-8 %	-6 %	31 %	52 %
	59	75 %	78 %	-8 %	-7 %	31 %	51 %
	61	84 %	88 %	12 %	16 %	25 %	45 %
	78	86 %	88 %	27 %	24 %	34 %	57 %
Median		84 %	85 %	15 %	19 %		
Mean		81 %	83 %	17 %	20 %		

Table 22 Ten largest events within the **warm** period according to the maximum black roof runoff for **Solution 2**, including peak delay for the detention-based green and grey roofs with respect to the black roof.

Event nr	Type	Start	Duration [hours]	Precipitation depth [mm]	Mean int. [mm/h]	Max 5-min int. [mm/h]	Peak delay	Peak delay	
							[black vs. grey]	[black vs. green]	
Solution 2	9	Rain	10.08.2018	29:49	57.2	1.9	30.0	no delay (-1)	0:00
	8	Rain	09.08.2018	0:09	2.2	15.0	19.2	0:02	0:04
	12	Rain	18.08.2018	41:10	13.2	0.3	12.0	0:01	0:07
	2	Rain	18.07.2018	9:40	6.8	0.7	19.2	0:01	no runoff
	29	Rain	25.09.2018	30:58	20.2	0.7	16.8	1:20	1:20
	7	Rain	09.08.2018	3:45	3.8	1.0	10.8	0:10	0:15
	21	Rain	12.09.2018	11:06	16.3	1.5	10.8	2:34	0:45
	6	Rain	05.08.2018	31:36	26.1	0.8	12.0	0:01	0:01
	27	Rain	22.09.2018	64:56	44.3	0.7	10.8	0:41	0:39
	45	Rain	23.10.2018	71:39	46.1	0.6	9.6	0:03	0:02
Median							0:03	0:07	
Mean							0:32	0:21	

Table 23 Ten largest events within the **warm** period according to the maximum black roof runoff for **Solution 2**, including peak and volume reduction for the detention-based green and grey roofs with respect to the black roof.

Event nr	Peak reduction	Peak reduction	Volume reduction	Volume reduction	Grey degree	Green degree	
	[black vs. grey]	[black vs. green]	[black vs. grey]	[black vs. green]	of saturation	of saturation	
Solution 2	9	88 %	90 %	1 %	7 %	27 %	37 %
	8	98 %	100 %	57 %	95 %	28 %	36 %
	12	97 %	98 %	-3 %	18 %	23 %	40 %
	2	97 %	100 %	79 %	100 %	19 %	13 %
	29	93 %	94 %	5 %	10 %	28 %	45 %
	7	98 %	99 %	69 %	98 %	27 %	34 %
	21	92 %	95 %	23 %	66 %	21 %	31 %
	6	91 %	95 %	12 %	85 %	20 %	14 %
	27	90 %	92 %	10 %	14 %	25 %	39 %
	45	85 %	87 %	0 %	-2 %	32 %	53 %
Median		93 %	95 %	11 %	42 %		
Mean		93 %	95 %	25 %	49 %		

Appendix B: Selected papers

The full version of the selected papers presented in this thesis are in the following chapter. The original formatting is preserved and does not conform to the general formatting of the thesis.

Paper 1

Hydrological performance of LECA-based roofs in cold climates

Hamouz, V., Lohne, J., Wood, J., & Muthanna, T. (2018).

Water, 10(3), 263. <https://doi.org/10.3390/w10030263>

Article

Hydrological Performance of LECA-Based Roofs in Cold Climates

Vladimír Hamouz ^{1,*}, Jardar Lohne ¹, Jaran R. Wood ² and Tone M. Muthanna ¹

¹ Department of Civil and Environmental Engineering, Norwegian University of Science and Technology, 7491 Trondheim, Norway; jardar.lohne@ntnu.no (J.L.); tone.muthanna@ntnu.no (T.M.M.)

² Leca International, Årnesvegen 1, 2009 Nordby, Norway; Jaran.Wood@Leca.no

* Correspondence: vladimir.hamouz@ntnu.no; Tel.: +47-410-70-318

Received: 15 December 2017; Accepted: 28 February 2018; Published: 3 March 2018

Abstract: Rooftops represent a considerable part of the impervious fractions of urban environments. Detaining and retaining runoff from vegetated rooftops can be a significant contribution to reducing the effects of urbanization, with respect to increased runoff peaks and volumes from precipitation events. However, in climates with limited evapotranspiration, a non-vegetated system is a convenient option for stormwater management. A LECA (lightweight expanded clay aggregate)-based roof system was established in the coastal area of Trondheim, Norway in 2016. The roof structure consists of a 200 mm-thick layer of LECA® lightweight aggregate, covered by a concrete pavement. The retention in the LECA-based roof was estimated at 9%, which would be equivalent to 0.27 mm/day for the entire period. The LECA-based configuration provided a detention performance for a peak runoff reduction of 95% (median) and for a peak delay of 1 h and 15 min (median), respectively. The relatively high moisture levels in the LECA-based roof did not affect the detention performance. Rooftop retrofitting as a form of source control may contribute to a change in runoff characteristics from conventional roofs. This study of the LECA-based roof configuration presents data and performance indicators for stormwater urban planners with regard to water detention capability.

Keywords: detention; cold climate; hydrological performance; LECA-based roof; lightweight aggregate; sustainable drainage systems (SuDS); water-detaining non-green roof

1. Introduction

Stormwater management is experiencing raised awareness due to an increased frequency of damaging rain-induced flood events across the world. The existing infrastructure is not typically fit to handle the combined effects of ever-increasing urbanization (including the proliferation of impervious surfaces) and climate change [1]. Densely-urbanized areas have limited space for retrofitting with green solutions, or for the reduction of imperviousness. This encourages communities to seek out new, emerging solutions. One possible way to rethink stormwater management is to focus on building rooftops. In developed cities, rooftops account for almost half of impervious surfaces [2].

New constructions and retrofitting existing buildings with sustainable drainage systems (SuDSs) seem to be efficient measures to counteract the effect of impervious covers in the cityscape [1,3,4]. Additionally, they contribute to the reduction of both sewer overflows and flood risks. Rooftop retrofitting differs from many other SuDS approaches, as it does not require additional land acquisition. Rooftop solutions such as green roofs belong to the first of the so-called three-step stormwater treatment train as a form of source control [5,6]. In 2008, the Norwegian Water Association adopted a national guideline for surface stormwater management that uses a three-step approach, where a source control should be able to collect and infiltrate runoff following small events (the rainfall intensity classification of small is location-specific) [7].

The main drivers behind rooftop source control are detention and retention of runoff. Retention occurs through the combined process of evapotranspiration for vegetated solutions, and its annual runoff reduction has been extensively investigated [8–13]. On the other hand, detention performance indicators are increasingly required by stormwater designers to alleviate urban flooding due to capacity exceedance in sewer systems [14,15]. Green roof performance depends largely on the local climate. Most studies scrutinized within the context of this research have reported limited hydrological performance in cold and wet climates, when evaporation and transpiration is limited due to climatic factors [14–20]. Johannessen et al. [20] investigated potential evapotranspiration in cold and wet regions across 14 locations in northern Europe, and concluded that retention on green roofs varied between 0% and 1% for Nordic countries in the winter period. In order to address the challenges outlined in the literature, it was decided to test the performance of a non-vegetated lightweight filter. For the sake of reference, this paper benchmarks the hydrological performance of the new non-vegetated solution against that of green roofs.

A LECA-based roof system was constructed at Høvringen (Trondheim, Norway), where the testing of roofs for water detention and retention are piloted. The Trondheim region registers an average of 150 days of precipitation a year [21]. Based on research studying the evapotranspiration and evaporation from vegetated and non-vegetated roofs, the water loss was comparable for both roofs for a period of approximately 50 h [22]. The following two weeks of dry period demonstrated that the additional ability of plants to transpire water outperformed the evaporation by more than 60%.

Hydrological performance indicators relevant to this study are peak flow reduction, peak flow delay with an event-based perspective, and retention within a long-term rainfall/runoff water balance perspective.

In order to address the hydrological performance of the LECA (lightweight expanded clay aggregate)-based roof, the following research questions were proposed:

- (1) What is the seasonal and annual retention capacity of the LECA-based roof in cold climates?
- (2) What is the event-based detention capacity of the LECA-based roof in cold climates?
- (3) How do antecedent stormwater events affect the hydrological performance of the examined roof?

Limitations to the Study

Given that this is an in-situ field setup, the study is limited to the actual weather phenomena that occurred during this period. As such, there was only one event with a return period greater than 2 years. Thus, a limited amount of data was collected to investigate the extreme performance of the roof.

2. A Brief Literature Review

A brief literature review was performed to address challenges within stormwater management, more specifically stormwater retention and detention on rooftops. Most of the relevant studies focused on rooftops with vegetation. Thus, water losses due to plant uptake show a clear difference when comparing results between vegetated and non-vegetated solutions. In this study, no transpiration was expected because of the non-vegetated setup. Furthermore, seasonally low evaporation rates were expected due to the cold and wet weather conditions [20,23]. The review identified the requirements of stormwater designers and planners regarding sustainable solutions that enable the reduction of annual runoff, as well as the management of short and large design vents. A dataset based on 18 studies was analyzed. Emphasis was given to studies which focused on non-vegetated roofs (including reference black roofs), as well as cold and wet climates. The majority of the studies were focused on retention performance, rather than detention.

Retention occurs during dry periods, when water is evaporated into the atmosphere. In terms of retention performance, VanWoert et al. [3] studied the total rainfall retention from different media. The retention ranged from 27.2% for gravel ballast to 50.4% for a bare growing media, and 60.6% for a green treatment. Similarly, Mentens et al. [1] compared the annual runoffs from green and gravel-covered roofs. They presented a 25% reduction for the gravel roof, and a 50% reduction for the green roof. Berghage et al. [22] reported the annual rainfall retention from three different setups. The retention ranged from 14.1% for an asphalt roof to 29.7% for a media roof, and 52.6% for a vegetated roof. Comparing LECA-based (non-vegetated) and vegetated setups, higher levels of retention were observed using vegetated beds [10], with an annual volumetric retention of 54.5% for a LECA-based setup and 75.1% for a green roof. Johannessen and Muthanna [24] presented an annual runoff reduction of 17–30% for three coastal cities in Norway. In a study focused on a long dry period, major differences were found in retention through evapotranspiration by vegetated and non-vegetated configurations [25]. Berretta et al. [9] studied moisture loss from a growing medium during a dry period of cold and warm months. They presented a mean moisture loss ranging from 0.34 mm/day to 1.65 mm/day in the period of March through July. Special attention should be given to the regeneration of roof storage capacity, which depends on physical configuration, precipitation patterns, and evaporation during dry periods [17]. Overall, the average retention performance is useful in a context where stormwater discharge to the sewer system is billable.

The detention effect occurs when temporally detained stormwater is subsequently released [14,15,18]. The evapotranspiration effect, which restores storage capacity during dry periods, may be neglected at this time in the interest of detention. Comparing detention performance, Liu et al. [26] and Villarreal et al. [14] presented peak flow reductions and peak delays of an intensive green roof on an event basis. The peak reductions varied between 25% and 65%, and peak delays varied between 20 min and 40 min. Stovin et al. [10] concluded that peak reduction for rainfall larger than 10 mm varied from 29% for a LECA-based bed to 68% for a sedum roof. They also noted that vegetated beds with brick-based substrates offer consistently greater attenuation compared with the LECA-based substrate. Stovin et al. [2] investigated the performance of an extensive green roof subjected to events with a return period of over one year. They presented a per-event peak reduction of 59.22% (mean) and 58.67% (median), and a per-event peak-to-peak delay of 54.16 min (mean) and 18 min (median). Li et al. [27] reviewed the typical hydrological performance of green roofs. It was shown that they attenuate a peak flow of 22% to 93%, and delay a peak flow of 0 to 30 min.

3. Materials and Methods

3.1. Geometrical Description and Structure Composition of the LECA-Based Roof

A full-scale LECA-based setup (Figure 1) was built to monitor the hydrological balance between rainfall and runoff on the roof of a wastewater treatment plant at Høvringen in Trondheim, Norway, approximately 50 m a.s.l. (63°26′47.5″ N; 10°20′11.0″ E). According to the Köppen-Geiger climate classification map (<http://koeppen-geiger.vu-wien.ac.at>), Trondheim is situated at the interface of oceanic (Cfb) and subarctic (Dfc) climates [23]. Main characteristics are strong seasonality, short summers, and no predominant dry seasons. The Norwegian Meteorological Institute recorded an annual precipitation of 950 mm and an annual average temperature of 3.8 °C in 2016. Cold climate is defined as a climate where the mean temperature of at least one month per year is below +1 °C [28]; in Trondheim, this occurs in January, February, November, and December [21].

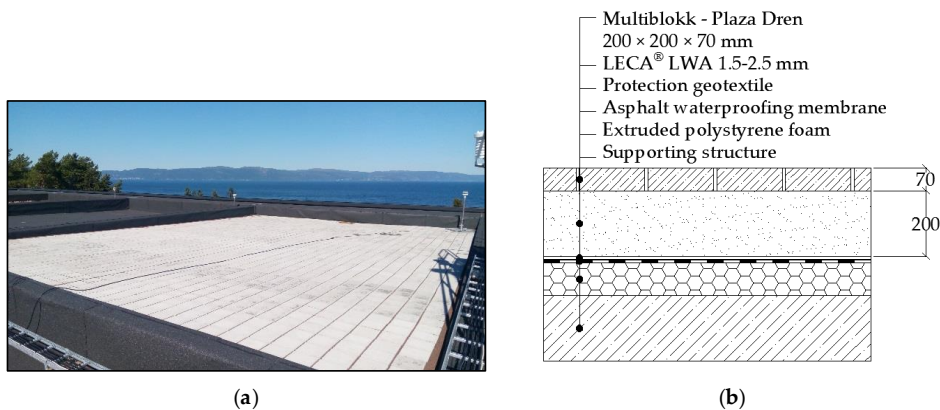


Figure 1. The LECA-based roof with concrete paving stones and its cross-section. LWA: lightweight aggregate. (a) The full-scale LECA-based roof at Høvringen (Trondheim, Norway); (b) The LECA-based roof components in a cross-section

The dimensions of the LECA-based roof-cells are 8×11 m, with a longitudinal slope of 2%. The full-scale configuration prevents impact associated with the scaling factor, which is important when accounting for the lateral flow across the roof-to-roof drain. The structure composition is made up of an underlying protection layer, a 200 mm thick layer of LECA® lightweight aggregates (LWA), and covering concrete pavers ($200 \times 200 \times 70$ mm). A geotextile is used as a separation layer, and to prevent fine particles from being washed out. LECA® LWA is an expanded lightweight crushed clay aggregate with a bulk density of 500 kg/m^3 , a particle density of 1050 kg/m^3 , and a particle size range of 1.5–2.5 mm [29]. Laboratory tests were also performed. The specific fraction was found to be ~60% of the proportion of voids in a sample, with a maximum water holding capacity (MWHC) of 26.2%, which is defined as the water content of a substance after two hours draining post-saturation. The tests were performed according to the Guidelines for the Planning, Construction and Maintenance of Green Roofing of the German Landscape Development and Landscaping Research Society [30]. The saturated hydraulic conductivity was measured to be 143.2 cm/h . The weight of the LECA-based roof was calculated at 251 kg/m^2 based on completely dry materials, and 310 kg/m^2 for wet conditions (MWHC). This includes LECA and pavers.

3.2. Data Collection and Event Analysis

Hydrological data were collected for all four seasons, from January 2017 to November 2017. Precipitation was monitored by a heated tipping bucket rain gauge (Lambrecht meteo GmbH 1518 H3, Lambrecht meteo GmbH, Göttingen, Germany) with a resolution of 0.1 mm at 1-min intervals. The runoff collection was measured using a weight-based system with two tanks downstream of the drainage outlets. The collection tanks had two conditions for emptying: they were automatically emptied either every 30 min, or when the weight of the water approached the capacity of the tank (30 kg).

A CR1000 data logger (Campbell Scientific, Inc., Logan, UT, USA) recorded all the parameters at 1-min intervals. Single precipitation events were defined according to a minimum period of 6 h of antecedent dry weather (ADWP), as commonly used by several previous studies, among others [2,3]. A threshold precipitation depth of 0.5 mm was used to exclude insignificant precipitation events. Similarly, a threshold discharge of 0.1 L/min was set to specify the start and end of runoff events. The moisture content in LECA® LWA was recorded using Decagon 5TM soil moisture and temperature sensors, which were delivered at the end of June. The moisture sensors were pre-calibrated in the laboratory for minimum and maximum degrees of saturation (0% and 100% saturation). Events were identified and sorted into five groups based on the type of precipitation: *rain*, *rain on snow*,

snow, snowmelt, and mixed. A total of 127 events were registered in the period between January 2017 and November 2017: 94 rain events, 12 rain on snow events, 9 snow events, 4 snowmelt events, and 8 mixed events. The events which were designated as mixed typically had a long duration (several days) and experienced several changes of precipitation type.

3.3. Retention Capacity

Retention was considered as long-term permanent water removal on a monthly basis, and a mean value for the entire studied period. Retention capacity was determined as follows:

$$Ret = P - R, \quad (1)$$

where P is precipitation, R is runoff and Ret is retention.

The retention at any given time will be the sum of the evapotranspiration and the water currently stored in the LECA medium.

3.4. Detention Capacity

The detention capacity of the LECA-based roof was assessed as the ability to attenuate and delay peak flows compared to the response of the black roof. This analysis was carried out on an event basis. In some cases, several peaks were observed in a single event due to the long duration (several days). In these cases, only the highest peak per event was analyzed. Peak flow reduction (PR) was determined as follows:

$$PR = 1 - \frac{Q_{LR,max}}{Q_{BR,max}}, \quad (2)$$

where $Q_{LR,max}$ is the maximum flow recorded per event from the LECA-based roof (LR), and $Q_{BR,max}$ is the maximum flow recorded per event from the black roof (BR). Peak delay (PD) was determined as follows:

$$PD = T_{LR,max} - T_{BR,max}, \quad (3)$$

where $T_{LR,max}$ is the time of maximum flow recorded per event from the LECA-based roof (LR) and $T_{BR,max}$ is the time of maximum flow recorded per event from the black roof (BR). Additionally, any delays were analyzed as delays of centroid of individual events.

4. Results

4.1. Precipitation Events and Time for Regeneration of the LECA-Based Roof Storage Capacity

The event durations and precipitation depths varied considerably. Of the selected highest-intensity events, the shortest lasted 8 min in July, and the longest lasted 122 h in October. This presents a widespread range; therefore, the median value of 8.2 h might be more representative. In terms of total precipitation depths, the events ranged from 0.5 mm to 85.4 mm. The total duration of precipitation events and dry periods were determined. Assuming the 6 h ADWP, precipitation occurred 22% of the time during these eleven months. This leaves 78% of the time (dry period) for the regeneration of the roof storage capacity, considered as time between events.

The precipitation at Høvringen (11-months dataset) was compared to the Risvollan stations, located 82 m a.s.l, at an areal distance of 7 km, due to the unavailability of Intensity–Duration–Frequency (IDF) curves at Høvringen. For the observation period, there was 8% more precipitation recorded at Høvringen than at Risvollan. The higher elevation of Risvollan makes this difference expected. Comparing the observed events at Høvringen with the IDF curves from the Risvollan station, one can see that all the events fall below a 2-year return period, with the exception of one from August 19, which lasted more than 1 day (Figure 2). The figure also shows a zoom to a 30 min resolution, where eventual rapid storms can be found. However, they registered low precipitation depths.

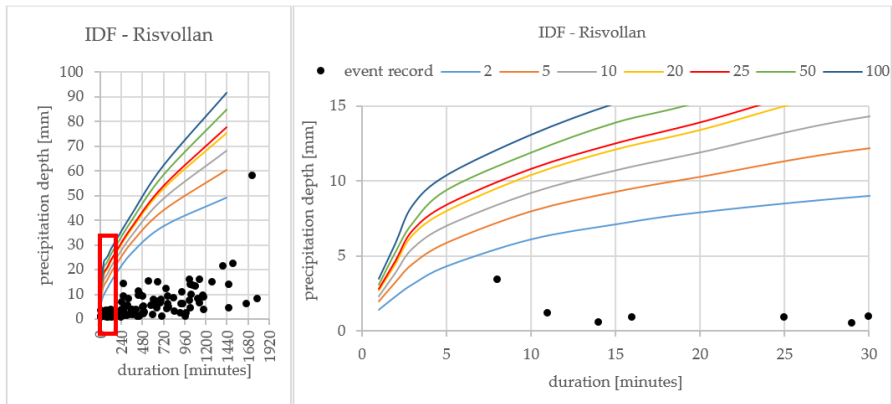


Figure 2. (left) The event record comparison with Risvollan Intensity–Duration–Frequency (IDF) curves for different return periods; (right) 30-min resolution.

The mean event intensities ranged from 0.1 mm/h to 25.6 mm/h. Particularly, the maximum mean intensity from July 26 that lasted 8 min exceeded the rest of the values; however, it is still below a 2-year return period event.

4.2. Retention Performance

The total rainfall-runoff rate can be observed between 23 January 2017 and 30 November 2017. During this period, the precipitation gauge measured 937.6 mm precipitation. The runoff depths during the examined period were 912.1 mm and 852.4 mm for the black and LECA-based roofs, respectively (Figure 3, Table 1). This indicated a discrepancy of 59.7 mm (black vs. LECA-based roof) and 85.2 mm (precipitation gauge vs. LECA-based roof), which is the evaporated volume. Overall, the difference between the precipitation and runoffs was a 3% volume reduction by the black roof, and 9% for the LECA-based roof.

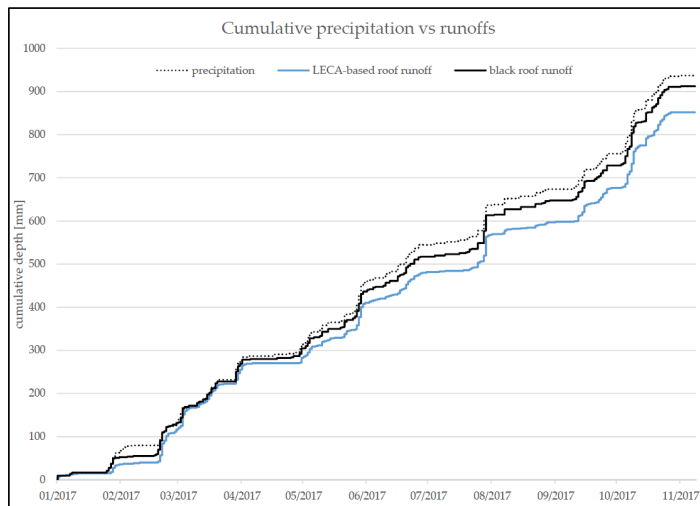


Figure 3. Cumulative hydrograph from the rain gauge and runoffs of the black and the LECA-based roofs.

The seasonal variations are shown in Table 1. The 11 months were divided into four groups: November, January, February, and March represent the winter period; April, May, and June represent the spring period; July and August represent the summer period; and September and October represent the fall period. The winter period confirmed zero evaporation during the cold climate condition. The minor negative difference between the black roof and the precipitation gauge can be attributed to signal noise and measuring uncertainties. The snowfall measurements are most likely the most significant here. Evaporation in the spring season exceeded values from the summer season (Table 1). This could be explained by an alteration of rainfall patterns in the summer season, when higher intensity rainfalls occur, resulting in decreased retention.

Table 1. Seasonal variation in retention performance.

Season	Number of Days	Total Precipitation (mm)	Total Runoff (mm)		Runoff Reduction (%)		Retention (mm)		Normalized Daily Retention (mm/day)	
			LECA	Black	LECA	Black	LECA	Black	LECA	Black
2017		Rain Gauge								
Winter	97	349.4	343.6	355.3	2%	−2%	5.7	−5.9	0.06	−0.06
Spring	91	301.3	251.9	276.7	16%	8%	49.4	24.7	0.54	0.27
Summer	62	182.7	160.9	179.1	12%	2%	21.8	3.7	0.35	0.06
Fall	61	104.2	96.0	101.1	8%	3%	8.3	3.2	0.14	0.05
Total	311	937.6	852.4	912.1	9%	3%	85.2	25.5	0.27	0.08

The runoff coefficients calculated from total precipitation and runoff records were 0.97 for the black roof and 0.91 for the LECA-based roof. The normalized daily retention estimated from total precipitation and runoff measurements was 0.27 mm per day. This reflects the fact that the climate in the Trondheim region is relatively cold and wet. The detention in the expanded clay aggregate (LECA), followed by a subsequent slow drainage of the system, was much greater than the evaporation loss rate.

4.3. Detention Performance

The detention capacity of the system was evaluated using peak flow delay and peak flow reduction. Evaluating the LECA-based roof using a wide range of performance indicators for all events indicated that the performance was mainly influenced by duration, intensity, moisture content, and ADWP of the individual events. At the same time, the detention indicators were highly sensitive to the chosen subsets of the rainfall dataset which was used in the calculations. Therefore, the eight events with the highest 5-min peak intensity were selected for detailed examination. Figure 4 illustrates the eight largest events, ranging in duration from 8 min to almost 3 days, with depths of 3.2 mm to 59.6 mm (Table 2). Additionally, the largest snowmelt (event 24) and rain-on-snow event (event 27) were included to show the different types of events observed on the roofs. For event 24 (the pure snowmelt event), there was a negative lag time delay between the black and the LECA-based roof. This can be explained by the observed temperatures in the LECA-based roof, which were more stable compared to the black roof. The black roof was typically colder than the LECA-based roof, meaning that higher net radiation was needed to initiate snowmelt. Though this was the largest snowmelt event, it was a relatively small compared to the other events in Tables 2 and 3, making the peak flow reduction less relevant. Event 27 (the rain-on-snow event) is very difficult to evaluate without knowing the mass of snow on the roofs at the onset of rain. It is not possible to compare peak lag times, as it is possible that the snowmelt initiated prior to the precipitation runoff. A complete mass balance would be needed of the initial snowfall until it was completely melted again. Due to these constraints, these two events were excluded from the comparisons in Tables 2 and 3.

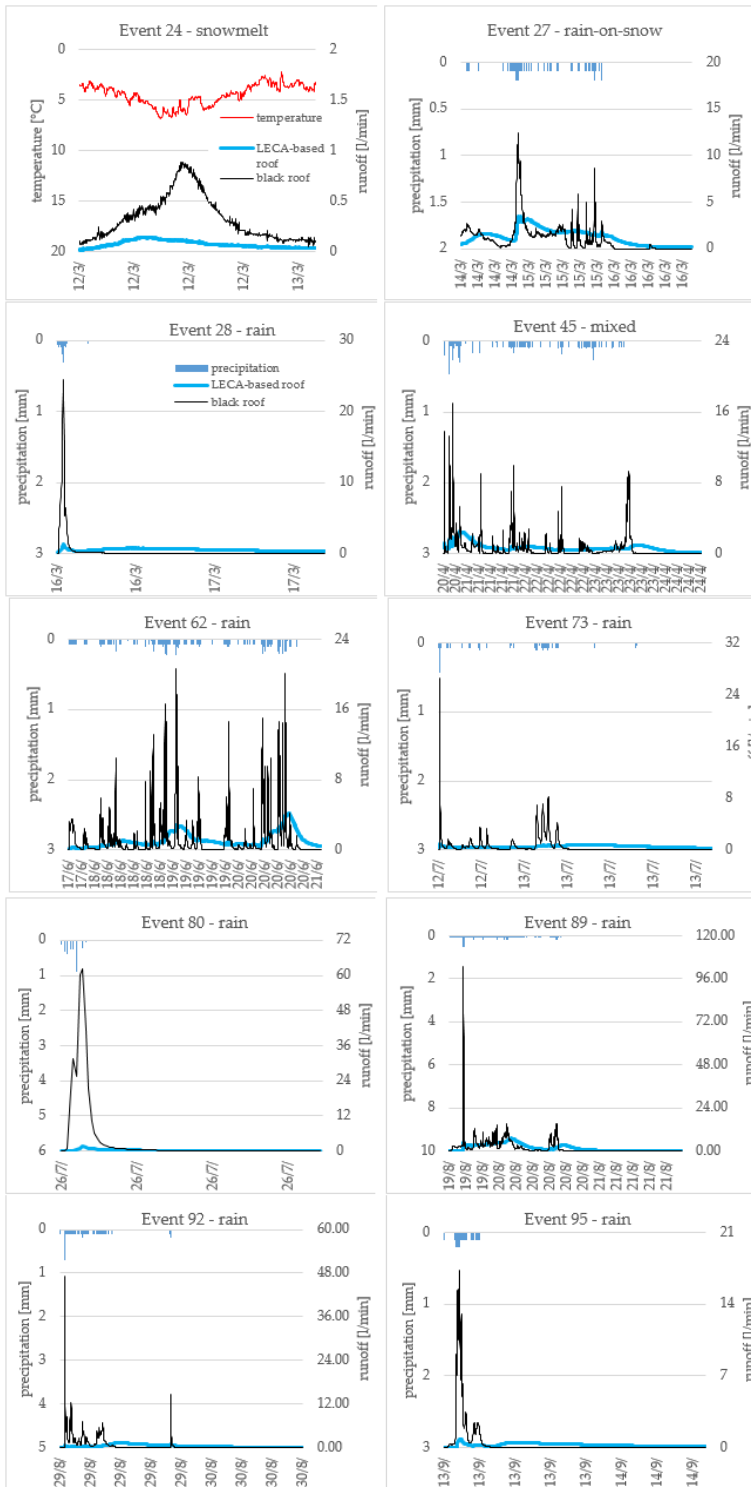


Figure 4. The events with the highest peak 5-min intensity.

Two alternative precipitation intensities were presented. The mean intensity indicates the ratio between the depth and duration, whereas the peak 5-min intensity is the peak intensity measured over 5 min. Event 45 turned to snow at a later stage, followed by a snowmelt in the end, and therefore the event type was classified as mixed. However, this event was used in the final evaluation, since the peak 5-min intensity and corresponding runoff occurred during “rainy” conditions. Event 80 was quite untypical in terms of mean intensity, which was more than ten times higher than the remaining events. With respect to the return period, event 89 was the only one that fell between the 2-year and 5-year return period (Figure 2).

Table 2. Rainfall characteristics for the significant events.

Event	Type	Start	Duration (hh:mm)	Precipitation Depth (mm)	Mean Intensity (mm/h)	Peak 5-min Intensity (mm/h)
28	rain	16.03.2017 19:43	1:38	3.3	2.13	14.40
45	mixed	20.04.2017 19:04	69:34	35.6	0.57	17.64
62	rain	17.06.2017 16:47	74:38	59.6	0.81	11.64
73	rain	12.07.2017 16:53	19:35	8.8	0.46	16.32
80	rain	26.07.2017 16:20	0:08	3.2	25.58	21.60
89	rain	19.08.2017 13:41	28:47	57.7	2.02	40.80
92	rain	29.08.2017 02:52	7:15	11.2	1.57	21.60
95	rain	13.09.2017 03:05	5:25	7.9	1.51	12.00

Table 3 summarizes responses of both black and LECA-based roofs for the eight events. Here, individual events were characterized by comparing the maximum (peak) values registered from the roofs. Overall, the peak delay totaled 1 h and 15 min in median and 7 h and 23 min in mean. A long dry period before the events naturally led to the freeing of the storage capacity. However, this does not necessarily mean ideal conditions for delaying peak runoffs, as can be seen for event 95. On the contrary, the short dry period led to a sufficient delay for event 45. A focus on maximum values was not always the best solution when evaluating the runoff delays. One can see very long delays for the long-duration events 62 and 89. Event 62 even experienced two heavier rainfalls, which obviously led to two responses. Because of this, two alternative solutions of peak delays were suggested (Figures 5 and 6).

In terms of peak reduction (Table 3), the roof demonstrated a high efficiency, with a reduction rate of 80% to 97%, irrespective of the length of the antecedent dry period or the degree of previous saturation. The latter indicates the extent to which the voids in the expanded clay aggregates are filled with water. The saturation measurements ranged between 31% and 61% for the period after which the sensors were installed. In addition to the degree of saturation, the initial runoff may also be used as a performance corrector or predictor. Higher initial runoffs correlate to higher degrees of saturation in the media from previous events.

Table 3. Comparison of runoff characteristics of black and LECA-based roofs for the significant events. ADWP: antecedent dry weather period.

Event	ADWP (hh:mm)	Peak Delay	Peak Reduction	Initial Degree of Saturation (%)	Initial Runoff (L/min)	Runoff Duration	Runoff Duration
		Peak-to-Peak (hh:mm)	Peak-to-Peak (%)			Black (hh:mm)	LECA (hh:mm)
		28	23:41			0:00	95%
45	7:37	2:30	85%	-	0.7	69:42	93:40
62	17:14	36:42	80%	-	0.08	74:57	81:41
73	8:44	0:01	97%	35.7	0.42	13:00	27:02
80	23:56	0:00	97%	32.1	0	0:51	1:22
89	62:42	12:17	93%	32.5	0.02	29:25	58:04
92	66:36	7:35	97%	32.2	0.01	15:46	33:28
95	165:12	0:00	95%	32.1	0.01	4:56	29:51

There were large differences in the runoff duration between the examined roofs. The median runoff duration of the LECA-based roof (31.5 h) lasted 2.2 times longer than of the black roof (14.5 h). Considering average values, the mean runoff duration of the LECA-based roof (42.5 h) lasted 1.6 times longer than of the black roof (26.5 h).

Figure 5 serves to recognize centroid delays of individual runoffs. The steep rises in cumulative runoffs associated with the black roof response after intense rainfalls may be considered a potential cause of rapid floods. One can see that the LECA-based roof transformed these rises to either flat (effective detention performance) or—in extreme cases—gradual runoffs. The extreme cases may be seen in events 45, 62, and 89. Additionally, Figure 5 shows the largest snowmelt and rain-on-snow events; however, these were different types of events, shown only for comparison. Further calculations include only the eight largest events, as outlined in the methods.

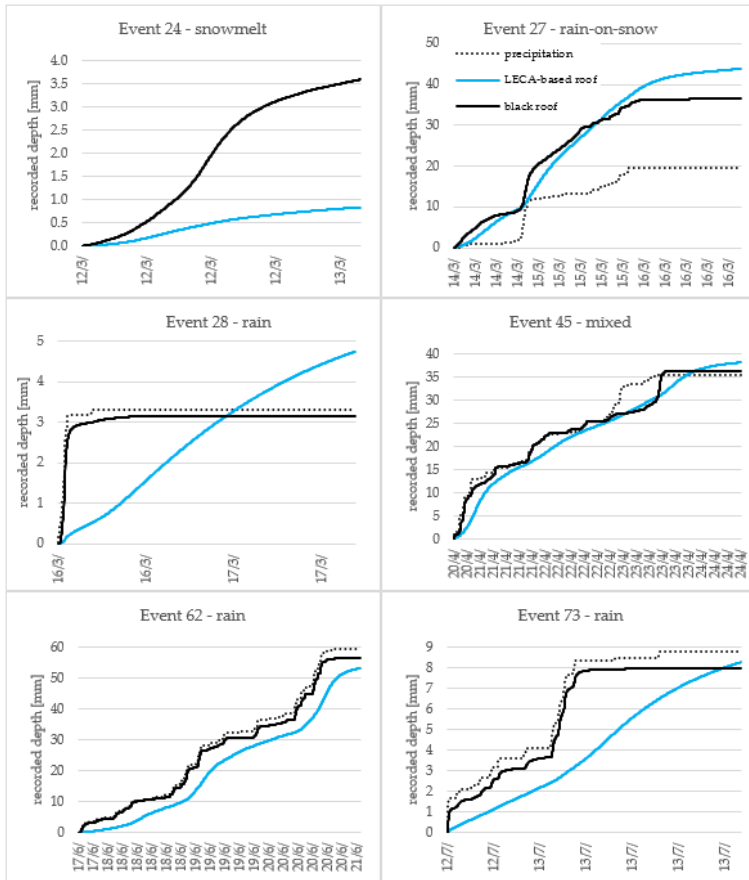


Figure 5. Cont.

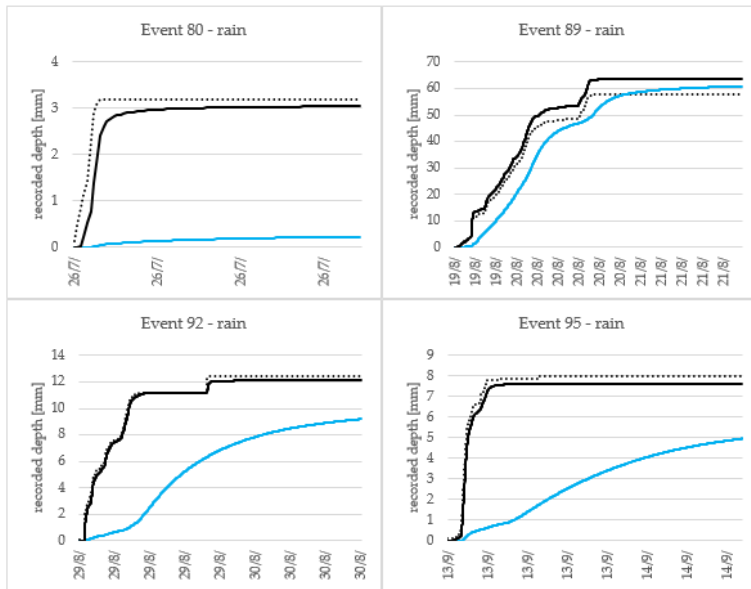


Figure 5. Cumulative runoff responses to the events with the highest peak 5-min intensity.

Considering shorter ADWP between events would result in a larger number of individual events. For instance, event 62 needed a 3 h ADWP to separate the event into two parts. Events 89 and 92, sharing a similar pattern, needed shorter breaks within the rainfall dataset (e.g., approximately 5–10 min), as there was continuous rainfall during this whole event. Using shorter breaks in the rainfall dataset would underestimate the total performance. For instance, the peak delay would change dramatically to 1 min (median) and 28 min (mean). Considering the centroids as the representative values, the peak delay counted 6 h (median) and 5 h and 51 min (mean).

Figure 6 presents a comparison of the alternative methods for runoff delays. The centroid delays were influenced by the short event 80, with small rainfall depth lasting only 8 min; this obviously led to a shortening of the centroid delay as well. During events 28 and 95, the quick responses can be clearly seen by the LECA-based roof runoffs, compared to the black roof peak runoff at the very beginning. This was probably caused by water collecting directly in the outlet (0.25 m²). Therefore, those peak runoffs should not be considered as real responses of the LECA-based roof. Overall, the peak reduction presents 95% in median and 92% in mean.

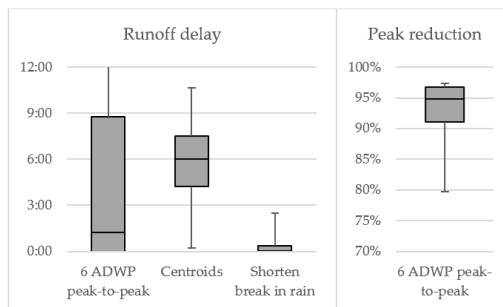


Figure 6. Comparison of the different methods of (left) the runoff delay and (right) the peak reduction.

5. Discussion

5.1. Retention Capacity

Retention is expected to be highest in the warm season. During the winter months, there was very limited measurable retention observed (2%). This is consistent with research [20] focused on potential evapotranspiration in cold and wet regions. Overall, the difference between the precipitation and runoff resulted in a 3% volume reduction for the black roof and 9% for the LECA-based roof. This is lower than the results presented by previous non-vegetated and green roof studies [1,3,10–13,22,24]. In terms of Norwegian conditions, Braskerud [31] presented a 25% runoff reduction in extensive green roofs in Oslo. This also agrees with the limited retention performance of the LECA-based roof. On the other hand, the result is most comparable with studies conducted in locations with wet and cool conditions [17,24]. The normalized daily retention during spring accounted for 0.54 mm per day, which is comparable with results from Beretta et al. [9]. As for the summer, 0.24 mm/day is about five times higher.

Nevertheless, it is a generally confirmed fact that water losses from vegetated roofs are higher due to evapotranspiration [25]. Beretta et al. [9] previously concluded lower daily moisture loss when using non-vegetated roofs compared to green roofs. Additionally, the reason for lower retention may be attributable to the concrete pavers, which cover and seal much of the surface area.

Average performance indicators may be useful for comparing different systems or even the same system exposed to different climatic conditions and/or for determining annual runoff, which does not have to be treated in a wastewater treatment plant. However, this data is very limited in terms of stormwater management design.

5.2. Detention Capacity

The performance indicators should reflect the performance in the non-daily events. Therefore, the eight largest events were examined. Evidence that the LECA-based roof can reduce peaks up to 95% (median) and 92% (mean) for significant events, as well as delay peaks by 1 h and 15 min (median) and 7 h 23 min (mean), provides support for its use in urban stormwater management strategies. The results of the peak reduction and delay, when neglecting the evapotranspiration effect, show a better performance than in the reviewed literature, for both the non-vegetated [10] and the green roofs [2,14,26,27,31].

The difficulties with defining events using the 6 h ADWP (resulting in some very long events) indicated that it might not be the best-suited time definition for the climate zone. These long duration events also cause decreasing mean intensity of individual events. Considering a maximum runoff as the representative value for an event may overestimate the overall performance in terms of the peak delay, even though it is more natural to compare events according to maximum registered values. The irregularity of natural rainfall patterns, combined with the variability within detention effect in specific events, complicates the identification of peak-to-peak delays. Centroid delays are perceived to be a more robust indicator of the delays in bulk runoff than peak delays [15]. Considering the centroids as the representative values, the peak delays total up to 6 h (median) and 5 h and 51 min (mean). Even though the vertical movement of stormwater (due to high saturated hydraulic conductivity; $K_{\text{sat}} = 143.2$ cm/hour) through the expanded clay aggregate is rather quick, the lateral movement through the media as well as the size of the roof (the distance between the sides to the outlet) and the slope of the roof are decisive and cause the high detention in the LECA-based roof.

5.3. Effect of Antecedent Events

Moisture levels in the expanded clay aggregate were higher than expected during dry periods. The expanded aggregate detains water for a long time, demonstrating why it is used for planting. However, very low saturation could be seen in November, when the moisture sensor registered low or negative temperatures. This can be explained by the inability of the sensor to accurately

measure moisture in low temperatures, or a measurement error due to frozen media. Between July and November (Figure 7), every month experienced a long dry period: 156 h in July, 172 h in August, 278 h in September, 166 h in October, and 191 h in November.

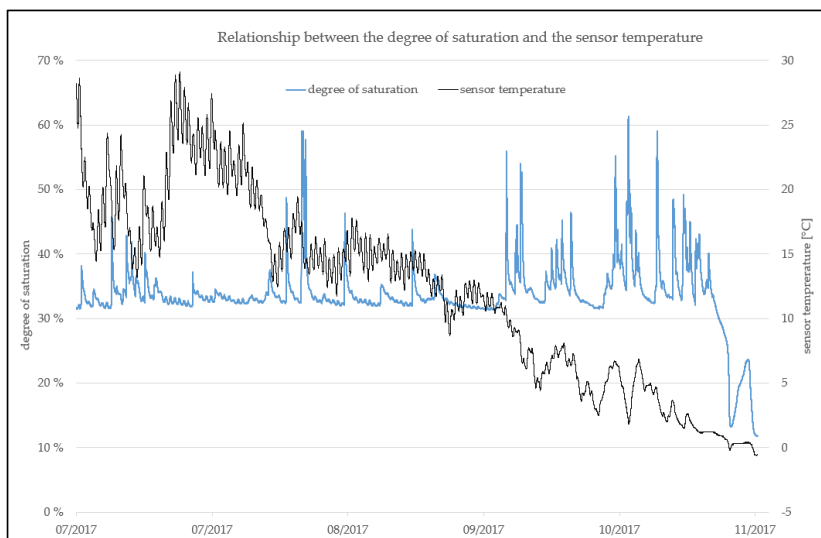


Figure 7. Variation of the degree of saturation within July and November.

Disregarding the long dry periods, the expanded clay aggregate kept a relatively high content of water within the medium. This clearly shows that the expanded clay aggregate was unable to fully regenerate its storage capacity to completely dry conditions, as in the laboratory. Despite the relatively high remaining saturation before an event, the LECA-based roof provided high performance in terms of peak reduction, as well as slowing down and transforming the runoff into a more natural flow for all seasons. Based on the moisture content measurements, a maximum storage capacity of 3.2 mm (0.28 m³) was determined. This was also validated by a maximum observed precipitation of 2.7 mm, which did not generate runoff. The total available voids space (120 mm) is permanently taken by an inaccessible volume of 31%. This could indicate that there might be some capacity that could be gained by optimizing the size fractions. The void space is a function of this LECA type, making this yet another parameter which could be further investigated for optimal water detention. However, the water is adsorbed by the void spaces in the LECA, which additionally makes the water detention capacity dependent on the rainfall intensity.

5.4. Practical Implications

In light of the results and limitations, the LECA-based retrofitting shows promising results in terms of handling runoff from precipitation depths as a source control. This solution outperformed the conventional green roof solutions [14,18,26,27] in several aspects. The hydrological performance was evaluated for retention and detention, as well as for resistance to different forms of precipitation and durability. The practical implication of the LECA-based roof with respect to the detention performance includes runoff delays and peak flow reductions. Extending the durations of the runoff may significantly decrease the number of combined sewer overflows or the design volume of underground detention basins. The hydrological performance did not decline during the largest events recorded in this study, giving a strong indication of its performance, even during the more intense precipitation events. The LECA-based solution offers a detention capacity on the roof without allowing

standing water on the roof membrane, as the water is held back and absorbed into the LECA material. An alternative solution would be an open or closed detention basin on the roof, or a cistern/closed tank system. A detention basin directly on the roof would exert water pressure on the roof membrane, increasing the risk of leaks. Standing water on the roof in a cold climate would freeze and contribute to blocked drains and ice formation on the roof. This would be a significant risk factor, as the ice expansion could also result in frost failure of the drains, which would lead to malfunctioning drains, and in the worst case, leaks into the underlying layers. A cistern-type solution would also experience freezing problems unless it was fully insulated or located indoors. The latter solution would be technically possible, as flat roofs always have internal roof drains in cold climates, again to minimize freezing of standing water. However, in urban areas where space is at a premium, it is more attractive to utilize the currently unused rooftop rather than sacrifice indoor space in buildings. The LECA-based solution is also an attractive solution to retrofit existing roofs, while the cistern solution would only be a feasible option for new buildings, due to the need for indoor space. Though it is not the only non-green alternative possible, the LECA-based system offers rooftop detention without introducing standing water pressure on the roof membrane, and with minimal ice formation risk due to the draining capacity, leaving no standing water on the roof.

In terms of estimated material costs per m^2 , the LECA-based roof is approximately 40 €/m², whereas a green roof is 70 €/m² (following consultations with providers). Since the LECA-based roof performance does not rely on the evapotranspiration effect, it can be used worldwide. The findings are specific to the LECA-based roof study and the specific actual rainfall that occurred during the study.

The weak points of the LECA-based roof in comparison to the green roof are in weight and in lower retention ability during warmer months. The LECA-based roof weighs 251 kg/m² in dry conditions and 310 kg/m² in wet conditions, whereas a green roof weighs 25 kg/m² in dry conditions and 50 kg/m² in wet conditions [32]. On the other hand, green roofs require irrigation during dry periods, periodical fertilization throughout the year, and have a deteriorated performance in extreme conditions [33].

6. Conclusions

The comparative study of precipitation and runoff data from two parallel rooftops (the LECA-based roof and the referenced “black” roof) was carried out at a coastal part of Trondheim, Norway. Eleven months of data were collected, analyzed, and divided into 127 events (94 rain events) according to a 6 h ADWP.

With respect to the previously reported findings, the retention performance of the LECA-based roof was lower than that of typical green roofs. This is because the water loss is only actuated by evaporation. For the entire studied period, the balance between precipitation and runoff of the LECA-based roof was estimated at 0.27 mm/day; this performance is 0.19 mm/day higher than the normalized daily retention of the black roof.

The runoff characteristics regarding to detention capacity of the LECA-based roof are particularly encouraging, even though the performance of source control systems typically struggle with intense rainfalls of short duration. Overall, the study demonstrated that the LECA-based configuration provided a large improvement compared with the black roof runoffs, with a peak reduction of 95% (median) and 92% (mean), and with a peak delay of 1 h 15 min (median) and 7 h 23 min (mean). This indicates that the LECA-based roof, with its improved detention performance, could be a good solution for the retrofitting of already-existing roof areas.

Acknowledgments: The field station was built with the support and contribution of the Klima2050 Centre for Research-based Innovation (SFI), financed by the Research Council of Norway and its consortium partners. The Klima2050 project aims to reduce the societal risks associated with climate change and the enhanced precipitation and floodwater exposure within urban areas [34].

Author Contributions: Vladimír Hamouz and Tone M. Muthanna conceived and designed the experiment. Vladimír Hamouz and Tone M. Muthanna performed the experiment and analyzed the data. Vladimír Hamouz

and Jaran R. Wood interpreted the results with a general discussion with all authors. Jardar Lohne helped with structure of the manuscript and language correction. Vladimír Hamouz wrote the majority of the text, with feedback and input from Tone M. Muthanna, Jardar Lohne and Jaran R. Wood.

Conflicts of Interest: The authors declare no conflict of interest.

References

- Mentens, J.; Raes, D.; Hermy, M. Green roofs as a tool for solving the rainwater runoff problem in the urbanized 21st century? *Landsc. Urban Plan.* **2006**, *77*, 217–226. [[CrossRef](#)]
- Stovin, V.; Vesuviano, G.; Kasmin, H. The hydrological performance of a green roof test bed under UK climatic conditions. *J. Hydrol.* **2012**, *414*, 148–161. [[CrossRef](#)]
- VanWoert, N.D.; Rowe, D.B.; Andresen, J.A.; Rugh, C.L.; Fernandez, R.T.; Xiao, L. Green roof stormwater retention. *J. Environ. Qual.* **2005**, *34*, 1036–1044. [[CrossRef](#)] [[PubMed](#)]
- Torgersen, G.; Bjerkholt, J.T.; Lindholm, O.G. Addressing flooding and suds when improving drainage and sewerage systems—A comparative study of selected Scandinavian cities. *Water* **2014**, *6*, 839–857. [[CrossRef](#)]
- Woods-Ballard, B.; Kellagher, R.; Martin, P.; Jefferies, C.; Bray, R.; Shaffer, P. *The Suds Manual*; CIRIA: London, UK, 2007; Volume 697.
- Fletcher, T.D.; Shuster, W.; Hunt, W.F.; Ashley, R.; Butler, D.; Arthur, S.; Trowsdale, S.; Barraud, S.; Semadeni-Davies, A.; Bertrand-Krajewski, J.-L. SUDS, LID, BMPs, WSUD and more—the evolution and application of terminology surrounding urban drainage. *Urban Water J.* **2015**, *12*, 525–542. [[CrossRef](#)]
- Lindholm, O.G.; Endresen, S.; Thorolfsson, S.T.; Sæggrov, S.; Jakobsen, G.; Aaby, L. Veiledning i klimatilpasset overvannshåndtering. *Rapport* **2008**, *162*, 2008.
- Berndtsson, J.C. Green roof performance towards management of runoff water quantity and quality: A review. *Ecol. Eng.* **2010**, *36*, 351–360. [[CrossRef](#)]
- Berretta, C.; Poë, S.; Stovin, V. Moisture content behaviour in extensive green roofs during dry periods: The influence of vegetation and substrate characteristics. *J. Hydrol.* **2014**, *511*, 374–386. [[CrossRef](#)]
- Stovin, V.; Poë, S.; De-Ville, S.; Berretta, C. The influence of substrate and vegetation configuration on green roof hydrological performance. *Ecol. Eng.* **2015**, *85*, 159–172. [[CrossRef](#)]
- Carson, T.; Marasco, D.; Culligan, P.; McGillis, W. Hydrological performance of extensive green roofs in New York City: Observations and multi-year modeling of three full-scale systems. *Environ. Res. Lett.* **2013**, *8*, 024036. [[CrossRef](#)]
- Gregoire, B.G.; Clausen, J.C. Effect of a modular extensive green roof on stormwater runoff and water quality. *Ecol. Eng.* **2011**, *37*, 963–969. [[CrossRef](#)]
- Garofalo, G.; Palermo, S.; Principato, F.; Theodosiou, T.; Piro, P. The influence of hydrologic parameters on the hydraulic efficiency of an extensive green roof in mediterranean area. *Water* **2016**, *8*. [[CrossRef](#)]
- Villarreal, E.L. Runoff detention effect of a sedum green-roof. *Hydrol. Res.* **2007**, *38*, 99–105. [[CrossRef](#)]
- Stovin, V.; Vesuviano, G.; De-Ville, S. Defining green roof detention performance. *Urban Water J.* **2017**, *14*, 574–588. [[CrossRef](#)]
- Bengtsson, L.; Grahn, L.; Olsson, J. Hydrological function of a thin extensive green roof in Southern Sweden. *Hydrol. Res.* **2005**, *36*, 259–268.
- Stovin, V.; Poë, S.; Berretta, C. A modelling study of long term green roof retention performance. *J. Environ. Manag.* **2013**, *131*, 206–215. [[CrossRef](#)] [[PubMed](#)]
- Locatelli, L.; Mark, O.; Mikkelsen, P.S.; Arnbjerg-Nielsen, K.; Jensen, M.B.; Binning, P.J. Modelling of green roof hydrological performance for urban drainage applications. *J. Hydrol.* **2014**, *519*, 3237–3248. [[CrossRef](#)]
- Vanuytrecht, E.; Van Mechelen, C.; Van Meerbeek, K.; Willems, P.; Hermy, M.; Raes, D. Runoff and vegetation stress of green roofs under different climate change scenarios. *Landsc. Urban Plan.* **2014**, *122*, 68–77. [[CrossRef](#)]
- Johannessen, B.G.; Hanslin, H.M.; Muthanna, T.M. Green roof performance potential in cold and wet regions. *Ecol. Eng.* **2017**, *106*, 436–447. [[CrossRef](#)]
- Norwegian Meteorological Institute (MET). Available online: www.met.no (accessed on 23 January 2018).
- Berghage, R.D.; Beattie, D.; Jarrett, A.R.; Thuring, C.; Razaeei, F.; O'Connor, T.P. Green roofs for stormwater runoff control. 2009. Available online: <http://nepis.epa.gov/exe/zypurl.cgi?dockey=p1003704.txt> (accessed on 23 January 2018).

23. Peel, M.C.; Finlayson, B.L.; McMahon, T.A. Updated world map of the köppen-geiger climate classification. *Hydrol. Earth Syst. Sci. Discuss.* **2007**, *4*, 439–473. [[CrossRef](#)]
24. Johannessen, B.G.; Muthanna, T. Hydraulic performance of extensive green roofs in cold climate. *Contrôle À La Source/Source Control*. 2016. Available online: <http://documents.irevues.inist.fr/bitstream/handle/2042/60499/1B1P04-134JOH.pdf> (accessed on 2 March 2018).
25. Poë, S.; Stovin, V.; Berretta, C. Parameters influencing the regeneration of a green roof's retention capacity via evapotranspiration. *J. Hydrol.* **2015**, *523*, 356–367. [[CrossRef](#)]
26. Liu, K.; Minor, J. Performance evaluation of an extensive green roof. Presented at Green Rooftops for Sustainable Communities, Washington, DC, USA, 5–6 May 2005; Volume 1, pp. 1–11.
27. Li, Y.; Babcock, R.W. Green roof hydrologic performance and modeling: A review. *Water Sci. Technol.* **2014**, *69*, 727–738. [[CrossRef](#)] [[PubMed](#)]
28. Smith, D.W. *Cold Regions Utilities Monograph*; American Society of Civil Engineers: Reston, VA, USA, 1996.
29. Filtralite. Available online: <http://www.filtralite.com/> (accessed on 23 January 2018).
30. Forschungsgesellschaft Landschaftsentwicklung Landschaftsbau (FLL). *Guidelines for the Planning, Construction and Maintenance of Green Roofing: Green Roofing Guideline*; Forschungsgesellschaft Landschaftsentwicklung Landschaftsbau: Bonn, Germany, 2008.
31. Braskerud, B.C. *Grønne Tak Og Styrregn*; NVE: Oslo, Norway, 2014.
32. Bergknapp. Available online: <http://www.bergknapp.no/hjem> (accessed on 23 January 2018).
33. Committee, M.S.S. *The Minnesota Stormwater Manual*; Minnesota Pollution Control Agency: St.Paul, MN, USA, 2005.
34. Klima2050. Available online: <http://www.klima2050.no/> (accessed on 23 January 2018).



© 2018 by the authors. Licensee MDPI, Basel, Switzerland. This article is an open access article distributed under the terms and conditions of the Creative Commons Attribution (CC BY) license (<http://creativecommons.org/licenses/by/4.0/>).

Paper 2

Detention-based green roofs for stormwater management under extreme precipitation due to climate change

Hamouz, V., Pons, V., Sivertsen, E., Raspati, G. S., Muthanna, T. M., & Bertrand-Krajewski, J-L.

Accepted for publication: Blue-Green Systems - IWA

Detention-based green roofs for stormwater management under extreme precipitation due to climate change

Vladimír Hamouz^{a,*}, Vincent Pons^a, Edvard Sivertsen^b, Gema Sakti Raspati^{IWA^b}, Jean-Luc Bertrand-Krajewski^{IWA^c} and Tone Merete Muthanna^{IWA^a}

^a Department of Civil and Environmental Engineering, Norwegian University of Science and Technology (NTNU), N-7491 Trondheim, Norway

^b SINTEF AS, S.P. Andersens veg 3, N-7465 Trondheim, Norway

^c Université de Lyon, INSA Lyon, DEEP (EA 7429), 11 rue de la Physique, F-69621, Villeurbanne cedex, France

*Corresponding author. E-mail: vladimir.hamouz@ntnu.no

Abstract

Rooftops cover a large percentage of land area in urban areas, which can potentially be used for stormwater purposes. Seeking adaptation strategies, there is an increasing interest in utilising green roofs for stormwater management. However, the impact of extreme rainfall on the hydrological performance of green roofs and their design implications remain challenging to quantify. In this study, a method was developed to assess the detention performance of a detention-based green roof (underlaid with 100 mm of expanded clay) for current and future climate conditions under extreme precipitation using an artificial rainfall generator. The green roof runoff was found to be more sensitive to the initial water content than the hyetograph shape. The green roof outperformed the black roof for performance indicators (time of concentration, centroid delay, T50 or peak attenuation). While the time of concentration for the reference black roof was within 5 minutes independently of rainfall intensity, for the green roof was extrapolated between 30 and 90 minutes with intensity from 0.8 to 2.5 mm/min. Adding a layer of expanded clay under the green roof substrate provided a significant improvement to the detention performance under extreme precipitation in current and future climate conditions.

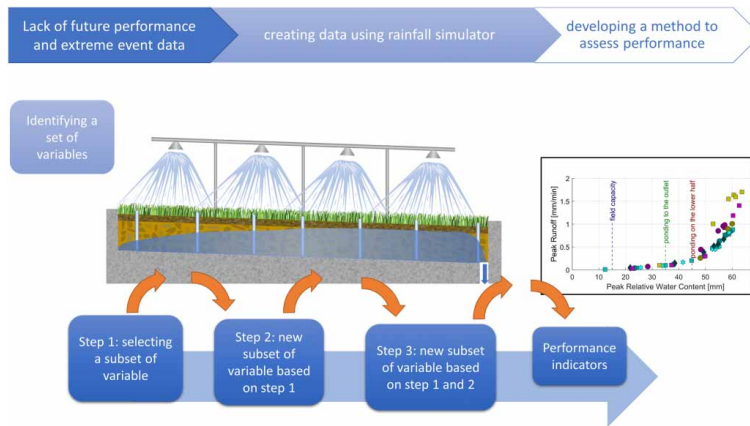
Key words: 20-year return period, climate change, depth duration frequency curves, design rainfall, detention-based green roofs, performance indicators

Highlights

- A method to assess the performance of a green roof under extreme events with a rainfall simulator was developed.
- Underlying a thin extensive green roof with expanded clay provided significant improvement to the detention performance.
- The study demonstrated that extensive green roofs with an added detention layer can have an effect also for extreme precipitation events including a climate factor.
- New knowledge on the water distribution within the roof from antecedent precipitation and how it affects the future performance.
- Demonstrating that the runoff can be predicted from the initial moisture, showing that for this roof the runoff exponentially increased with increasing initial moisture.

This is an Open Access article distributed under the terms of the Creative Commons Attribution Licence (CC BY 4.0), which permits copying, adaptation and redistribution, provided the original work is properly cited (<http://creativecommons.org/licenses/by/4.0/>).

Graphical Abstract



INTRODUCTION

Climate change is increasing the exposure and vulnerability of urban environments to local flooding (among others: Few 2003; Miller & Hutchins 2017; Hettiarachchi *et al.* 2018). The increasing frequency of extreme precipitation and growing urbanization have amplified the need for sustainable design and management of stormwater measures in urban areas (Mentens *et al.* 2006; Arnbjerg-Nielsen *et al.* 2013; Zhou 2014). Consequently, green roofs have become a common and popular green infrastructure solution around the world (Stovin 2010; Voyde *et al.* 2010; Fassman-Beck *et al.* 2013). The use of green roofs as a stormwater solution is rapidly growing across the Nordic countries, and several municipalities have set targets for their implementation (Copenhagen 2011).

Norway has adopted a three-step approach to stormwater management, where step 1 aims to infiltrate all small events onsite (a well-established and effective solution to reduce peak runoff from impervious surfaces), step 2 aims to safely detain all medium-size events, while step 3 aims to ensure safe floodways for all extreme events (Lindholm *et al.* 2008). Green roofs target events covering both step 1 and step 2. Although there is no infiltration into the ground from green roofs, the small events typically do not generate runoff from the roofs as the water is retained in the substrate and later released through evapotranspiration. Small to medium events are both partly retained in the roof and partly detained and released as delayed runoff. Recently, new research dealing with a lightweight expanded clay-based roof (also called grey roof) has demonstrated the potential to attenuate intense rainfall (Hamouz *et al.* 2018). However, little research has been conducted on the performance of green and grey roofs during extreme events. Extreme events, by their nature, occur neither regularly nor frequently, and they are therefore difficult to capture. Additionally, due to climate change, extreme events are expected to increase in intensity and frequency (Stocker 2014; Hanssen-Bauer *et al.* 2017; Hoegh-Guldberg *et al.* 2018). A great amount of uncertainty is linked to the change in extreme events as the trajectory of climate change itself remains uncertain. This is why several scenarios depending on impact of human activities on climate have been developed to evaluate and predict this change (Hanssen-Bauer *et al.* 2017).

Green roofs offer stormwater solutions that can conceivably contribute to the management of extreme events as they allow the opportunity to deal with stormwater directly at the source. The critical performance provided by green roofs is their retention and detention capacity. Detention performance is principally related to runoff delay, attenuation, and peak flow reduction (Stovin *et al.* 2017; Hamouz *et al.* 2018) which are crucial to dealing with extreme events since retention capacities are limited

during extreme precipitation (VanWoert *et al.* 2005; Villarreal & Bengtsson 2005; Speak *et al.* 2013; Johannessen *et al.* 2018). The use of a combined solution comprised of both green and expanded clay-based (grey) elements is expected to provide a way to design a structure able to achieve long-term retention and event-based detention performance capable of dealing with both conventional and extreme events. There is a consensus in the literature that the performance of green roofs is subject to local weather patterns (Berndtsson 2010; Li & Babcock 2014; Stovin *et al.* 2017). Common practices to study the performance of green roofs under various locations rely on: field studies limited by available data and location, and modelling studies limited by available data and the transferability of the model (Johannessen *et al.* 2019). The assessment of detention performance can be challenging due to the irregularity of natural precipitation patterns and the variable storage capacity available at the time of a given precipitation event (Stovin *et al.* 2017). Due to the difficulties involved with identifying detention metrics that describe the performance of green roofs for natural precipitation and lack of data on extreme rainfall events, the use of a rainfall simulator was found to be an effective method for testing the roof under extreme 'input-controlled' (e.g. hyetograph and initial water content) variables and evaluating the roof performance. Artificial rain has already been used to simulate various hyetographs to deal with lack of data associated with intense rain (Bengtsson 2005; Villarreal & Bengtsson 2005). Spatial uniformity of the simulated rainfall has been investigated in a certain number of studies (Naves *et al.* 2017; Naves *et al.* 2019). However, no research was found to apply the rainfall simulator to test different hyetographs on a full-scale green roof under changing initial climate conditions.

As a green roof's performance is dependent on water content, the use of a rainfall simulator might be a solution for controlling storm characteristics and initial conditions, including initial water content for a full-scale roof. Due to the rare occurrence of extreme events, utilising artificial rain is a way to fill the knowledge gap. Therefore, the purpose of this research is to assess a procedure for using artificial rain to study the hydrological performance of a detention-based green roof under extreme events. More precisely, this study focuses on 20-year return period (RP) rain events for three Norwegian cities (Bergen, Oslo, Trondheim), taking into account climate change.

The main objectives of this research were as follows:

1. Develop a method to test extreme precipitation on a full-scale, detention-based green roof using a rainfall simulator.
2. Assess the hydrological performance of a detention-based green roof under extreme precipitation, exceeding a 20-year return period in current and future conditions and including a 1.4 climate factor.

MATERIALS AND METHODS

The study area

A full-scale field setup was built on top of a roof located approximately 10 meters above ground and 50 meters above sea level. The setup was built to study the hydrological performance of different roof configurations at Høvringen in Trondheim, Norway (63°26'47.5" N 10°20'11.0" E). In this paper, a green (underlaid with 100 mm of expanded clay – material characteristics in Appendix, Table A2) (FLL 2008) and a black roof, which both had a total area of 88 m² and a longitudinal slope of 2%, were considered (Figure 1). More information about the field setup may be found in previous studies (Hamouz *et al.* 2018; Hamouz & Muthanna 2019). The detention-based green roof, referred hereafter as the green roof, was tested in this study. The black roof was used as a reference for comparison.

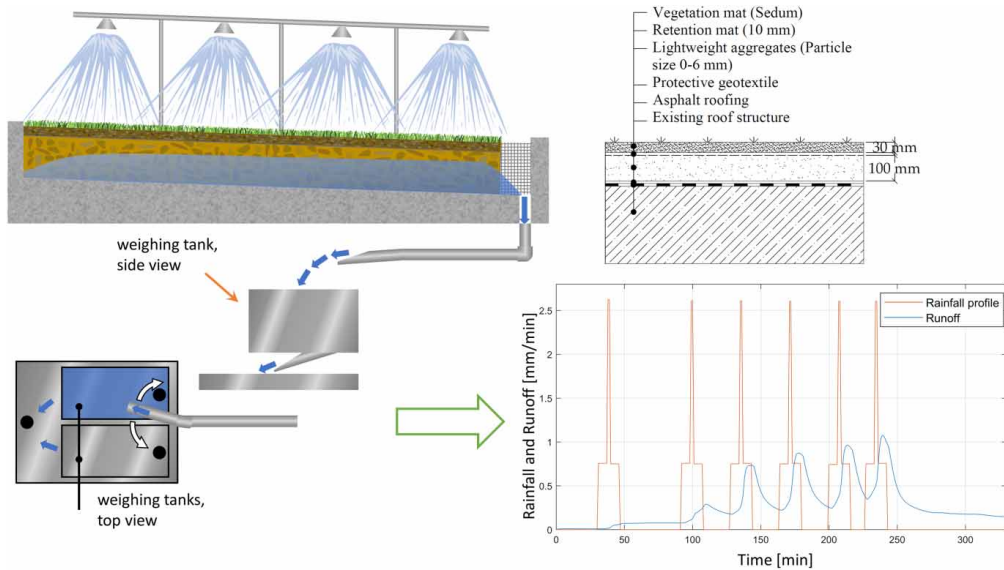


Figure 1 | Conceptual view of the roof, irrigation system and measurement device (on the left), the green roof in a cross-section (on the top right), example of a daily experiment (on the bottom right).

Field data collection

The meteorological and experimental data were collected during a period lasting from May 2019 to October 2019. Natural precipitation was measured by a heated tipping bucket rain gauge (Lambrecht meteo GmbH 1518 H3, Lambrecht meteo GmbH, Göttingen, Germany) with a resolution of 0.1 mm at 1-min intervals and with an uncertainty of $\pm 2\%$. Runoff was measured using a weight-based system (accuracy class C3 according to OIML R60) with two tanks located downstream of the drainage outlet (a 110 mm pipe). All data were recorded at 1-min intervals using a CR 1000 data logger (Campbell Scientific, Inc.). More information related to the instrumentation may be found in other studies (Hamouz *et al.* 2018; Hamouz & Muthanna 2019). Additionally, eight plexiglass tubes were buried vertically along the longitudinal edge of the roof for visual observation and estimation of spatial water distribution within the roof at the beginning and the end of each individual event during the tests.

Rainfall simulator and future climate scenarios

The field site was equipped with a setup using a grid of non-regulated nozzles (4 nozzles per line, 4 lines) connected to a water supply pipe that was used to generate the precipitation input. The nozzles were placed 1.5 m above the roof to ensure the maximal spreading effect of water. The enlarged uncertainty (BIPM *et al.* 2009) with respect to the water spatial distribution was $\pm 3\%$. The enlarged uncertainty of inflow was estimated to be ± 0.06 mm/min and caused by variations in inflow (i.e. a pressure drop in the water supply).

The inflow rates were measured by an electromagnetic flowmeter (Siemens Sitrans FM MAG 5000; uncertainty $\pm 0.4\%$ of the flow rate) and regulated using two valves to allow changes of inflow duration and intensity. The decision was made to run rainfalls with different durations, intensities, and inter-event periods (ranging from 5 minutes to more than 74 minutes) to enable different initial water contents (IWC) in the roof and differently shaped hyetographs. The range of intensities (from

0.8 to 2.5 mm/min) was limited by the minimal flow due to nozzle spread and maximum flow by the capacity of the flow measuring tanks.

Climate change was considered in this study through an increase in precipitation using a climate factor. The Norwegian Climate Centre (<https://klimaservicesenter.no/>) published recommendations for future short-term precipitation until 2100 (Hanssen-Bauer *et al.* 2017; Dyrørdal & Førland 2019). Based on this recommendation, a 1.4 climatic factor (CF) is advised in Norway. Firstly, precipitation depths for the 20-year return period (RP) were derived from Depth-Duration-Frequency (DDF) curves for three different cities: Bergen (BER), Oslo (OSL), and Trondheim (TRO) (Table 1). The locations were chosen because of their different climatic conditions. Secondly, these DDF curves were multiplied by a climate factor of 1.4 to estimate expected rainfall in the period between 2071 and 2100, including a worst-case scenario with Representative Concentration Pathway (RCP) 8.5 for short-term events. The use of this factor was also suggested in other studies (Kristvik *et al.* 2018; Kristvik *et al.* 2019).

Experimental design

To study the behaviour and performance of the roof under extreme rainfall, four primary variables were identified: (1) IWC (based on water balance), (2) rainfall duration, (3) mean intensity of the rainfall, and (4) shape of the hyetograph (impact of varying intensity). Additionally, secondary variables (depending on primary variables) were considered: (5) depth of the rainfall, depending on its duration and mean intensity and (6) location and climate change scenario, linking duration and mean intensity using Intensity-Duration-Frequency (IDF) or Depth-Duration-Frequency (DDF) curves.

The main objective was to identify the most significant variables governing the behaviour of the roof. The experimental design has been driven by the Bayesian principle to minimise the number of experiments. This means that the method has been updated by considering the results obtained in the previous steps. The experiments' three main steps were as follows:

1. The first step was conducted to include a primary analysis of the behaviour of the roof. The influence of rainfall intensity was measured by performing the time of concentration (TC) test. The TC was defined as the time for the roof's runoff to equal inflow under constant intensity rainfall. Subsequently, the water drainage was assessed.
2. Based on the results of the first step, the second experiment was conducted to compare the influence on runoff of a change in hyetograph to a change in IWC.
3. Finally, the third step, based on the results of the first two steps, was conducted to study the influence of the duration and intensity while considering the impact of water content (WC).

Step 1: assessing hydrological behaviour of the roof

To fulfil the first step, the green roof TC was estimated for different inflow intensities (0.8, 1.0, 1.2, 1.4, 1.7, 2.0, and 2.5 mm/min) and compared with the black roof TC. The duration of each event was monitored to ensure that both inflow ($\pm 2\%$) and outflow ($\pm 2\%$) lay within the boundaries for measurement uncertainty which was set as a threshold for ending the individual tests.

The roof drainage was studied as part of the first step by recording the outflow after the end of the inflow (precipitation) stopped at the conclusion of the TC test. The drainage curves were later updated with the data from steps 2 and 3 to refine the results.

As the performance of the roof depends to a large degree on WC, and given the fact that short, intense rainfalls typically pose the biggest challenge to urban drainage systems, the choice was made to focus on short-duration events by running the rainfalls successively during step 2 and 3. Each hyetograph presented below in step 2 and 3 was applied in a sequence separated by dry-periods (from 5 to 74 min). Each hyetograph was repeated 3–9 times (see example Figure 1). The

Table 1 | Summary of the tested rainfall events derived from DDF curves for three locations: Trondheim, Oslo, and Bergen both with and without CF

ID	Intensity [mm/min]	Depth [mm]	Duration [mm:ss]	Number of blocks [-]	Return Period			Return period CF = 1.4			Notes
					TRO [YYYY]	OSL	BER	TRO [YYYY]	OSL	BER	
TRO 1	1.7	12	07:00	9	200	20–25	100	20	5	5–10	–
TRO 2	1.0	16	16:00	8	200	5–10	100	20	2	5	16 min with 1 mm/min intensity
TRO 2a	1.0	16	16:00	7	200	5–10	100	20	2	5	2 min with 2.6 mm/min followed by 14 min with 0.8 mm/min
TRO 2b	1.0	16	16:00	8	200	5–10	100	20	2	5	14 min with 0.8 mm/min followed by 2 min with 2.6 mm/min
TRO 2c	1.0	16	16:00	6	200	5–10	100	20	2	5	7 min with 0.8 mm/min followed by 2 min with 2.6 mm/min and 7 min with 0.8 mm/min
TRO 2d	1.0	16	16:00	6	200	5–10	100	20	2	5	2 min with 2.6 mm/min three times
TRO 3	2.6	9	03:30	9	200	100–200	100	20	10	5–10	–
TRO 4	0.8	20	26:00	6	200	5–10	100	20	2	5	–
OSL 1	1.7	23	16:00	5	>>200	200->200	>>200	>200	20	200->200	–
OSL 2	1.0	45	44:00	3	>>200	200->200	>>200	>200	20	200	–
BER 1	1.7	16	09:00	6	>200	50–100	>200	50	5–10	20	–
BER 2	1.0	28	23:00	5	>200	20	>200	50	5	20	–

Bold entries show the events with 20 RP; the rest was transposed to other locations.

inter-event duration was adapted with real-time control of runoff to increase IWC: (1) the peak of runoff had to be reached, (2) IWC had to increase, (3) the set of IWC had to be evenly distributed.

Step 2: influence of the hyetograph

In the second step, the choice was made to run events with different hyetographs in order to identify to what hyetograph the roof runoff is the most sensitive as well as to assess the significance of the WC in contrast with the hyetograph. In this step, all simulated hyetographs corresponded to the same overall rainfall depth (16 mm) and duration (16 minutes), although with different distributions named TRO 2, 2a, 2b, 2c, and 2d (see Table 1). The duration and intensity were based on the 20-year return period curve of Trondheim with the 1.4 climatic factor.

Step 3: influence of duration and intensity

The third step was split in two sub-steps. Firstly, four events were selected on the 20-year return period curve of Trondheim with the 1.4 climate factor (TRO 1, TRO 2, TRO 3, and TRO 4, see Table 1). Secondly, based on the results of the first sub-step, the list of events was expanded through selecting events from the DDF curves of Bergen and Oslo (Figure 2). The intensities of TRO2 and TRO3 were chosen to select the events and study the influence of the rain duration: two events for Oslo

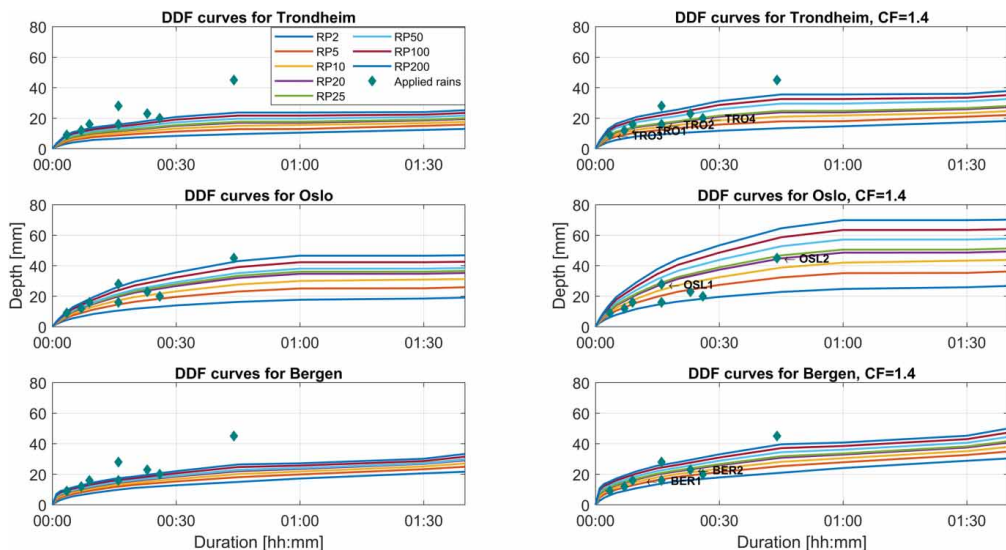


Figure 2 | DDF curves for different return periods, locations, both with (on the right) and without (on the left) the CF of 1.4.

(OSL 1 and OSL 2) and two events for Bergen (BER 1 and BER 2) (Table 1 and Appendix, Table A3 and Table A4). An overview of the individual events was plotted for the different locations – both with and without the climatic factor as shown in Figure 2.

Performance indicators and condition indicators

For all simulated rainfall events, a set of performance indicators was estimated:

- *Peak Runoff [mm/min]*: maximum runoff at 1 min intervals;

- *Peak Attenuation* $[-] = \frac{\text{Peak Rainfall} - \text{Peak Runoff}}{\text{Peak Rainfall}}$ where *Peak Rainfall* [mm/min] is the maximum rainfall intensity at 1 min interval;
- *Peak Delay* [min]: the time between the peak rainfall (the maximum and the last peak when observing multiple peaks) and peak runoff;
- *Centroid Delay* [min]: delay between the mass centre of the rainfall and mass centre of the associated runoff;
- *T50* [min]: a delay between 50% of the volume of the rain supplied on the roof and 50% of the volume released out of the roof. *T50 delay* was only computable when more than 50% of the rain depth was drained from the roof, whereas *Centroid Delay* and *Peak Delay* rely only on runoff (they do not consider retained water).

Condition indicators:

- *Initial Relative Water Content* [mm]: IWC for each event was based on water balance;
- *Peak Relative Water Content* [mm]: PRWC highest value of WC observed before peak runoff (especially, for constant intensity rainfall it corresponds to the WC at the end of the test).

Data processing

The water balance equation was applied to compute WC within a 1-min time resolution. It was not possible to know the IWC; hence, the WC was computed using the stable tail of the outflow (see section ‘Drainage of the roof’) as a reference:

$WC_t = WC_{t+1} + R_t - P_t$ if $t < t_{ref}$ and $WC_t = WC_{t-1} + R_{t-1} + P_{t-1}$ if $t > t_{ref}$ with t_{ref} the daily reference time on the stable tail of the outflow, R the runoff, P the rainfall depth and t the time. The unit was kept as mm to facilitate comparison with rainfall depth. The enlarged uncertainty of WC due to water balance was estimated to be ± 0.7 mm based on the Monte Carlo Method. The raw data were analysed using custom MATLAB[®] scripts.

Due to the short inter-event period between artificial rains, it was not possible to use raw data to compute centroid delay and T50-delay for each rain. Thus, with respect to the first step results, the falling limb between two events was best-fitted using the data from the observed drainage curve. Linear interpolation between successive time intervals was used to minimize the error between the falling limb during dry periods and the roof measured drainage curve. The fitting with the falling limb was evaluated using Nash-Sutcliffe efficiency (NSE). The data from each event was completed to ensure that the outflow volume is equal to the inflow volume and that most of the indicators were computable. Natural precipitation recorded during the experimentation was included in the analysis. However, since the intensity of natural rainfalls was very low compared to the artificial rainfall, the impact of the natural rainfall could be disregarded.

RESULTS AND DISCUSSION

Hydrological analysis of the roof

Time of concentration

To study the behaviour of the roof, the time of concentration (TC), was first assessed. Figure 3 shows the TC curves for different intensities for both the black and the green roofs. TC of the green roof was found inversely proportional to the intensity, i.e. decreasing from 90 minutes to 30 minutes for increasing intensity from 0.8 mm/min to 2.5 mm/min. In contrast, TC of the black roof was found around 5 minutes independently of the intensity. The events defined by their TC and corresponding

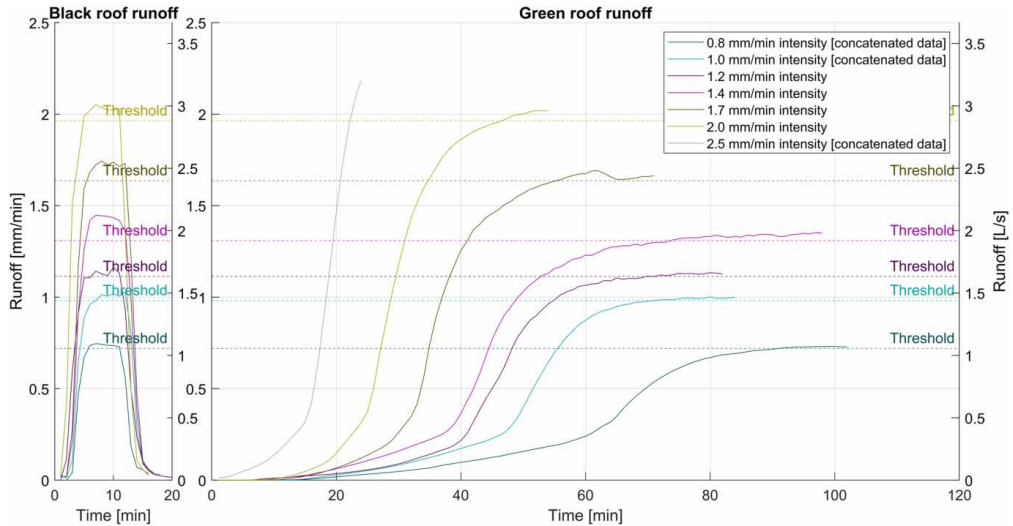


Figure 3 | The TC for different rainfall intensities and rooftop solutions. The TC test for 0.8, 1.0 and 2.5 mm/min intensity started on a partially saturated roof and the curves were completed using concatenation.

mean intensity were found to be close or greater than a 200-year return period (RP) event in Trondheim, Bergen and Oslo, having a 1.4 climate factor. The exact TC was challenging to estimate due to its sensitivity to IWC and its slow asymptotic convergence. Moreover, in the 0.8 mm/min and 1.0 mm/min tests, TC was based on concatenation of the runoff, which might have altered the result. Data from concatenation were monitored under different conditions, inner porosity was saturated (inner porosity was hypothesized to distinguish water standing between the aggregates and water stored in the aggregates), which could have led to underestimating TC. The beginning of an event is subject to a transient state (explained later in ‘Sensitivity to hyetograph’) leading to overestimating TC, even though the transient state was excluded as much as possible. Due to the characteristics of the tested extreme rainfall events, ponding was observed. It was visually inspected that this was linked to the detention properties of the expanded clay and that the outlet was not submerged. [Figure 1](#) shows water distribution in the longitudinal cross section in the middle of the roof.

Dynamic spatial distribution of water within the roof

During all the tests, the spatial distribution of water through the roof longitudinal cross-section was assessed by manual measurement, i.e. the depth of water standing in the roof measured in the 8 plexi-glass tubes. This measurement showed the head loss along the flow path toward the outlet. It was found that different distributions of water within the roof for different rainfall events could lead to the same average WC. In addition, it was also observed that, for high WC (more than 35–45 mm of WC), the same average WC could lead to minor differences in outflows (the uncertainty increases with the WC), which is likely linked to different spatial distributions of water within the roof. This phenomenon was understood as the dynamic effect linked to both the dual-porosity properties of the detention layer (expanded clay) and the size of the roof as the water cannot be instantly transferred to the outlet. [Figure 4](#) shows that the water distribution within the roof at the end of an artificial rainfall was not linear. It was found, especially in OSL 1, BER 1, and BER 2, that the water distribution was dependent on the rainfall intensity and duration acting as a feedback loop: higher intensity led to higher runoff and greater dynamic effect, leading in turn to higher runoff. In

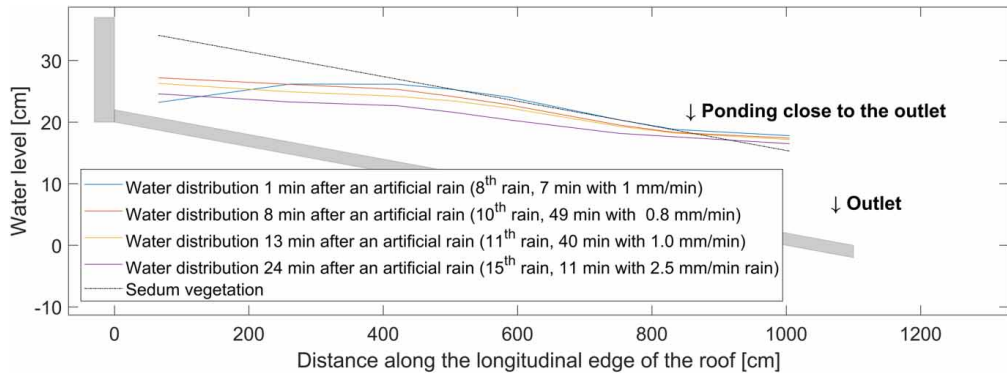


Figure 4 | Cross-section of water distribution in the roof with 50 mm of WC. Data measured during 10.7.2019 along one of the longitudinal edges of the roof. The shaded area (grey) represents the existing concrete structure.

the upper part of the roof (right side of Figure 4), the water level followed a parabolic distribution. During the inter-event period, the water distribution tended to maintain a steady state influenced by gravity and detention properties (the distribution became more linear). Variation of water distribution was explained by capillarity and gravity effect in the detention medium. It was also influenced by both the imperfection of the rainfall simulator (the rainfall spread was not perfectly homogeneous with $\pm 3\%$), and the upper side of the roof having a boundary effect (i.e. close to the top of the roof, no flow was coming from upstream). In addition, a different distribution near the outlet would have been expected if the measurement longitudinal cross section aligned with the outlet due to a different boundary condition. It was also hypothesized that inner conductivity (i.e. the aggregates hydraulic conductivity) was lower than the medium hydraulic conductivity. After saturating the medium, the inner porosity was not yet completely saturated. For this reason, it was not found relevant to simplify the behaviour of the roof as initial losses until field capacity was reached and followed by runoff, as these two processes are interconnected.

Drainage of the roof

For all events, a smooth falling limb, decreasing exponentially, was observed from a nearly saturated roof after various rainfall events (Figure 5). The drainage curves were plotted and processed together with the same starting value. Figure 5 presents the median-observed runoff curve estimated from 14 different events, including the 5th and 95th percentiles. Falling limbs strongly affected by natural rains were excluded from the sample. Additionally, the corresponding relative WC was computed. Even with a minor variation of observed drainage curve, the difference from the 5th percentile to the 95th percentile led to significant variations when computing WC. The WC used with performance indicators was computed based on raw data; hence, while any instability of WC computing should not affect the results presented here, it does highlight the sensitivity of the water balance during long-term events. The WC curve suggests that the detention time is long: starting with 60 mm of WC, it took 3 hours to drain 50% of the water and 6 hours to drain 66% of the water. The analysis of the dynamic distribution of water within the roof and the hypothesis of a dual porosity of the roof material suggests a relevant explanation to interpret the roof drainage curve. The standing water was drained during the first hour, inducing a quick change of outflow. During the second phase, the outflow had smaller variations as the runoff was driven by its exchange with inner WC (i.e. water in the aggregate). The roof has a long saturation and inner porosity drainage time. Therefore, the previous day rainfall and the corresponding detained water can have a significant influence

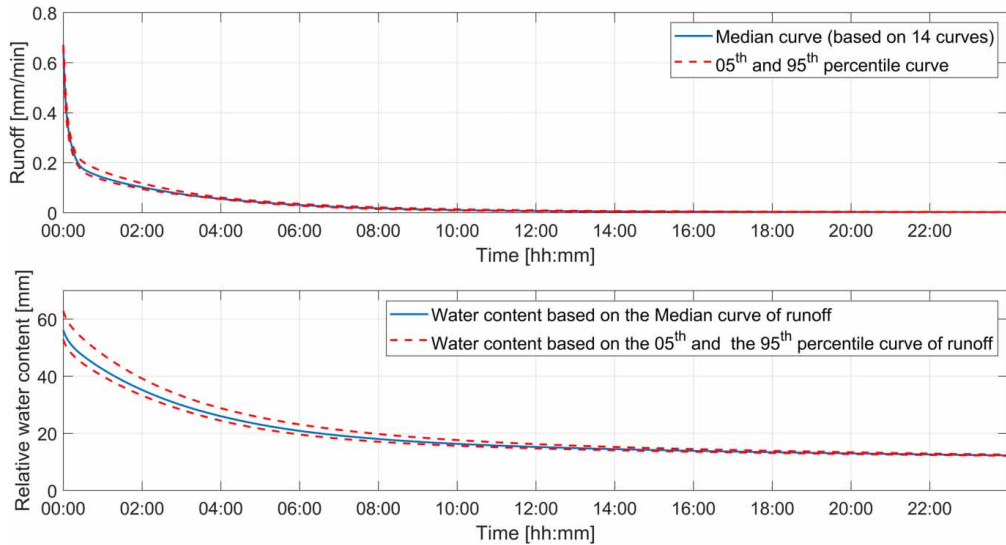


Figure 5 | Median-observed drainage curve for the green roof with 5th and 95th percentile.

on the roof performance. Based on this it was chosen to run short events several times per day to experience a range of WC during the experiments second and third steps.

Sensitivity to hyetograph

The hydrological performance of the roof as a source control may be explained and understood using a variety of indicators, as can be seen in the Appendix, Table A3 and Table A4. When the IWC was low (e.g. lower than field capacity), a plateau of runoff occurred (Figure 6). Consequently, it was not possible to close the event's mass balance, which might slightly alter some indicators. The five artificial events (Table 1 and Table A3) chosen to study the influence of the hyetograph shape on the runoff hydrograph were plotted and compared (Figure 6). Tables A3 and A4 show the roof initial condition, which is represented by starting outflow and starting relative water content (soil moisture), both of which were found to be important for the performance of the roof. As the peak runoff rose, the roof performance deteriorated with respect to the peak attenuation, T50, centroid delay, and peak delay. The performance of each artificial rain cannot be compared directly without considering these initial conditions.

The green roof was tested using different hyetographs (Figure 6). Absolute values of runoff increased in proportion with increasing IWC. Similarly, a dependency between the initial runoff and peak runoff was found. Running different hyetographs enabled the identification of the sensitivity of the roof. As shown in Figure 6, the position of the peak at the end (TRO 2b) of the rainfall had a large impact on the green roof performance. Following TRO 2b, the green roof generated higher and steeper peak outflows than following TRO2 a, c, d or e. Regarding event flow duration, one can easily read the duration of runoff above a threshold and compare this with the hyetograph. For example, only hyetographs peaking in the middle (TRO 2c) and at the end (TRO 2b) generated runoff from the roof that was greater than 1 mm/min.

There are four observable parts in each runoff hyetograph (illustrated with shaded area on Figure 6):

- the start, a transient state influenced by rainfall (a sudden change of the runoff's gradient);
- the increase, a steady state of the gradient influenced by rainfall;

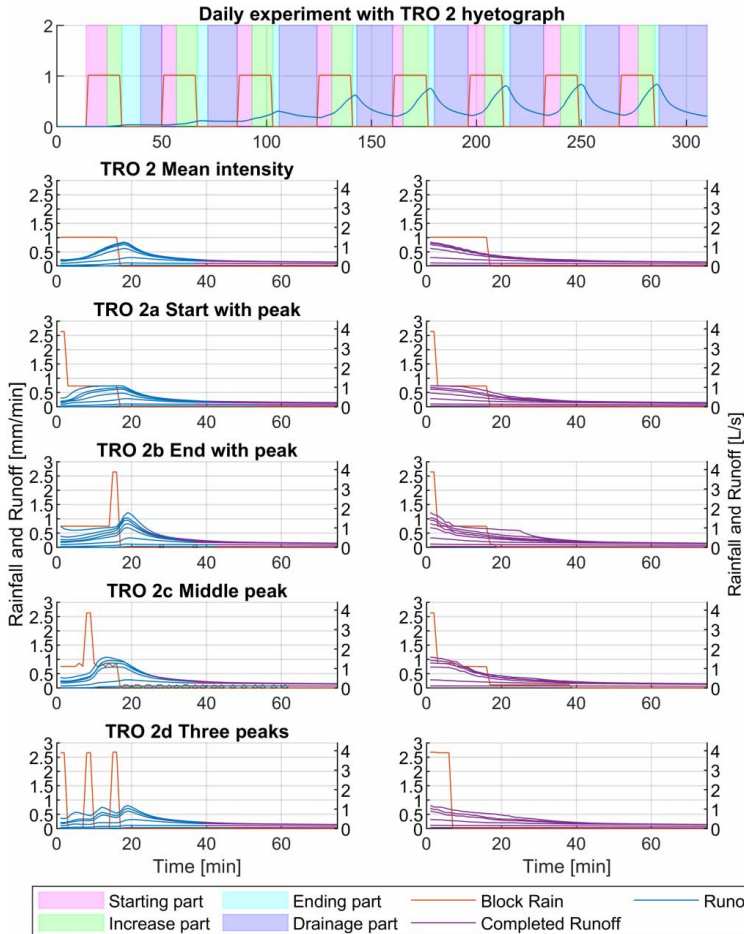


Figure 6 | Comparison of event flow duration for several artificial rainfalls and runoffs for the green roof after 16:00-min blocks with 1.0 mm/min intensity. Mean rainfall depth = 15.9 mm and std = 0.5 mm for all 35 runs.

- the end, a transient state after rainfall stopped that is linked to the dynamic water distribution in both the roof and peak delay (a drop of the gradient);
- the drainage, a steady state of the gradient not influenced by rainfall.

The gradient of the runoff changed smoothly under constant rainfall or without rainfall. Between two stable stages, the gradient changed abruptly: it is the transient stage. The duration of the transition was influenced by the size of the roof and the IWC.

The three indicators selected to assess the effect of the hyetographs are shown in Figure 7. Similarly to previous research (Villarreal & Bengtsson 2005; Li & Babcock 2014; Locatelli *et al.* 2014), there was a relationship between IWC and peak runoff. Given the same IWC, having the peak at the end (TRO 2b) or in the middle of the rainfall (TRO 2c) event caused higher peak runoff. However, the relationship between the peak runoff and peak relative WC was not notably influenced by the hyetograph. The same conclusion may be drawn by analysing centroid delay in comparison with the IWC. Centroid delay, representing the delay between the centres of mass of rainfall and runoff, was not sensitive to the shape of the hyetographs.

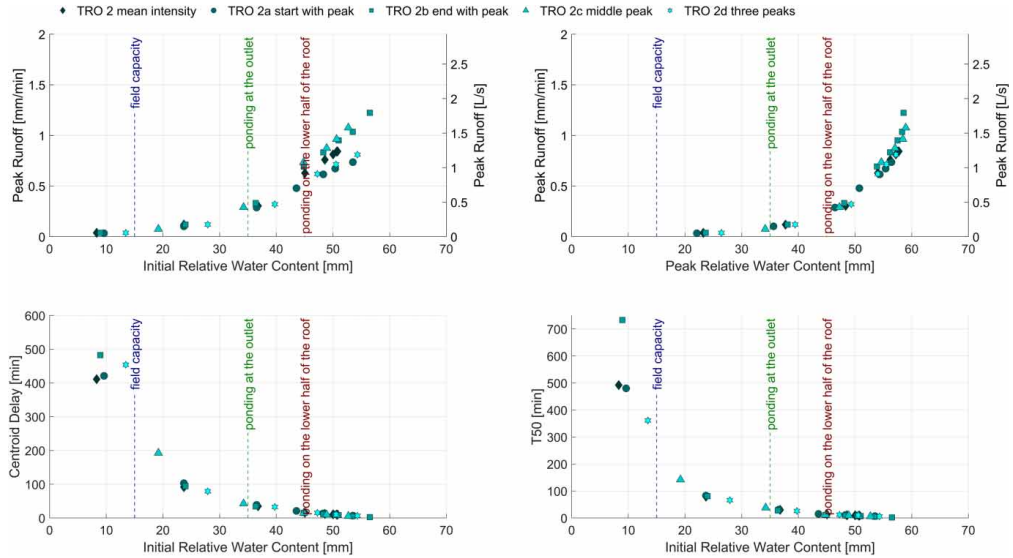


Figure 7 | Observed peak runoff versus IWC and peak relative WC, and centroid delay versus IWC for different hyetographs.

Sensitivity to the rainfall duration and intensity

It was concluded from the second step that the IWC had a stronger influence on performance than the shape of short-term rainfall. Therefore, in order to investigate the roof sensitivity to the rainfall intensity and duration, constant intensity events were studied. Events were chosen based on the 20-year RP IDF curves to ensure realistic values and facilitate a comparison between rainfall events. It should be noted that both future 20-year RP events for Oslo were larger or equal to 200-year RP events under current conditions in Trondheim and Bergen. The roof provided a peak attenuation higher than 93% with the exception of OSL 2. It strengthened the roof's resilience and the capacity to handle a short duration 20-year return period rain in a future climate.

The events corresponding to the Oslo curve generally generated higher runoffs with respect to IWC than events from Bergen and Trondheim (Figure 8). High IWC caused the peak runoff to be close to the peak rainfall. However, when specifically considering the low IWC, the roof was more sensitive to longer rainfalls with lower intensity (e.g. worse performance under OSL 2 than under OSL 1 with IWC lower than field capacity). The roof with a high starting IWC was more vulnerable to shorter events with higher intensity (e.g. worse performance under OSL 1 than under OSL 2 with IWC higher than 30 mm). Although the same analysis could have been done with OSL 2 and BER 1, or BER 1 and BER 2, the shift appeared with a higher WC (50 mm). Consequently, the roof is sensitive to different short-duration rainfalls depending on its initial condition. Thus, in addition to the DDF curves, the design should be location specific, and based on different events depending on a range of IWC.

Comparing the last artificial rains for TRO 1 and TRO 2 with 50 mm WC, it is noticeable that the peak runoffs were very similar (Table A4, Figure 8). However, the peak attenuation remained very different, showing 50% for TRO 1 and 17% for TRO 2. Moreover, similar observations could be done for TRO 2 and TRO 2 a b c d (Table A3). For TRO 2 and TRO 2 a b c d that had the same rainfall depth, but different hyetographs; comparable peak runoffs were found, but the attenuation remained different. Thus, even though peak reduction is a popular performance indicator, it should be presented carefully.

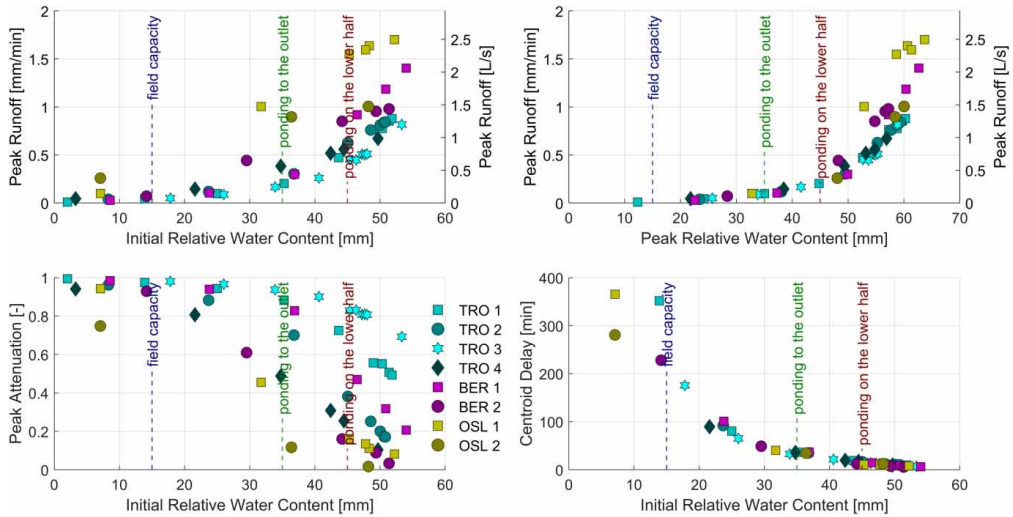


Figure 8 | Comparison between peak runoff, peak attenuation and centroid delay for different locations, including the 1.4 CF.

Peak runoff against peak relative WC followed an exponential tendency independent of the type of artificial rain. However, a scattering of peak runoffs was observed with a high peak of relative WC (over 45 mm, with ponding in the middle of the roof), which could be explained by the dynamic spatial distribution of water within the roof. This scattering effect is governed by the mean intensity of previous intervals (i.e. considering previous artificial rain and dry periods). If the roof had not been saturated, a high mean intensity prior to an artificial rain led to a more curved distribution of water within the roof, i.e. to a higher peak runoff than the other events having the same peak relative WC. OSL 2 was the event with the most significant rainfall depth, and thus, it also had the longest inter-event period. This led to smaller dynamic effect, resulting in a steady water distribution across the roof. On the contrary, OSL 1 and BER 2, due to shorter inter-event durations (and to a pipe disconnection during one of the BER 2 tests), underwent more intense antecedent rainfall, which explains why the scatter effect is more noticeable.

The centroid delay in contrast to initial relative WC may be separated into two domains. Having an IWC lower than field capacity, the centroid delay was over 200 minutes. The centroid delays having IWC at field capacity were independent of the rainfall intensity and duration. When the IWC ascended from field capacity (of approximately 15 mm) to 55 mm, the centroid delay decreased by an exponential decay from 200 min to between 5 and 10 minutes, which showed that even a nearly saturated roof outperformed the black roof. Comparable results were found using the T50 delay, which means that the hyetograph, intensity, and duration do not influence centroid delay or T50 delay, i.e. the performance only depends on the IWC.

Performance depending on location

Events linked to Oslo lead to worst performance as their characteristics are more intense than Trondheim or Bergen events. Nevertheless, the performance of the roof depends to a large extent on the IWC. To assess the performance of the roof under a given location those aspects shall be considered. The IWC depends on the climate, i.e. the number and succession of events and the temperature are supposed to greatly influence those parameters. There are more warm days in Oslo than in Trondheim or Bergen. Consequently, a higher Potential Evapotranspiration (PET) is expected in Oslo, even

though limited in Nordic climates evapotranspiration is expected to influence the IWC. Moreover, the PET is likely to rise with temperature increase (Hanssen-Bauer *et al.* 2017). The number of rainy days per year and annual precipitation were found for each location: Bergen (205 ± 18 days, $2,715 \pm 450$ mm), Oslo (122 ± 15 days, 861 ± 146 mm) and Trondheim (174 ± 14 days, $1,191 \pm 184$ mm) according to the Norwegian Meteorological Institute (<https://www.met.no/>). This shows that initial conditions are likely to change according to each location. This also means that it is necessary to know the IWC conditions to assess future roof performance.

The worst performance of a short-term artificial rainfall (with <45 min for all the rainfalls) linked to the DDF curves of Oslo does not mean that a higher peak is likely to occur in Oslo than in Bergen. According to the number of days with rainfall, the IWC is expected to be higher in Bergen and Trondheim than in Oslo. However, defining a rainfall with a 6-hour antecedent dry weather period, the initial relative WC could not be higher than 25 mm due to the roof's characteristics (Figure 4). A more realistic initial condition would be to consider one that is less than 20 mm. When initial conditions are between field capacity and 20 mm of WC, the roof's performance would be slightly worse in Oslo than in Bergen for short-term rainfalls. It appeared that OSL 2 (0.25 mm/min peak runoff), with initial conditions lower than field capacity, led to worse performance than TRO 1, 2, 3, and 4 with 20 mm of IWC (less than 0.15 mm/min peak runoff). Nonetheless, it did not perform significantly worse than BER 1 and 2 with 20 mm of IWC. In this case, the peak runoff would depend more on the characteristics of the hyetograph than on the location. The centroid delay does not depend on the hyetograph and is likely to be higher in Oslo (more than 200 min) with lower initial conditions than in Bergen (between 200 and 100 min). Nevertheless, these expectations only consider short-term rainfalls up to 45 min. Understandably, 20-year return period events are likely to be more intense in Bergen than in Oslo, having a duration over 140 minutes. This study does not reach a conclusion about long duration rainfalls, which occur more often in Bergen and Trondheim than in Oslo. The hyetograph was not significant in comparison to the IWC with short-term rain. Nevertheless, it would affect a long duration rain.

CONCLUSION

In this study, a method to test extreme precipitation on a full-scale detention-based green roof consisting of sedum mats underlaid with expanded clay was developed using an artificial rainfall simulator. Rainfall events with 20-year return periods, including a climatic factor of 1.4, were derived from DDF curves for three different cities: Bergen, Oslo, and Trondheim, and tested at the field station in Trondheim. This multistep method that compares different variables depending on the previous steps was found relevant to analyse the global performance of the roof.

The assessment of the hydrological performance showed that retrofitting the black roof as a green roof increased the performance significantly. Furthermore, the roof was found to be sensitive to water content strengthened by long drainage and time of concentration. The study also strengthened the understanding of dynamic phenomena governing the flow within the roof and the limitations that are linked to the use of artificial rainfalls. The use of various short-term hyetographs led to different roof performance. It was found that the hyetographs with a peak at the end caused the worst performance, and that the initial water content had a greater influence on the performance than the shape of the hyetograph. Considering water content as a main variable, an indicator such as centroid delay that depends on the initial relative water content is suitable for characterizing the roof without depending on the hyetograph. Indeed, the lower the initial water content was, the longer the detention was observed.

With respect to the general performance of the roof and considering initial conditions according to the location, it was possible to assess that the same roof would perform better in Trondheim than in

Oslo. It was also found that rainfall in Bergen (BER 1 and 2, with a higher initial water content) and Oslo (OSL 1 and 2, with lower initial water content) is likely to lead to similar peak runoff. Consequently, initial conditions need to be taken into account for design purposes as a more favourable hietograph may be counterbalanced by a high initial water content. This study has highlighted the relevance of using performance indicators as a function of input parameters instead of using a single-value performance indicator and discussing commonly used indicators. Based on these results, further study is needed to provide statistics to extend the results to longer lasting rainfalls and make generalizations about locations using modelling.

ACKNOWLEDGEMENTS

The study was supported by the Klima2050 Centre for Research-based Innovation (SFI) and financed by the Research Council of Norway and its consortium partners (grant number 237859/030).

DECLARATION OF INTERESTS

None.

DATA AVAILABILITY STATEMENT

All relevant data are included in the paper or its Supplementary Information.

REFERENCES

- Arnbjerg-Nielsen, K., Willems, P., Olsson, J., Beecham, S., Pathirana, A., Bülow Gregersen, I., Madsen, H. & Nguyen, V. T. V. 2013 *Impacts of climate change on rainfall extremes and urban drainage systems: a review*. *Water Science and Technology* **68** (1), 16–28.
- Bengtsson, L. 2005 *Peak flows from thin sedum-moss roof*. *Hydrology Research* **36** (3), 269–280.
- Berndtsson, J. C. 2010 *Green roof performance towards management of runoff water quantity and quality: a review*. *Ecological Engineering* **36** (4), 351–360.
- BIPM, I., IFCC, I., ISO, I., IUPAP, O. 2009 Evaluation of measurement data- an introduction to the ‘Guide to the expression of uncertainty in measurement’ and related documents. *JCGM* **104**, 1–104.
- Copenhagen, C. o. 2011 *Copenhagen Carbon Neutral by 2025, Copenhagen Climate Adaptation Plan*.
- Dyrørdal, A. V. & Førland, E. J. 2019 *Klimapåslag for korttidsnedbør – Anbefalte verdier for Norge, Norwegian Climate Service Center*.
- Fassman-Beck, E., Voyde, E., Simcock, R. & Hong, Y. S. 2013 *4 living roofs in 3 locations: does configuration affect runoff mitigation?* *Journal of Hydrology* **490**, 11–20.
- Few, R. 2003 *Flooding, vulnerability and coping strategies: local responses to a global threat*. *Progress in Development Studies* **3** (1), 43–58.
- FLL 2008 *Guidelines for the Planning, Construction and Maintenance of Green Roofing: Green Roofing Guideline*. Forschungsgesellschaft Landschaftsentwicklung Landschaftsbau, Landscape, Research, Development & Construction Society, Bonn, Germany.
- Hamouz, V. & Muthanna, T. M. 2019 *Hydrological modelling of green and grey roofs in cold climate with the SWMM model*. *Journal of Environmental Management* **249**, 109350.
- Hamouz, V., Lohne, J., Wood, J. R. & Muthanna, T. M. 2018 *Hydrological performance of LECA-based roofs in cold climates*. *Water* **10** (3), 263.
- Hanssen-Bauer, I., Førland, E. J., Haddeland, I., Hisdal, H., Mayer, S., Nesje, A., Nilsen, J. E. Ø., Sandven, S., Sandø, A. B., Sorteberg, A. & Ådlandsvik, B. 2017 *Climate in Norway 2100 – A Knowledge Base for Climate Adaptation*. Norsk klimasenter.
- Hettiarachchi, S., Wasko, C. & Sharma, A. 2018 *Increase in Flood Risk Resulting From Climate Change in A Developed Urban Watershed-the Role of Storm Temporal Patterns*.

- Hoegh-Guldberg, O., Jacob, D., Bindi, M., Brown, S., Camilloni, I., Diedhiou, A., Djalante, R., Ebi, K., Engelbrecht, F., Guiot, J., Hijikata, Y., Mehrotra, S., Payne, A., Seneviratne, S. I., Thomas, A., Warren, R., Zhou, G., Halim, S. A., Achlatis, M., Alexander, L. V., Allen, M., Berry, P., Boyer, C., Byers, E., Brilli, L., Buckeridge, M., Cheung, W., Craig, M., Ellis, N., Evans, J., Fischer, H., Fraedrich, K., Fuss, S., Ganase, A., Gattuso, J. P., Greve, P., Bolaños, T. G., Hanasaki, N., Hasegawa, T., Hayes, K., Hirsch, A., Jones, C., Jung, T., Kanninen, M., Krinner, G., Lawrence, D., Lenton, T., Ley, D., Liverman, D., Mahowald, N., McInnes, K., Meissner, K. J., Millar, R., Mintenbeck, K., Mitchell, D., Mix, A. C., Notz, D., Nurse, L., Okem, A., Olsson, L., Oppenheimer, M., Paz, S., Petersen, J., Petzold, J., Preuschmann, S., Rahman, M. F., Rogelj, J., Scheuffele, H., Schleussner, C.-F., Scott, D., Séférian, R., Sillmann, J., Singh, C., Slade, R., Stephenson, K., Stephenson, T., Sylla, M. B., Tebboth, M., Tschakert, P., Vautard, R., Wartenburger, R., Wehner, M., Weyer, N. M., Whyte, F., Yohe, G., Zhang, X. & Zougmore, R. B. 2018 *Impacts of 1.5°C Global Warming on Natural and Human Systems*. IPCC Special Report.
- Johannessen, B., Muthanna, T. & Braskerud, B. 2018 *Detention and retention behavior of four extensive green roofs in three nordic climate zones*. *Water* **10** (6), 671.
- Johannessen, B. G., Hamouz, V., Gragne, A. S. & Muthanna, T. M. 2019 *The transferability of SWMM model parameters between green roofs with similar build-up*. *Journal of Hydrology* **569**, 816–828.
- Kristvik, E., Kleiven, G. H., Lohne, J. & Muthanna, T. M. 2018 *Assessing the robustness of raingardens under climate change using SDSM and temporal downscaling*. *Water Science and Technology* **77** (6), 1640–1650.
- Kristvik, E., Johannessen, B. G. & Muthanna, T. M. 2019 *Temporal downscaling of IDF curves applied to future performance of local stormwater measures*. *Sustainability* **11** (5), 1231.
- Li, Y. & Babcock, R. W. 2014 *Green roof hydrologic performance and modeling: a review*. *Water Science and Technology* **69** (4), 727–738.
- Lindholm, O., Endresen, S., Thorolfsson, S., Sægrov, S., Jakobsen, G. & Aaby, L. 2008 *Veiledning i klimatilpasset overvannshåndtering*. *Rapport* **162**, 2008.
- Locatelli, L., Mark, O., Mikkelsen, P. S., Arnbjerg-Nielsen, K., Jensen, M. B. & Binning, P. J. 2014 *Modelling of green roof hydrological performance for urban drainage applications*. *Journal of Hydrology* **519**, 3237–3248.
- Mentens, J., Raes, D. & Hermy, M. 2006 *Green roofs as a tool for solving the rainwater runoff problem in the urbanized 21st century?* *Landscape and Urban Planning* **77** (3), 217–226.
- Miller, J. D. & Hutchins, M. 2017 *The impacts of urbanisation and climate change on urban flooding and urban water quality: a review of the evidence concerning the United Kingdom*. *Journal of Hydrology: Regional Studies* **12**, 345–362.
- Naves, J., Jikia, Z., Anta, J., Puertas, J., Suárez, J. & Regueiro-Picallo, M. 2017 *Experimental study of pollutant washoff on a full-scale street section physical model*. *Water Science and Technology* **76** (10), 2821–2829.
- Naves, J., Anta, J., Puertas, J., Regueiro-Picallo, M. & Suárez, J. 2019 *Using a 2D shallow water model to assess Large-Scale Particle Image Velocimetry (LSPIV) and Structure from Motion (SfM) techniques in a street-scale urban drainage physical model*. *Journal of Hydrology* **575**, 54–65.
- Speak, A., Rothwell, J., Lindley, S. & Smith, C. 2013 *Rainwater runoff retention on an aged intensive green roof*. *Science of the Total Environment* **461**, 28–38.
- Stocker, T. 2014 *Climate Change 2013: The Physical Science Basis: Working Group I Contribution to the Fifth Assessment Report of the Intergovernmental Panel on Climate Change*. Cambridge University Press.
- Stovin, V. 2010 *The potential of green roofs to manage urban stormwater*. *Water and Environment Journal* **24** (3), 192–199.
- Stovin, V., Vesuviano, G. & De-Ville, S. 2017 *Defining green roof detention performance*. *Urban Water Journal* **14** (6), 574–588.
- VanWoert, N. D., Rowe, D. B., Andresen, J. A., Rugh, C. L., Fernandez, R. T. & Xiao, L. 2005 *Green roof stormwater retention*. *Journal of Environmental Quality* **34** (3), 1036–1044.
- Villarreal, E. L. & Bengtsson, L. 2005 *Response of a Sedum green-roof to individual rain events*. *Ecological Engineering* **25** (1), 1–7.
- Voyde, E., Fassman, E. & Simcock, R. 2010 *Hydrology of an extensive living roof under sub-tropical climate conditions in Auckland, New Zealand*. *Journal of Hydrology* **394** (3), 384–395.
- Zhou, Q. 2014 *A review of sustainable urban drainage systems considering the climate change and urbanization impacts*. *Water* **6** (4), 976–992.

Paper 3

Hydrological modelling of green and grey roofs in cold climate with the SWMM model

Hamouz, V., & Muthanna, T. M. (2019).

Journal of environmental management, 249, 109350. <https://doi.org/10.1016/j.jenvman.2019.109350>



Contents lists available at ScienceDirect

Journal of Environmental Management

journal homepage: www.elsevier.com/locate/jenvman

Research article

Hydrological modelling of green and grey roofs in cold climate with the SWMM model



Vladimír Hamouz*, Tone Merete Muthanna

Department of Civil and Environmental Engineering, Norwegian University of Science and Technology (NTNU), N-7491, Trondheim, Norway

ARTICLE INFO

Keywords:

Green roofs
Grey roofs
Storm water management model (SWMM)
Hydrological performance
Decision support
Urban snowmelt modelling

ABSTRACT

Rooftop retrofitting targets the largest land-use type available for reduction in impervious surfaces area in urban areas. Extensive green and grey roofs offer solution for retention and detention of stormwater in densely developed urban areas. Among the available green roof types, the extensive green roof has become a popular selection and commonly adopted choice. These solutions provide multiple benefits for stormwater and environmental management due to stormwater retention and detention capacities. The Storm Water Management Model (SWMM) 5.1.012 with Low Impact Development (LID) Controls was used to model the hydrological performance of a green and a grey (non-vegetated detention roof based on extruded lightweight aggregates) roof (located in the coastal area of Trondheim, Norway) by defining the physical parameters of individual layers in LID Control editor. High-resolution 1-min data from a previously monitored green and grey roof were used for calibration. Six parameters within the individual LID layers: soil (four parameters) and drainage mat (two parameters) were selected for calibration. After calibration, the SWMM model simulated runoff with a Nash-Sutcliffe model efficiency (NSME) of 0.94 (green roof) and 0.78 (grey roof) and a volume error of 3% for the green roof, and 10% for the grey roof. Validation of the calibrated model indicates good fit between observed and simulated runoff with a NSME of 0.88 (green roof) and 0.81 (grey roof) and with volume errors of 29% (green roof) and 11% (grey roof). Concerning the snowmelt modelling, the calibrated model showed a NSME of 0.56 (green roof) and 0.37 (grey roof) through the winter period. However, regarding volume errors, additional model development for winter conditions is needed; 30% (green roof) and 11% (grey roof). Optimal parameter sets were proposed within both the green and grey configurations. The results from calibration and especially validation indicated that SWMM could be used to simulate the performance of different rooftop solutions. The study provides insight for urban planners of how to target and focus the implementation of rooftop solutions as stormwater measures.

1. Introduction

The combined effect of urban growth and climate change is altering the hydrological balance in developed urban areas (Gill et al., 2007; Leopold, 1968; Semádeni-Davies et al., 2008). They is also an increase public awareness of the impact of stormwater on flash flood occurrence and water quality in receiving water bodies (Jia et al., 2015). Generally, rooftops remain unused, even though they cover a large part of the impervious surfaces. Rooftop retrofitting, using either vegetated (Stovin et al., 2012) or non-vegetated (in this paper: “grey” detention roof based on extruded lightweight aggregates, which profits from its filter media while attenuating stormwater runoff) (Hamouz et al., 2018) solutions, has shown multiple benefits in terms of hydrology, building physics, biodiversity, and usage as living areas (allowing for working and/or recreational purposes) (Ahiablame and Shakya, 2016; Berndtsson, 2010). The rooftop retrofitting offers a method to manage stormwater at the

source while providing retention and runoff detention in already urbanized areas (Cipolla et al., 2016).

1.1. Urban green roof runoff modelling

A large part of the research has been conducted as monitoring studies to understand the hydrological performance of green roofs. However, it remains challenging to predict the hydrological performance in general, as each performance reflect a specific type of green roof and its location. There has been several attempts to simulate green roof runoffs on an individual roof scale (Carson et al., 2013; Hilten et al., 2008; Johannessen et al., 2019; Kasmin et al., 2010; Krebs et al., 2016; Locatelli et al., 2014; Metselaar, 2012; Stovin et al., 2012; Villarreal, 2007) or a catchment scale (Ashbolt et al., 2013; Carter and Jackson, 2007; Krebs et al., 2013, 2014; Palla and Gnecco, 2015; Rosa et al., 2015; Warsta et al., 2017). These models can either be categorized as data-based, where runoff is calculated as an empirical function of rainfall or

* Corresponding author.

E-mail address: vladimir.hamouz@ntnu.no (V. Hamouz).<https://doi.org/10.1016/j.jenvman.2019.109350>

Received 15 January 2019; Received in revised form 17 July 2019; Accepted 1 August 2019

Available online 12 August 2019

0301-4797/ © 2019 The Authors. Published by Elsevier Ltd. This is an open access article under the CC BY license

<http://creativecommons.org/licenses/by/4.0/>.

process-based methods, where the flow is calculated from the green roof water balance (Carson et al., 2017; Li and Babcock, 2014; Stovin et al., 2013). Urban hydrology is a complex system, where a model has to account for an array of possible physical processes: surface runoff, infiltration, groundwater, snowmelt, flow routing, surface ponding, and water quality routing. Green roof systems, which calculate the runoff by solving the water balance equation, account for precipitation, irrigation, storage and evapotranspiration processes (Rossman, 2015). Even though the green roofs might be a quite simple system consisting of several layers, all the processes within each layer must be controlled dynamically. Based on these considerations, the physically based SWMM model has been considered the best choice for further work as it includes all previously mentioned processes as well as snowmelt simulation (Elliott and Trowsdale, 2007; Moghadas et al., 2016).

1.2. Urban snowmelt modelling

Snowmelt and rain-on-snow events in urban areas in the coastal Nordic regions are complex processes. Frontal systems drive low pressure systems as they hit the coast. The path and precipitation intensities are often difficult to accurately predict, resulting in a rapidly changing weather pattern. The winter season often brings heavy snowfall followed by rainfall events, which results in flood risk in urban areas due to mixing of rainfall and snowmelt for these rain-on-snow events, (Moghadas et al., 2017). Moreover, in coastal regions such as Trondheim, continuous changing in freezing and thawing periods can create an intermittent impermeable cover in cold and wet areas (e.g., the coast of Norway) (Matheussen, 2004; Paus et al., 2016). Furthermore, the snow-pack distribution is influenced by meteorological variables (temperature, precipitation, wind, radiation), spatial disposition (topography, vegetation, insulation conditions, albedo) and anthropogenic activities ((Beven, 2011; Førland et al., 1996; Matheussen and Thorolfsson, 2004; Moghadas et al., 2016; Semádeni-Davies, 2000), among others). This adds challenges to the urban snowmelt modelling as snow characteristics (e.g., snow density, albedo, grain size porosity, solar energy absorption) in urban areas vary substantially from rural areas (Bengtsson and Westerström, 1992; Gray and Male, 1981; Semádeni-Davies, 2000; Sundin et al., 1999).

There is a knowledge gap in the hydrological performance of the different solutions under variable climates and geographical locations, especially on a large scale, rather than a small pilot test. Applying modelling software in combination with observed data offers a tool to simulate expected hydrological performance under various current and future climate conditions (Peng and Stovin, 2017). Therefore, a more generic approach has been adopted in order to model green and grey roof hydrological performance on-site. In this study, the Storm Water Management Model (SWMM) including the LID module for green roofs has been applied for simulating runoff from the aforementioned green and grey roof located in the coastal area of Trondheim, Norway.

The literature review has revealed that there have been several attempts to model retention performance of small-scale green roofs using the SWMM model. However, there is still a lack of knowledge with respect to modelling of detention performance of green roofs. This moreover applies to a very new concept of grey detention roofs which has shown promising results especially for stormwater detention and it ought to be mentioned that in this study the green and grey roof has been tested in the full-scale size (i.e., area of a family house with 100 m²). Another major gap within the SWMM model is the transferability of initial parameters representing runoff characteristics (Johannessen et al., 2019). This study revealed the importance of calibration against local meteorological data.

Several urban snowmelt models have been developed; however, a challenging part in snowmelt modelling remains in terms of finding an optimal level of complexity. This is because more sophisticated models do not necessarily provide better results in a diverse urban environment due to the lack of available data (Moghadas et al., 2016). The previous attempts to model snowmelt in urban areas were performed on a catchment scale (Ho and Valeo, 2005; Moghadas et al., 2017; Semádeni-Davies, 1997, 2000). However, one of the main issues linked to snowmelt modelling is caused by snow redistribution in an urban environment as aforementioned reported. In this study, the focus is given to rooftops only, where human-made snow redistribution is not

expected. This might facilitate snowmelt simulation from a single green or grey rooftop.

The research questions that this study aims to answer are:

1. What is the performance of the SWMM model after calibration for long-term continuous simulations¹ in terms of the Nash-Sutcliffe model efficiency and volume error of green and grey roofs in coastal regions during warm² period?
2. Does the model calibration provide an optimal parameter set, which will satisfy both the objective functions; the Nash-Sutcliffe model efficiency and volume error?
3. Is the SWMM model able to accurately simulate snowmelt and rain-on-snow events from a green and grey roof in coastal regions during cold³ period?

2. Materials and methods

2.1. Characteristics of the green and grey roof

A full-scale field setup was built (approximately 10 m above ground and 50 m.a.s.l.) in order to study the hydrological performance of three different roof configurations at Høvringen in Trondheim, Norway (63°26'47.5" N 10°20'11.0" E). A conventional (black) roof with bituminous waterproofing served as a reference to the green and grey roof. The dimensions of each roof were 8 × 11 m, with a longitudinal slope of 2%. Thus, 88 m² served for green/grey roof retrofitting within each field, but an additional 12 m² were accounted for runoff contribution from impervious surroundings. The structural composition of the grey roof was made up of an underlying protection layer, a 200 mm thick layer of lightweight extruded clay aggregates (LWA) and covered with concrete pavers (200 × 200 × 70 mm). The green roof consisted of an underlying protection layer, a 25 mm plastic drainage layer (egg box), a 10 mm retention mat and a 30 mm pre-grown reinforced extensive Sedum mat (Fig. 1). Based on (FL, 2008), the maximum water holding capacity (MWHC) was estimated having 52.8 mm for the grey roof and 20.6 mm for the green roof (theoretical values⁴). A more detailed description of the grey roof setup can be found in the previous study (Hamouz et al., 2018).

2.2. Input data

The data was collected at the field station within the period from May 2017 to April 2018. Precipitation was measured by a heated tipping bucket rain gauge (Lambrecht meteo GmbH 1518 H3, Lambrecht meteo GmbH, Göttingen, Germany) with a resolution of 0.1 mm at 1-min intervals and with accuracy ± 2%. Runoff was measured using a weight-based system (accuracy class C3 according to OIML R60) with two tanks downstream of the drainage outlets. The collection tanks were automatically emptied every 30 min, and when the collected water reached the capacity of the tank. All the data were recorded at 1-min intervals with a CR 1000 data logger (Campbell Scientific, Inc.). Air temperature was registered using a thermosensor (Vaisala HMP155A Temperature and Humidity with accuracy ± 0.03 °C), and wind speed using an ultrasonic anemometer (Luftt VENTUS Ultrasonic anemometer, 240W heater with an accuracy ± 2%). Actual evapotranspiration was estimated as the water loss from direct measurements of precipitation and runoff. Soil moisture sensors were not available during the model calibration

¹ Long-term continuous simulation means simulation through several months, including several events in this paper.

² Period without snow and negative temperatures.

³ Period with snow and temperatures that can influence runoff (<= 0 °C).

⁴ The values of MWHC are, however, very theoretical since the method assumes a comparison between a wet and oven-dry sample, which is not possible to achieve in the field conditions. At the same time, the methodology assumes dripping away over 2 h following total immersion for 24 h where the dripping period is questionable for such detention materials used in the green/grey roof build-up.

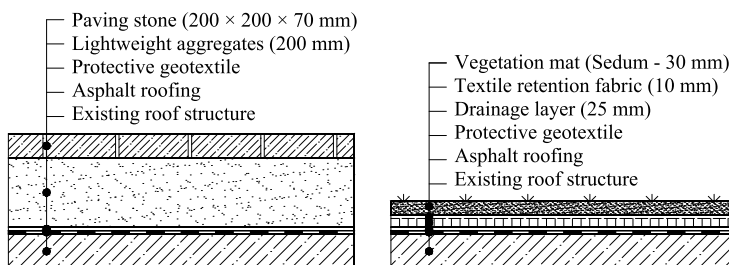


Fig. 1. Grey (left) and green (right) rooftop configurations in a cross-section. (For interpretation of the references to colour in this figure legend, the reader is referred to the Web version of this article.)

process. Therefore, the initial moisture was estimated, and the first rainfall event was used as a warm-up period.

2.3. Model application and parameters estimation

The Storm Water Management Model (SWMM) 5.1.012, including the Low Impact Development (LID) Controls module specifically designed for modelling SUDS (Sustainable Urban Drainage Systems) structures, was used for long-term and short-term simulation of runoff quantity using the rainfall/runoff process with 1-min reporting time step. The green and the grey roofs were modelled as a subcatchment in SWMM, where the rooftop occupied 88% of the subcatchment, and the remaining 12% by impervious area. This impervious area is covered by a standard asphalt roofing, same as used for the reference roof. For this layer, the Manning's surface roughness was set to 0.015 and the depression storage to 0.01 mm. Simultaneously, the impervious area was routed to the LID module. The LID module consists of three layers (surface, soil and drainage mat). Only parameters included in the soil and drainage layers were selected for calibration (Table 1), as the surface layer is assumed not to contribute to the retention or detention performance in the LID module due to the high infiltration capacity. Within the soil layer the porosity (indicating potential space within soil layer for storing stormwater), field capacity (indicating the amount of water in the soil layer after free water

drainage), conductivity (indicating the velocity, which the water can flow through a porous medium), conductivity slope (indicating the slope of the curve of log (conductivity) vs. soil moisture content) were calibrated, in addition, two parameters within the drainage mat; the void fraction (indicating the ratio of void volume to total volume in the mat) and roughness (used to compute the lateral flow rate of drained water through the mat). The initial green and grey roof parameters as well as lower and upper bound used during the calibration were estimated from field measurements, literature (Carson et al., 2017; Krebs et al., 2016; Peng and Stovin, 2017; Rosa et al., 2015), or defaults (Rossman and Huber, 2016a, 2016b). The thickness of the substrate layer of the grey roof, which is 200 mm, was used in the LID module for both the soil layer as well as a part within the drainage mat layer. The estimation of the drainage mat thickness, which could represent the flow through the lightweight aggregate was set to 5% of the whole thickness, thus 10 mm. This was estimated based on the high infiltration capacity of the lightweight aggregate where saturated hydraulic conductivity was experimentally determined in the laboratory to be 1432 mm/h. The Green-Ampt and the curve number infiltration method were used for the green roof and the grey roof, respectively. The kinematic wave routing method, which solves the continuity equation with a simplified form of the momentum equation, was applied for overland flow calculations (Rossman and Huber, 2016a, 2016b).

Table 1
LID Green roof control editor and its parameters with initial values and lower and upper bounds.

Control name	Green roof		Grey roof		Data source
	Initial value	Range	Initial value	Range	
SURFACE					
Berm Height (mm)	500	–	500	–	a
Vegetation Volume Fraction	0.1	–	0	–	b
Surface Roughness (Manning's n)	0.05	–	0.015	–	c
Surface Slope (%)	2	–	2	–	a
SOIL					
Thickness (mm)	30	–	200	–	a
Porosity (volume fraction)*	0.5	0.45–0.60	0.6	0.45–0.65	b, c, d, e, f
Field Capacity (volume fraction)*	0.3	0.20–0.45	0.1	0.02–0.2	b, c, d, e, f
Wilting Point (volume fraction)	0.05	–	0.01	–	b, c, d, e, f, g
Conductivity (mm/hr)*	25	10–1000	1432	500–3000	b, c, d, e, f
Conductivity Slope*	15	5–60	10	5–60	b, c, d, e, h
Suction Head (mm)	110	–	10	–	b, c, d, g
DRAINAGE MAT					
Thickness (mm)	10	–	10	–	a
Void Fraction*	0.5	0.01–1	0.5	0.01–1	b
Roughness (Manning's n)*	0.1	0.01–0.4	0.1	0.01–0.4	b
Site specific					
Rossman (2015)	a		Laboratory analysis		e
Rossman and Huber (2016a)	b		FLI (2008)		f
Rossman and Huber (2016b)	c		Rosa et al. (2015)		g
	d		Palla and Necco (2015)		h

* parameters for calibration.

Table 2
Individual events used for evaluating the model performance within calibration (C) and validation (V) period and their hydrometeorological properties. The table also shows overall model performance for long-term continuous periods (total period*) as well as individual events that occurred during the calibration and validation period.

ev.num	RAINFALL		RUNOFF		CALIBRATION/ VALIDATION	RAINFALL			RUNOFF PEAK		
	start	end	start	end		DURATION [hh:mm]	DEPTH [mm]	MEAN INTENSITY [mm/h]	MAX 5MIN INTENSITY [mm/h]	MAX BLACK [L/min]	MAX GREEN [L/min]
1	21.05.2017 16:19	24.05.2017 06:24	C1		35:29	18.8	0.5	6.0	10.73	1.2	
2	12.06.2017 09:15	14.06.2017 05:59	C2		16:57	15.1	0.9	6.7	14.62	4.22	
3	17.06.2017 16:47	23.06.2017 04:01	C3		74:39	65.4	0.9	11.6	20.63	12.78	
4	11.07.2017 04:47	15.07.2017 10:29	C4		55:41	26.4	0.5	16.3	26.55	3.31	
5	26.07.2017 16:21	26.07.2017 17:50	C5		0:07	3.2	27.4	21.6	62.12	2.87	
6	16.08.2017 04:53	18.08.2017 02:26	V1		18:06	12.8	0.7	7.2	12.1	3.24	
7	19.08.2017 13:41	22.08.2017 00:50	V2		28:47	57.7	2.0	40.8	102.74	26.03	
8	29.08.2017 02:52	30.08.2017 13:05	V3		15:34	12.4	0.8	21.6	48.07	2.21	
9	13.09.2017 03:05	14.09.2017 10:30	V4		9:39	7.9	0.8	12.0	17.3	1.38	
10	05.10.2017 22:59	09.10.2017 20:31	V5		75:56	23.7	0.3	9.6	19.83	5.84	
11	26.10.2017 03:18	03.11.2017 08:06	V6		167:47	94.7	0.6	9.6	12.67	10.21	

(continued on next page)

Table 2 (continued)

ev.num	RUNOFF PEAK				RUNOFF VOLUME					
	MAX GREY	BLACK OBSERVED	GREEN OBSERVED	GREEN SIMULATED	VE	NSME	GREY OBSERVED	GREY SIMULATED	VE	NSME
	[L/min]	[mm]	[mm]	[mm]	[%]	[-]	[mm]	[mm]	[%]	[-]
1	1.4	18.3	5.6	6.5	-15.9	0.44	15.4	8.4	45.3	0.33
2	2.08	15.9	6.9	8.0	-16.3	0.61	14.8	12.4	16.1	0.44
3	4.17	62.4	57.5	52.7	8.3	0.98	62.6	60.6	3.1	0.78
4	0.91	25.5	19.6	19.3	1.5	0.89	22.7	22.9	-0.7	0.61
5	1.65	3.0	0.2	0.0	96.6	-0.13	0.2	0.2	30.8	0.59
6	2.08	13.9	6.3	2.6	59.4	0.38	12.5	10.8	13.5	0.24
7	7.09	63.8	58.6	46.3	21.0	0.88	61.3	54.7	10.7	0.80
8	1.34	12.2	5.6	2.3	59.4	0.26	9.2	10.5	-14.0	0.06
9	0.87	7.7	0.7	0.8	-10.0	-0.90	5.0	6.9	-38.6	-1.74
10	2.3	26.3	24.4	16.7	31.5	0.86	25.7	27.5	-6.7	0.53
11	5.85	97.3	94.6	77.6	17.9	0.84	96.6	92.1	4.7	0.80
total - calibration period		241.5	147.4	143.3	2.8	0.94	214.4	193.5	9.7	0.78
total - validation period		331.2	259.7	185.1	28.7	0.88	315.6	279.7	11.4	0.81
total - cold period		390.0	371.0	259.0	30.2	0.56	384.0	340.0	11.5	0.37

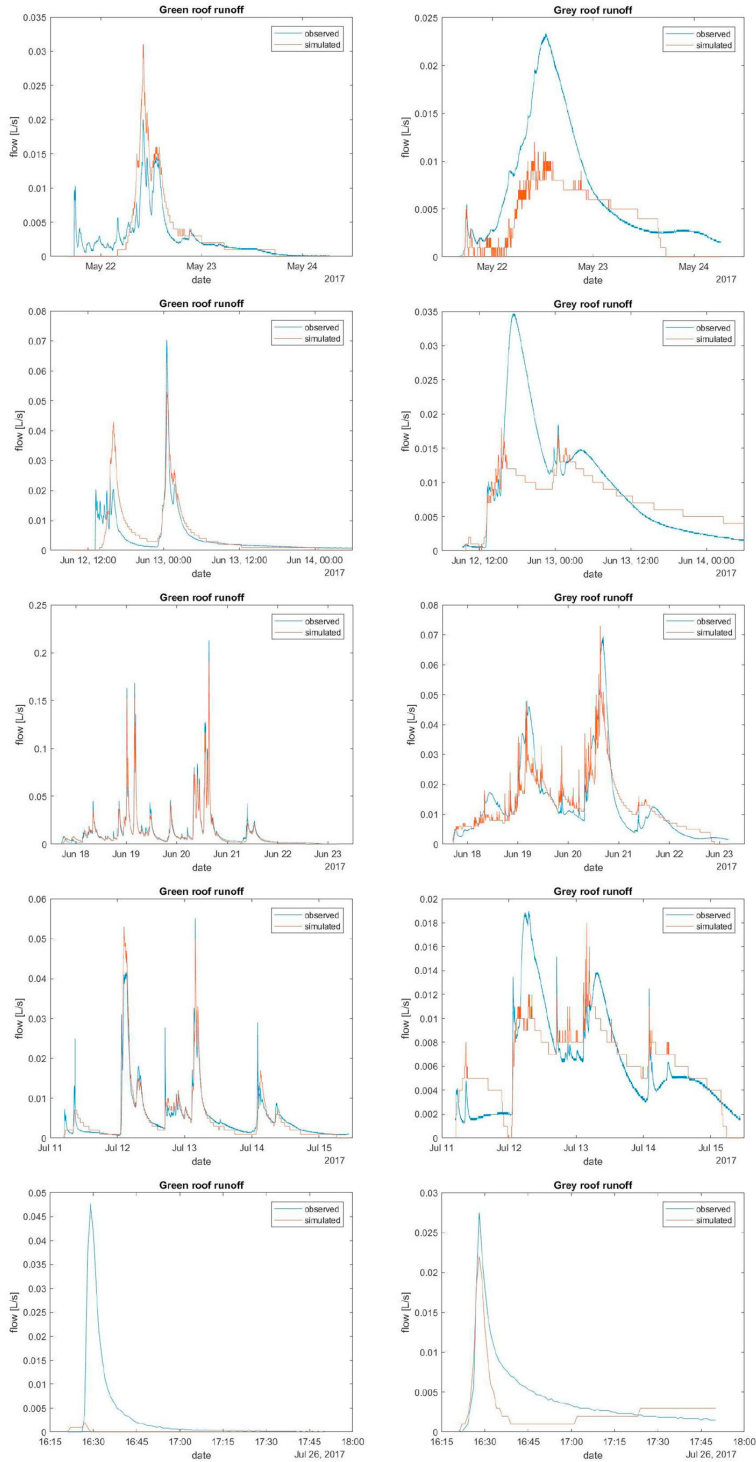


Fig. 2. Comparison of observed and simulated runoff from the green (left) and grey (right) roof. Five events that occurred during the calibration period were chosen, namely C1, C2, C3, C4, and C5 (Table 2). (For interpretation of the references to colour in this figure legend, the reader is referred to the Web version of this article.)

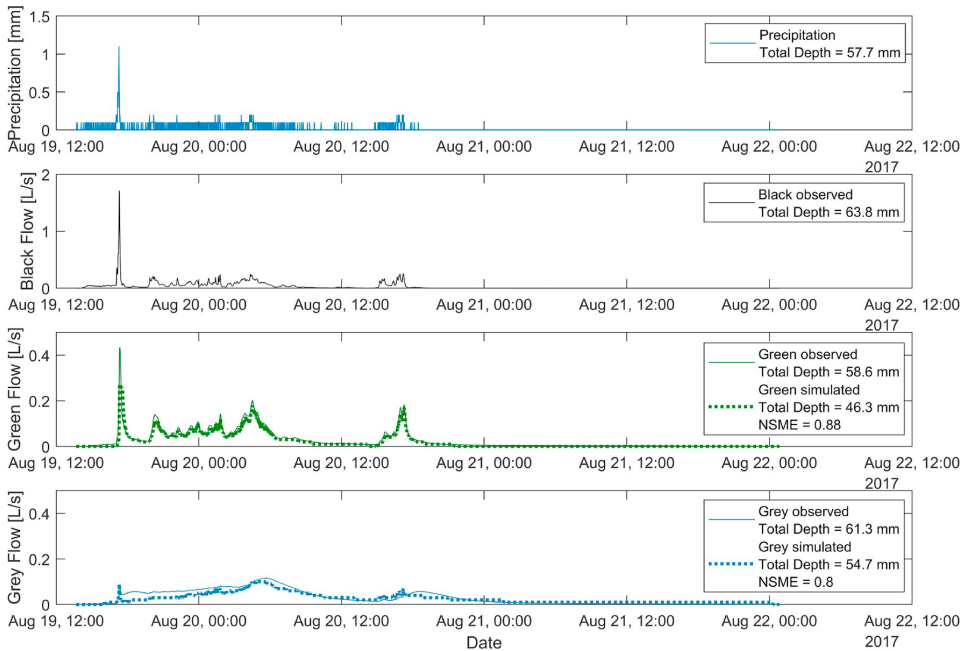


Fig. 3. Calibrated time-series rainfall, observed runoff, and simulated runoff for the largest event registered between 19th and 22nd of August 2017.

2.4. Model performance

Two objective functions were applied to evaluate the model performance. The model accuracy was quantitatively assessed with the Nash-Sutcliffe model efficiency (NSME) (eq. (1)) (Nash and Sutcliffe, 1970), which aims to evaluate the peak performance. Regarding water balance evaluation, the volume error (VE) (eq. (2)) was used to calculate discrepancies between observed and simulated (modelled) runoff.

$$NSME = 1 - \frac{\sum_1^n (Q_{obs,i} - Q_{sim,i})^2}{\sum_1^n (Q_{obs,i} - \bar{Q}_{obs})^2}, \tag{1}$$

$$VE = \frac{V_{obs} - V_{sim}}{V_{obs}} * 100, \tag{2}$$

where $Q_{obs,i}$ is the observed discharge and $Q_{sim,i}$ is the modelled discharge, \bar{Q}_{obs} is the mean of observed discharge, and V_{obs} and V_{sim} are the observed and simulated runoff volumes, respectively. The measured precipitation and outflow were used to evaluate how well the model matched this outflow using the NSME ranging from $-\infty$ to 1. The NSME was used as an objective function in order to find the optimal parameter set, and to measure the goodness of fit. In general, the closer the model efficiency is to 1, the more accurate the model can predict the performance of green roofs, whilst an NSME greater than 0.5 indicates acceptable model performance (Rosa et al., 2015). The final parameters were achieved by applying the Shuffle Complex Evolution (SCE) algorithm (Duan et al., 1992). The SCE method is based on four concepts that aims for efficient global optimization. The calibration process was based on random sampling from a predefined variable range where each parameter had lower and upper bound delineated. The SCE algorithm uses an initial guess to generate a sequence of improving approximate solutions in order to reach the highest NSME; where the n-th approximation was derived from the previous ones. The termination criteria of the calibration process were based on the principle of convergence (objective function stabilizes) (Duan et al., 1992).

2.5. Model calibration and validation

A long-term continuous calibration was chosen in order to prevent eventual validation issues while comparing events with different characteristics. Data between 11th of May and 31st of July served for the model calibration. The calibration period included five larger events; while six events were used for model validation (Table 2). The model was evaluated by the NSME and VE in both the calibration and validation period using a long-term continuous dataset as well as an event-based dataset.

2.6. Snowmelt modelling

The model, which was calibrated against long-term continuous observed flows generated from rain events only, was applied for a period between November 2017 and April 2018 in order to identify the essential parameters for the snowmelt processes. Time series with hourly temperature and wind speed were used to distinguish between liquid and solid precipitation as well as recognise snowmelt generation. The SWMM model employs either the degree-day method or a simplified energy budget method (Anderson, 1968; Rossman and Huber, 2016a). The degree-day method was used for all snow events except rain-on-snow events to compute the melt rate for any particular day (eq. (3)). Minimum and maximum snowmelt coefficients are used to estimate a melt coefficient that varies by day of the year (Rossman and Huber, 2016a). The relationship between snowmelt and air temperature can be expressed as:

$$SM = C_M * (T_A - T_B), \tag{3}$$

where SM is the snowmelt generated (mm/day), C_M is the melt coefficient (mm/°C/day), T_A is the index air temperature in °C (used the mean daily temperature according to the observation from the field station), and T_B is the base temperature in °C (used 0°C according to (Rossman and Huber, 2016a)). Minimum ($C_{Mmin} = 0.01$ mm/h/°C) and maximum ($C_{Mmax} = 0.123$ mm/h/°C) melt coefficients were derived from observed snowmelts. Other parameters were kept default; Dividing Temperature Between Snow and Rain ($DT = 0^\circ C$), Antecedent Temperature Index ($ATI = 0.5$), Negative Melt Ratio ($NMR = 0.6$), Fraction Free Water

Capacity (FFWC = 0.1) (Rossman and Huber, 2016a). The simplified energy budget (heat budget) method is applied during rain-on-snow events where the energy is supplied by sensible heat (from the air) and advective heat (from rain). Other forms of energy, as well as albedo and snow age, are neglected. Within this method, snowmelt increases with increasing air temperature, wind speed and rainfall intensity (used data from the field station). In this study, the human-made snow redistribution did not occur, therefore, to avoid any snow redistribution the depth, at which snow removal begins, was set to 1000 mm.

3. Results and Discussion

The main intention of this chapter is to present result from the model calibration and validation of the green/grey roof, evaluate six parameters which were calibrated as well as test the calibrated model during the cold period. However, data from monitoring including several rooftop management aspects (retention and detention) can be also derived from Table 2 where comparison of peak runoffs and volume generation from individual rooftops can be seen.

3.1. Calibrated long-term continuous simulation

Long-term continuous simulations using initial uncalibrated parameter sets indicated agreement between observed and simulated runoff from the green roof with the NSME equaled to 0.5. The same did not apply for the simulated runoff from the grey roof with the NSME equaled to - 2.87 where calibration was required.

Six parameters within two LID layers (namely the soil and the drainage mat) were calibrated. Their values prior and after calibration are presented in Table 1. Within the green roof, the overland flow does not usually occur due to high infiltration capacity of the soil where ponding is not allowed. Therefore, the parameters associated with the surface layer were excluded from the calibration process. Some of the parameters (berm height, surface slope, thickness) were kept fixed to preserve the physical description of the field setup as well as avoid overparameterization. Substantial improvement of model performance was achieved after the calibration of both the green and grey roof parameters. The NSME calculated from observed and simulated runoff from the green roof improved from 0.50 to 0.94, of the grey roof improved from insufficient -2.87 to 0.78. It should be noted that the NSME values include inter-events periods (periods without rain) since the increased detention effect (led to higher baseflow) made it challenging to distinguish when runoff stopped.

Long-term continuous model simulation and comparison of the observed and simulated runoff from the green and the grey roof following calibration is shown in Appendix in Figs. A7, A9 and A10. These figures show a better fit within the calibration period of the green roof which can be visually seen in data spread of observed versus simulated runoff or mathematically when expressed with the lowest value of norm of residuals (and mean squared error MSE, coefficient of determination R² and correlation coefficient). The model simulated lower volumes (flow rates) than observed in most of the cases

which is also shown by slope and intercept of the regression line. Visually, the models simulated the runoffs fairly well. The simulated runoff from both the green and grey roof tended to underestimate the observed peak flow responses to rainfalls with the highest intensity. At the same time, the model had difficulties in simulating the tails of grey roof runoff more than in the green roof. The simulated cumulative runoffs (total volumes) were close to the observed data.

In comparison, the volume errors between the simulated and observed runoff from the grey roof counted 10% and from the green roof counted 3%. Firstly, the volume errors were caused by inaccurately estimated seasonal evapotranspiration rates, which occur during dry periods and cause regeneration of the storage capacity of the roof. Secondly, the volume errors were caused by inaccurate model simulations of runoffs. It was noted that actual ET rates decay with time during the dry period but the SWMM model assumes a fixed ET rates (Peng and Stovin, 2017). Thirdly, the model runoff outputs had coarser resolution than the observed runoff which made the volume comparison more challenging.

Five events were chosen to evaluate the model performance in term of event-based simulation during the calibration period (Fig. 2). One can see the difficulties with the simulation and the underestimation of the runoff tails in the grey roof (Fig. 4). This leads to that the ability of the model to simulate runoff detention is partly limited. Thus, the equations describing the detention processes as well as the detention parameters, namely porosity, soil conductivity, soil conductivity slope and soil suction head within soil layer and the parameters within the drainage mat serving to the estimation of the baseflow, should be further investigated in order to improve runoff prolongation.

3.2. Validation

In order to assess model performance for the non-calibration period, the calibrated green and grey roof models were tested in terms of the NSME and VE through a part of the summer and whole autumn (may be seen in Appendix in Figs. A8, A11 and A12). During this study, only one event with a 2-year return period was registered via rain gauge at Høvringen, Trondheim in August 2017 (Fig. 3). However, several larger events were also used to validate the model performance as well as a long-term continuous dataset with a high resolution of 1-min.

Six events were chosen to evaluate the model performance in term of event-based simulation during the validation period (Fig. 4). Events V2 and V6 offered interesting results reaching the NSME of 0.8 and higher for both roofs, and the volume error fell into reasonable limits as well. Both events lasted several days, and relatively large volumes were registered, and one can conclude that such events are of interest due to the fact that the SWMM model showed its ability to reproduce registered runoffs and that the roofs were able to reduce the maximal flow (Table 2). The green roof runoff was simulated reasonably well except for one event in September during the validation period (Fig. 4), which followed an almost one-week dry period, which intensely dried the roof storage capacity. This was, however, captured with the model of the grey roof,

Table 3
Six calibrated model parameters of the green and grey roofing and their statistics after selecting NSME higher than 0.7.

Statistics/parameter	Porosity	Field Capacity	Conductivity	Conductivity Slope	Void Fraction	Manning's n
			GREEN (NSME > 0.7)			
Initial value	0.500	0.300	25	15.0	0.500	0.100
Median	0.568	0.269	11	31.4	0.019	0.022
Mean	0.567	0.270	86	32.7	0.060	0.050
Standard deviation	0.015	0.019	159	4.5	0.112	0.072
Optimal value	0.559	0.267	11.1	31.5	0.016	0.010
			GREY (NSME > 0.7)			
Initial value	0.600	0.010	1432	10.0	0.500	0.100
Median	0.450	0.095	2973	27.7	0.663	0.205
Mean	0.452	0.094	2881	27.4	0.667	0.183
Standard deviation	0.005	0.006	218	0.8	0.016	0.045
Optimal value	0.450	0.095	2975	27.7	0.663	0.205

Table 4
 Model sensitivity to parameters adjustment $\pm 10\%$ and $\pm 50\%$. Abbreviation: GN = Green roof, GY = Grey roof, 10UP = 10% increment, 10DOWN = 10% decrement, 50UP = 50% increment, 50DOWN = 50% decrement, P = porosity, FC = field capacity, C = conductivity, CS = conductivity slope, VF = void fraction and Mn = Manning's n. Orange marking applies for performance deterioration and green marking for performance improvement.

PERIOD	GREEN ROOF PARAMETERS											GREY ROOF PARAMETERS										
	GN_P_DOWN	GN_C_DOWN	GN_CS_DOWN	GN_VF_DOWN	GN_Mn_DOWN	GN_P_UP	GN_C_UP	GN_CS_UP	GN_VF_UP	GN_Mn_UP	GN_P_DOWN	GN_C_DOWN	GN_CS_DOWN	GN_VF_DOWN	GN_Mn_DOWN	GN_P_UP	GN_C_UP	GN_CS_UP	GN_VF_UP	GN_Mn_UP		
NAME	0.83	0.84	0.86	0.87	0.88	0.85	0.85	0.85	0.82	0.82	0.84	0.84	0.82	0.82	0.84	0.84	0.85	0.85	0.82	0.82	0.84	
VE	25.9%	25.9%	25.9%	25.9%	25.9%	24.83%	24.83%	24.83%	24.83%	24.83%	25.83%	25.83%	25.83%	25.83%	25.83%	26.83%	26.83%	26.83%	26.83%	26.83%	27.83%	
Wpon perf	1.00	0.97	0.96	0.95	0.98	0.94	0.98	0.98	0.98	0.98	0.96	0.96	0.96	0.96	0.96	1.02	1.02	1.02	1.02	1.02	1.04	
INTERCEPT	0.00064	0.00064	0.00067	0.00076	0.00067	0.00066	0.00067	0.00067	0.00067	0.00067	0.00070	0.00066	0.00067	0.00067	0.00066	0.00074	0.00073	0.00073	0.00073	0.00073	0.00074	
CORRELATION	0.94	0.94	0.94	0.94	0.94	0.94	0.94	0.94	0.94	0.94	0.94	0.94	0.94	0.94	0.94	0.94	0.94	0.94	0.94	0.94	0.94	
VE_CAL	21.8%	20.8%	20.1%	18.7%	20.2%	18.5%	18.5%	18.5%	18.5%	18.5%	20.2%	20.2%	20.2%	20.2%	20.2%	21.8%	21.8%	21.8%	21.8%	21.8%	23.4%	
Calibration RQ	0.85	0.83	0.83	0.84	0.83	0.88	0.83	0.83	0.83	0.83	0.83	0.83	0.83	0.83	0.83	0.83	0.83	0.83	0.83	0.83	0.83	
Validation RQ	0.88	0.89	0.89	0.88	0.89	0.82	0.89	0.89	0.89	0.89	0.87	0.87	0.87	0.87	0.87	0.89	0.89	0.89	0.89	0.89	0.89	
INTERCEPT	0.00037	0.00025	0.00025	0.00038	0.00025	0.00031	0.00025	0.00025	0.00025	0.00025	0.00030	0.00025	0.00025	0.00025	0.00025	0.00034	0.00034	0.00034	0.00034	0.00034	0.00034	
CORRELATION	0.94	0.94	0.94	0.94	0.94	0.94	0.94	0.94	0.94	0.94	0.94	0.94	0.94	0.94	0.94	0.94	0.94	0.94	0.94	0.94	0.94	
NAME	0.79	0.87	0.81	0.89	0.88	0.86	0.86	0.86	0.81	0.81	0.84	0.84	0.86	0.86	0.84	0.84	0.86	0.86	0.86	0.86	0.86	
VE	25.9%	25.9%	25.9%	25.9%	25.9%	27.8%	27.8%	27.8%	27.8%	27.8%	28.7%	28.7%	28.7%	28.7%	28.7%	29.7%	29.7%	29.7%	29.7%	29.7%	31.6%	
Wpon perf	1.07	0.95	0.96	0.92	1.04	0.99	0.92	0.98	1.04	1.04	0.96	0.96	0.96	0.96	0.96	1.02	1.02	1.02	1.02	1.02	1.04	
INTERCEPT	0.00070	0.00052	0.00041	0.00039	0.00056	0.00066	0.00066	0.00066	0.00066	0.00066	0.00071	0.00066	0.00066	0.00066	0.00066	0.00074	0.00073	0.00073	0.00073	0.00073	0.00074	
CORRELATION	0.94	0.94	0.94	0.94	0.94	0.94	0.94	0.94	0.94	0.94	0.94	0.94	0.94	0.94	0.94	0.94	0.94	0.94	0.94	0.94	0.94	
VE_CAL	24.5%	11.0%	19.7%	18.1%	20.2%	20.2%	20.2%	20.2%	20.2%	20.2%	20.2%	20.2%	20.2%	20.2%	20.2%	21.8%	21.8%	21.8%	21.8%	21.8%	23.4%	
Calibration RQ	0.88	0.87	0.88	0.89	0.89	0.83	0.83	0.83	0.83	0.83	0.83	0.83	0.83	0.83	0.83	0.83	0.83	0.83	0.83	0.83	0.83	
Validation RQ	0.94	0.88	0.94	0.86	0.97	0.93	0.93	0.93	0.93	0.93	0.93	0.93	0.93	0.93	0.93	0.93	0.93	0.93	0.93	0.93	0.93	
INTERCEPT	0.00042	0.00044	0.00044	0.00044	0.00044	0.00044	0.00044	0.00044	0.00044	0.00044	0.00044	0.00044	0.00044	0.00044	0.00044	0.00044	0.00044	0.00044	0.00044	0.00044	0.00044	
CORRELATION	0.94	0.94	0.94	0.94	0.94	0.94	0.94	0.94	0.94	0.94	0.94	0.94	0.94	0.94	0.94	0.94	0.94	0.94	0.94	0.94	0.94	
NAME	0.83	0.87	0.81	0.89	0.88	0.86	0.86	0.86	0.81	0.81	0.84	0.84	0.86	0.86	0.84	0.84	0.86	0.86	0.86	0.86	0.86	
VE	25.9%	25.9%	25.9%	25.9%	25.9%	27.8%	27.8%	27.8%	27.8%	27.8%	28.7%	28.7%	28.7%	28.7%	28.7%	29.7%	29.7%	29.7%	29.7%	29.7%	31.6%	
Wpon perf	1.07	0.95	0.96	0.92	1.04	0.99	0.92	0.98	1.04	1.04	0.96	0.96	0.96	0.96	0.96	1.02	1.02	1.02	1.02	1.02	1.04	
INTERCEPT	0.00070	0.00052	0.00041	0.00039	0.00056	0.00066	0.00066	0.00066	0.00066	0.00066	0.00071	0.00066	0.00066	0.00066	0.00066	0.00074	0.00073	0.00073	0.00073	0.00073	0.00074	
CORRELATION	0.94	0.94	0.94	0.94	0.94	0.94	0.94	0.94	0.94	0.94	0.94	0.94	0.94	0.94	0.94	0.94	0.94	0.94	0.94	0.94	0.94	

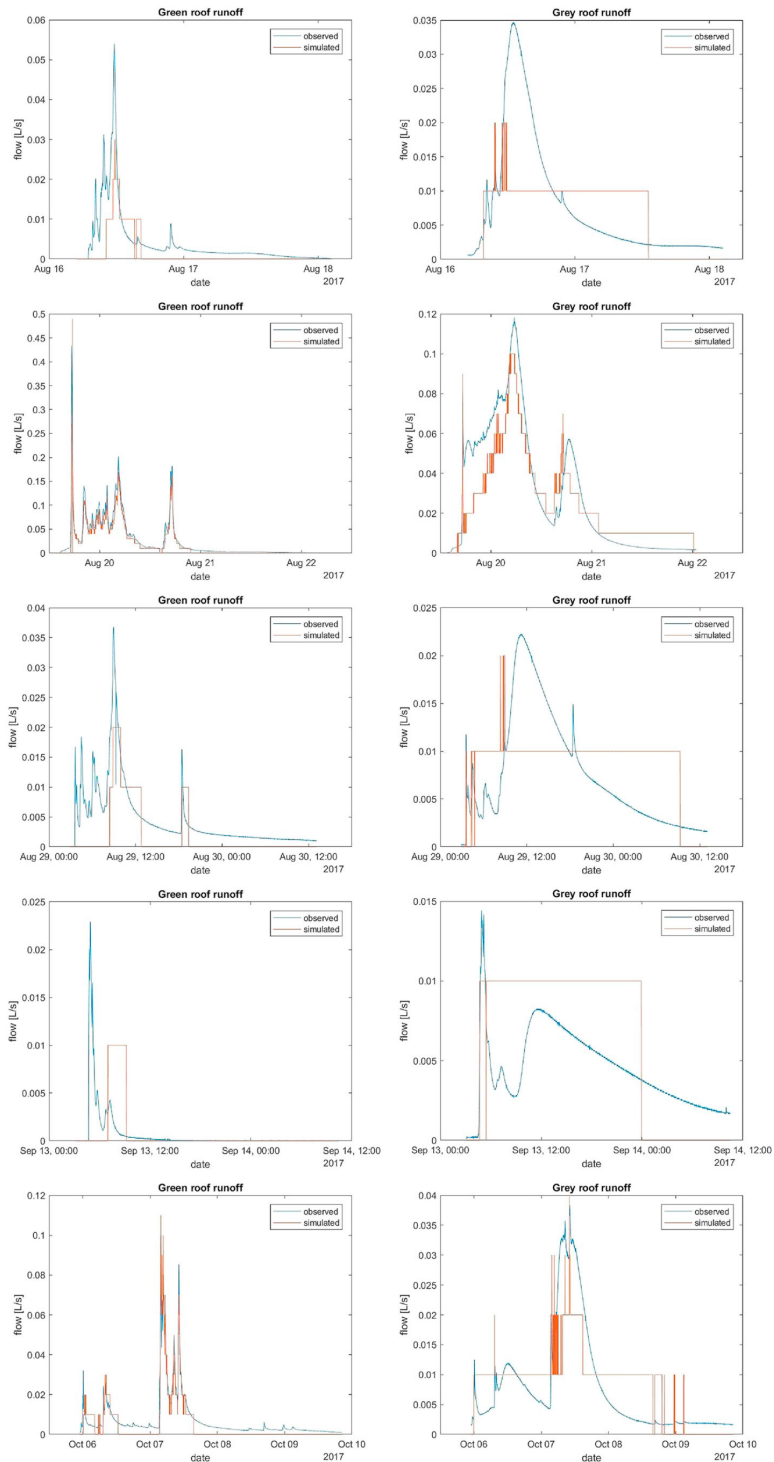


Fig. 4. Comparison of observed and simulated runoff from the green (left) and grey (right) roof. Six events that occurred during the validation period were chosen, namely V1, V2, V3, V4, V5, and V6 (Table 2). It should be noted that the model output is on much coarser resolution than the observed runoff. (For interpretation of the references to colour in this figure legend, the reader is referred to the Web version of this article.)

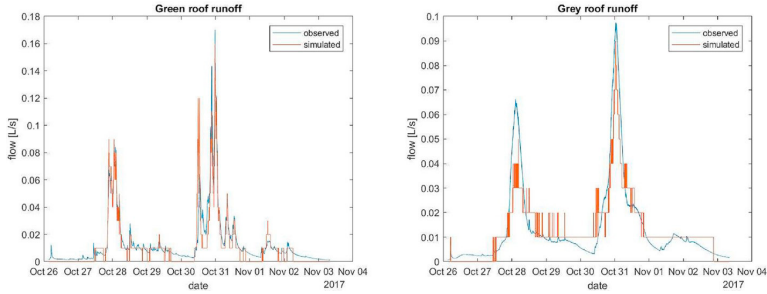


Fig. 4. (continued)

which generally showed a poorer fit to peak runoffs.

Overall evaluation of the model performance is presented in Table 2. One can see that the green roof model performance deteriorated regarding the NSME from 0.94 to 0.88 and VE from 3% to 29% during validation within the long-term continuous datasets while the grey roof model experienced improvement in terms of the NSME from 0.78 to 0.81.

3.3. Parameter evaluation

During the calibration process, nearly 2300 iterations were carried out within the green roof and nearly 2700 for the grey roof. Each parameter was plotted using a 3D histogram in order to see a representation of the distribution of a sample achieved during calibration (Figs. A13 and A14). The optimal value of each parameter is corresponding to the highest column of each graph. One can see the lower and upper bound of the individual parameters as well as a pattern in the histograms, which tended to be skewed to one side of the bound.

The randomly sampled numerical data of six calibrated parameters were sorted based on the NSME where only values higher than 0.7 were taken into consideration (Table 3). The table shows the initial value, median, mean and optimal value of each parameter where the medians of

most parameters are very close to optimal values. The optimal parameters between the roofs show very different values. The standard deviation, showing individual parameter dispersion of the grey roof parameters achieved lower values in comparison with the green roof parameters, except for conductivity. Thus, the conductivity of the grey roof experienced the largest data point spread. Overview of distribution of each the parameter vs. the NSME from the calibration and the low data spread of the parameters can be visually detected from Figs. A13 and A14. However, having a low standard deviation of a parameter shows that the model might be sensitive to this parameter.

Four parameters within the soil layer were calibrated (Table 3). The calibrated porosity (P) of 0.559 (green) and 0.45 (grey) was comparable with suggested values from the SWMM manual (Rossman and Huber, 2016a) (P = 0.4–0.5). Similarly, Krebs et al. (2016) achieved P = 0.41 after calibration and concluded that porosity was the most sensitive parameter. Other researchers decided to use the measured value of the porosity and did not calibrate it (Peng and Stovin, 2017). The field capacity (FC) was obtained to be 0.267 (green) and 0.095 (grey) after calibration. This is in line with the SWMM manual, which suggests field capacity of various soils between 0.062 and 0.378, other research presented FC = 0.29 (Krebs et al., 2016). The calibrated conductivity (C)

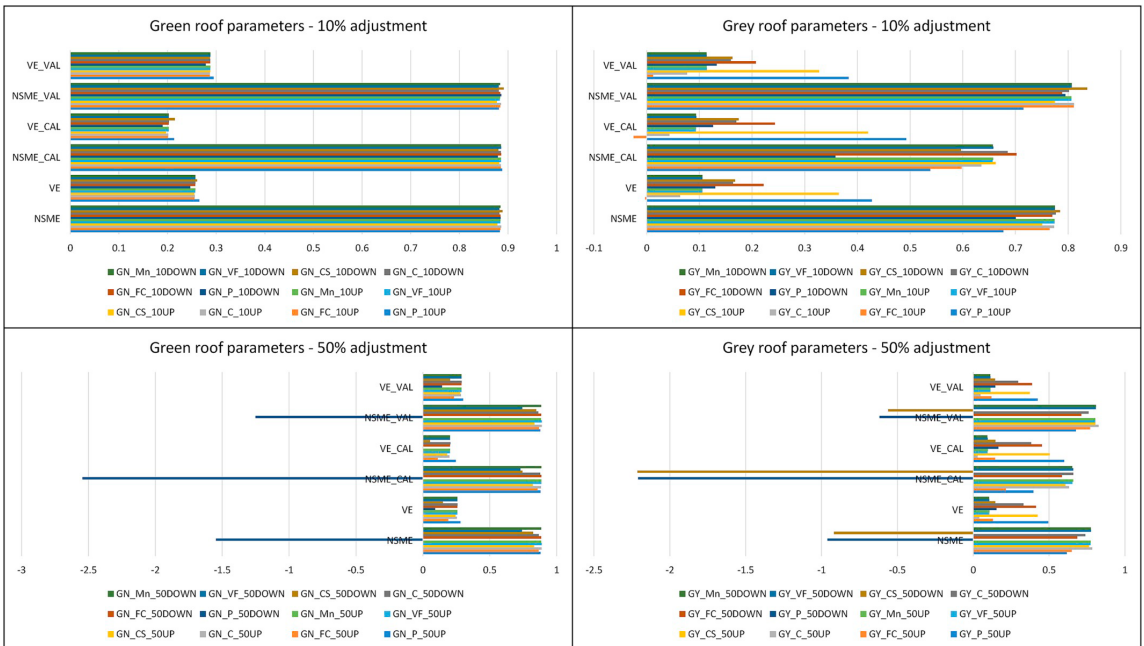


Fig. 5. Impact of parameters adjustment ± 10% and ± 50% to model performance (NSME and VE).

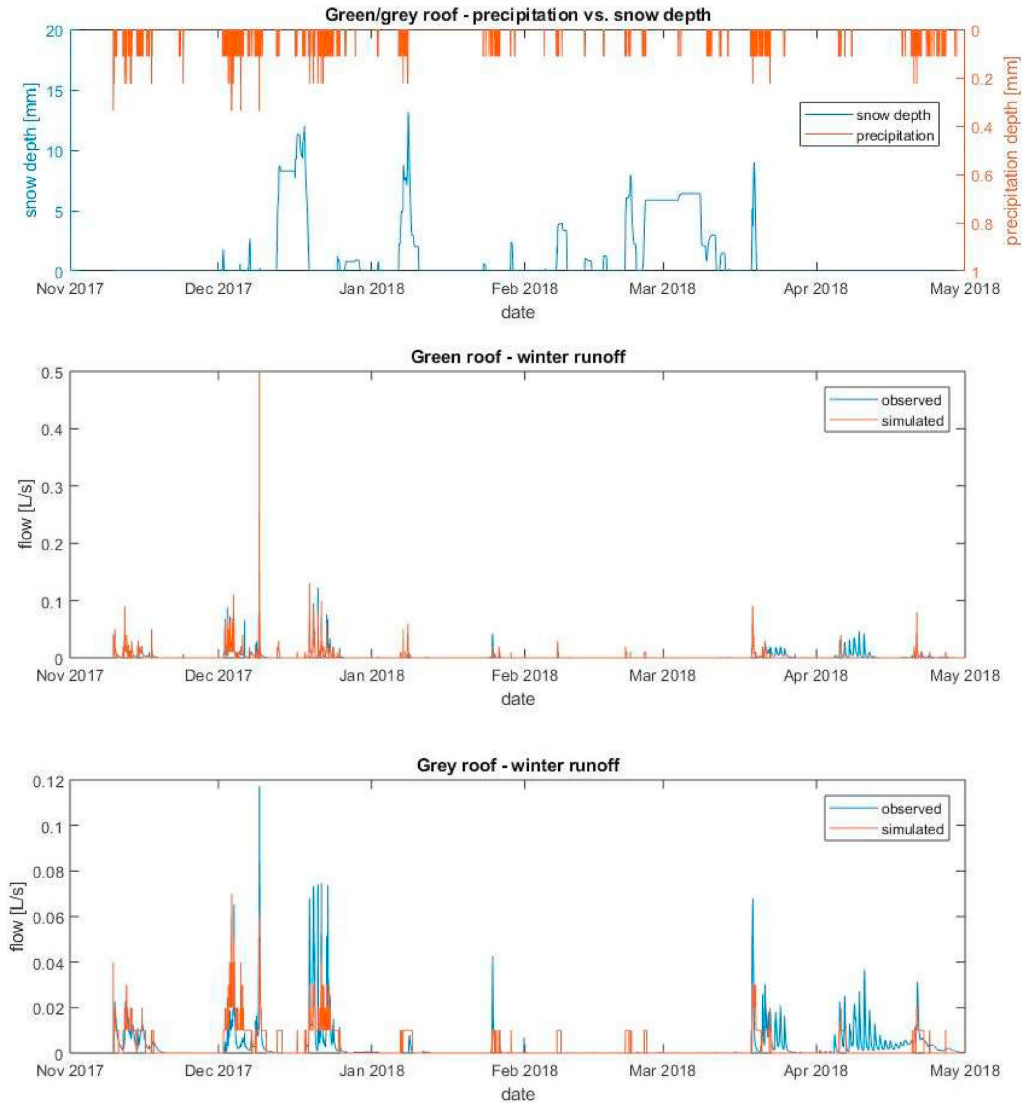


Fig. 6. Time series of precipitation during the winter season and subsequent snow depth expressed as the depth of water equivalent. Simulated runoff compared to long-term continuous observed from the green (left) and grey (right) roof during the winter period between November 2017 and April 2018. (For interpretation of the references to colour in this figure legend, the reader is referred to the Web version of this article.)

reached 11 mm/h (green) and 2975 mm/h (grey). The SWMM manual suggests soil conductivity values in the range 0.3–120 mm/h. This range is applicable for the green roof as well as a recommendation from (Krebs et al., 2016) ($C = 37.9$). The grey roof conductivity showed to be out of the range, similarly as other research (Peng and Stovin, 2017) $C = 1000$ mm/h. The calibrated conductivity slope (CS) reached 31.5 (green) 27.7 (grey) and was closest to the SWMM manual recommendation ($CS = 30$ – 60) as well as others (Krebs et al., 2016) ($CS = 40$) and (Peng and Stovin, 2017) ($CS = 50$).

The parameters representing the drainage layer varied substantially between the green and grey roof. The void fraction (VF) was 0.016 (green) 0.663 (grey). This is slightly out of the typical values recommended by the SWMM manual (VF = 0.2–0.4) but comparable to other research with VF = 0.6 (Peng and Stovin, 2017). The Manning's n roughness (MR ended up

on 0.01 (green) 0.205 (grey) after the calibration. The green roof parameter was comparable with the suggested values of 0.01–0.03 in the SWMM manual and with others researches (Peng and Stovin, 2017) MR = 0.03 and (Krebs et al., 2016) MR = 0.01. The grey roof served more like a detention solution and the green roof as a retention solution. Therefore, the parameters representing runoff detention (conductivity, void fraction and Manning's roughness) showed variation compared to the SWMM manual or other green roof researches. The model consists of a large number of physical parameters where some of the parameters might be determined from laboratory or field measurements (e.g., porosity, conductivity). This is however questionable as the SWMM model is unable to fully represent the green and grey roof structure design (e.g., lightweight aggregates representing both the soil layer and drainage mat layer; and/or the plastic drainage layer (egg box) affecting retention parameters) (Johannessen et al., 2019).

The model sensitivity to parameters deviation ($\pm 10\%$ and $\pm 50\%$ adjustment) was evaluated comparing the model performance including the objective functions (NSME and VE) for different periods (calibration period, validation period and whole period) in terms of the NSME and VE (Table 4 and Fig. 5). Additionally, several basic statistics (Pearson product moment correlation coefficient, slope of the linear regression line with intersect the y-axis and correlation coefficient between the observed and simulated data) were supplied. A $\pm 10\%$ adjustment had little impact on the model performance of the green roof whereas for the grey roof some variation in model performance was observed. One can conclude that 10% increment of the field capacity of the grey roof had a positive impact on the VE (-2.48% – -1.21%) whereas 10% increment of the porosity worsen the VE (38.31%–49.26%). The green roof model was mainly sensitive to 50% decreasing of the porosity which resulted in negative NSMEs (-1.251 – -2.546). However, in contrary this adjustment resulted in improvement of the VE (0.01 %–14.32%). The grey roof model was mainly sensitive to 50% decreasing of the porosity and conductivity slope which resulted in negative NSMEs (-0.617 to -2.209 and -0.561 - - 2.214). 50% increasing of the porosity resulted in large VEs (42.48%–59.95%). A positive impact on the model performance was achieved 50% increasing of the conductivity which resulted in low VEs (2.8%–4.82%) and NSMEs (0.631–0.826) remained relatively high as well.

3.4. Snowmelt modelling

The SWMM model, which was calibrated over a rainfall period, was tested during the winter period between November 2017 and April 2018. Within this period solid precipitation, as well as temperatures (degrees Celsius) which formed water into ice, were registered. Therefore, some of the winter precipitation did not directly contribute to the runoff but remained on the roofs in the form of snow (Fig. 6). This was driven by a temperature equal to 1°C below which precipitation falls as snow instead of rain. During the period, the heated rain gauge alone registered 346 mm of precipitation which was considerably lower than the cumulative precipitation registered from the reference black roof 390 mm (both located at the field station). Therefore, the total cumulative precipitation was corrected according to the reference black roof assuming that the error is based on wind and snow drift.

The model was able to simulate snowmelt and rain-on-snow reasonably well (Fig. 6). The observed volume equalled to 371 mm of the green roof runoff and 384 mm of the grey roof runoff and the model simulated 259 mm of the green roof and 340 mm of the grey roof. Regarding model evaluation, the green roof runoff was simulated with the NSME of 0.56 and VE of 30%. The grey roof runoff was simulated with the NSME of 0.37 and VE of 11%. One can see that the model had difficulties in simulating remaining water in the roof soil layers (substrate in the green roof, lightweight aggregate in the grey roof), which was slowly released in the first half of April. Limitation in terms of the snowmelt simulation was setting of the start and end of the cold period which may affect control of water balance.

Modelling remarks:

- The model was less accurate for short intense rainfall following a long antecedent dry period. This shows that the model assumed that the storage capacity of the green roof was regenerated and does not take into account detention of the roof and/or climatic effect (condensation of atmospheric vapor).
- NSME improved within the grey roof from calibration to validation from 0.78 to 0.81. Median and mean values of the observed flow used during calibration were 0.0012 L/s (median) vs. 0.003 L/s (mean) and during validation 0.006 L/s (median) vs. 0.0036 L/s (mean). Thus, there was double higher baseflow during calibration and slightly peaky runoff during validation. This can mean that the wetter part of the year performed better during the dryer part and reveal a question of using the same part of the year for validation.
- The calibrated SWMM models reproduced the observed runoffs sufficiently, but the calibration revealed that there might be several parameters sets which perform equally good. This makes the parameters valid only for the roof setups and climatic conditions of the study site or potentially roofs that have the same components as the

roofs tested with similar climatic conditions. The reason for skewness in the parameters sets could be due to the optimization algorithm, which instead of finding the global minimum, maybe found only local minima. Sensitivity analysis of the tested parameters showed that the porosity is most sensitive parameter for the green roof. In terms of the grey roof, the porosity and conductivity slope were found to be the most sensitive parameters (Table 4 and Fig. 5).

- Limitation due to equifinality, which states the non-uniqueness of the optimized parameter sets. The issue here is that similarly performing optimized parameter sets may not all be equivalent in terms of transferability and sensitivity. This will also affect the distribution of parameters into identifiable regional patterns; two similar models may have different optimized parameter sets. It is also likely that the optimized parameter sets should be transferred in its entirety and not as individual parameters Beven and Freer, 2001.
- Limitation due to singularity: Information contained in the optimized parameter set is specific to the modelled roof, and thus not transferable to another roof model. This might be due to data error compensation (precipitation or/and runoff) as the precipitation measurements are affected with the wind and intense rain undercatches. Another likely issue is the bias induced to the model by the optimization period and its specific climatic conditions and the model conceptualization error Poissant et al., 2017. There is a possible explanation for the mismatch between observed and simulated runoffs during the winter period. The SWMM model simulates runoff from rainfall or snow accumulation from snowfall according to observed air temperature. This temperature, however, does not correspond to temperature inside the medium (substrate) or around the outlet. Having negative air temperatures and positive medium temperatures may, therefore, lead to continuously observed runoff while the model accounts for snow accumulation. Additionally, rainfall measurement was performed over a period of 4 months using manual rain gauges (simple plastic non-digital cones which must be handled manually) (8 gauges per roof) in order to see rainfall distribution over the roofs and if the roof receives an equal amount of precipitation during non-snow period. There were not found differences between registered volumes. However, the volume error which raised from 3% during the warm period to 29% during the cold period revealed that the wind effect during cold period has to be still considered. Limitation within this manuscript is the actual dataset duration which spans over less than one year and that there was only one event with a return period greater than 2 years. This may also raise the question of whether it is appropriate to validate the model using periods with different season within the same year.

3.5. Practical implications for environmental management

In light of the results and limitations, one can conclude that the SWMM model can simulate the hydrological performance of green/grey roof solutions. It is a user-friendly tool, which may support urban planners and decision makers in activities related to project planning, implementation, and assessment. From the management point of view, important results are presented in Table 2. The grey roof outperforms the reference black roof and extensive green roof in terms of stormwater detention while changing extreme runoff to more natural flow with a low peak and long duration (Hamouz et al., 2018; Mentens et al., 2006; Stovin, 2010). The runoff attenuation may also be seen between the green and grey roof in the figures in chapter Results and Discussion (Figs. 2, 4 and 6 and in Appendix in Figs. A7 and A8). This difference will influence the number of CSO events as well as the duration of the events. (Ahiablame and Shakya, 2016).

Considering stormwater retention, the green roof discharged 407 mm of stormwater (during the warm period) and 371 mm (during the cold period). The grey roof discharged 530 mm (warm period) and 384 mm (cold period). While the black reference roof had 573 mm (warm period) and 390 mm (cold period). This confirms earlier findings where low retention effect can be observed during cold period (Hamouz et al., 2018; Johannessen et al., 2017; Mentens et al., 2006; Poë et al., 2015; Stovin et al., 2015; Teemusk and Mander, 2007; Xu, 2000), among others). In contrast, the green roof retained a considerable amount of 166 mm of precipitation in comparison with the

reference black roof during a warm period while the grey roof retained 46 mm. This clearly shows that the green roofs should be favoured from a retention point of view.

This study is an important step prior to a large-scale implementation of green and grey roofs in a watershed. More interest should be given to the grey roof, in particular for cool season locations due to low maintenance of the roof and the fact that evapotranspiration is a limiting factor for the green roofs in cold climates.

4. Conclusions

In this study, the runoff from a green and grey rooftop retrofitting were simulated using the model SWMM version 5.1. The model was able to simulate runoff with a good fit, 0.94 (green roof) and 0.78 (grey roof) values of the Nash-Sutcliffe model efficiency (NSME) within the calibration period. Similarly, a good fit was achieved during the validation period with 0.88 (green roof) and 0.81 (grey roof) values of NSME. The model was able to simulate the water balance satisfactorily during the calibration period with volume errors of 3% (green roof) and 10% (grey roof). Remarkable deterioration was observed within the validation period of the green roof with volume error of 29%, within the grey roof almost no change occurred with volume error of 11%. Concerning snowmelt modelling, the calibrated model

showed the NSME of 0.56 (green roof) and 0.37 (grey roof) with the volume error of 30% (green roof) and 11% (grey roof) through the winter period. The results indicate that there is a need for further research related to the volume errors during the winter season.

The SWMM model allows simulating runoff from the green and grey roof with a good fit between observed and simulated runoff but after calibration and with limitation to the specific local climate. The parameters may deviate with different roof layers build-up, geometry, and climate, which was confirmed after comparing with other studies and laboratory measurements but still being within the recommendation and limits of green roof standards and manuals. The study provides insight for urban planners who may use the output from the SWMM model as an aid in the implementation of roof retrofitting in urban watersheds.

Acknowledgements

The study was supported by the Klima2050 Centre for Research-based Innovation (SFI), financed by the Research Council of Norway and its consortium partners (grant number 237859/030). We would like to acknowledge Ashenafi Seifu Grange for providing a script used for calibration and advices related to hydrological modelling.

Appendix

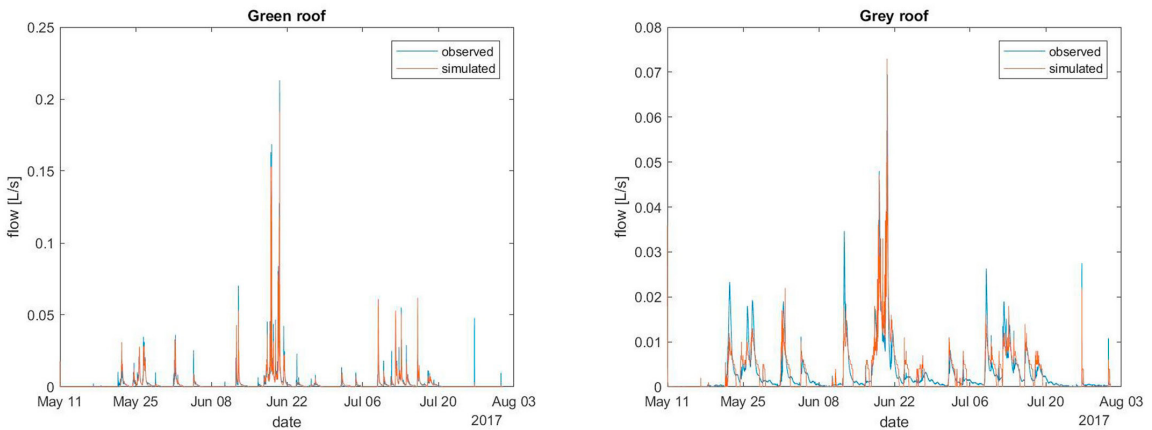


Fig. A7. Comparison of long-term continuous observed and simulated runoff from the green (left) and grey (right) roof from the calibration period between May and July 2017.

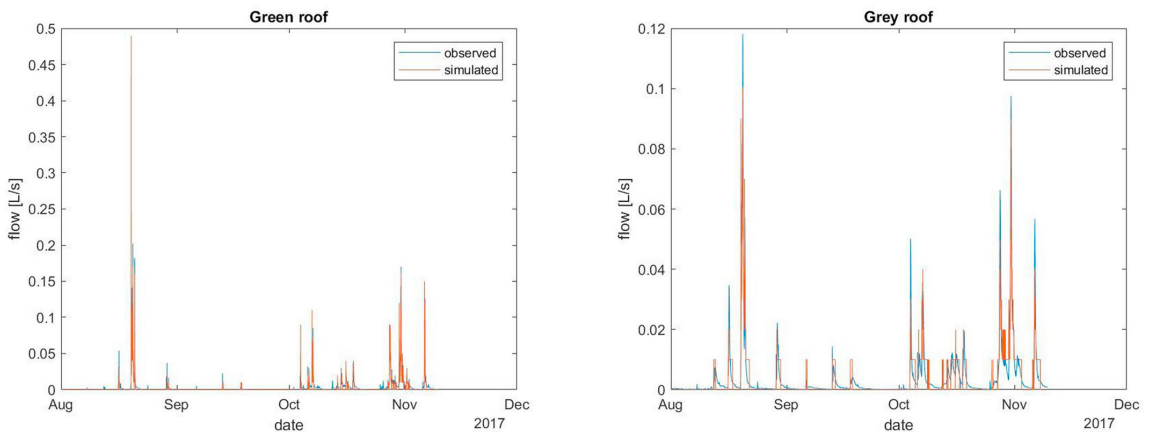


Fig. A8. Comparison of long-term continuous observed and simulated runoff from the green (left) and grey (right) roof from the validation period between August and November 2017.

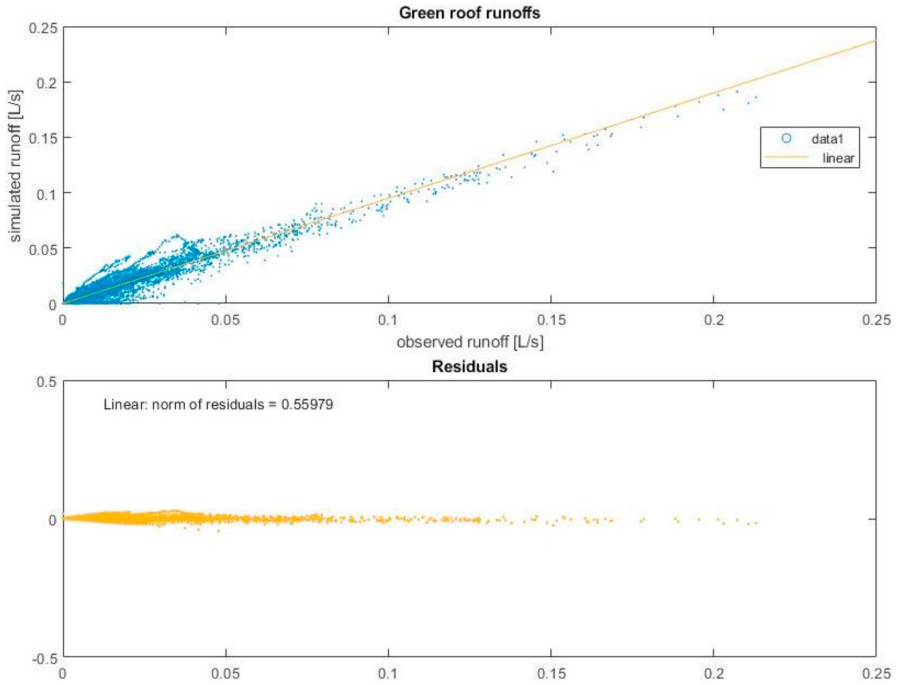


Fig. A9. Comparison of long-term continuous observed and simulated runoff from the green roof and its residuals chosen from the calibration period between May and July 2017; NSME = 0.94; MSE = 0.000003; $R^2 = 0.941$; Correl = 0.97.

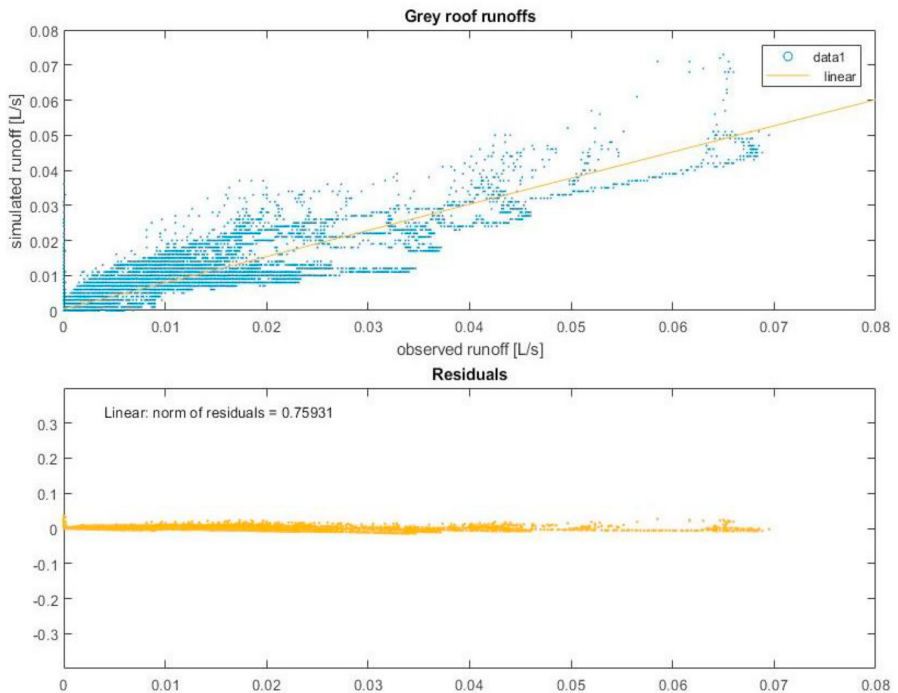


Fig. A10. Comparison of long-term continuous observed and simulated runoff from the grey roof and its residuals chosen from the calibration period between May and July 2017; NSME = 0.78; MSE = 0.000005; $R^2 = 0.785$; Correl = 0.886.

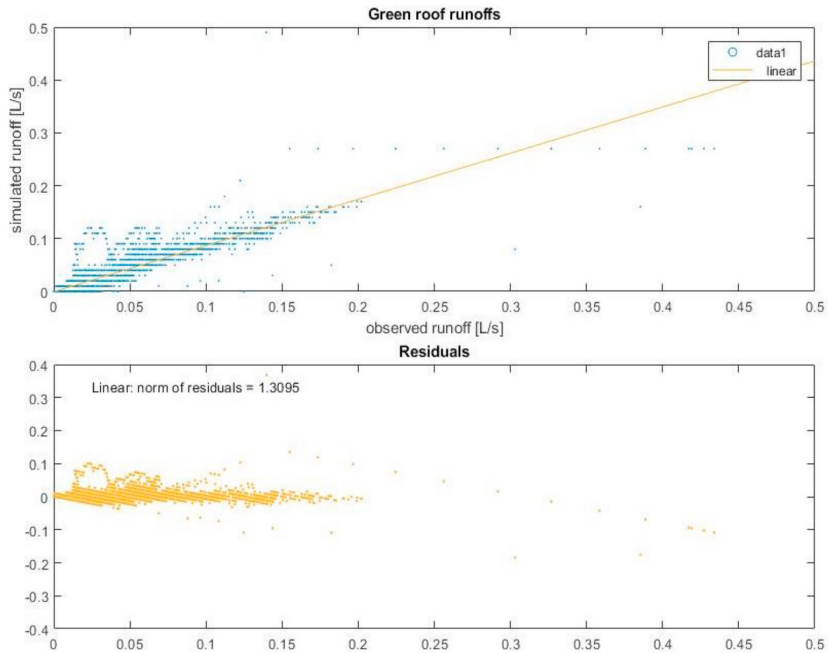


Fig. A11. Comparison of long-term continuous observed and simulated runoff from the green roof and its residuals chosen from the validation period between August and November 2017; NSME = 0.88; MSE = 0.000012; $R^2 = 0.89$; Correl = 0.943.

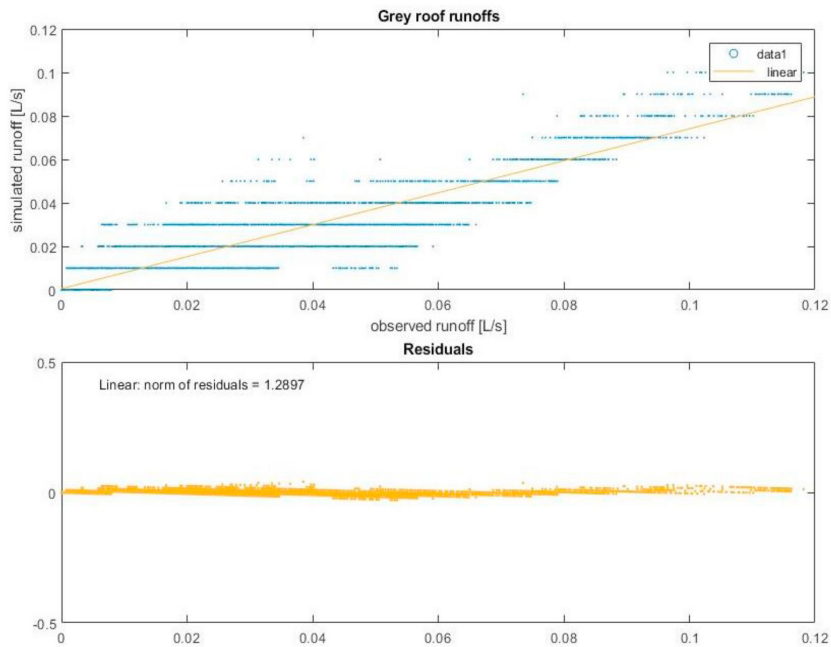


Fig. A12. Comparison of long-term continuous observed and simulated runoff from the grey roof and its residuals chosen from the validation period between August and November 2017; NSME = 0.81; MSE = 0.000011; $R^2 = 0.816$; Correl = 0.903.

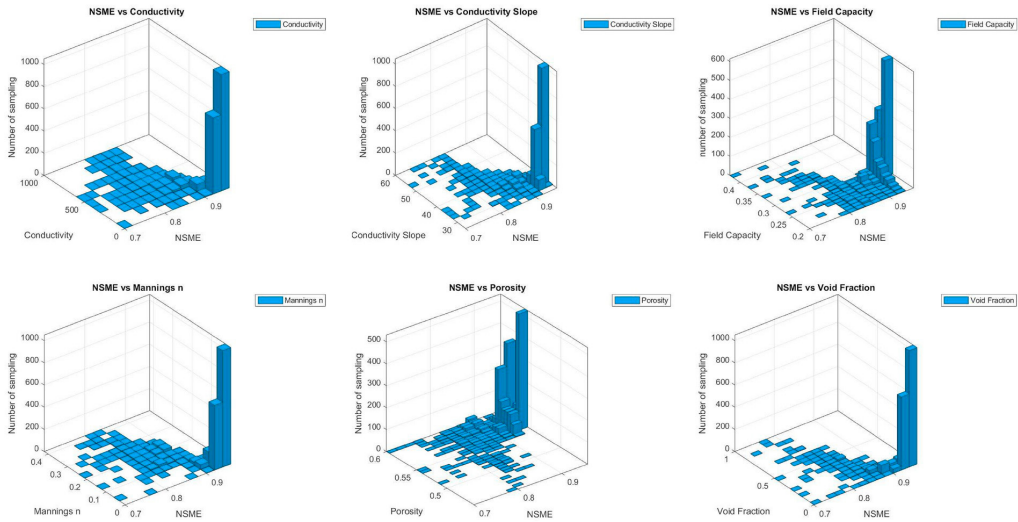


Fig. A13. 3D plots of calibrated parameters, NSME and number of sampling of the green roof.

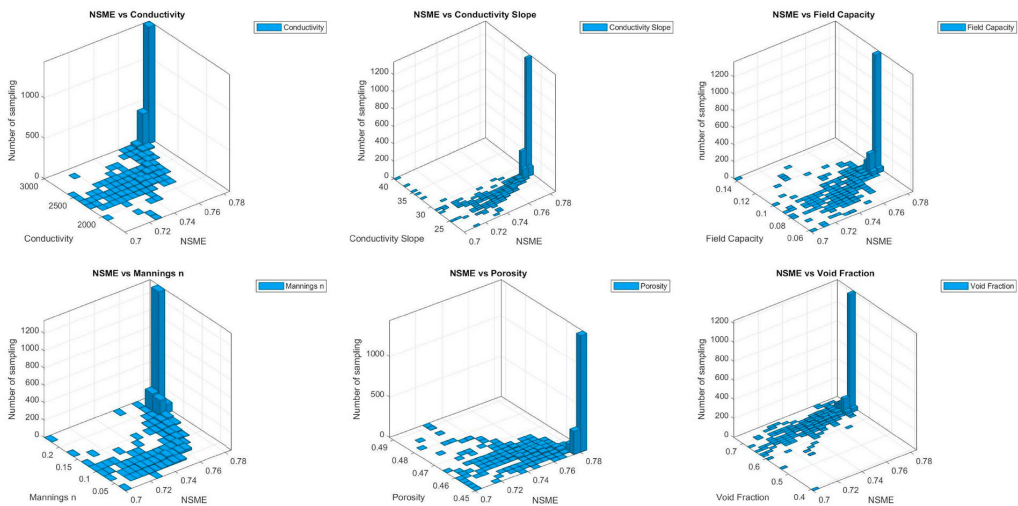


Fig. A14. 3D plots of calibrated parameters, NSME and number of sampling of the grey roof.

References

Ahiablame, L., Shakya, R., 2016. Modeling flood reduction effects of low impact development at a watershed scale. *J. Environ. Manag.* 171, 81–91.
 Anderson, E.A., 1968. Development and testing of snow pack energy balance equations. *Water Resour. Res.* 4, 19–37.
 Ashbolt, S., Aryal, S., Petrone, K., McIntosh, B., Maheepala, S., Chowdhury, R., Gardner, T., 2013. Can stormwater harvesting restore pre-development flows in urban catchments in South East Queensland? *Water Sci. Technol.* 67, 446–451.
 Bengtsson, L., Westerström, G., 1992. Urban snowmelt and runoff in northern Sweden. *Hydrol. Sci. J.* 37, 263–275.
 Berndtsson, J.C., 2010. Green roof performance towards management of runoff water quantity and quality: a review. *Ecol. Eng.* 36, 351–360.
 Beven, K., Freer, J., 2001. Equifinality, data assimilation, and uncertainty estimation in mechanistic modelling of complex environmental systems using the GLUE methodology. *J. Hydrol.* 249, 11–29.
 Beven, K.J., 2011. *Rainfall-runoff Modelling: the Primer*. John Wiley & Sons.
 Carson, T., Keeley, M., Marasco, D.E., McGillis, W., Culligan, P., 2017. Assessing methods for predicting green roof rainfall capture: a comparison between full-scale observations and four hydrologic models. *Urban Water J.* 14, 589–603.

Carson, T., Marasco, D., Culligan, P., McGillis, W., 2013. Hydrological performance of extensive green roofs in New York City: observations and multi-year modeling of three full-scale systems. *Environ. Res. Lett.* 8, 024036.
 Carter, T., Jackson, C.R., 2007. Vegetated roofs for stormwater management at multiple spatial scales. *Landscape Urban Plan.* 80, 84–94.
 Cipolla, S.S., Maglionico, M., Stojkov, I., 2016. A long-term hydrological modelling of an extensive green roof by means of SWMM. *Ecol. Eng.* 95, 876–887.
 Duan, Q., Soroshian, S., Gupta, V., 1992. Effective and efficient global optimization for conceptual rainfall-runoff models. *Water Resour. Res.* 28, 1015–1031.
 Elliott, A., Trowsdale, S.A., 2007. A review of models for low impact urban stormwater drainage. *Environ. Model. Softw.* 22, 394–405.
 FLL, 2008. Guidelines for the planning, construction and maintenance of green roofing: green roofing guideline. Forschungsgesellschaft Landschaftsentwicklung Landschaftsbau.
 Forland, E., Allerup, P., Dahlström, B., Elomaa, E., Jónsson, T., Madsen, H., Perälä, J., Rissanen, P., Vedin, H., Vejen, F., 1996. Manual for operational correction of Nordic precipitation data. *Klima Report* 24, 96.
 Gill, S.E., Handley, J.F., Ennos, A.R., Pauleit, S., 2007. Adapting cities for climate change: the role of the green infrastructure. *Built Environ.* 33, 115–133.
 Gray, D.M., Male, D.H., 1981. *Handbook of Snow: Principles, Processes, Management & Use*. Pergamon Press.

- Hamouz, V., Lohne, J., Wood, J.R., Muthanna, T.M., 2018. Hydrological performance of LECA-based roofs in cold climates. *Water* 10, 263.
- Hilten, R.N., Lawrence, T.M., Tollner, E.W., 2008. Modeling stormwater runoff from green roofs with HYDRUS-1D. *J. Hydrol.* 358, 288–293.
- Ho, C., Valeo, C., 2005. Observations of urban snow properties in Calgary, Canada. *Hydrol. Process.: Int. J.* 19, 459–473.
- Jia, H., Yao, H., Tang, Y., Shaw, L.Y., Field, R., Tafuri, A.N., 2015. LID-BMPs planning for urban runoff control and the case study in China. *J. Environ. Manag.* 149, 65–76.
- Johannessen, B.G., Hamouz, V., Gragne, A.S., Muthanna, T.M., 2019. The transferability of SWMM model parameters between green roofs with similar build-up. *J. Hydrol.* 569, 816–828.
- Johannessen, B.G., Hanslin, H.M., Muthanna, T.M., 2017. Green roof performance potential in cold and wet regions. *Ecol. Eng.* 106, 436–447.
- Kasmin, H., Stovin, V., Hathway, E., 2010. Towards a generic rainfall-runoff model for green roofs. *Water Sci. Technol.* 62, 898–905.
- Krebs, G., Kokkonen, T., Valtanen, M., Koivusalo, H., Setälä, H., 2013. A high resolution application of a stormwater management model (SWMM) using genetic parameter optimization. *Urban Water J.* 10, 394–410.
- Krebs, G., Kokkonen, T., Valtanen, M., Setälä, H., Koivusalo, H., 2014. Spatial resolution considerations for urban hydrological modelling. *J. Hydrol.* 512, 482–497.
- Krebs, G., Kuoppamäki, K., Kokkonen, T., Koivusalo, H., 2016. Simulation of green roof test bed runoff. *Hydrol. Process.* 30, 250–262.
- Leopold, L.B., 1968. *Hydrology for Urban Land Planning: A Guidebook on the Hydrologic Effects of Urban Land Use.*
- Li, Y., Babcock, R.W., 2014. Green roof hydrologic performance and modeling: a review. *Water Sci. Technol.* 69, 727–738.
- Locatelli, L., Mark, O., Mikkelsen, P.S., Ambjerg-Nielsen, K., Jensen, M.B., Binning, P.J., 2014. Modelling of green roof hydrological performance for urban drainage applications. *J. Hydrol.* 519, 3237–3248.
- Matheussen, B.V., 2004. *Effects of Anthropogenic Activities on Snow Distribution, and Melt in an Urban Environment.*
- Matheussen, B.V., Thorolfsson, S.T., 2004. *Risvöllan Urban Hydrological Model (RUHM) - Preliminary Results.* Ninth International Conference on Urban Drainage (9ICUD).
- Mentens, J., Raes, D., Herm, M., 2006. Green roofs as a tool for solving the rainwater runoff problem in the urbanized 21st century? *Landsc. Urban Plan.* 77, 217–226.
- Metselaar, K., 2012. Water retention and evapotranspiration of green roofs and possible natural vegetation types. *Resour. Conserv. Recycl.* 64, 49–55.
- Moghadas, S., Gustafsson, A.-M., Muthanna, T.M., Marsalek, J., Viklander, M., 2016. Review of models and procedures for modelling urban snowmelt. *Urban Water J.* 13, 396–411.
- Moghadas, S., Leonhardt, G., Marsalek, J., Viklander, M., 2017. Modeling urban runoff from rain-on-snow events with the US EPA SWMM model for current and future climate scenarios. *J. Cold Reg. Eng.* 32, 04017021.
- Nash, J.E., Sutcliffe, J.V., 1970. River flow forecasting through conceptual models part I—a discussion of principles. *J. Hydrol.* 10, 282–290.
- Palla, A., Gnecco, I., 2015. Hydrologic modeling of Low Impact Development systems at the urban catchment scale. *J. Hydrol.* 528, 361–368.
- Paus, K.H., Muthanna, T.M., Braskerud, B.C., 2016. The hydrological performance of bioretention cells in regions with cold climates: seasonal variation and implications for design. *Nord. Hydrol.* 47, 291–304.
- Peng, Z., Stovin, V., 2017. Independent validation of the SWMM green roof module. *J. Hydrol. Eng.* 22, 04017037.
- Poë, S., Stovin, V., Berretta, C., 2015. Parameters influencing the regeneration of a green roof's retention capacity via evapotranspiration. *J. Hydrol.* 523, 356–367.
- Poissant, D., Arsenault, R., Brisette, F., 2017. **Impact of parameter set dimensionality and calibration procedures on streamflow prediction at ungauged catchments.** *J. Hydrol. Reg. Stud.* <https://doi.org/10.1016/j.ejrh.2017.05.005>.
- Rosa, D.J., Clausen, J.C., Dietz, M.E., 2015. Calibration and verification of SWMM for low impact development. *JAWRA Journal of the American Water Resources Association* 51, 746–757.
- Rossman, L., 2015. *SWMM 5.1 Storm Water Management Model User's Manual.* US Environmental Protection Agency, Cincinnati, OH.
- Rossman, L., Huber, W., 2016a. *Storm Water Management Model Reference Manual Volume I—Hydrology (Revised).* US Environmental Protection Agency, Cincinnati, OH, USA.
- Rossman, L., Huber, W., 2016b. *Storm Water Management Model Reference Manual: Volume III—Water Quality.* US Environmental Protection Agency, Office of Research and Development, National Risk Management Laboratory, Cincinnati, OH, USA.
- Semádeni-Davies, A.F., 1997. Monthly snowmelt modelling for large-scale climate change studies using the degree day approach. *Ecol. Model.* 101, 303–323.
- Semádeni-Davies, A.F., 2000. Representation of snow in urban drainage models. *J. Hydrol. Eng.* 5, 363–370.
- Semádeni-Davies, A.F., Hernebring, C., Svensson, G., Gustafsson, L.-G., 2008. The impacts of climate change and urbanisation on drainage in Helsingborg, Sweden: suburban stormwater. *J. Hydrol.* 350, 114–125.
- Stovin, V., 2010. The potential of green roofs to manage urban stormwater. *Water Environ. J.* 24, 192–199.
- Stovin, V., Poë, S., Berretta, C., 2013. A modelling study of long term green roof retention performance. *J. Environ. Manag.* 131, 206–215.
- Stovin, V., Poë, S., De-Ville, S., Berretta, C., 2015. The influence of substrate and vegetation configuration on green roof hydrological performance. *Ecol. Eng.* 85, 159–172.
- Stovin, V., Vesuviano, G., Kasmin, H., 2012. The hydrological performance of a green roof test bed under UK climatic conditions. *J. Hydrol.* 414, 148–161.
- Sundin, E., Andreasson, P., Viklander, M., 1999. An energy budget approach to urban snow deposit melt. *Nord. Hydrol.* 30, 39–56.
- Teemusk, A., Mander, Ü., 2007. Rainwater runoff quantity and quality performance from a greenroof: the effects of short-term events. *Ecol. Eng.* 30, 271–277.
- Villarreal, E.L., 2007. Runoff detention effect of a sedum green-roof. *Nord. Hydrol.* 38, 99–105.
- Warsta, L., Niemi, T.J., Taka, M., Krebs, G., Haahti, K., Koivusalo, H., Kokkonen, T., 2017. Development and application of an automated subcatchment generator for SWMM using open data. *Urban Water J.* 14, 954–963.
- Xu, C.-Y., 2000. Modelling the effects of climate change on water resources in central Sweden. *Water Resour. Manag.* 14, 177–189.

Paper 4

The transferability of SWMM model parameters between green roofs with similar build-up

Johannessen, B. G., Hamouz, V., Gagne, A. S., & Muthanna, T. M. (2019).

Journal of hydrology, 569, 816-828. <https://doi.org/10.1016/j.jhydrol.2019.01.004>



Contents lists available at ScienceDirect

Journal of Hydrology

journal homepage: www.elsevier.com/locate/jhydrol

Research papers

The transferability of SWMM model parameters between green roofs with similar build-up



Birgitte Gisvold Johannessen*, Vladimír Hamouz, Ashenafi Seifu Gagne, Tone Merete Muthanna

Department of Civil and Environmental Engineering, Norwegian University of Science and Technology (NTNU), N-7491 Trondheim, Norway

ARTICLE INFO

This manuscript was handled by G. Syme,
Editor-in-Chief

Keywords:
Green roofs
Design
Storm Water Management Model (SWMM)
LID
Calibration
Validation

ABSTRACT

While extensive green roofs are popular measures for reducing and delaying stormwater runoff, design tools are needed to better predict roof performance based on material properties, geometry and climate. This paper investigates the EPA's Storm Water Management Model's (SWMM) green roof module for this purpose based on observed runoff from several roofs with different build-ups, geometry, and climates. First, the general model performance was investigated and secondly transferability of model parameters for similar roofs but different geometries and climates was tested. Individual models reproduced runoff hydrographs well (NSE 0.56–0.96), while the long-term modelling showed relatively large volume errors most likely due to insufficient representation of evapotranspiration in the model. Model parameters obtained at one site were only partly transferable to similar roof build-up at other sites. Transferability was better from models calibrated with wetter climates and higher intensity events to drier climates, than the opposite way. Multi-site calibration resulted in model parameters performing well for most sites, giving model parameters that could be used for the design of similar roof build-ups in comparable climates. However, large variability in obtained model parameters, large volume errors and the fact that the calibrated model parameters did not directly correspond to measured material properties, place concerns on the generality of the SWMM green roof module as a design tool.

1. Introduction

Green roofs are popular measures for stormwater management, while also providing a set of other positive aspects to local environment ranging from reduced energy consumption for buildings, reduction in heat island effects, increase in urban habitats, and bringing visual improvements to urban areas (Besir and Cuce, 2018; Oberndorfer et al., 2007; Saadatian et al., 2013).

A substantial amount of green roof research has been published over the last decade wherein performance of green roofs has been examined in terms of both permanent (retention) and temporary (detention) storage of water in the green roof build ups (Akther et al., 2018; Berndtsson, 2010; Carter and Rasmussen, 2006; Li and Babcock, 2014). There is a large variation in reported performance, which has been explained by several factors ranging from natural (e.g. climate, precipitation patterns and amounts (Alfredo et al., 2010)) to material properties (e.g. layer build-up (Souliis et al., 2017a)) and roof geometry (size, shape and slope (Carson et al., 2013; Hakimdavar et al., 2014)). This makes field observations difficult to directly use for design purposes (Stovin et al., 2017).

Most engineers designing stormwater solutions prefer simplified

methods in terms of schematic values, plots or the use of well-known modelling tools. Preferable methods should be able to show performance as a function of applied materials (measured material properties and depths), roof geometry and local climate to simplify the design process. The necessary parameters and coefficients should be readily available without extensive field experiments. Different approaches have been applied to represent green roof's performance from the traditional applied runoff coefficients and curve numbers, via single or multiple regression equations to more complex conceptual or physical models (Li and Babcock, 2014). This paper briefly presents different published approaches, before thoroughly testing one of the modelling tools, the United States Environmental Protection Agency's (EPA) Storm Water Management Model (SWMM) green roof Low Impact Development (LID) module, for general model performance and for a comparison of calibrated model parameters between sites and to material properties.

Curve numbers (CN) and volumetric runoff coefficients (C_v) combined with design storms are widely applied methods for calculating surface runoff, making coefficients for green roofs highly sought after. Fassman-Beck et al. (2016) made a thorough investigation of retention performance from rainfall-runoff data from 21 living roofs. The authors

* Corresponding author.

E-mail address: birgitte.g.johannessen@ntnu.no (B.G. Johannessen).

<https://doi.org/10.1016/j.jhydrol.2019.01.004>

Received 30 October 2018; Received in revised form 2 January 2019; Accepted 4 January 2019

Available online 08 January 2019

0022-1694/© 2019 Elsevier B.V. All rights reserved.

emphasize the fact that the coefficients poorly represent the performance variability of green roofs, but due to the demand for such numbers, they suggest a climate specific modified approach using CN and C_v to predict green roof runoff.

Regression models showing a second-order relation between precipitation and runoff depth have been found useful in representing runoff at a specific site by Fassman-Beck et al. (2013) and Carson et al. (2013), but these types of models are not transferable to other climates, roof build-ups and roof geometries. Stovin et al. (2012) performed multiple linear regression analysis to predict hydrological performance, but these showed poor predictive capability. It was suggested that a continuous simulation approach based on substrate moisture flux is better suited to predict retention performance because it can deal with the complex inter-event processes.

Conceptual water balance models, as presented by Kasmin et al. (2010), have been proven successful for modelling green roof retention in several later studies if adequate evapotranspiration estimates are implemented (Johannessen et al., 2017; Starrý et al., 2016; Stovin et al., 2013). Moreover, conceptual models have been extended with reservoir routing models or runoff coefficients to model detention processes (Kasmin et al., 2010; Locatelli et al., 2014; Soulis et al., 2017b; Vesuviano and Stovin, 2013; Yio et al., 2013). Model parameters have been linked to materials, roof slopes and drainage length. Although these conceptual models have proven to successfully reproduce the observed green roof performance, they are highly dependent on laboratory or field testing and hence are not transferable to green roofs with different materials, layer build-up and geometry.

Several physically based models have also been suggested useful in reproducing green roof runoff like the Soil Water Atmosphere and Plant model (SWAP) (Metselaar, 2012), Hydrological Evaluation of Landfill Performance (HELP) (Carson et al., 2017) and Integrated Hydrological Model at Residential Scale (IHMORS) (Herrera et al., 2018). All these models include the possibility to model several consecutive substrate layers, while SWAP and IHMORS lack the ability to model lateral flow and are thus unable to include the detention effect resulting from the horizontal flow through the drainage layer in the green roof geometry. HYDRUS, a commercial physically based model for water movement in variably saturated media has been applied to several green roof studies in the one (1D) (Hilten et al., 2008; Palla et al., 2012; Soulis et al., 2017b), two (2D) (Li and Babcock, 2015) or three dimensional (3D) model version (Brunetti and Simunek, 2016) showing adequate performance. The model is based on a quite large number of physical parameters defined either from laboratory measurements or from model calibration, introducing high computational requirements and challenging calibration with variability in calibrated parameters (Soulis et al., 2017b).

Even though a large number of modelling tools have shown good abilities to reproduce observed green roof runoff, few of these models are applied among practitioners, who need tools to estimate runoff from green roofs to further combine with other stormwater measures for system design purposes. This could be due to little knowledge of some of these specialized modelling tools or inability to estimate model parameters accurately. For many stormwater engineers, a green roof modeling tool that combines with existing stormwater models and is based on generic material parameters would be preferable.

SWMM is an easily accessible, widely known and applied open source physically based dynamic rainfall-runoff simulation model used for predicting flows from contributing subcatchments and for analyzing wastewater and stormwater flow in piped systems (Rossman, 2015). The first attempts of applying SWMM to green roofs were carried out by modelling the green roof as permeable area coupled with a runoff coefficient, a curve number or modelled as a storage node (Alfredo et al., 2010; Roehr and Kong, 2010). Later, after a bioretention LID module was added to SWMM, green roof runoff was simulated with this module (Burszta-Adamiak and Mrowiec, 2013; Cipolla et al., 2016). The bioretention module includes; a surface layer describing possible

surface storage and overland flows; a soil layer describing the properties of the substrate affecting temporary and permanent water storage and infiltration properties; a separate water storage layer based on available volume and depth; and a drain function based on a drain coefficient (C) and a drain exponent (n) creating runoff (Rossman, 2015). Cipolla et al. (2016) reported satisfactory performance of the calibrated bioretention module, while Burszta-Adamiak and Mrowiec (2013) found the module to have limited capabilities in correctly simulating the runoff hydrographs. The main objection to this approach for green roof modelling is the use of two drain parameters predicting runoff without including parameters describing roof geometry and drainage layer materials. The SWMM green roof LID module was introduced in 2014. It has the same surface and soil layers as the bioretention module but with a drainage mat as its bottommost layer. The drainage mat provides volume for temporary storage of water while the runoff from the green roof is calculated based on Manning's equation with a specific roughness coefficient for the drainage layer. Evapotranspiration can be modelled based on a constant, on monthly values, an external input time series (climate file) or calculated by a climatology editor using the Hargreaves method with a possibility to add a monthly soil recovery pattern (Rossman and Huber, 2016a).

Palla and Gnecco (2015), Krebs et al. (2016) and Peng and Stovin (2017) applied the SWMM green roof module, including calibration and validation of the model parameters. Krebs et al. (2016) and Peng and Stovin (2017) used field studies and evaluated the model both with continuous data, to account for the retention process, and with events, to account for the detention parameters, while Palla and Gnecco (2015) applied synthetic rainfall events. All studies reported that the calibrated models represented the overall runoff generation process very well, with better performance for high-intensity rainfall events (i.e. events with high runoff to rainfall ratio when compared to low runoff events). On the other hand, Krebs et al. (2016) and Peng and Stovin (2017) discovered the inability of the models to physically represent and predict performance of the plastic board drainage layer to be an important limiting factor. Furthermore, Peng and Stovin (2017) attribute SWMM's limitations in estimating evapotranspiration to its shortcomings in accounting for the influence of the substrate moisture, a simplification which Krebs et al. (2016) found to be of limited effect on initial moisture content in a Nordic climate. All reported studies of the SWMM green roof module are calibrated based on small-scale units (2–6 m²) with 2–8% slope, substrate depth of 80–120 mm and an egg-cup shaped conjugated plastic drainage mat as the bottommost layer.

Calibrated SWMM green roof models have shown promising results when simulating green roof runoff from specific small-scale test roofs, while there is still lack of knowledge to whether the model parameters are true material constants transferable to other roofs with deviating climates, geometry and build-up making this a generic tool for design and performance evaluation. This study investigates the performance of the SWMM green roof module in general for several roofs with varying roof build-ups, sizes, slopes and climates. Calibrated model parameters for identical roof build-ups with deviating geometries and climates have been compared, assuming that if model parameters were comparable this would be an indication that these were true material constants that could be used for design purposes. Transferability of parameters has further been investigated by cross-validation of parameters among the study sites and by implementing a multi-site calibration procedure. Calibrated model parameters have been compared to other comparable studies and laboratory measurements, to see if these could be a source for parameter values when field tests are missing.

The objectives of the study have been:

1. Evaluate model performance of the SWMM green roof module with respect to long-term retention performance and event-based reproduction of the runoff hydrograph across geographical different climates.
2. Evaluate the use of the SWMM green roof module as a generic tool,

Table 1
Description of individual test sites.

Id	Size [m ²]	Slope [%]	Berm Height[mm]	Soil Thickness [mm]	Drainage mat Thickness [mm]	Build-up	Calibration period	Validation period	Tot. prec. [mm]	Tot. runoff [mm]
RIS1	15	16	10	30	10	Type A green roof	01.05–31.10.16	01.01–31.10.17	839	404
RIS3	15	16	10	80	25	Type C green roof	01.05–31.10.16	01.01–31.10.17	912	488
BER1	8	16	10	30	10	Type A green roof	01.05–31.10.16	01.01–31.10.17	2888	2240
BER3	8	16	10	80	75	Type C green roof	01.05–31.10.16	01.01–31.10.17	2888	2203
BER4	8	16	10	30	3	Type B green roof	01.05–31.10.16	01.01–31.10.17	2888	2288
SAN1	9	27	10	30	10	Type A green roof	01.05–31.10.16	01.01–31.10.17	1764	1180
SAN2	9	27	10	80	75	Type C green roof	01.05–31.10.16	01.01–31.10.17	1764	1219
SAN3	9	27	10	30	3	Type B green roof	01.05–31.10.16	01.01–31.10.17	1764	1293
OSL1	8	5.5	-	-	-	Reference roof	01.05–31.10.12	01.01–31.10.10	1339	1241
HOV1	100	2	500	200	20	Gray roof	11.05–15.08.17	16.08–30.11.17	627	582
HOV2	100	2	-	-	-	Reference roof	11.05–15.08.17	16.08–30.11.17	627	629
HOV3	100	2	500	30	36	Type B green roof	11.05–15.08.17	16.08–30.11.17	627	459
LAB1	4	2	-	-	-	Reference roof	one event	no validation	27	27
LAB2	4	2	10	1	10	Type A drain mat	one event	no validation	27	27
LAB3	4	2	10	0	7	Type B drain mat	one event	no validation	27	27
LAB4	4	2	10	30	47	Type B green roof	one event	no validation	27	27
LAB6	4	2	10	100	10	Gray roof	one event	no validation	27	27

* Slope applied to both the subcatchment and the LID surface.

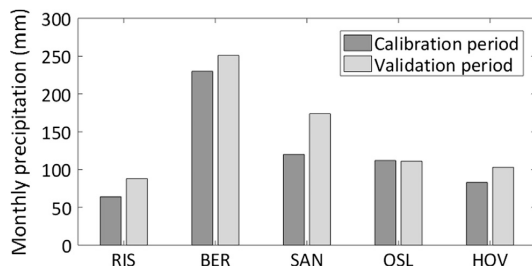


Fig. 1. Comparison of monthly precipitation within individual field stations.

by comparing estimated parameters across different sites, roof build-ups and geometries.

2. Materials and methods

2.1. Site descriptions

Various field studies, containing mainly extensive green roofs but also black bitumen reference roofs and a non-vegetated media (gray roof), with various scale were built to increase knowledge in terms of stormwater retention and runoff detention in cold climate (Table 1). Laboratory tests were conducted to supplement field studies. Test plots (8–15 m²), as well as full-scale (100 m²) field sites, were set up in different cities representing the typical coastal climate with various rainfall pattern across Norway: Bergen (BER), Oslo (OSL), Sandnes (SAN) and Trondheim. In Trondheim, data from two different test sites were included, Risvollan (RIS) and Høvrvingen (HOV). Each monitored roof is identified by its location and a number (e.g. BER1 and BER3). Bergen experienced most precipitation per month followed by Sandnes and Oslo, while the two sites in Trondheim were the driest (Fig. 1). In the figure, one can see a comparison between individual sites as well as periods chosen for calibration and validation. In two sites (OSL1 and HOV2), a black bitumen roof was used as a reference roof, while a gray roof was tested in one site (HOV1). Three groups of extensive green roofs from three different suppliers (A, B and C), which henceforth shall be referred to as Type A, Type B and Type C, were tested. The Type A designed for sloped roofs (RIS1, BER1, and SAN1) consisted of a vegetation mat (30 mm substrate in a reinforced net of fiber, pre-cultivated and sedum-based) over a 10 mm thick textile retention fabric (Fig. 2b). The Type B for sloped roofs (BER4, SAN3) have vegetation mat similar to Type A, but with a 3 mm thick textile retention mat (Fig. 2b). The Type B for a flat roof (HOV3) also included a thicker textile retention mat (11 mm) over a 25 mm conjugated plastic drainage layer (Fig. 2c). This configuration where a thin sedum vegetation mat (30 mm) constitute the total substrate depth is typical for the Scandinavian market, where they are preferred due to fast establishment, low weight and low maintenance needs, and where the drought risks are lower than in central Europe and United States due to the cold and wet climate. In general, little green roof research is published on these thin configurations, and to the knowledge of the authors, no applications of the SWMM green roof module are published. The Type C for sloped roofs consisted of a 30 mm vegetation mat over 50 mm of extra substrates, a 25 mm conjugated plastic drainage layer (RIS3) or a 75 mm polystyrene drainage layer (BER3, SAN2) and with a 10 mm textile retention mat in the bottom for all (Fig. 2d).

The non-vegetated gray roof (HOV1) consisted of a 200 mm layer of lightweight expanded clay aggregates, covered by paving stones (Fig. 2a). The expanded clay layer served partially as the soil layer as well as the drainage layer. For model purposes 10% of the total thickness was assumed to represent the drainage layer. For more information about the field experiments, see Johannessen et al. (2018) and Hamouz et al. (2018). Besides field tests, laboratory experiments were

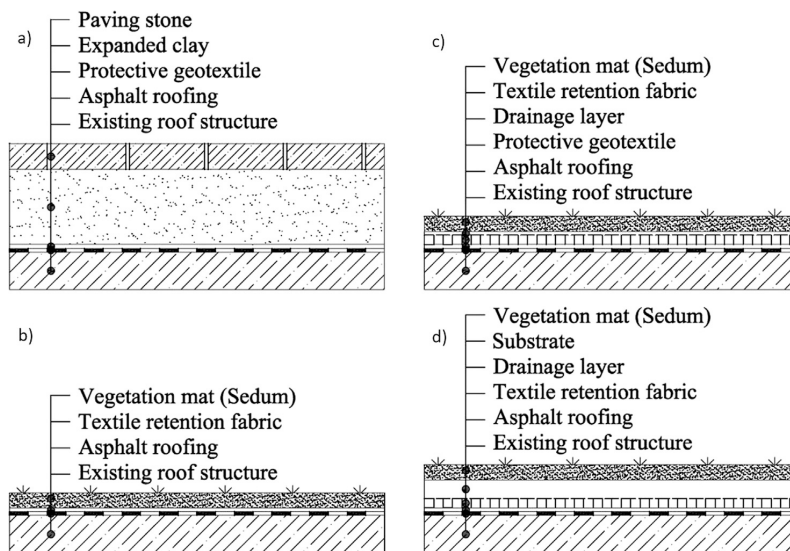


Fig. 2. Components of various rooftop configurations in a cross-section: a) Non-vegetated roof (HOV1, LAB6); b) Green roof Type A and B for sloped roofs (RIS1, BER1, SAN1, BER4, SAN3); c) Green roof Type B for flat roofs (HOV3); d) Green roof Type C for sloped roofs (RIS3, BER3, SAN2).

Table 2
Parameters chosen for calibration in SWMM (*parameters for calibration).

PARAMETER	GREEN ROOF			GRAY ROOF			REFERENCE ROOF		
	Initial value	Lower bound	Upper bound	Initial value	Lower bound	Upper bound	Initial value	Lower bound	Upper bound
Subcatchment									
Surface Roughness (Manning's n)*							0.011	0.001	0.2
Depression storage (mm)*							1	0.1	2.5
Initial saturation*	50	10	95	50	10	95	–	–	–
Soil recovery coefficient*	0.5	0.1	1.0	0.5	0.1	1.0	0.5	–	–
LID CONTROL									
Surface							No LID		
Berm Height (mm)	Site specific			Site specific					
Vegetation Volume Fraction	0.15			0					
Surface Roughness (Manning's n)	0.15			0.015					
Surface Slope (%)	Site specific			Site specific					
SOIL									
Thickness (mm)	Site specific			Site specific					
Porosity (volume fraction)*	0.6	0.45	0.7	0.6	0.45	0.7			
Field Capacity (volume fraction)*	0.35	0.2	0.45	0.03	0.01	0.2			
Wilting Point (volume fraction)*	0.05	0.01	0.1	0.05	0.01	0.1			
Conductivity (mm/hour)*	100	10	1000	2500	100	5000			
Conductivity Slope*	30	5	60	30	5	60			
Suction Head (mm)*	10	1	100	10	1	100			
Drainage mat									
Thickness (mm)	Site specific			Site specific					
Void Fraction*	0.5	0.01	1	0.5	0.01	1			
Roughness (Manning's n)*	0.1	0.01	0.4	0.1	0.01	0.4			

performed in order to test whether or not laboratory experiments could give material parameters comparable to the one obtained from field experiments. This includes vegetated and non-vegetated roofs as well as simply individual layers (retention mats) and a reference roof. The laboratory experiments were conducted according to the procedure given in the German Green Roofing Guideline published by the Landscape Development and Landscaping Research Society (FLL) (FLL, 2008). For more information on the laboratory tests see Schärer (2018).

2.2. Data collection

Continuous time series from the field rooftops and short-term

(event-based) data records from the laboratory were used as inputs to the hydrological model (Table 1). The RIS, BER, SAN and OSL field studies are based on two years of data, while the HOV field study is based on a total of 6.5 months of data. Winter data were excluded due to challenges with snow accumulation and melt. Precipitation was measured on site for all field experiments with a heated tipping bucket rain gauge. Runoff was measured with a pressure transducer measuring changes in a collection tank for all sites except Høvringen where a weight-based system was applied. Precipitation and runoff data were recorded with time intervals of 1-minute (Bergen, Sandnes, Risvollan and Høvringen,), 5-minutes (Oslo) and 3-second (laboratory experiments). Details on instrumentation and data collection can be found in

Hamouz et al. (2018), Johannessen et al. (2018) and Schärer (2018). Laboratory measurements of porosity, field capacity and wilting point for the green roof Type C substrate and the HOV1 and LAB6 material was performed based on a porous plate apparatus method (Richards, 1948), while the saturated hydraulic conductivity of Type C substrate was tested according to the German Green Roofing Guidelines water permeability method (FLL, 2008).

2.3. Model description

The SWMM version 5.1.012, including the green roof LID module was applied. The rooftop test beds were modeled as subcatchments that were 100% occupied (88% for HOV1 and HOV3) by the LID. The parameters in SWMM’s Green roof module, consisting of the individual LID layers: soil and drainage mat, as well as two parameters from the surface subcatchment (Surface Roughness – Manning’s n and Depression storage) were used in the calibration process (Table 2). Initial parameter values as well as lower- and upper-bounds for the calibration were estimated from field observations, laboratory experiments, adopted from other studies (Cipolla et al., 2016; Krebs et al., 2016; Palla and Gnecco, 2015; Peng and Stovin, 2017; Rosa et al., 2015) or from SWMM manuals (Rossman, 2015; Rossman and Huber, 2016b). However, parameters describing physical features such as thicknesses, slopes, berm heights, and elements of the surface LID layer were excluded from the calibration. The values of these parameters were obtained directly from the field experiment setups (Table 1). Potential evapotranspiration rates were determined using Hargreaves method (Hargreaves and Allen, 2003), computing daily evaporation rates from the daily air temperature records provided in an external climate file, while soil recovery coefficients were calibrated in order to achieve the best model fit.

2.4. Model calibration and evaluation

A uniform prior distribution was assumed for all calibration parameters given in Table 2. The optimal model parameters were identified through model calibration using the Shuffled Complex Evolution (SCE) algorithm (Duan et al., 1992). The Nash–Sutcliffe Efficiency (NSE) (Eq. (1)) (Nash and Sutcliffe, 1970) and the relative percentage difference (RPD) (Eq. (2)) were used for model evaluation. First as objective functions for the calibration period, referred to as model calibration. Then applied as metrics for measuring model performance when the calibrated parameters were applied in the validation period, referred to as model validation. In general, the closer the NSE is to 1, the more accurately the model can predict the observed performance, whilst an NSE greater than 0.5 indicates acceptable model performance (Rosa et al., 2015). Parameter spans giving acceptable model performance were defined as the 5–95% percentile of all parameters fulfilling the requirement of $NSE > 0.5$ or $|RPD| < 25\%$.

$$NSE = 1 - \frac{\sum_{i=1}^n (Q_{obs,i} - Q_{sim,i})^2}{\sum_{i=1}^n (Q_{obs,i} - Q_{obs})^2} \quad \text{Eq. (1)}$$

$$RPD = \frac{V_{obs} - V_{sim}}{V_{obs}} * 100, \quad \text{Eq. (2)}$$

Model performance was further evaluated visually using the quantile–quantile (Q-Q) plots. A quantile-based evaluation provides a more comprehensive analysis approach where whether or not the simulated and observed runoff series exhibit consistent distributions can be assessed directly (Thyer et al., 2009). Observed and simulated runoff from the event based calibration was classified in to 100 bins, plotted against each other and compared to a 1:1 line to evaluate the model performance at different flow regimes. A Q-Q plot along the 1:1 line indicates that the distribution of the simulated runoff series is consistent with

that of the observed runoff; hence, good model performance. Any deviation of a Q-Q plot from the 1:1 line implies inconsistent uncertainty in the simulated and observed runoff time series. With the 1:1 line as a reference, sections where the Q-Q data points plot above this line indicate an overestimation while data points that fall under this line indicate an underestimation of the simulated flows.

A two-step calibration procedure separating the volume calibration (retention performance) from the peak runoff (detention performance) calibration, was carried out. Retention related parameters (soil field capacity, soil wilting point and soil recovery constant) were calibrated with a continuous time-series first and evaluated based on volume errors (RPD). These parameters were then kept constant while the remaining, detention-related, parameters were calibrated on selected events with high intensity precipitation and evaluated with NSE. Similar calibration approaches calibrating both on retention and detention performance were also carried out by (Krebs et al., 2016) and (Peng and Stovin, 2017) for the SWMM green roof module. For the continuous calibration, the observed time series were divided in two equal parts for calibration and validation (Table 1). For the event-based evaluation, the four to five largest events were chosen for the calibration and validation period respectively. The maximum 5-minute intensities of the chosen events are given in Fig. 3 together with intensities of the two and five year return period events from local Intensity Duration Frequency (IDF) curves. Some events exceeded the two and five year return periods, while most of the applied events had return periods less than two years. For the laboratory experiments based on only one event, NSE alone was used for model calibration.

Model parameters were first calibrated for each site and configuration individually. Transferability of model parameters among models of similar roof build-ups was further tested with three different approaches. The first approach was carried out by manually selecting a common set of parameter values for all Type A sloped roofs, Type B sloped roofs, Type C sloped roofs and reference roofs and evaluating the performance. These parameters were set as close to the optimal values obtained in the individual calibration as possible. The second approach was based on a cross-validation of parameters among sites. For example, optimal parameters of the Type A sloped roof in Trondheim (RIS1) were applied at Sandnes (SAN1) and Bergen (BER1) sites and evaluated, and so on for all comparable roof build-ups. The third approach was carried out as a multi-site calibration, by artificially creating a combined time series of all comparable roofs, running a calibration and validating the performance based on both the combined series and the individual sites. To reduce the influence of variability in runoff flows, the runoff was normalized 0 (Q_{min}) to 1 (Q_{max}) for each

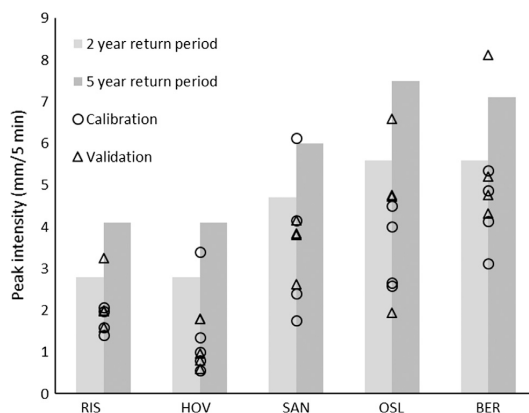


Fig. 3. Events used for calibration and validation. Maximum five minute precipitation and two and five year return period events from local IDF-curves for all sites.

Table 3
Model evaluation from individual model calibration.

Id	NSE		RPD	
	Calibration events	Validation events	Calibration period	Validation period
RIS1	0.65	0.85	4%	9%
BER1	0.77	0.75	−4%	3%
SAN1	0.66	0.75	4%	1%
BER4	0.77	0.82	−1%	3%
SAN3	0.92	0.87	21%	17%
RIS3	0.60	0.56	5%	4%
BER3	0.85	0.85	0%	6%
SAN2	0.87	0.80	12%	10%
HOV3	0.90	0.88	28%	14%
OSL1	0.80	0.66	2%	−5%
HOV2	0.96	0.95	18%	9%
HOV1	0.90	0.83	25%	17%
LAB1	0.89			
LAB2	0.84			
LAB3	0.84			
LAB4	0.82			
LAB5	0.80			
LAB6	0.60			

series in the last approach.

3. Results and discussion

3.1. Individual model evaluation

The individual model calibration procedure resulted in volume errors ranging from −4 to 28% in the calibration period and from −5 to 17% in the validation period (Table 3). While some of the models showed acceptable volume errors (six models with errors less than < 6%), others exhibit large volume errors (3 models with errors larger than 20%). This is most likely due to the fact that the model does not fully represent the evapotranspiration processes taking place, as suggested by earlier studies (e.g. Peng and Stovin (2017)), however it could also be due to measurement inaccuracies and uncertainties. The model represents evapotranspiration by the Hargreaves method combined with a soil recovery coefficient and does not include the influence of soil moisture which has been shown to have an important impact on evapotranspiration in green roofs (Berretta et al., 2014; Stovin et al., 2013). The calibration was based on one soil recovery coefficient for the whole model period, however it is possible that individual coefficients for each month might improve the performance. Larger volume errors were found for all tested configurations at Høvringen (HOV). One explanation might be uncertainties in the precipitation measurement related to placement of the field station at Høvringen, located by the coast exposed to an open fjord area and therefore experience higher wind stress. This model was also the only where the LID occupied only 88% compared to 100% for the other models, which might have influenced the model performance. Another aspect that could introduce volume errors are possible temporal variations in model parameters, not accounted for in the model. This aspect will be further discussed in Chapter 4.2.

The individual model's ability to reproduce the observed runoff hydrograph was evaluated by NSE coefficients (Table 3). All model runs provided NSE larger than 0.56, with an average of 0.80 for both the calibration and the validation period, which can be considered adequate performance for a rainfall-runoff model based on field observations (Rosa et al., 2015).

Fig. 4 shows Q-Q plots of the observed versus simulated runoff at the study sites. Each data point represent 1% of the data, and it can be

seen that most of the data fall in the low to medium flow regime (under the 75% percentile). The individual model calibrations showed good model performance for all data up to the 98–99% percentile, while peak flows were overestimated (HOV3, BER3) or underestimated (HOV2, RIS1, BER1, RIS3) for several of the models (Fig. 4).

3.2. Model parameters

Optimal model parameters for all calibrated models are given in Table 4a–e together with NSE values from the calibration.

3.2.1. Reference roofs

Three models of reference roofs (OSL1, HOV2, LAB1) were calibrated resulting in model parameters that could be useful for design purposes when comparing different roof configurations to conventional roofs (Table 4a). All reference roofs were based on black bitumen roofing but with varying roof size, slope and type of experiment. Optimal model parameters from individual calibration were comparable. Good model performance was found for both the manually chosen common parameter set and the multi-site calibration (Table 4a, Fig. 4b, Fig. 5b), indicating that the SWMM model reproduces the runoff satisfactory and can be used for modeling reference roofs of variable sizes and locations. The laboratory experiments were conducted with one high-intensity rainfall event, which differed significantly from the conditions in the field experiments, and gave larger spans of model parameters but still comparable optimal values. Recommended model parameters for reference roofs based on this study are a Manning's roughness coefficient of 0.01, as also found by Cipolla et al. (2016) in an earlier study, and a depression storage of 0.03.

3.2.2. Model retention performance

The available water storage capacity in green roofs in the SWMM green roof module is defined by the pore space between the field capacity and the wilting point combined with the soil thickness. No storage capacity is included in the drainage layer of the model even if the properties of the drainage layer might allow for water to be stored there, i.e. in cups in the conjugated plastic drainage layers or soaked up in the textile retention drainage mats. In some initial tests, separate monthly soil recovery patterns were applied, while in the individual calibration reported here only one soil recovery coefficient was applied.

The individual model calibrations showed large variation in optimal parameters for both field capacities (24–44%) and wilting points (1–15%) for the same material at different sites, and the resulting parameters seem to be influenced by local climate conditions (Table 4b–e). The highest field capacities were found for the wettest site (BER). The highest calibrated wilting points were found for the thickest configurations (Type C), possibly due to the fact that the total available storage capacities for the thickest configurations in a Norwegian climate are seldom utilized (Johannessen et al., 2017). Little or no data when the roof reaches its wilting point is expected to be present in the observed data used to calibrate the model, and this might affect the model's ability to predict these parameters properly. The span between the field capacity and the wilting point was only 3% for the Type B flat roof (HOV3). This model also has a volume error of 28% for the calibration period, indicating that the model is unable to reproduce the retention processes of this roof. Laboratory experiments of Type C substrate gave a field capacity of 21% and a wilting point of 1.5%. This is a large deviation from the individual calibrations (giving field capacity 24–44% and wilting point 7–15%) but corresponds quite well to the field capacity obtained in the multi-site calibration (23%).

Tests conducted with monthly soil recovery coefficients resulted in large seasonal variability in the predicted coefficients and a median span of model parameters of 0.19. Median model parameter span increased to 0.30 in the calibration including only one soil recovery coefficient. For some of the configurations (like RIS3), the monthly variations could be explained by variations in precipitation pattern with

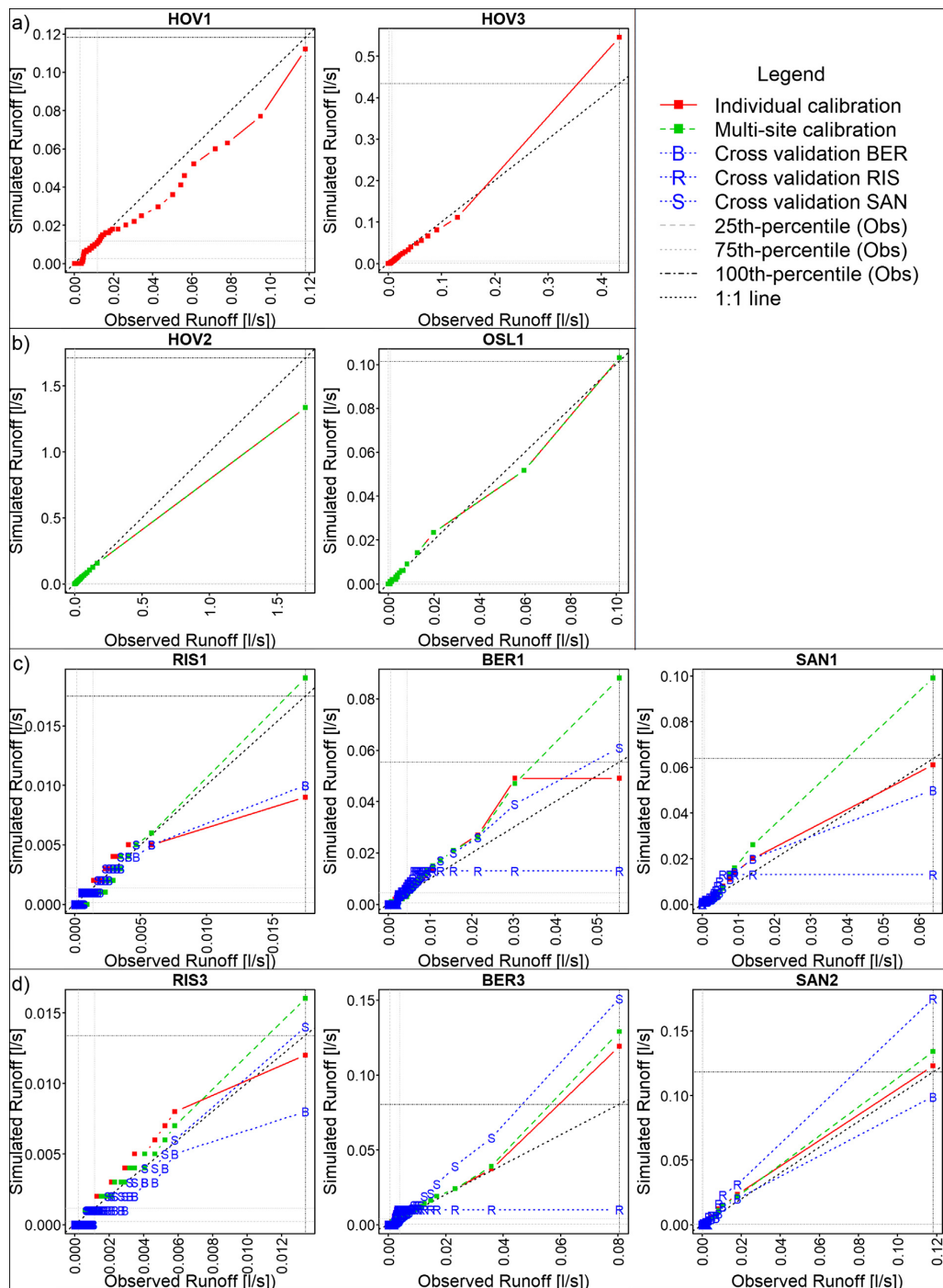


Fig. 4. Q-Q plots based on all calibration events showing observed versus simulated runoff at; a) gray roof (HOV1) and green roof (HOV3) at Høvringen Trondheim, b) reference roofs at Høvringen, Trondheim (HOV1) and in Oslo (OSL1), c) Type A roofs at Risvollan, Trondheim (RIS1), Bergen (BER1) and Sandnes (SAN1), d) Type C roofs at Risvollan, Trondheim (RIS3), Bergen (BER3) and Sandnes (SAN2).

Table 4

Optimal model parameters and NSE performance for individual calibration, manual chosen parameters and multi-site calibration; a) Reference roofs, b) Type A green roofs, c) Type B green roofs, d) Type C green roofs, e) Gray roof and Type B flat roof. a).

a)	Individual calibration			Manual	Multi-site cal	
	OSL1	HOV2	LAB1	ALL	ALL	
Surface Parameters						
Manning's n	0.03	0.01	0.02	0.02	0.01	
Depression storage (mm)	0.20	0.30	0.60	0.30	0.30	
Model evaluation						
NSE			0.89		0.90	
NSE OSL1	0.80			0.79	0.81	
NSE HOV2		0.96		0.95	0.96	
b)	Individual calibration				Man-ual	Multi-site cal
	RIS1	BER1	SAN1	LAB2	ALL	ALL
Soil Parameters						
Field Capacity (%)	31	44	29		32	43
Wilting Point (%)	2	1	9		5	2
Porosity (%)	70	70	70		70	61
Conductivity (mm/hr)	65	43	63		60	42
Conductivity Slope	14	16	15		15	32
Suction Head	77	13	6		40	28
Drain Parameters						
Void Fraction	0.01	0.03	0.03	0.10	0.03	0.56
Manning's n	0.18	0.22	0.21	0.10	0.21	0.32
Model evaluation						
NSE				0.84		0.52
NSE RIS1	0.65				< 0.5	< 0.5
NSE BER1		0.77			< 0.5	0.77
NSE SAN1			0.66		< 0.5	0.59
c)	Individual calibration			Man-ual	Multi-site cal	
	BER4	SAN3	LAB4	ALL	ALL	
Soil Parameters						
Field Capacity (%)	44	28	17	30	35	
Wilting Point (%)	4	10	7	7	10	
Porosity (%)	70	69	47	70	67	
Conductivity (mm/hr)	183	108	982	180	292	
Conductivity Slope	24	18	16	23	20	
Suction Head	39	51	71	45	18	
Drain Parameters						
Void Fraction	0.13	0.11	0.02	0.13	0.16	
Manning's n	0.09	0.10	0.23	0.10	0.09	
Model evaluation						
NSE			0.82		0.85	
NSE BER4	0.77			< 0.5	0.82	
NSE SAN3		0.92		< 0.5	0.89	
d)	Individual calibration				Man-ual	Multi-site cal
	RIS3	BER3	SAN2	LAB3	ALL	ALL
Soil Parameters						
Field Capacity (%)	24	44	32		30	23
Wilting Point (%)	15	7	15		2	14
Porosity (%)	43	59	50		60	40
Conductivity (mm/hr)	782	549	1 183		800	596
Conductivity Slope	43	46	47		45	53
Suction Head	55	64	45		50	90
Drain Parameters						
Void Fraction	0.01	0.47	0.06	0.21	0.20	0.89
Manning's n	0.13	0.07	0.24	0.11	0.15	0.01
Model evaluation						

Table 4 (continued)

d)	Individual calibration				Man-ual	Multi-site cal
	RIS3	BER3	SAN2	LAB3	ALL	ALL
NSE				0.82		0.83
NSE RIS3	0.60				< 0.5	0.81
NSE BER3		0.85			0.86	0.82
NSE SAN2			0.87		0.71	0.89
e)	Individual calibration					
	HOV1	HOV3		LAB6		
Soil Parameters						
Field Capacity (%)	15		18		27	
Wilting Point (%)	15		15		10	
Porosity (%)	35		49		57	
Conductivity (mm/hr)	3 366		645		80	
Conductivity Slope	48		60		19	
Suction Head	79		41		49	
Drain Parameters						
Void Fraction	0.72		0.64		0.40	
Manning's n	0.48		0.07		0.35	
Model evaluation						
NSE HOV1	0.90					
NSE HOV3		0.90				
NSE LAB6					0.60	

drier conditions in some months giving lower soil moisture content which again reduces the actual evapotranspiration (Fig. 6a bottom). However, if this was properly represented in the model, the same pattern should be found in all configurations at the same site experiencing the same local climate. This was not the case for the modelled sites, as shown for RIS1 which shows a deviating pattern from RIS3 (Fig. 6a top). Large variation in optimal values at the same site was also found when applying only one soil recovery coefficient, while model parameter spans were overlapping for all green roofs at the same site (Fig. 6b). Both the large volume errors and the large variation in calibrated parameters for soil recovery coefficients, field capacities and wilting points confirms earlier findings indicating that the modelling of evapotranspiration in the SWMM LID module based on the Hargreaves method combined with a soil recovery coefficient is not adequately representing the actual evapotranspiration, and thereby also the retention processes taking place (Feng and Burian, 2016; Peng and Stovin, 2017). This insufficient representation of the evapotranspiration processes in the model is also expected to affect the detention performance and detention parameters, as the observed runoff pattern is a combination of initial retention and detention.

3.2.3. Green roof drainage layers parameters

The drainage layer parameters are expected to play an important role in runoff generation, especially for full-scale roofs, as they will define the detention process associated with the horizontal water movement.

The only flat green roof included in the study resulted in a drainage layer void fraction of 0.64 and a Manning's n of 0.07. Model studies with similar conjugated plastic drainage layers resulted in comparable calibrated void fractions of 0.4–0.6 but lower Manning's roughness coefficients of 0.01–0.03 (Krebs et al., 2016; Palla and Gnecco, 2015; Peng and Stovin, 2017). These studies were based on table scale green roof units with drainage lengths of 2–3 m, which could explain the differences in the findings. The SWMM manual suggests a void fraction of 0.2–0.4 and Manning's n values of 0.01–0.03, but without specifying the drainage layer build-up (Rossman and Huber, 2016b).

The sloped green roofs included in the study were all equipped with textile retention mats as the bottommost layer, while the total thickness

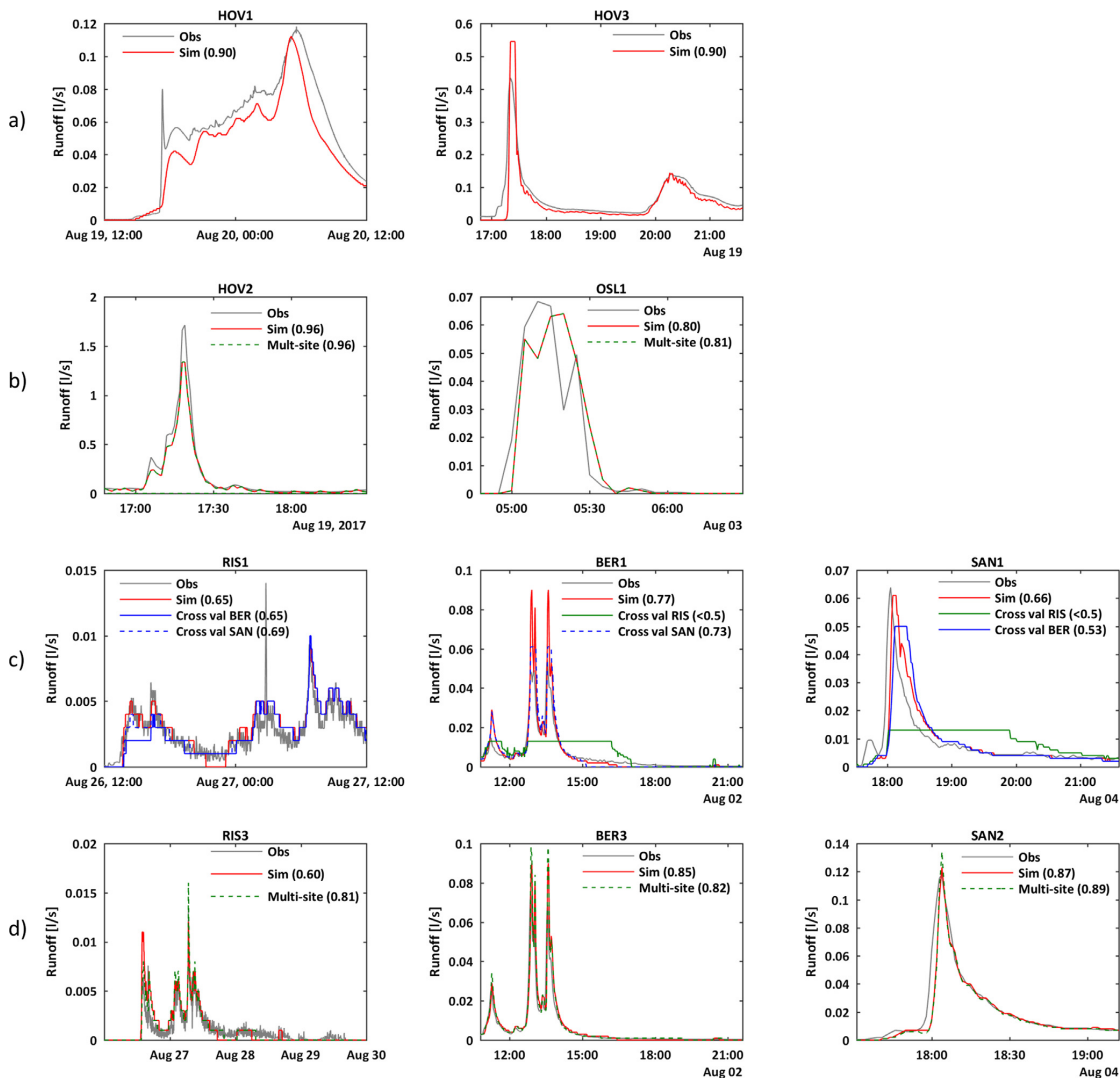


Fig. 5. Runoff hydrographs for one of the calibration events at; a) grey roof (HOV1) and green roof (HOV3) at Høvringen Trondheim, b) reference roofs at Høvringen, Trondheim (HOV1) and in Oslo (OSL1), c) Type A roofs at Risvollan, Trondheim (RIS1), Bergen (BER1) and Sandnes (SAN1), d) Type C roofs at Risvollan, Trondheim (RIS3), Bergen (BER3) and Sandnes (SAN2). Observed runoff (Obs), simulated runoff after the one-step (One-step), the two-step calibration (Sim), the multi-site calibration (Multi-site) and with model parameters transferred from the other sites (Cross val).

of the drainage layer varied between the different types. The drainage layer parameters were the parameters that showed the largest variation, both between the individual models of same type, between individual models and multi-site calibrated models for the same type and between the different types, in spite of the similarities of the bottommost layer. This indicated that the SWMM green roof module have limited ability to represent the water movement through the drainage layer, a process considered by the authors to be quite important for modelling detention properly on large scale roofs. This limitation of the model was also mentioned by Krebs et al. (2016), who also applied a textile retention mat as the bottommost layer, and by Peng and Stovin (2017), who applied a slightly different configuration with a plastic drainage layer as the bottommost layer.

The laboratory experiments of the textile retention mats alone were

carried out to test whether these kinds of experiments could give model parameters for different materials. The results showed large parameter spans and not comparable optimal parameters to the parameters obtained from field studies, and can therefore not be recommended to use for determining model parameters. Laboratory experiments were calibrated based on only one high-intensity event. Repeated tests with varying intensities might change the results but this was not tested.

3.2.4. Green roof soil parameters

Porosities were found to be larger for the reinforced vegetation mats compared to the Type C roofs which also had an extra separate substrate layer, and with small variations within the same type of green roofs. Laboratory experiments on the Type C extra substrate gave a porosity of 58%, which corresponded with one of the model's optimal

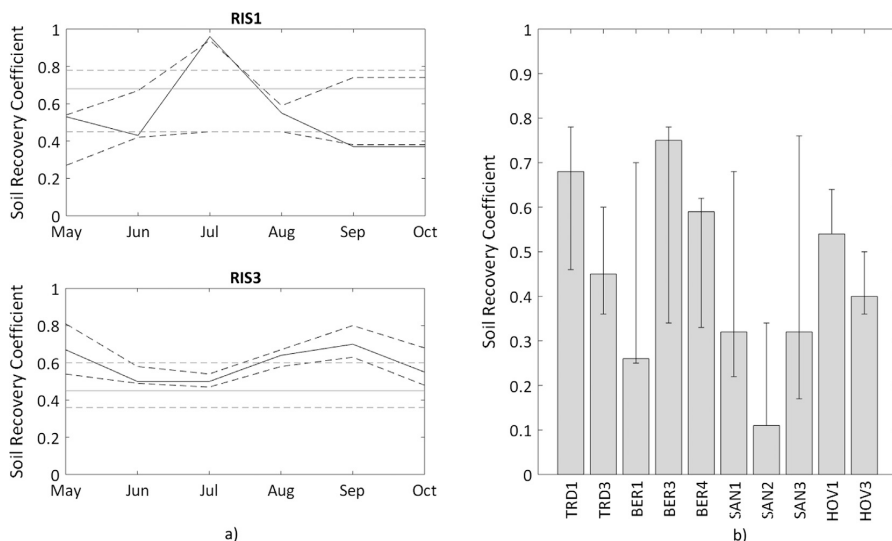


Fig. 6. Calibrated soil recovery coefficients. a) Comparison of monthly (black) or a constant (grey) value showing both median (solid) and parameter spans (dotted). b) Calibrated soil recovery coefficients using one constant value showing optimal values and parameter spans.

value of 59% but this was higher than the other models and the multi-site calibration value. Unfortunately, it was not possible to measure the porosities of the vegetation mats due to the reinforced structure, but based on visual observations it is likely that the porosities are higher in these, as also found in the model calibration.

Soil conductivity varied both between and within the different types of green roofs (42–1276 mm/hour), while there was slightly less variation in the obtained parameters for conductivity slope (14–60) and suction head (6–69). The SWMM manual suggests Soil Conductivity values in the range 1000–2500 mm/hr (Rossman and Huber, 2016b), while the German Green Roofing Guidelines give a requirement for water permeability in the range 36–4200 mm/hr (FLL, 2008). Laboratory experiments with the Type C substrate gave water permeability from 370 to 570 mm/hr, which is lower than the model parameters found in the individual models but closer to the multi-site calibrated value of 596 mm/hr. Krebs et al. (2016) applied a pregrown vegetation mat (Type A) over a thicker substrate and found a Soil Conductivity of 38 mm/hr, while (Palla and Gnecco, 2015) and (Peng and Stovin, 2017) found it to be 1000 mm/hr.

3.2.5. Gray roofs

Two models of gray roofs, one from the laboratory (LAB6) and one field site (HOV1), were calibrated in the same way as the green roofs. Both gray roofs were based on a lightweight expanded clay aggregate but with varying particle size, roof size, and type of experiment (continuous versus laboratory). The drainage parameters of HOV1 showed greater values than all other configuration (Manning's $n = 0.48$). This corresponds well to the observed runoff, with prolonged runoff compared to the green roofs, however the calibrated parameters might be too high as high flows had a tendency to be slightly underestimated (Fig. 4a, Fig. 5a). Since the soil conductivity (vertical movement) was very high, the horizontal movement through the expanded clay layer was expected to provide substantial detention.

Porosity was found to be lower for the gray roof than for the green roofs, conductivity higher, while conductivity slope and suction heads were found to be comparable. Laboratory measured porosity was 54.2% for the HOV1 material, much higher than the calibrated model porosity of 35%. Field capacity and the wilting point, determining the soil retention, was found to both be 15% according to the calibrated model

parameters for HOV1. Laboratory measurements of the same material gave a field capacity of 15.6% consistent to the model parameter, while the wilting point was measured to be 12.6% indicating that there was a small potential retention capacity in the material that was not found in the model parameters. Identical values for field capacity and wilting point in the model corresponds to no available storage capacity and explains the large volume error of the model (Table 3). This is a strong indication that the model does not properly represent the retention processes. The LAB6 model gave a porosity close to the laboratory measured 54%, while field capacity (10%) and wilting point (6.5%) deviated largely from the model derived parameters of respectively 27% and 10%.

Runoff hydrographs were well reproduced according to NSE values (Table 3), while the model underestimated the runoff for the upper 15% of the data (Fig. 4a).

4. Practical implications

4.1. Laboratory measured material properties

Laboratory measurements of porosity, field capacity and wilting point were carried out for the extra substrates used in the continuous field observations for Type C green roofs and the HOV1 gray roof. Laboratory measured porosities were higher than the model calibrated porosities, while the wilting points were found to be lower in laboratory measurements than in the model. Field capacities in the model, however, were found to be comparable to laboratory measurements of these. Laboratory measurements of water permeability according to the method described in the German Green Roofing Guidelines were slightly lower than the saturated hydraulic conductivity found in the models based on the same material. This method has been questioned for its accuracy and the large deviation from other methods (double-ring infiltrometer) earlier (Fassman and Simcock, 2012). Calibrated model parameters from the synthetic rain laboratory runoff tests did not show comparable model parameters to the models calibrated with field observations and cannot be used to obtain model parameters. This indicates that laboratory measurements should be used with caution in the SWMM green roof module. Alternatively, one could argue that physical measurements, when available, should be used in a physically

Table 5

Evaluation of model transferability. Cross validation of parameters between identical green roof build ups (Type A, Type B and Type C). Bold values indicate acceptable model performance.

Calibration	Validation								
	Type A			Type B			Type C		
	RIS1	BER1	SAN1	BER4	SAN3	RIS3	BER3	SAN2	
RIS1		< 0.5	< 0.5						
BER1	0.65		0.53						
SAN1	0.69	0.73							
BER4					0.85				
SAN3				0.75					
RIS3							< 0.5	< 0.5	
BER3							< 0.5	0.84	
SAN2						0.61	< 0.5		

based model to improve the model's ability to represent unmeasured systems. The challenges with such an approach in this study are discussed in Section 4.2. However, such an approach would simplify the use of the model and should be investigated further with respect to model performance and which parameters could be based on physical measurements and which need to be calibrated.

4.2. Can the SWMM green roof LID module provide generic material parameters?

The individually calibrated models reproduced the observed green runoff patterns during precipitation events sufficiently, as documented by acceptable NSE values (Table 4) and by the quantile plots (Fig. 4), while the long-term retention processes were less well reproduced giving variable volume errors. The SWMM green roof module is a model based on the physical properties and processes in a green roof. Provided that the model sufficiently reproduces the reality and measurement inaccuracies are limited, similar generic model parameters should be obtained when calibrating green roofs with the same roof build up at different sites and with different climate and geometry. Such transferable model parameters could then further be used for design purposes in sites without experimental data. The individually calibrated optimal model parameters were in some cases similar, while in other cases quite different for the same type of roofs (Table 4a–d). One of the challenges with model calibration is that it provides a set of optimal parameters which together give the best model performance without addressing the possible interdependency of the parameters. Several different parameter sets can give an adequate model performance, which could explain some of the variations in the obtained parameters for the same roof types. One could hypothesize that by using fewer model parameters for calibration, less variation could be found. Revealing parameter interdependencies could give information that further could be used to reduce the number of parameters for calibration. Interdependency of parameters was investigated by visually comparing all sets of acceptable parameter values ($NSE > 0.5$), by plotting all parameter values against each other (e.g. soil porosity versus soil conductivity, soil porosity versus conductivity slope and so on) for each individual model. No repeated patterns that could have given information about interdependencies of model parameters in the SWMM LID module were found in the plots, and this approach was therefore abandoned. The number of model parameters could also be reduced by fixing some of the substrate properties measured in laboratory (e.g. water storage capacity calculated from field capacity and wilting point in the model, which are measurable in laboratory). This would have been a feasible approach if all water storage took place in a single layer and was easily measurable. This was not the case in our green roof build-ups where water storage took place in several layers (vegetation mat, extra substrate layer, drainage layer and in textile retention mats).

Similarly, no standardized infiltration test for measuring green roof hydraulic conductivity in multiple layers exist. Based on this, rather than reducing the number of calibrated parameters, this study focused further on the transferability of model parameters between comparable roof build-ups at different sites as a method to investigate the credibility of the obtained model parameters.

The first approach by manually selecting a common set of parameter values for similar roofs build-ups at different sites showed poor performance with respect to reproducing the green roofs runoff pattern for Type A and B roofs ($NSE < 0.5$), while the reference roof runoff and two of the Type C roofs gave acceptable model performance ($NSE > 0.5$) (Table 4a–d). The results indicated that the model parameter spans could not be used individually as a basis for choosing parameter values. This was not surprising considering the interdependency of some of the parameters. The second approach, cross-validation of parameters between sites for the Type A roof showed that the parameters obtained in RIS were not transferable to the other sites, while the parameters obtained in BER and SAN were transferable to the other sites when evaluated based on NSE and quantile plots (Table 5, Fig. 4c, Fig. 5c). The Type B roofs showed a good transferability between the two sites BER and SAN (Table 5). The Type C roof parameters were transferable only from BER to SAN and from SAN to RIS (Table 5, Fig. 4d). The third approach, the multi-site calibration was more successful, resulting in common parameter sets for each green roof type as shown in Table 5b–d, Fig. 4b–c and Fig. 5d. Model evaluation showed these parameters to sufficiently reproduce green roof runoff patterns ($NSE > 0.5$) for all tested roof types except for the Type A roofs at Risvollan, but with some challenges associated with overestimation of the highest flows (Fig. 4c–d). Volume errors, however, were still variable and quite large as also shown and discussed in relation to the individual model calibrations.

There seems to be a better transferability of model parameters between BER and SAN, than to RIS. BER and SAN are comparable in terms of roof size and drainage length, while the slope of the roofs are 16% in RIS and BER and 27% in SAN (Table 1). Slope and size were accounted for in the model but due to the experienced differences in obtained parameters, this could not be ruled out as a possible cause. Another more likely explanation to the differences are the differences in precipitation. Total precipitation amount was lowest in RIS, almost double in SAN and around tripled in BER (Table 1, Fig. 1). The same pattern can be found for the size of the events used for model calibration and validation (Fig. 3). The results indicate that the model parameters are partly influenced by local conditions, and not totally generic model parameters representing only the used materials. Results showed that models calibrated with high precipitation amounts and peak intensities were transferable to drier sites, but not the other way around. This finding would also limit the use of models for higher intensity events than included in the calibration process. De-Ville et al. (2018) investigated temporal variations in hydraulic parameters as retention, by studying field capacity, and detention, by studying the scale parameter in a fitted reservoir routing model. The study revealed large sub-annual variations in the studied parameters, and suggested this to be caused by temporal variation in substrate hydrophobicity/ water repellency. This could also be a possible explanation to why model parameters differ between similar build-ups in different climates, as some of the sites were considerably wetter than others. The findings could also complicate the modelling concept in general, and introduce errors, as model parameters are expected to be constant and material dependent. The multi-site calibration approach produced model parameters giving acceptable model performance for several sites, resulting in what seemed to be a more robust model applicable for roofs with varying geometry and climate, leading us closer to a generic model. However, there are still questionable whether the models are generic, since the model parameters deviate both between individual models with the same roof build-up, between individual models and multi-site calibrated models and from several of the laboratory measurements of material properties.

5. Conclusions

The individual model calibration procedure using two objective functions, RPD for volume errors and NSE for hydrograph reproduction, gave an acceptable model performance. Runoff hydrographs for each individual model were well reproduced ($NSE > 0.56$ for all individual models, average $NSE = 0.80$), while the long-term modelling gave relatively high volume errors (average absolute volume error of 9%), indicating that the water storage and evapotranspiration processes are not well represented in the SWMM green roof LID module.

Manually chosen parameter sets for a given green roof build-up based on individual model results showed in general poor model performance. Model parameters obtained at one site was only partly transferable to similar roof build-up at other sites. Transferability was better from models calibrated with wetter climates and higher intensity events to drier climates, than the opposite way.

Multi-site calibration resulted in model parameters performing well for all sites and roof types except one of the configurations in Trondheim, giving model parameters that could be used for design of similar roof build-ups with varying geometry and climates. However the large variability in obtained model parameters, the large volume errors and the fact that the calibrated model parameters did not directly correspond to measured material properties, places concerns on the generality of the SWMM green roof LID module as design tool.

Declaration of interests

None.

Acknowledgements

This work was founded by The Research Council of Norway (grant no 241827), The Municipality of Trondheim, Norway and The Klima2050 Centre for Research-based Innovation (SFI), financed by the Research Council of Norway and its consortium partners.

References

- Akther, M., He, J.X., Chu, A., Huang, J., van Duin, B., 2018. A review of green roof applications for managing urban stormwater in different climatic zones. *Sustainability* 10 (8). <https://doi.org/10.3390/su10082864>.
- Alfredo, K., Montalto, F., Goldstein, A., 2010. Observed and modeled performances of prototype green roof test plots subjected to simulated low- and high-intensity precipitations in a laboratory experiment. *J. Hydrol. Eng.* 15 (6), 444–457. [https://doi.org/10.1061/\(ASCE\)JHE.1943-5584.0000135](https://doi.org/10.1061/(ASCE)JHE.1943-5584.0000135).
- Berndtsson, J.C., 2010. Green roof performance towards management of runoff water quantity and quality: a review. *Ecol. Eng.* 36 (4), 351–360. <https://doi.org/10.1016/j.ecoleng.2009.12.014>.
- Berretta, C., Poe, S., Stovin, V., 2014. Moisture content behaviour in extensive green roofs during dry periods: the influence of vegetation and substrate characteristics. *J. Hydrol.* 511, 374–386. <https://doi.org/10.1016/j.jhydrol.2014.01.036>.
- Besir, A.B., Cuce, E., 2018. Green roofs and facades: A comprehensive review. *Renew. Sustain. Energy Rev.* 82, 915–939. <https://doi.org/10.1016/j.rser.2017.09.106>.
- Brunetti, G., Simunek, J., Piro, P., 2016. A comprehensive analysis of the variably saturated hydraulic behavior of a green roof in a mediterranean climate. *Vadose Zone J.* 15 (9). <https://doi.org/10.2136/vzj2016.04.0032>.
- Burszta-Adamiaik, E., Mrowiec, M., 2013. Modelling of green roofs' hydrologic performance using EPA's SWMM. *Water Sci. Technol.* 68 (1), 36–42. <https://doi.org/10.2166/wst.2013.219>.
- Carson, T.B., Keeley, M., Marasco, D.E., McGillis, W.R., Culligan, P., 2017. Assessing methods for predicting green roof rainfall capture: A comparison between full-scale observations and four hydrologic models. *Urban Water J.* 14 (6), 589–603. <https://doi.org/10.1080/1573062X.2015.1056742>.
- Carson, T.B., Marasco, D.E., Culligan, P.J., McGillis, W.R., 2013. Hydrological performance of extensive green roofs in New York City: observations and multi-year modeling of three full-scale systems. *Environ. Res. Lett.* 8 (2), 13. <https://doi.org/10.1088/1748-9326/8/2/024036>.
- Carter, T.L., Rasmussen, T.C., 2006. Hydrologic behavior of vegetated roofs. *J. Am. Water Resour. Assoc.* 42 (5), 1261–1274. <https://doi.org/10.1111/j.1752-1688.2006.tb05611.x>.
- Cipolla, S.S., Maglionico, M., Stojkov, I., 2016. A long-term hydrological modelling of an extensive green roof by means of SWMM. *Ecol. Eng.* 95, 876–887. <https://doi.org/10.1016/j.ecoleng.2016.07.009>.
- De-Ville, S., Menon, M., Stovin, V., 2018. Temporal variations in the potential hydrological performance of extensive green roof systems. *J. Hydrol.* 558, 564–578. <https://doi.org/10.1016/j.jhydrol.2018.01.055>.
- Duan, Q.Y., Sorooshian, S., Gupta, V., 1992. Effective and efficient global optimization for conceptual rainfall-runoff models. *Water Resour. Res.* 28 (4), 1015–1031. <https://doi.org/10.1029/91wr02985>.
- Fassman-Beck, E., et al., 2016. Curve number and runoff coefficients for extensive living roofs. *J. Hydrol. Eng.* 21 (3). [https://doi.org/10.1061/\(ASCE\)JHE.1943-5584.0001318](https://doi.org/10.1061/(ASCE)JHE.1943-5584.0001318).
- Fassman-Beck, E., Voyde, E., Simcock, R., Hong, Y.S., 2013. 4 Living roofs in 3 locations: does configuration affect runoff mitigation? *J. Hydrol.* 490, 11–20. <https://doi.org/10.1016/j.jhydrol.2013.03.004>.
- Fassman, E., Simcock, R., 2012. Moisture measurements as performance criteria for extensive living roof substrates. *J. Environ. Eng.-Asce* 138 (8), 841–851. [https://doi.org/10.1061/\(ASCE\)EE.1943-7870.0000532](https://doi.org/10.1061/(ASCE)EE.1943-7870.0000532).
- Feng, Y.C., Burian, S., 2016. Improving evapotranspiration mechanisms in the US environmental protection agency's storm water management model. *J. Hydrol. Eng.* 21 (10). [https://doi.org/10.1061/\(ASCE\)JHE.1943-5584.0001419](https://doi.org/10.1061/(ASCE)JHE.1943-5584.0001419).
- FLI, 2008. Guidelines for the Planning, Research Society for Landscape Development and Landscape Construction, Bonn, Germany, Construction and Maintenance of Green Roofing.
- Hakimdavar, R., Culligan, P.J., Finazzi, M., Barontini, S., Ranzi, R., 2014. Scale dynamics of extensive green roofs: quantifying the effect of drainage area and rainfall characteristics on observed and modeled green roof hydrologic performance. *Ecol. Eng.* 73, 494–508. <https://doi.org/10.1016/j.ecoleng.2014.09.080>.
- Hamouz, V., Lohne, J., Wood, J., Muthanna, T., 2018. Hydrological Performance of LECA-Based Roofs in Cold Climates. *Water* 10 (3), 263. <https://doi.org/10.3390/w10030263>.
- Hargreaves, G.H.A., Allen, R.G., 2003. History and evaluation of hargreaves evapotranspiration equation. *J. Irrig. Drain. Eng.* 129 (1), 53–63. [https://doi.org/10.1061/\(ASCE\)0733-9437\(2003\)129:1\(53\)](https://doi.org/10.1061/(ASCE)0733-9437(2003)129:1(53)).
- Herrera, J., et al., 2018. Using a hydrological model to simulate the performance and estimate the runoff coefficient of green roofs in semiarid climates. *Water* 10 (2). <https://doi.org/10.3390/w10020198>.
- Hilten, R.N., Lawrence, T.M., Tollner, E.W., 2008. Modeling stormwater runoff from green roofs with HYDRUS-1D. *J. Hydrol.* 358 (3–4), 288–293. <https://doi.org/10.1016/j.jhydrol.2008.06.010>.
- Johannessen, B.G., Hanslin, H.M., Muthanna, T.M., 2017. Green roof performance potential in cold and wet regions. *Ecol. Eng.* 106, 436–447. <https://doi.org/10.1016/j.ecoleng.2017.06.011>.
- Johannessen, B.G., Muthanna, T.M., Braskerud, B.C., 2018. Detention and retention behavior of four extensive green roofs in three nordic climate zones. *Water* 10 (6), 671. <https://doi.org/10.3390/w10060671>.
- Kasmin, H., Stovin, V.R., Hathway, E.A., 2010. Towards a generic rainfall-runoff model for green roofs. *Water Sci. Technol.* 62 (4), 898–905. <https://doi.org/10.2166/wst.2010.352>.
- Krebs, G., Kuoppamaki, K., Kokkonen, T., Koivusalo, H., 2016. Simulation of green roof test bed runoff. *Hydrol. Process.* 30 (2), 250–262. <https://doi.org/10.1002/hyp.10605>.
- Li, Y.L., Babcock, R.W., 2014. Green roof hydrologic performance and modeling: a review. *Water Sci. Technol.* 69 (4), 727–738. <https://doi.org/10.2166/wst.2013.770>.
- Li, Y.L., Babcock, R.W., 2015. Modeling Hydrologic Performance of a Green Roof System with HYDRUS-2D. *J. Environ. Eng.* 141 (11). [https://doi.org/10.1061/\(ASCE\)JHE.1943-7870.0000976](https://doi.org/10.1061/(ASCE)JHE.1943-7870.0000976).
- Locatelli, L., et al., 2014. Modelling of green roof hydrological performance for urban drainage applications. *J. Hydrol.* 519 (Part D), 3237–3248. <https://doi.org/10.1016/j.jhydrol.2014.10.030>.
- Metselaar, K., 2012. Water retention and evapotranspiration of green roofs and possible natural vegetation types. *Resour. Conserv. Recycl.* 64, 49–55. <https://doi.org/10.1016/j.resconrec.2011.12.009>.
- Nash, J.E., Sutcliffe, J.V., 1970. River flow forecasting through conceptual models part I—a discussion of principles. *J. Hydrol.* 10 (3), 282–290. [https://doi.org/10.1016/0022-1694\(70\)90255-6](https://doi.org/10.1016/0022-1694(70)90255-6).
- Oberdorfer, E., et al., 2007. Green roofs as urban ecosystems: Ecological structures, functions, and services. *Bioscience* 57 (10), 823–833. <https://doi.org/10.1641/b571005>.
- Palla, A., Gnecco, I., 2015. Hydrologic modeling of Low Impact Development systems at the urban catchment scale. *J. Hydrol.* 528, 361–368.
- Palla, A., Gnecco, I., Lanza, L.G., 2012. Compared performance of a conceptual and a mechanistic hydrologic models of a green roof. *Hydrol. Process.* 26 (1), 73–84. <https://doi.org/10.1002/hyp.8112>.
- Peng, Z., Stovin, V., 2017. Independent validation of the SWMM green roof module. *J. Hydrol. Eng.* 22 (9). [https://doi.org/10.1061/\(ASCE\)JHE.1943-5584.0001558](https://doi.org/10.1061/(ASCE)JHE.1943-5584.0001558).
- Richards, L.A., 1948. Porous plate apparatus for measuring moisture retention and transmission by soil. *Soil Sci. Soc. J.* 66 (2), 105–110. <https://doi.org/10.1097/00010694-194808000-00003>.
- Roehr, D., Kong, Y., 2010. Stormwater runoff reduction achieved by green roofs: Comparing SWMM method to TR-55 method, 2010 International Low Impact Development Conference - Redefining Water in the City, San Francisco, CA, pp. 1012–1021. DOI:[https://doi.org/10.1061/41099\(367\)88](https://doi.org/10.1061/41099(367)88).
- Rosa, D.J., Clausen, J.C., Dietz, M.E., 2015. Calibration and Verification of SWMM for Low Impact Development. *J. Am. Water Resour. Assoc.* 51 (3), 746–757. <https://doi.org/10.1111/jawr.12272>.
- Rossman, L.A., 2015. StormWater Management Model User's Manual Version 5.1. EPA-600/R-14/413b.
- Rossman, L.A., Huber, W.C., 2016a. Storm Water Management Model Reference Manual Volume I - Hydrology (Revised). EPA/600/R-15/162A.
- Rossman, L.A., Huber, W.C., 2016b. Storm Water Management Model Reference Manual

- Volume III - Water Quality. EPA/600/R-16/093.
- Saadatian, O., et al., 2013. A review of energy aspects of green roofs. *Renew. Sustain. Energy Rev.* 23, 155–168. <https://doi.org/10.1016/j.rser.2013.02.022>.
- Schärer, L.A., 2018. Comparing experimentally measured runoff coefficients with field observations for detention-based roofs. Norwegian University of Science and Technology, Trondheim, Norway, pp. 48.
- Soulis, K.X., Ntoulas, N., Nektarios, P.A., Kargas, G., 2017a. Runoff reduction from extensive green roofs having different substrate depth and plant cover. *Ecol. Eng.* 102, 80–89. <https://doi.org/10.1016/j.ecoleng.2017.01.031>.
- Soulis, K.X., Valiantzas, J.D., Ntoulas, N., Kargas, G., Nektarios, P.A., 2017b. Simulation of green roof runoff under different substrate depths and vegetation covers by coupling a simple conceptual and a physically based hydrological model. *J. Environ. Manage.* 200, 434–445. <https://doi.org/10.1016/j.jenvman.2017.06.012>.
- Starry, O., Lea-Cox, J.D., Ristvey, A., Cohan, S., 2016. Parameterizing a water-balance model for predicting stormwater runoff from green roofs. *J. Hydrol. Eng.* 21 (12). [https://doi.org/10.1061/\(ASCE\)HE.1943-5584.0001443](https://doi.org/10.1061/(ASCE)HE.1943-5584.0001443).
- Stovin, V., Poe, S., Berretta, C., 2013. A modelling study of long term green roof retention performance. *J. Environ. Manage.* 131, 206–215. <https://doi.org/10.1016/j.jenvman.2013.09.026>.
- Stovin, V., Vesuviano, G., De-Ville, S., 2017. Defining green roof detention performance. *Urban Water J.* 14 (6), 574–588. <https://doi.org/10.1080/1573062X.2015.1049279>.
- Stovin, V., Vesuviano, G., Kasmin, H., 2012. The hydrological performance of a green roof test bed under UK climatic conditions. *J. Hydrol.* 414, 148–161. <https://doi.org/10.1016/j.jhydrol.2011.10.022>.
- Thyer, M., et al., 2009. Critical evaluation of parameter consistency and predictive uncertainty in hydrological modeling: a case study using Bayesian total error analysis. *Water Resour. Res.* 45, 22. <https://doi.org/10.1029/2008wr006825>.
- Vesuviano, G., Stovin, V., 2013. A generic hydrological model for a green roof drainage layer. *Water Sci. Technol.* 68 (4), 769–775. <https://doi.org/10.2166/wst.2013.294>.
- Yio, M.H.N., Stovin, V., Werdin, J., Vesuviano, G., 2013. Experimental analysis of green roof substrate detention characteristics. *Water Sci. Technol.* 68 (7), 1477–1486. <https://doi.org/10.2166/wst.2013.381>.

Paper 5

Modelling runoff reduction through implementation of green and grey roofs in urban catchments using PCSWMM

Hamouz, V., Møller-Pedersen P., & Muthanna, T. M.

In review: Urban water Journal

This paper is awaiting publication and is not included in NTNU Open

Secondary papers and conference presentations

This appendix presents two presented conference papers and presentation titles two on which some the selected papers are built. The full bibliographies and abstract are presented.

Secondary papers

Hydrological performance of a blue-grey roof in a cold climate

Vladimír Hamouz, Tone Merete Muthanna

Department of Civil and Environmental Engineering, Norwegian University of Science and Technology (NTNU)

Keywords: Blue-grey roof, hydrological performance, cold climate, detention, retention.

Summary: Rooftop areas represents a considerable part of the impervious fractions of urban areas. Detaining and retaining runoff from rooftops can significantly contribute to reduction of runoff peaks and volumes from urban areas. Typically a vegetated green roof has been the one most commonly used to achieve this. However, in climates with limited evapotranspiration, a blue-grey system of a detention filtermedia can be a option. A blue-grey field site was established at a coastal area of Trondheim during 2016. It will provide long-term data collection and serve to increase knowledge in terms of design and behavior of blue-grey roofs as stormwater controls in cold climate.

Modelling of Green and Grey Roofs in Cold Climates using EPA's Storm Water Management Model

Vladimir Hamouz, Tone Merete Muthanna

Department of Civil and Environmental Engineering, Norwegian University of Science and Technology (NTNU).

Keywords: Green/grey roof; Storm Water Management Model (SWMM); Hydrological performance; Long-term simulation.

Abstract: Rooftops retrofitting, typically extensive green roofs, is a favoured sustainable drainage system technology in densely developed urban areas. They provide multiple benefits in terms of stormwater retention and runoff detention. The latest version of Storm Water Management Model (SWMM) 5.1.012 with Low Impact Development (LID) Controls was used to model hydrological the performance of a green and grey (non-vegetated) roof by defining the physical parameters of individual layers in LID Control editor. In this study, high-resolution 1-minute data from a previously monitored green and grey roof were used to calibrate the SWMM LID Green Roof module. Results from the un-calibrated model were unsatisfactory considering the hydrological response of the green and grey roof. After calibration, the observed and simulated runoff had Nash-Sutcliffe model efficiency (NSME) of 0.88 (green roof) 0.68 (grey roof). This indicates that better fit between observed and modelled runoff could be achieved with calibration, primarily of the grey roof. Ideally the calibrated parameter set of the LID modules should be transferable between watersheds given the same LID structural build up. This should be investigated through further research finding the optimal parameter set, and data validation of proposed parameters across catchments.

Conference presentations

1. Hamouz, V., & Muthanna, T. M. (2017). Water retention on non-vegetated roofs in Nordic climates. Nordic Wastewater Conference (NORDIWA2017). 10-12 October 2017, Aarhus, Denmark.
 2. Hamouz, V., & Muthanna, T. M. (2019). How can blue-green/grey roof solutions contribute to runoff reductions in urban catchments? Nordic Wastewater Conference (NORDIWA2019). 23-25 September 2019, Helsinki, Finland.
-

Co-Author Statements

This appendix includes the statements from the co-authors confirming co-authorship and the contribution made by the Ph.D. candidate.



NTNU

Encl. to application for assessment of PhD thesis

STATEMENT FROM CO-AUTHOR

(cf. section 10.1 in the PhD regulations)

Vladimír Hamouz applies to have the following thesis assessed:

Name of candidate

Retention and detention-based roofs for stormwater management in urban environments in cold climates

Title

*) The statement is to describe the work process and the sharing of work and approve that the article may be used in the thesis.

*)

Statement from co-author on article:

Hamouz, V., Lohne, J., Wood, J., & Muthanna, T. (2018). Hydrological performance of LECA-based roofs in cold climates. *Water*, 10(3), 263; <https://doi.org/10.3390/w10030263>

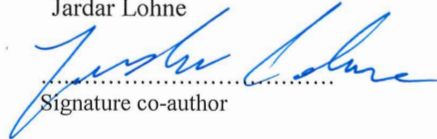
I hereby declare that the article mentioned above, of which I am co-author, will form part of the Ph.D. thesis by the Ph.D. candidate Vladimír Hamouz who made a major contribution to the work in the experiment, data analysis and writing phase.

.....
Place, date

Oslo, 04.01.2020
Place, date

Trondheim 10.02.2020
.....
Place, date

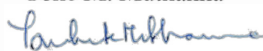
Jardar Lohne


.....
Signature co-author

Jaran R. Wood


.....
Signature co-author

Tone M. Muthanna


.....
Signature co-author

**STATEMENT FROM CO-AUTHOR**

(cf. section 10.1 in the PhD regulations)

Vladimír Hamouz applies to have the following thesis assessed:

Name of candidate

Retention and detention-based roofs for stormwater management in urban environments in cold climates



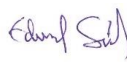



Title

*) The statement is to describe the work process and the sharing of work and approve that the article may be used in the thesis.

*) Statement from co-author on article:

Hamouz, V., Pons, V., Sivertsen, E., Raspati, G. S., Bertrand-Krajewski, J-L., & Muthanna, T. M., Detention-based green roofs for stormwater management under extreme precipitation due to climate change. (Accepted for publication: Blue-Green Systems - <https://iwaponline.com/bgs>)

I hereby declare that the article mentioned above, of which I am co-author, will form part of the Ph.D. thesis by the Ph.D. candidate Vladimír Hamouz.

Author	Roles	Place, date	Signature co-author
Vladimír Hamouz	Conceptualization, data curation, formal analysis, investigation, methodology, visualization, writing the original draft.	Oslo, 26.5.2020	
Vincent Pons	Conceptualization, data curation, formal analysis, investigation, methodology, visualization, writing the original draft.	Trondheim, 27.05.2020	
Edvard Sivertsen	Conceptualization, investigation, methodology, review, editing.	Trondheim, 27.05.2020	
Gema Sakti Raspati	Conceptualization, investigation, methodology, review, editing.	Trondheim, 27.05.2020	
Jean-Luc Bertrand-Krajewski	Supervision, review, editing.	Villeurbanne, 27/05/2020	
Tone Merete Muthanna	Supervision, review, editing.	Trondheim, 27.05.2020	



STATEMENT FROM CO-AUTHOR

(cf. section 10.1 in the PhD regulations)

Vladimír Hamouz applies to have the following thesis assessed:

Name of candidate

Retention and detention-based roofs for stormwater management in urban environments in cold climates

Title

*) The statement is to describe the work process and the sharing of work and approve that the article may be used in the thesis.

*)	
Statement from co-author on article:	
Hamouz, V., & Muthanna, T. M. (2019). Hydrological modelling of green and grey roofs in cold climate with the SWMM model. Journal of environmental management, 249, 109350, https://doi.org/10.1016/j.jenvman.2019.109350 .	
I hereby declare that the article mentioned above, of which I am co-author, will form part of the Ph.D. thesis by the Ph.D. candidate Vladimír Hamouz who made a major contribution to the work in the experiment, data analysis and writing phase.	
	Tone M. Muthanna
... Trondheim 10.02.2020.....
Place, date	Signature co-author



STATEMENT FROM CO-AUTHOR

(cf. section 10.1 in the PhD regulations)

Vladimír Hamouz applies to have the following thesis assessed:

Name of candidate

Retention and detention-based roofs for stormwater management in urban environments in cold climates

Title

*) The statement is to describe the work process and the sharing of work and approve that the article may be used in the thesis.

*)


Statement from co-author on article:


Johannessen, B. G., Hamouz, V., Gragne, A. S., & Muthanna, T. M. (2019). The transferability of SWMM model parameters between green roofs with similar build-up. *Journal of hydrology*, 569, 816-828.


<https://doi.org/10.1016/j.jhydrol.2019.01.004>


Author Contribution Statement

Author	Roles
Birgitte G. Johannessen	Conceptualization, Data curation, Formal analysis, Investigation, Methodology, Visualization, Writing original draft
Vladimir Hamouz	Conceptualization, Data curation, Formal analysis, Investigation, Methodology, Visualization, Writing original draft
Ashenafi S. Gragne	Conceptualization, Investigation, Methodology, Software, review & editing
Tone M. Muthanna	Supervision, review & editing


Birgitte G. Johannessen Trondheim, Norway Oct 30 2018


Vladimir Hamouz Trondheim, Norway Oct 30 2018


Ashenafi S. Gragne Trondheim, Norway Oct 30 2018


Tone M. Muthanna Lyon, France Oct 30 2018



STATEMENT FROM CO-AUTHOR

(cf. section 10.1 in the PhD regulations)

Vladimír Hamouz applies to have the following thesis assessed:

Name of candidate

Retention and detention-based roofs for stormwater management in urban environments in cold climates

Title

*) The statement is to describe the work process and the sharing of work and approve that the article may be used in the thesis.

*)

Statement from co-author on article:

Hamouz, V., Møller-Pedersen P., & Muthanna, T. M., Modelling runoff reduction through implementation of green and grey roofs in urban catchments using PCSWMM. (In review: Urban Water Journal - <https://www.tandfonline.com/toc/nurw20/current>)

I hereby declare that the article mentioned above, of which I am co-author, will form part of the Ph.D. thesis by the Ph.D. candidate Vladimír Hamouz who made a major contribution to the work in the experiment, data analysis and writing phase.

Trondheim, 27/5/2020

Place, date

Per Møller-Pedersen

Per Møller-Pedersen
Signature co-author

Trondheim 27.05.2020

Place, date

Tone M. Muthanna

Tone M. Muthanna
Signature co-author

